GERMANIUM HYDRIDE DERIVATIVES

OF

TRANSITION METAL CARBONYLS

A thesis

submitted to the

University of Waikato

for the degree of

Doctor of Philosophy

by

Judith Anne Christie M.Sc., (Hons., First Class)

School of Science

University of Waikato

July, 1981.

TABLE OF CONTENTS

TABLE OF CONTENTS (Continued)

TABLE OF CONTENTS (Continued)

TABLE OF CONTENTS (Continued)

TABLE OF CONTENTS (Continued)

TABLE OF CONTENTS (Continued)

TABLE OF CONTENTS (Continued)

LIST OF TABLES

LIST OF TABLES (continued)

LIST OF TABLES (continued)

LIST OF FIGURES

LIST OF FIGURES (Continued)

LIST OF FIGURES (Continued)

ACKNOWLEDGEMENTS

I am extremely grateful to my supervisor, Professor K. M. Mackay for his guidance and encouragement throughout the course of this research.

I also wish to thank Dr B. K. Nicholson for his very helpful words of advice.

My thanks I also extend to all my colleagues, and especially to Dr D. N. Duffy, Dr K. R. Ronaldson, Mrs L. Briggs, Mr R. Thompson, and Miss C. C. Ngo.

Many thanks, too, to the university staff, particularly Mr G. Purdy, the glassblower, Mr A. Brennan for the recording of the mass spectra, and Dr A. L. Wilkins for the 90MHz spectra.

Thanks also to: the Ruakura Animal Research Centre; Dr P. Holland; Mr D. McGaverston for their help with and use of the mass spectroscopic facilities; to Auckland University; Dr M. J. Taylor and Mr F. Povil for the use and recording of Raman spectra.

I thank the New Zealand University Grants Committee for a Post-Graduate Scholarship during the tenure of which this work was carried out.

Finally, I wish to thank Mrs M. V. Quilter for her most efficient preparation of the typescript.

Judy Christie

ABSTRACT

Compounds of the type $Fe(CO)_4(GeR_3)_2$ containing two different methylgermyl substituents have been prepared and characterised. The preparation was *via* the exchange reaction

$$Fe(CO)_4(GeR_3)_2 + [Mn(CO)_5]^- \longrightarrow [Fe(CO)_4(GeR_3)]^- + Mn(CO)_5(GeR_3)$$

$$[Fe(CO)_4(GeR_3)]^- + GeXR'_3 \longrightarrow Fe(CO)_4(GeR_3)(GeR'_3)$$

The compounds characterised were $Fe(CO)_4(GeMeH_2)(GeH_3)$ $Fe(CO)_4(GeMe_2H)(GeH_3)$, $Fe(CO)_4(GeMe_2H)(GeMeH_2)$, $Fe(CO)_4(GeMe_3)(GeH_3)$ $Fe(CO)_4(GeMe_3)(GeMeH_2)$ and $Fe(CO)_4(GeMe_3)(GeMe_2H)$. Of these, the species $Fe(CO)_4(GeMeH_2)(GeH_3)$, $Fe(CO)_4(GeMe_2H)(GeH_3)$ and $Fe(CO)_4(GeMe_3)(GeH_3)$ were characterised fully by infrared, proton nmr and mass spectroscopic studies.

The self-reaction

$$2Fe(CO)_4(GeR_3)_2 \longrightarrow [Fe(CO)_4(GeR_2)]_2 + 2GeR_4$$

has also been examined in some detail. The methylgermane was eliminated in preference to GeH_4 and species of the type $[Fe(CO)_4(GeH_3)]_2$-GeR_2 were also identified in two cases.

Halogenation of $Fe(CO)_4(GeMeH_3)(GeH_3)$ and $Fe(CO)_4(GeMe_2H)(GeH_3)$ was followed by ^1H nmr studies. $CC\ell_4$ results in the substitution of Ge-H, while $HC\ell$ cleaves Fe-Ge bonds.

While $Fe(CO)_4(GeMe_2H)(GeMeH_2)$, $Fe(CO)_4(GeMe_3)(GeMeH_2)$ and $Fe(CO)_4(GeMe_3)(GeMe_2H)$ have been prepared, spectroscopic identification of these species is rather tenuous as these samples were found always to be contaminated with either the symmetrically substituted species $Fe(CO)_4(GeR_3)_2$ and/or products from the self-reaction.

$Mn(CO)_5(GeR_3)$ species obtained in the above syntheses react with $Co_2(CO)_8$ to yield the species $[Co_3(CO)_9][Mn(CO)_5]Ge$, $[Co_2(CO)_7][Mn(CO)_5]GeMe$ and possibly $[Co(CO)_4][Mn(CO)_5]GeMe_2$.

These species were characterised by their infrared and mass spectroscopic properties.

Abbreviations

$M_a(CO)_xM'_bR_y$ is used throughout this work as an abbreviation for group IVB derivatives of transition metal carbonyls;

M	transition metal	d	days
M'	main group IV metal	hr	hours
R	organic moiety or halide	min	minutes
X	halide (typically Cℓ, Br)	nmr	nuclear magnetic resonance
L	ligand, not necessarily of the type $M'R_y$	ms	mass spectrum
Me	methyl CH_3-	*ir*	infrared
Et	Ethyl, C_2H_5-	*R*	Raman
Pr	propyl, C_3H_7-	*R*p	Raman polarised
Bu	butyl, C_4H_9-	w	weak
Cp	Cyclopentadienyl, C_5H_4-	m	medium
Ph	phenyl, C_6H_5-	s	strong
acac	acetylacetonato, $C_5H_7O_2$-	v	very
Na/Hg	sodium amalgam	br	broad
Et_2O	diethylether,	sh	shoulder
THF	tetrahydrofuran,	P^+,	p.m.i - parent molecular ion
RT	room temperature	a_{11}	$(a_1)_1$ or a_1
octacarbonyl - structure *14*, page 4.		a_{12}	$(a_1)_2$ or a_1

spectra; typically routine scans have been included in this work as figures - more detailed spectra were usually expanded, and run more slowly.

X or C = contaminant

nmr spectra; Benzene solvent and associated spinning side bands etc, are massive peaks compared with the quantity of material used in nmr reactions. As benzene was used as a reference in this work it was recorded at much lower gain than the rest of the spectrum. A small break in the spectra separates the peaks associated with benzene from the rest of the spectrum.

CHAPTER ONE

GENERAL INTRODUCTION TO GROUP IVB TRANSITION METAL CARBONYLS

Compounds of the general formula $M_a(CO)_xM'_bR_y$ where M = transition metal amd M' = group IV metal, have been known for many years.(1) Several excellent reviews in this field have been published.(2-14) The majority of compounds known to date are simple molecules involving only one transition metal atom, (see Table 1.1, page 2). As with the group IV metals and parent transition metal carbonyls, a major feature of these compounds is the tendency to form polymetallic complexes. This area has been little explored, but promises to be a dynamic, and rewarding - though challenging - area for future study.

General features of $M_a(CO)_xM'_bR_y$ complexes that are of particular interest to this work are outlined in the following sections: structural types; preparative methods; chemical properties; physical properties and bonding aspects.

1.1 Structural types

Most of the work to date has focussed on the isolation and identification of the more abundant lower molecular weight complexes of the type shown in Figure 1.1, page 3. The range of diverse structural possibilities becomes apparent in complexes with two transition metal atoms as is illustrated in Figure 1.2, page 4. Few higher molecular weight complexes have been identified, but some examples of polymetallic complexes are given in Figure 1.3, page 5.

TABLE 1.1

Examples of $M_a(CO)_xM'_bR_y$ complexes where M=Mn, Fe, Co and R=H

	Structure	Preparation	Ref.		Structure	Preparation	Ref.
MANGANESE							
$Mn(CO)_5SiH_3$	2	a	(15)	$[Mn(CO)_5]_2SiH_2$	9	a	(16)
$Mn(CO)_5SiCl_2H_2$	2	a	(16)	$[Mn(CO)_5][Co(CO)_4]SiClH$	9	b	(16)
$Mn(CO)_5GeH_3$	2	a	(17)	$[Mn(CO)_5]_2GeH_2$	9	b	(18)
$Mn(CO)_5GeMeH_2$	2	a	(19)	$Mn(CO)_5GeMe_2H$	2	a	(20)
$Mn(CO)_5GePh_2H$	2	a	(21)	$Mn(CO)_5Ge_2H_5$	2	a	(22)
$Mn(CO)_5Ge_3H_7$	2	a	(22)	$[Mn(CO)_5(GeH_2)]_2$	14	a	(22)
$Mn(CO)_5SnPh_2H$	2	a	(21)	$[Mn(CO)_5]_2SnH_2$	9	a	(21)
$[Mn(CO)_5]_3SnH$	28	a	(21)	$[Mn(CO)_5]_4Sn_2H_2$	30	b	(161)
IRON							
$Fe(CO)_4(SiH_3)_2$	3	a	(23)	$Fe(CO)_4(SiH_3)H$	3	a	(23)
$Fe(CO)_2Cp(SiH_3)$	6	a	(24)	$Fe(CO)_2Cp(SiMe_2H)$	6	a	(25)
$[Fe(CO)_2Cp]_2SiMeH$	9	a	(159)	$[Fe_2(CO)_3Cp_2]SiMeH$	9	a	(159)
$Fe(CO)_4(GeH_3)(SiH_3)$	3	a	(33)				
$Fe(CO)_4(GeH_3)_2$	3	a	(26)	$Fe(CO)_4(GeH_3)H$	3	a	(26)
$[Fe(CO)_4(GeH_2)]_2$	14	b	(12)	$[Fe(CO)_4(GeXH)]_2$	14	b	(27)
$Fe(CO)_4(GeMeH_2)_2$	3	a	(29)	$Fe(CO)_4(GeMeH_2)H$	3	a	(29)
$Fe(CO)_4(GeMeH_2)(GeXMeH)$	3	b	(28)	$[Fe(CO)_4(GeMeH)]_2$	14	b	(29)
$Fe(CO)_4(GeMe_2H)_2$	3	a	(30)	$Fe(CO)_4(GeMe_2H)H$	3	a	(30)
$Fe(CO)_2Cp(GeH_3)$	6	a	(26)	$Fe_2(CO)_6(GePh_2)(GePhH)$	3	b	(31)
$[Fe(CO)_2Cp]_2GeH_2$	9	b	(32)	$Fe(CO)_4(Ge_2H_5)(GeH_3)$	3	a	(33)
$Fe(CO)_4(Ge_2H_5)_2$	3	a	(33)				
COBALT							
$Co(CO)_4SiH_3$	6	a	(34)	$Co(CO)_4SiMeH_2$	6	b	(35)
$Co(CO)_4SiMe_2H$	6	a	(16)	$Co(CO)_4SiPh_2H$	6	b	(36,37)
$Co(CO)_4SiCl_2H$	6	a	(16)	$[Co(CO)_4]_2SiH_2$	9	a	(16)
$Co(CO)_4Si_2Me_4H$	6	b	(54)				
$Co(CO)_4GeH_3$	6	a	(38)	$Co(CO)_4GeMeH_2$	6	a	(39)
$Co(CO)_4GeMe_2H$	6	a	(20)	$[CoCO)_4]_2GeMeH$	9	b	(39)
$Co(CO)_4Ge_2H_5$	6	a	(40)	$[Co(CO)_4]_2(Ge_2H_4)$	7	a	(22)
$[Co(CO)_3(PBu_3)]_3SnH$	28	b	(41)				

a. Salt elimination (see Section 1.2.1)

b. Neutral molecule addition and/or elimination, exchange reactions, insertion reactions, (see Section 1.2.2)

X. Cl, Br

* See compounds with similar structures in Figures 1.1, 1.2, 1.3, pages 3. to 5 .

Figure 1.1

The structure of some $M(CO)_xM'_bR_y$ complexes

1, (11)

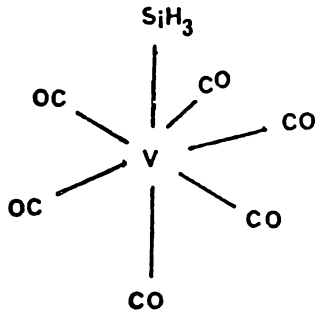

2, (17)

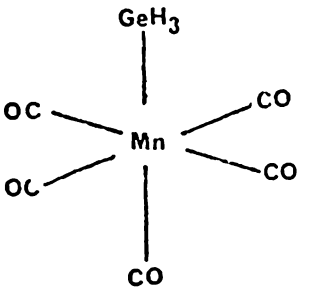

3, (26)

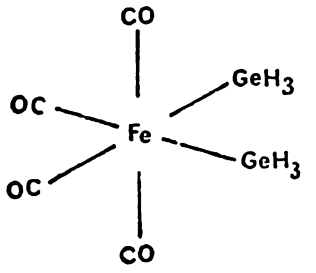

4, (160)

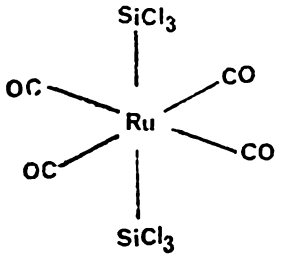

5, (82)

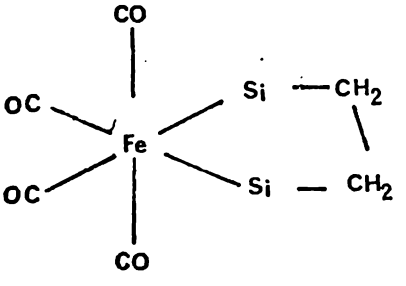

6, (38)

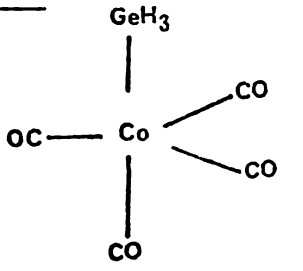

Figure 1.2

Structures with two transition metal atoms; $M_2(CO)_xM'_bR_y$

7, (54)

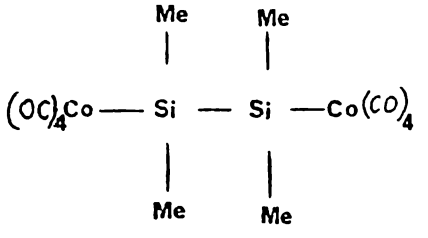

8, (95)

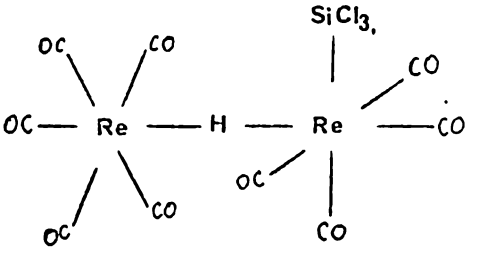

9, (96)

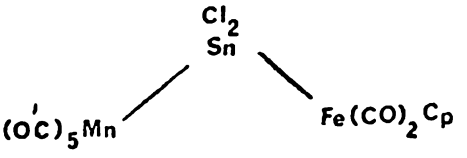

10, (164)

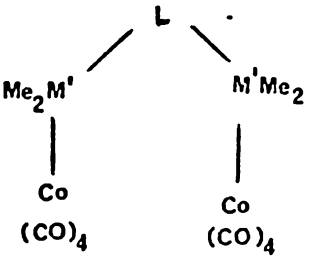

11, (97)

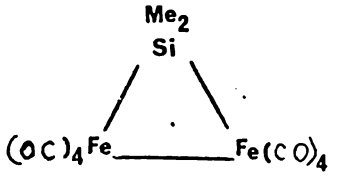

12, (135)

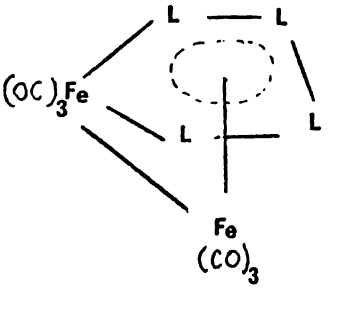

L= $COSiMe_3$

Figure 1.2 (Continued)

Structures with two transition metal atoms; $M_2(CO)_xM'_bR_y$

13, (53,94)

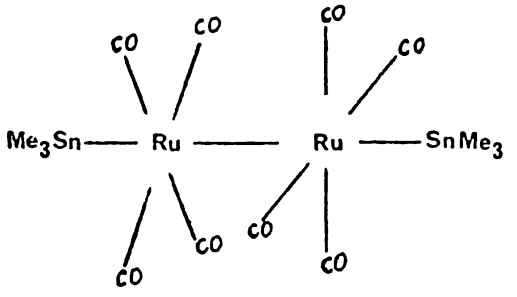

14, (99-101)

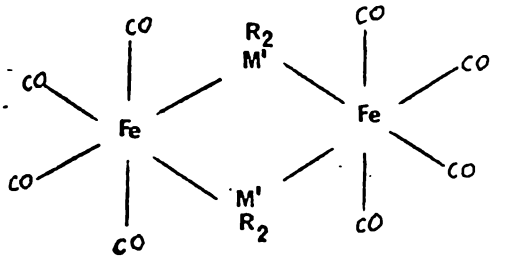

15, (12)

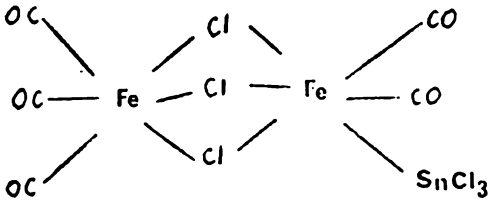

16, (103)

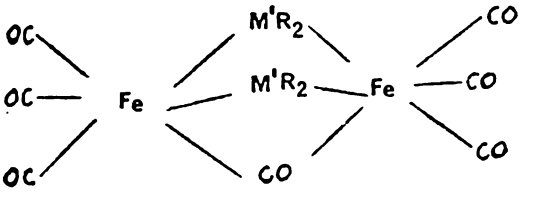

17, (104)

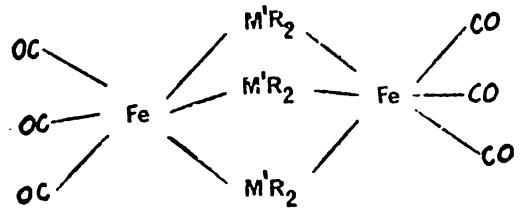

18, (102)

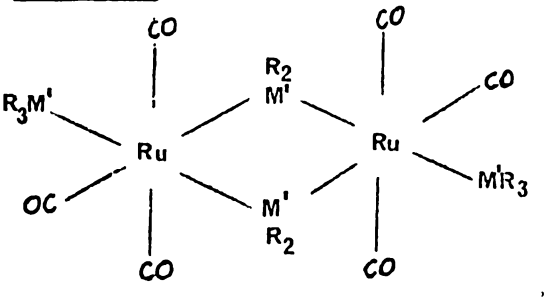

Figure 1.2 (Continued)

Structures with two transition metal atoms; $M_2(CO)_xM'_bR_y$

19, (157)

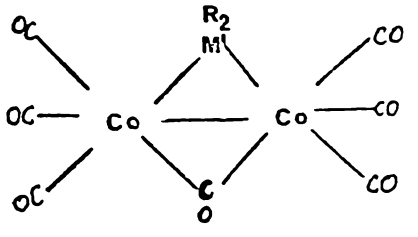

20, (106)

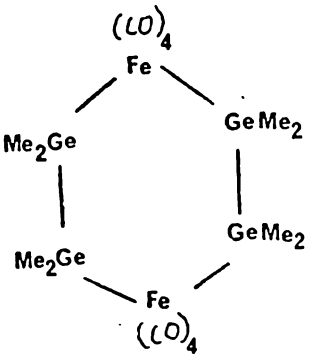

21, (105)

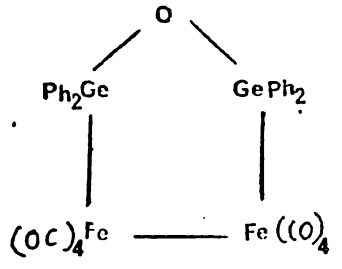

22, (106)

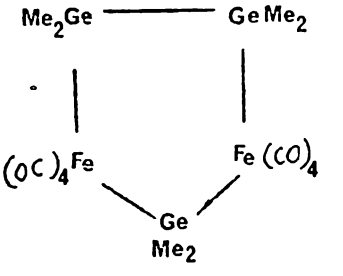

Figure 1.3

Complexes with three or more transition metal atoms; $M_a(CO)_xM'_bR_y$ ($a \geq 3$)

23, (107)

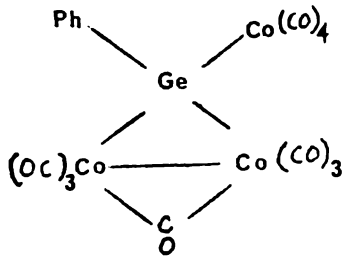

24, (108)

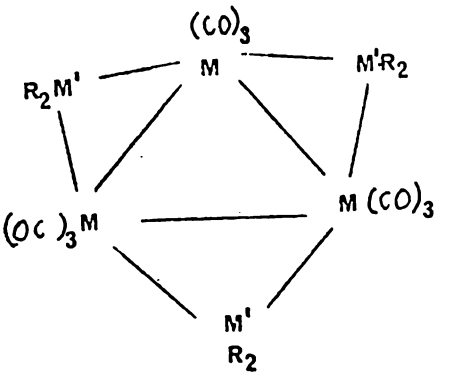

25, (14)

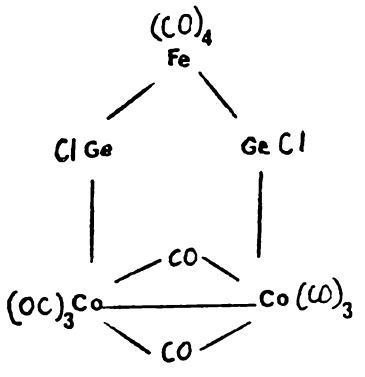

26, (21)

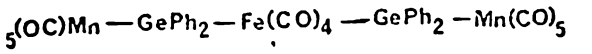

27, (179)

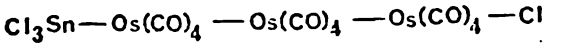

28, (21)

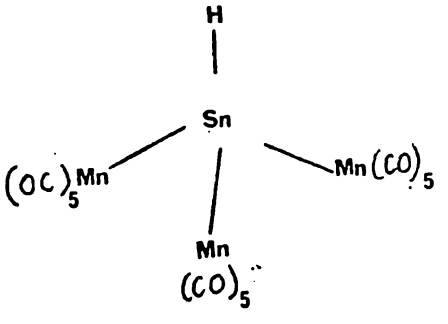

29, (154)

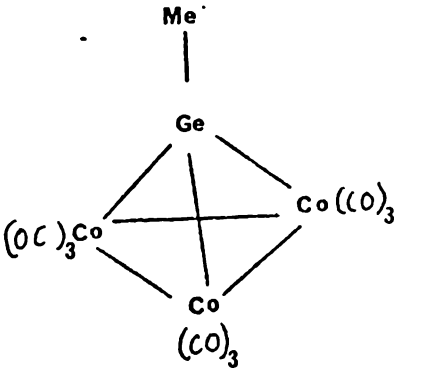

Figure 1.3 (Continued)

Complexes with four transition metals; $M_4(CO)_xM'_bR_y$

30, (161)

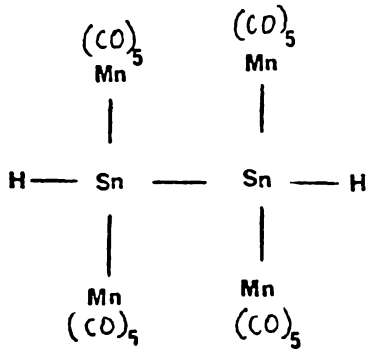

31, (112)

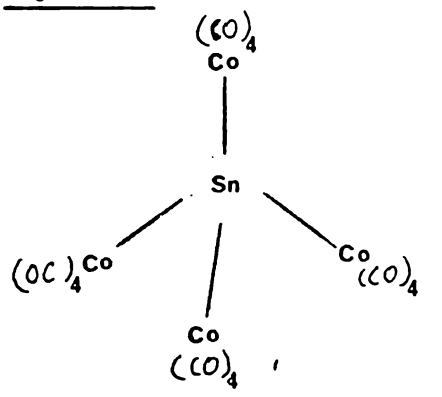

32, (110)

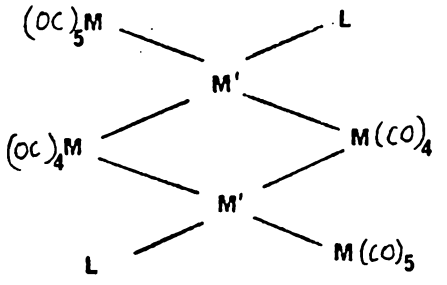

33, (109)

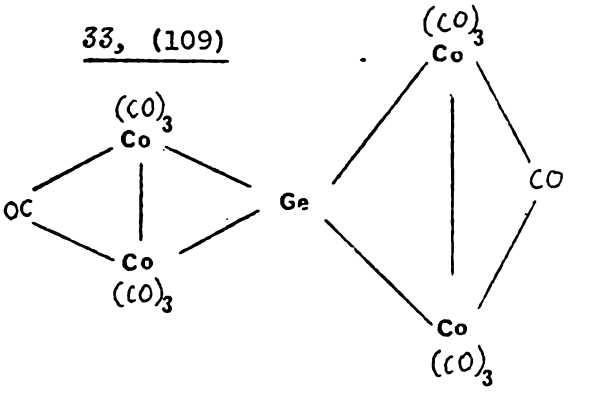

34, (111)

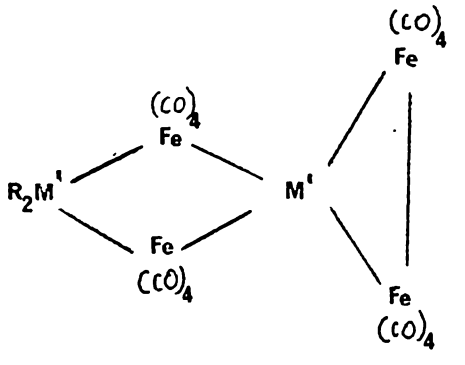

35, (101)

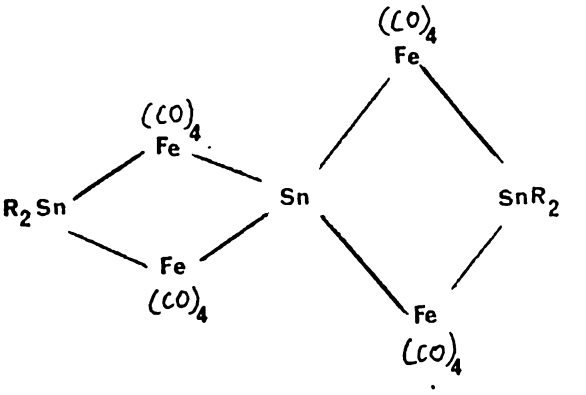

Figure 1.3 (Continued)

Complexes with five or more transition metal atoms, $M_a(CO)_xM'_bR_y$

36, (114)

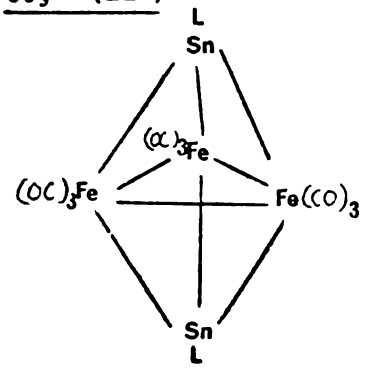

L = $Fe(CO)_2Cp$

37, (109)

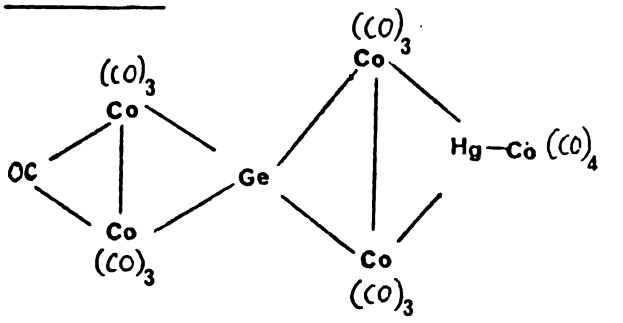

38, (115)

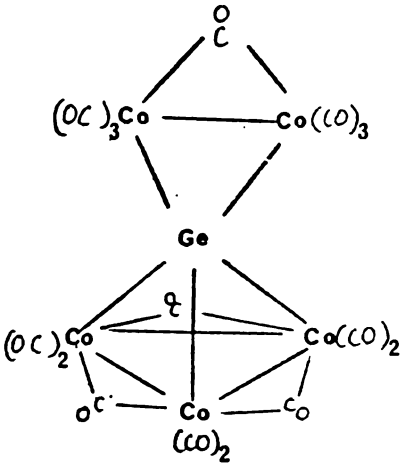

39, (16)

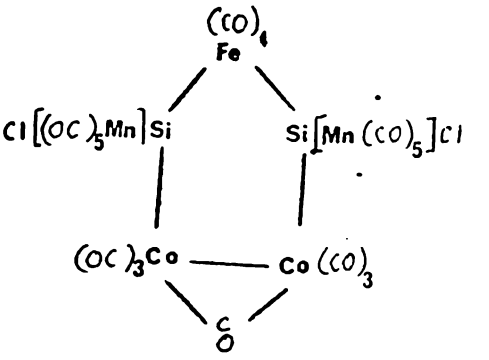

40, (115b)

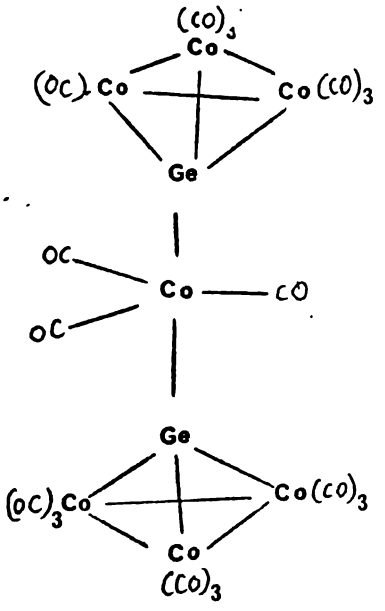

41, (115c)

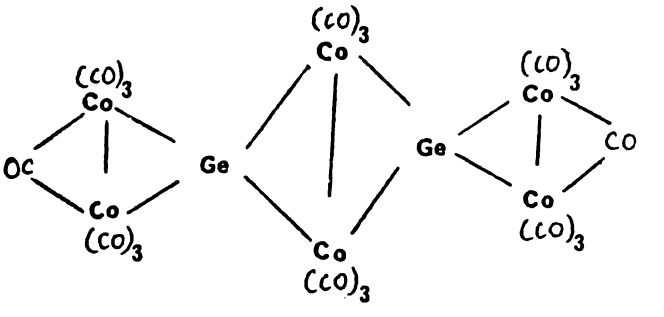

More detailed examination of structural aspects of these complexes is included in recent reviews.(12,13,14)

As attention in this work has been focussed on complexes containing iron carbonyl germanium hydrogen bonds, examples referred to in this chapter have been chosen with this bias. Table 1.1 page 2 , lists complexes of this type, together with group IV hydrogen containing derivatives of manganese and cobalt.

1.2 Preparative methods

Methods of preparation are many and varied, and have been outlined in previous reviews. (2-14) The majority of known compounds have been prepared either by the salt elimination method or by neutral molecule addition and/or elimination.

1.2.1 Salt elimination

This is the most widely used method of preparing $M(CO)_x M'_b R_y$ species.

$$GeBrH_3 + NaMn(CO)_5 \rightarrow Mn(CO)_5(GeH_3) + NaBr \quad (17,42)$$

$$GeCl_2Me_2 + Na_2Fe(CO)_4 \rightarrow [Fe(CO)_4(GeMe_2)]_2 + 2NaCl \quad (43)$$

$$Re(CO)_5Br + [Ru(CO)_4GeMe_3]^- \rightarrow [Re(CO_5][Ru(CO)_4](GeMe_3) + Br^- \quad (44)$$

1.2.2 Neutral molecule addition/neutral molecule elimination

Direct reaction between neutral molecules often occurs under mild conditions:

$$2Fe(CO)_5 + GeCl_4 \xrightarrow{RT} Fe(CO)_4(GeCl_3)_2 + FeCl_2 + 6CO \quad (45)$$

$$Co_2(CO)_8 + 2SiR_3H \xrightarrow{RT} 2Co(CO)_4(SiR_3) + H_2 \quad (46)$$

Polymetallic complexes are typically obtained under more vigorous conditions for example, by photolysis or thermal reactions of the parent carbonyls with group IV metal hydrides or halides, or by reaction of complexes which already have M-M' bond(s).

$$[Co(CO)_4]_2SnMe_2 \xrightarrow{h\nu} [Co_2(CO)_7]SnMe_2 + CO \quad (47)$$

$$Fe_3(CO)_{12} + GeMe_2H_2 \xrightarrow{65^{o}} Fe_2(CO)_6(GeMe_2)_3 + \text{other neutral species} \quad (48)$$

These reactions often yield a complex mixture of products and are sometimes called condensation reactions. Reactions between $M'X_2$ and species containing M-M or M-X bonds are often called insertion reactions.

$$[Fe(CO)_2Cp]_2 + M'X_2 \longrightarrow [Fe(CO)_2Cp]_2M'X_2 \quad (14)$$

The formation of metal-metal bonds by elimination of Hg is also known (2).

$$Fe(CO)_5 + Hg(SiMe_3)_2 \xrightarrow{h\nu} Fe(CO)_4(SiMe_3)_2 + Hg[Fe(CO)_4(SiMe_3)]_2 \quad (49)$$

A very interesting compound recently isolated by addition of $[Co(CO)_4]^-$ to $[Co_2(CO)_7]_2Ge$, is $[Et_4N]^+[\{Co_5(CO)_{16}\}Ge]^-$ (structure (38) in Figure 1.3, page 5). The $[\{Co_5(CO)_{16}\}Ge]^-$ anion is the first known penta-coordinate germanium with metal-metal bonds to five transition metals (115a). Several penta and hexa-coordinate germanium-main group compounds, *e.g.*, GeX_5^-, GeX_4L_2 (L = Base) are however, known. $[\{Co_5(CO)_{16}\}Ge]^-$ contains structural units which are related to two well-known structural types: $[Co_2(CO)_7]Ge$ and $[Co_3(CO)_9]Ge$, [structures (*19*) and (*29*) on pages 4 and 5 respectively].

In most cases, X-ray crystallographic data exist for compounds of the type illustrated in Figure 1.1, 1.2 and 1.3. In a few cases however, this type of evidence does not exist. For instance, no crystal structure is known by this author for compounds of the type illustrated by Structure *10*, (164) in Figure 1.2, which are thermolabile, and decompose slowly at -78° under nitrogen.

General structural features exhibited by $M_a(CO)_x M'_b R_y$ complexes include: (i) the M' atom is usually tetrahedrally surrounded by ligands,

(ii) coordination around M is determined by the 18 electron rule and hence, the number of ligands is pre-determined.

(iii) severe steric interactions are common,

(iv) the M-M' bond is shorter than expected.

Complexes which have M_2M' triangles also exhibit:

(i) acute MM'M angles

(ii) shorter MM' bonds than terminal MM' bonds,

(iii) M-M distances shorter than equivalent unbridged ones but longer than carbonyl bridged analogues,

(iv) unsymmetrical bridges, where significantly different M-M' bond lengths occur.

1.3 Chemical Properties

The reactions of transition metal-group IV metal compounds fall into three categories; reaction at the group IV metal, reaction at the transition metal, and reaction at the M-M' bond. These reactions were presented in a useful form by Aylett (11) and this is shown in Figure 1.4.

FIGURE 1.4

Modes of reaction of $M(CO)_nSiH_3$

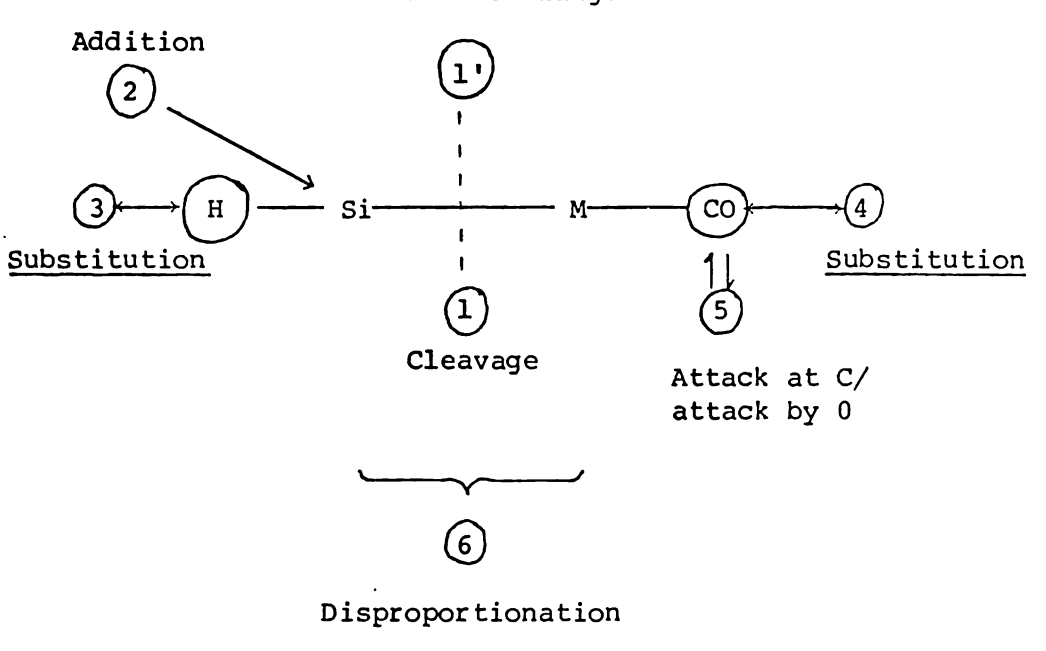

1.3.1 Reaction at the group IV metal

The common reactions at M' are illustrated by the examples which follow. See also, reactions with bases, 2.2.

(a) Substitution

$$Re(CO)_5GeH_3 + xHBr \longrightarrow Re(CO)_5GeBr_2H_{3-x} + xH_2 \qquad (50)$$

(no solvent, 20°, 48 hr.,)

(b) Redistribution

$$Mn(CO)_5GeBrPh_2 + Mn(CO)_5GeBr_3 \longrightarrow 2Mn(CO)_5GeBr_2Ph \qquad (3)$$

(c) Addition of donor

This is often followed by cleavage (11)

$$Mn(CO)_5SiH_3 + 2py \longrightarrow Mn(CO)_5(SiH_3).2py \longrightarrow [Mn(CO)_5][SiH_3.py]^+$$

(d) Insertion

$$Mn(CO)_5SnPh_3 + SO_2 \longrightarrow Mn(CO)_5Sn[O(O)SPh]_x(Ph)_{3-x} \qquad (14)$$

Reactions at the group IV metal are essentially the same as those for $M'XnR_{4-n}$ compounds, though, replacing X with $M(CO)_x$ may alter the reactivity of the compound. For example, $M_n(CO)_5Ge_2H_5$ (22), is more thermally stable than either Ge_2H_6 or $Mn(CO)_5GeH_3$.

The α-hydrogens are preferentially substituted using $SiCl_4$ or CCl_4 and the products, such as $Mn(CO)_5(GeClHGeH_3)$, are stable in very marked contrast to $GeClH_2GeH_3$.

1.3.2 Reaction at the transition metal

Here, reactions that occur in $M_a(CO)_xM'_bR_y$ are analogous to those of the parent carbonyls, $M_a(CO)_x$.

(a) ligand exchange

$$M(CO)_4(GeMe_3)_2 + 2PPh_3 \longrightarrow M(CO)_2(PPh_3)(GeMe_3)_2 + 2CO \qquad (44)$$

(M = Ru, refluxed in C_6H_{12}, 1.5 hr, 79% yield)

(M = Os, hν, in C_6H_{14}, 21 hr, 76% yield).

(b) M-M bond formation with CO elimination

$$Ph_2Ge[Co(CO)_4]_2 \xrightarrow[0.5\,hr]{h\nu} Ph_2Ge[Co_2(CO)_7] + CO \qquad (51)$$

1.3.3 Reaction at the M-M' bond

(a) Cleavage

$$Mn(CO)_5GePh_3 + Br_2 \longrightarrow Mn(CO)_5Br + GeBrPh_3 \qquad (3)$$

(1:1 hexane, benzene, 2-3 hrs, R.T.)

Some $M(CO)_xM'_bR_y$ complexes react exothermically with oxygen in the atmosphere,

$$Mn(CO)_5SiH_3 + O_2 \longrightarrow Mn_2(CO)_{10}, CO_2, SiH_4 + Si\text{-}O \text{ species?} \qquad (15a)$$

$$Co(CO)_4SiH_3 + O_2 \longrightarrow Co(CO)_4(H) + (SiH_3)_2O \qquad (34)$$

(b) Exchange of group IV moiety

$$Ru(CO)_4(GeMe_3)_2 + SnMe_3H \longrightarrow Ru(CO)_4(SnMe_3)_2 + GeMe_3H \qquad (44)$$

(C_6H_{14}, 98°, 17 hr : no reaction with $SiMe_3H$)

Here, the general tendency is for $M'R_3$ groups bonded to transition metals to be displaced in the series; $SiR_3 \rightarrow GeR_3 \rightarrow SnR_3 \leftarrow PbR_3$

(c) Exchange of $M(CO)_x$ moiety

$$M(CO)_xSiH_3 + [M''(CO)_n]^- \rightleftharpoons M''(CO)_nSiH_3 + [M(CO)_x]^- \quad (11)$$

The tendency for $[M''(CO)_n]^-$ to form a bond with the SiH_3 moiety increases in the order

$$[V(CO)_6]^- < [Co(CO_4]^{2-} < [Fe(CO)_4X]^- < [Mn(CO)_5]^- < [Re(CO)_5]^-$$

It is thought that this trend follows the relative nucleophilicities of the $[M(CO)_n]^-$ moieties (14). A similar order is found for SiR_3 and GeH_3 species (185).

(d) Insertion

$$Mn(CO)_5GeMe_3 + C_2F_4 \longrightarrow Mn(CO)_5(CF_2CF_2GeMe_3) \quad (52)$$

The classification of reactions is not rigid nor exclusive. The same reagents can participate in any of the reactions with different compounds, or even participate in two or more of the reactions simultaneously. For example, types 1.3.1 and 1.3.3.

$$Mn(CO)_5GeMeH_2 + Br_2 \longrightarrow Mn(CO)_5GeBr_xMeH_{2-x} + GeBr_xMeH_{3-x} \quad (19)$$

For example, types 1.3.1 and 1.3.2

$$Mn(CO)_5(GeMeH_2) + (n+x)PF_3 \longrightarrow Mn(CO)_{5-n}(PF_3)_nGeF_xMeH_{2-x} + nCO + xPF_2H \quad (19)$$

For example, types 1.3.1, 1.3.2 and 1.3.3

(i) together with M-M bond formation

$$Ru(CO)_4(GeMe_3)_2 \longrightarrow [Ru(CO)_3(GeMe_2)]_3 \quad (53)$$

(see structure *24*, page 5).

(ii) Without concomitant M-M bond formation.

$$Fe(CO)_4(GeMe_2H_2) \longrightarrow [Fe(CO)_4(GeMe_2)]_2 + GeMe_2H_2 \quad (30)$$

(see page 4, Structure *14*)

The same compounds under different reaction conditions may react differently.

$$Mn(CO)_5GePh_3 + Br_2 \longrightarrow Mn(CO)_5Br + GeBrPh_3 \quad (3)$$

(1:1 hexane, benzene, 2-3 hrs, RT)

$$Mn(CO)_5GePh_3 + Br_2 \longrightarrow Mn(CO)_5GeBr_3 + 3PhBr$$

(dibromoethane, 5 hrs, 20° to 130°C)

Reactions of $M_a(CO)_xM'_bR_y$ are frequently exploited as preparative routes to new transition metal group IV metal complexes. The products are generally very sensitive to, and dependent on, the reaction conditions employed.

1.4 Physical properties

Germanium hydride derivatives of the type $M(CO)_xGeR_{3-y}H_y$ are colourless (or pale in colour), slightly volatile, solids or liquids, which are air and temperature sensitive (12,29,40). The polymetallic $M_a(CO)_xM'_bR_y$ complexes tend to be less volatile and more highly coloured (12). The stability of both the lower and higher molecular weight complexes appears in part to be dependent on the availability of a self-reaction sequence. (see Section 2.3 , page 52). However, the non-isolability of some compounds may be an artefact of the work-up technique rather than reflecting the stability of the compound concerned. An

illustration of this may be seen in attempts to isolate products from reactions between $Co_2(CO)_8$ and $Si_2Me_4H_2$ (see also Section 2.4.2, page 63). Here, the inability to isolate 'higher molecular weight' complexes was attributed to the inherent instability of these complexes (54). However, although $Co_4(CO)_{12}$ (a decomposition product) was observed in only 'small' amounts in most reaction mixtures, up to 41% of $Co_4(CO)_{12}$ was obtained together with 'voluminous gas evolution' when chromatographic separation procedures were attempted (54). Nevertheless, the possibility of kinetically controlled reactions should not be overlooked. Rate of removal of some product from an equilibrium reaction could drive the reaction in the directions of, say, decomposition of higher complexes. This can be particularly significant when CO is formed and products depend on whether the system is open, closed, or evacuated. Conditions of reactions can be varied so as to control the proportions of inter-related products. (21,152).

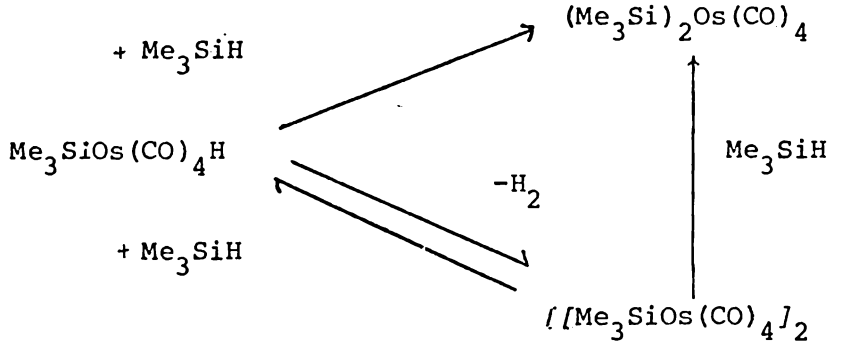

1.4.1 Spectroscopic and other physical parameters

X-ray crystallography is fundamental to the study of group IV-transition metal carbonyl complexes and will become even more vital as the number of atoms and the complexity of these compounds increases. However, the major compounds prepared in this work, the methyl germyl iron carbonyls,

$Fe(CO)_4(GeMe_xH_{3-x})_2$, are unsuitable for such study, since they are air, heat and light sensitive, low volatile liquids. In such cases, it is necessary to rely on detailed analysis of data collected from infrared, nmr and mass spectroscopy studies to identify such complexes.

Alternative techniques for obtaining physical data such as photoelectron spectroscopy, and mössbauer spectroscopy have, as yet, made little contribution to the understanding of $M_a(CO)_xM'_bR_y$ complexes (12,14).

1.4.2 Vibrational spectroscopy

(a) Infrared spectroscopy

Infrared spectroscopy is without doubt the most widely used, and hence most valuable tool in the study of $M_a(CO)_xM'_bR_y$ complexes. Not only does it serve to 'fingerprint' the complexes formed, but analysis of the position and intensity of the carbonyl stretching bands can give an insight into the symmetry of the molecule in question. (55,12). While attention has traditionally been focussed on the carbonyl region (12 - 19) the deformation modes of $M'H_x$ units also give important evidence.

(b) Raman spectroscopy

Raman spectroscopy, while complementary to infrared spectroscopy, is used less often. Relatively large amounts of sample are needed and it is still difficult to measure Raman spectra of coloured compounds. Photo-decomposition is also often a problem (182,190), particularly when the products are highly coloured as in $Co(CO)_4M'R_3$ systems. However, modern techniques allow some of these problems to be overcome (38). The inherently high Raman intensity of heavy-atom stretches is a major inducement to use the method.

1.4.2.1 Analysis of vibrational spectra

(i) Carbonyl stretching region

Factors which make the carbonyl stretching region the most diagnostic region of the infrared spectrum for these complexes include;

a) very intense absorptions from carbonyl stretches (arising from orbital following (57)),

b) little mixing of the carbonyl stretching modes with other vibrational modes (57),

c) clear division (*ca* 150 cm^{-1}) between carbonyl stretches of terminal carbonyls and bridging carbonyl ligands (12).

d) carbonyl stretches are highly sensitive to the environment (57). This makes them particularly useful for monitoring reactions (115).

e) carbon-13 bands, although weak, may aid analysis. For example, where several CO groups are involved, satellite bands are expected *ca* 35-40 cm^{-1} lower than out-of-phase modes and, a few reciprocal centimeters to the low frequency side of in-phase vibrations (12).

Factors which may lead to ambiguity include:

a) a deficit of modes (usually because of accidental superposition of fundamental modes).

b) conformational and/or stereoisomers. Even where a compound exists as only one isomer in the solid phase, two isomers may be present in solution (45,56,65,82).

c) an increase in the expected number (162) or intensity (83) of carbonyl modes may originate from distortions from ideal bond angles. For example, although *trans*-$Fe(CO)_4I_2$ is expected to have D_{4h} symmetry this compound exhibits D_{2d} symmetry.

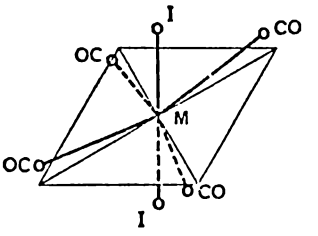

trans-$M(CO)_4I_2$ (M = Fe, Os).

(ii) M-M' stretching region

The infrared region *ca* 300 to 50 cm^{-1} where M-M' stretching frequencies occurs is rarely recorded in $M_a(CO)_xM'_bR_y$ complexes. For many compounds little information can be gleaned from absorptions in this region because, the M-M' stretches are typically weak, mixing with other modes of similar energy and like symmetry can occur (12), and bands arising from other M'R modes can be found in this region. It is perhaps worth mentioning that this region is also experimentally more difficult to observe.

In contrast to the infrared, νMM' data from Raman spectra may be readily obtained (58). The νMM' bands are usually relatively strong, and the symmetric modes are easily distinguished.

(iii) Other regions

Again, these regions are rarely reported. The region 1000 to 300 cm^{-1} often contains numerous weak to medium intensity absorptions due to δMCO, νMC and other modes associated with M'R ligands. Hence assignments may not be unambiguous. Mixing with other fundamentals of like symmetry and similar energy is highly probably. For these reasons, this region is unsuitable as a diagnostic region. (*cf.* the same number of modes are predicted for νMC as for νCO). Typically, medium to strong

Ge-H and Si-H deformations in the region *ca* 900-700 cm^{-1} and *ca* 1000-800 cm^{-1} respectively (12,23,184) are characteristic of $GeR_{3-x}H_x$ and $SiR_{3-x}H_x$ ligands. These bands may show vibrational fine structure in the gas phase spectra of lower molecular weight complexes (26).

(iv) A special case, the νGeH region

GeH stretching modes are found in the region *ca*2150-2000 cm^{-1}. Although similar frequency and like symmetry of νGeH and νCO modes, *e.g.* in $Co(CO)_4(GeH_3)$, C_{3v}, would appear to be ideal conditions for νGeH and νCO mixing, there is little evidence for this. For instance, deuteration of $Mn(CO)_5(GeH_3)$ and $Co(CO)_4(GeH_3)$ (17,38) show very little change in the *ca* 2120-1950 cm^{-1} region on substitution of GeD_3 (νGeD occurs in the region *ca*1500-1450 cm^{-1} in these complexes). Indeed the marked difference in force constants, K_{CO} *ca* 1700 Nm, K_{GeH} *ca*300Nm, precludes coupling of these vibrations. νGeH modes have been assigned to very strong absorptions occurring at *ca*2072-2055 cm^{-1} in $Co(CO)_4(GeH_3)$ and to the medium broad absorptions at *ca* 2065-2040 cm^{-1} in $Mn(CO)_5(GeH_3)$.

1.4.2.2 The vibrational spectra of $M(CO)_4(M'R_3)_2$

As infrared identification of $Fe(CO)_4(GeR_3)_2$ R = H, Me complexes is a vital component of this work, the vibrational data for analogous complexes will now be discussed in detail. $M(CO)_4(M'R_3)_2$ can be pure *cis*, pure *trans*, or a mixture of observable amounts of *cis* and *trans* isomers (which may or may not be in rapid equilibrium). Figure 1.5, page 19, illustrates predicted modes of vibration for both *cis* and *trans* $M(CO)_4(M'R_3)_2$ (62,66,67,74)

Figure 1.5

Predicted modes of vibration in $M(CO)_4(M'R_3)_2$

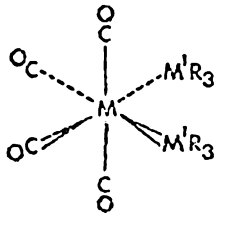

Cis, C_{2v}

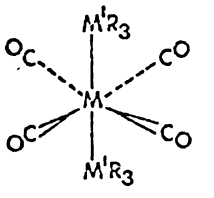

trans, D_{4h} *

* slight distortion to give D_{2d} symmetry gives similar predictions as those for D_{4h}

CO and MC Stretches

$2a_1 + b_1 + b_2$
(ir,Rp) (ir,R) (ir,R)

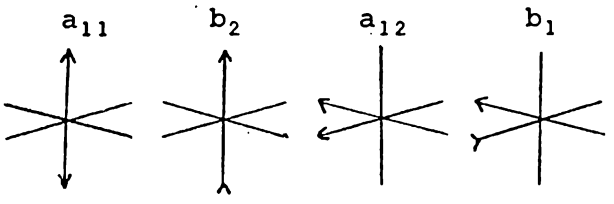

$a_{1g} + b_{1g} + e_u$
(Rp) (R) (ir)

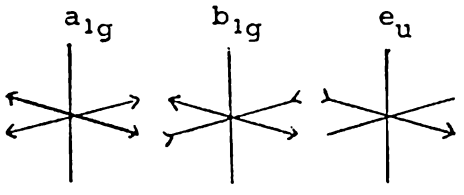

M-M' Stretches

$a_1 + b_1$
(ir,Rp) (R)

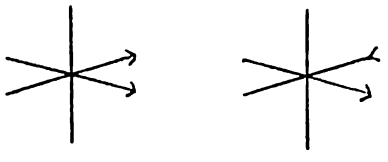

$a_{1g} + a_{2u}$
(Rp) (ir)

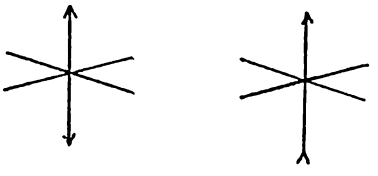

MCO deformations

$2a_1 + 2a_2 + 2b_1 + 2b_2$
(ir,Rp) (R) (ir,R) (ir,R)

$b_{2g} + e_u + a_{2u} + b_{2u}$
(R) (ir) (ir)

νCO region

For the *cis* isomers, the highest absorption is assigned to the νCO (axial, a_{11}) mode (61,62), while the band at lowest frequency is assigned as νCO (equatorial, b_1). However, the order of the a_{12} and b_2 bands is sensitive to the nature of M and $M'R_3$ (57), and may also be sensitive to the solvent (63). These effects not only cause changes in frequency but may also influence intensity and band width (65). In theory (57), the infrared intensities are predicted to be: a_{11}, - weak, a_{12} and b_1 - medium, b_2 - strong. In Raman spectra, b_2 is predicted to be weak (57). Figure 1.6, page 21, shows the νCO region in the infrared spectra of some typical *cis*-$M(CO)_4(M'R_3)_2$ species. As can be seen from Figure 1.6, page 21, many *cis* isomers show only three bands, as a_{12} and b_2 coincide. Figures 1.7, page 22, for $Fe(CO)_4(GeH_3)_2$ (27), and 1.8, page 22, for $Fe(CO)_4(GeMeH_2)_2$ (60), illustrate this (see Section 3.4 , page 96, and Section 3.5.2, page 102, for further discussion). Comparison of the gas and solution spectra of $Fe(CO)_4(GeMeH_2)_2$ clearly demonstrates the importance of the 'solvent shift' effect.

Trans-$M(CO)_4(M'R_3)_2$ complexes usually give one strong infrared band e_u. Weak bands at higher frequency, the a_{1g} and b_{1g} fundamentals gain intensity in the infrared in molecules where the symmetry of the molecule is actually slightly less (*e.g.*, D_{2d}) than the highest possible symmetry D_{4h} (66,162). An example is shown in Figure 1.9e, page 23 .

In many cases, the *cis* and *trans* isomers are present in equilibrium, and the carbonyl region shows a superposition of both spectra. Figure 1.9, page 23, shows the carbonyl stretching region of the infrared spectrum of some *cis* and *trans* mixtures of $M(CO)_4(M'R_3)_2$ complexes, $Ru(CO)_4(SnR_3)_2$ where R changes from Me through Et and Pr and Bu, cyclohexane (145). Here, the proportion of *trans* isomer increases from R=Me

Figure 1.6

Carbonyl stretching region of the infrared spectrum of some *cis*-$M(CO)_4(M'R_3)_2$ complexes, cm^{-1}

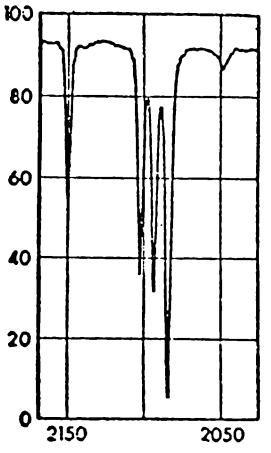

$Ru(CO)_4(SiCl_3)_2$ (59)

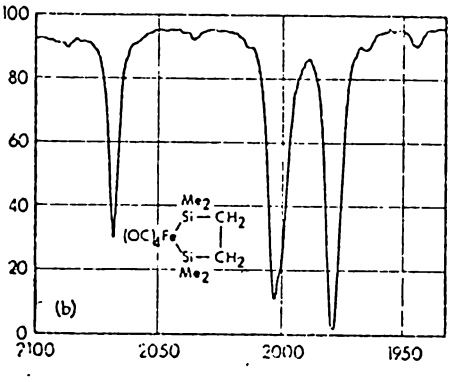

$Fe(CO)_4SiMeCH_2CH_2SiMe_2$ (82)

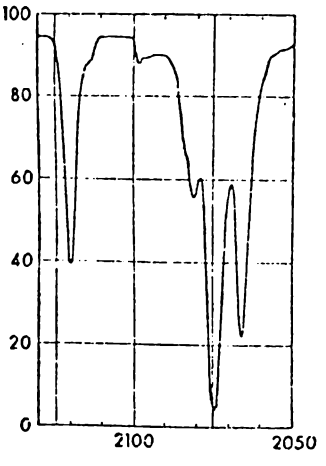

$Fe(CO)_4(SnBr_3)_2$ (45)

$Fe(CO)_4(Bu_2SnCl)_2$ (146)

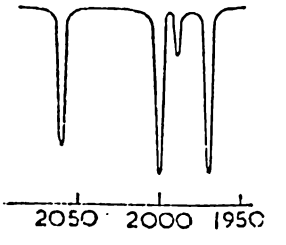

$Fe(CO)_4(SiMe_3)_2$ (146)

Figure 1.7

The carbonyl infrared region of $Fe(CO)_4(GeH_3)_2$, (27) : cm^{-1}

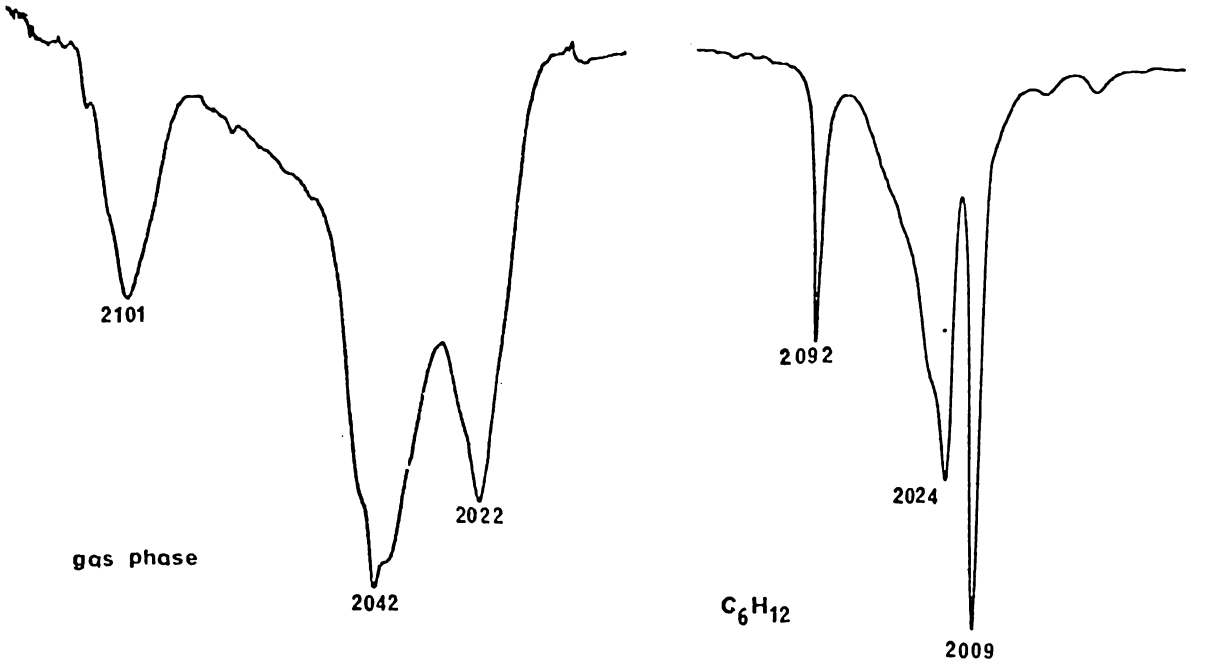

Figure 1.8

The carbonyl infrared region of $Fe(CO)_4(GeMeH_2)_2$, (178) : cm^{-1}

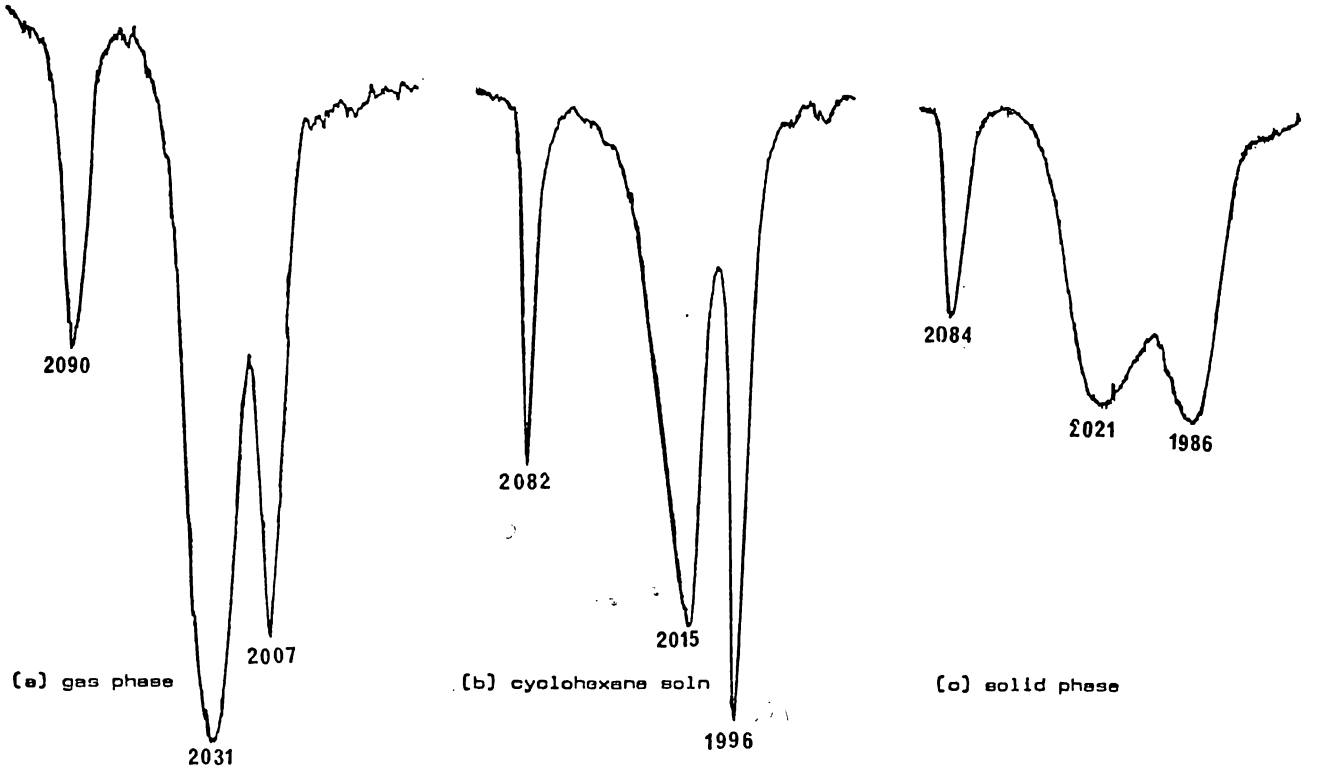

Figure 1.9

Carbonyl stretching region of the infrared spectrum of some *cis* and *trans*-$M(CO)_4(M'R_3)_2$ complexes

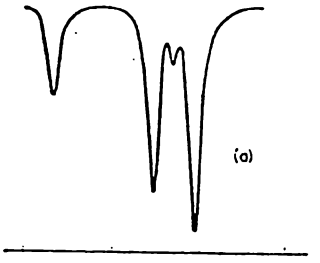

$Ru(CO)_4(SnMe_3)_2$ (145)

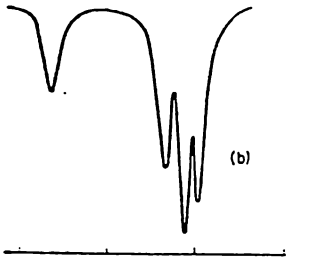

$Ru(CO)_4(SnEt_3)_2$ (145)

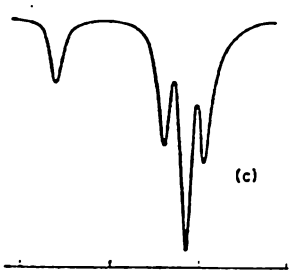

$Ru(CO)_4(SnPr_3)_2$ (145)

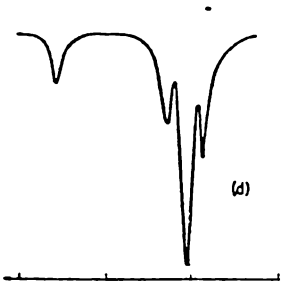

$Ru(CO)_4(SnBu_3)_2$ (145)

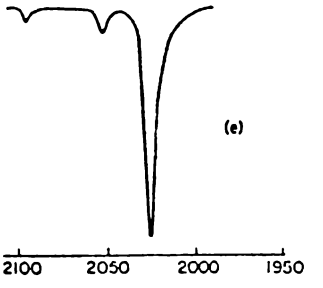

$Ru(CO)_4(SnPh_3)_2$ (145)

where only a small amount of *trans* is detectable to 100% *trans* when R=Ph.

Approximate carbonyl force constant analyses using Cotton-Kraihanzel field or modifications have been performed on several complexes (12): this is helpful for assigning the νCO modes.

νM-M' region

The $a_1 + b_1$ M-L stretching modes for *cis*-$M(CO)_4L_2$ complexes are allowed in the infrared and in the Raman. $Fe(CO)_4(GeRH_2)_2$ R=H or Me both exhibit two strong Raman bands (230-200 cm^{-1}). The higher frequency mode is polarised and coincident with a weak infrared mode. This has been assigned a_1 (26). In other complexes, for example $Mn(CO)_5(GeH_2GeH_3)$ and $[Mn(CO)_5]_2GeH_2$ the order of the symmetric and asymmetric MM stretches may be reversed, *i.e.*, the lower frequency band being the symmetric stretch.(26)

For a *trans*-$M(CO)_4L_2$ complex the expected νML modes are $a_{1g}(R_p)$, and a_{2u} (*ir*). A very weak absorption at 248 cm^{-1} (*ir*) and a strong one at 220 cm^{-1} (R_p) were assigned as νRuGe a_{2u} and a_{1g} respectively in *trans*-$Ru(CO)_4(GeCl_3)_2$ (12). Raman spectra of *trans*-$Os(CO)_4(SnPh_3)_2$, *trans*-$Os(CO)_4(SnBu_3)_2$, *trans*-$Os(CO)_4(SnCl_2Ph)_2$ and *trans*-$Os(CO)_4(SnBr_3)_2$ are reported to exhibit νOsSn a_{1g} modes at 112 cm^{-1}, 105 cm^{-1}, 113 cm^{-1}, and 138 cm^{-1} respectively. (68)

δMCO, νMC and δM'R regions

In *cis*-$Fe(CO)_4(GeR_3)_2$ R=H, Me the δMCO, νMC and $\delta M'R_x$ fundamentals occur in different regions in the infrared (20,27).

δGeH_3	900 - 800 cm^{-1}
δFeCO	630 - 600 cm^{-1}
νFeC	450 - 430 cm^{-1}

1.4.2.3 Vibrational spectra of polymetallic complexes

The carbonyl infrared region for selected polymetallic systems are discussed briefly.

(a) $[Co(CO)_4]_2GeR_2$

In the case where both R groups are the same, this complex (see Structure 9, page 4), exhibits C_{2v} symmetry, and seven infrared active carbonyl strretching modes; $3a_1$, $3b_1$, b_2 are predicted. In practice six or seven of these bands are observed (see Figure 1.10, page 26) (206,73).

In the case where one of the R groups is replaced by a different substituent, the symmetry drops to C_s and eight infrared active stretching frequencies are expected, $4a'$, $4a''$. That is, double the number of vibrations expected for $Co(CO)_4GeR_3$. Figure 1.10, page 26, illustrates 'doubling' of the number of modes in the νCO region on comparing the four bands of $Co(CO)_4GeCl_2Me$ with those of $[Co(CO)_4]_2GeClMe$ (20b). The bands in $[Co(CO)_4]_2GeClMe$ were not assigned. Although, intuitively, it would appear that the eight modes in $[Co(CO)_4]_2GeClMe$ arise from symmetric and asymmetric combinations of the modes in $Co(CO)_4GeCl_2Me$, it must be emphasised that mixing almost certainly occurs (*e.g.*, among the $4a'$ modes) so that simple descriptions are not fully valid.

(b) $[M(CO)_4(M'R_2)]_2$

Figure 1.11 describes the symmetry-allowed vibrations for a $[M(CO)_4(M'R_2)]_2$ complex. Examples of the carbonyl stretching region of the infrared spectrum of $[Fe(CO)_4(SnEt_2)]_2$ in n-hexadecane (72), $[Fe(CO)_4(GeI_2)]_2$ in cyclohexane (45), and $[Fe(CO)_4(SnBu_2)]_2$ in cyclohexane (146) are illustrated. The similarity in appearance of $M(CO)_4L_2$ spectra and spectra of $[M(CO)_4M'R_2]_2$ species led earlier workers (11,70) to assume there was no coupling between the $M(CO)_4$ units.

Figure 1.10

Comparison of the carbonyl infrared spectra of $Co(CO)_4GeCl_2Me$, $[Co(CO)_4]_2GeMe_2$, $[Co(CO)_4]_2GeClMe$

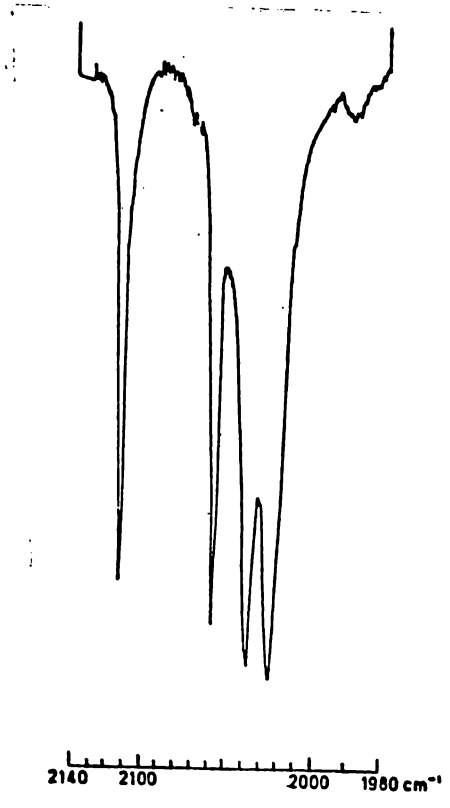

$MeGeCl_2Co(CO)_4$ (20)

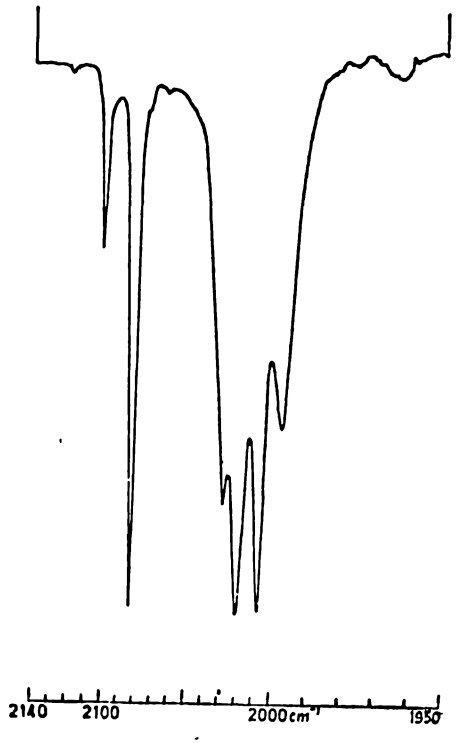

$Me_2Ge[Co(CO)_4]_2$ (20)

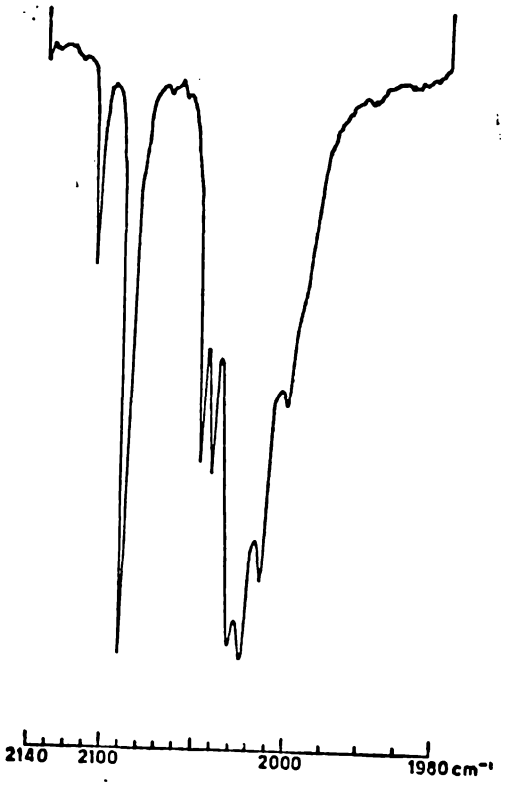

$MeGeCl[Co(CO)_4]_2$ (20)

Figure 1.11

Symmetry and spectra of $[M(CO)_4(M'R_2)]_2$ complexes

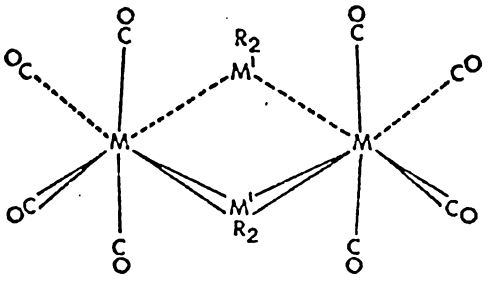

where M' is tetrahedrally surrounded by R groups and M atoms.

D_{2h}; Carbonyl stretching modes.

$$2a_g + b_{2g} + b_{3g} + 2b_{1u} + b_{2u} + b_{3u}$$

four infrared active (g) modes, four Raman active (u) modes, no coincidences.

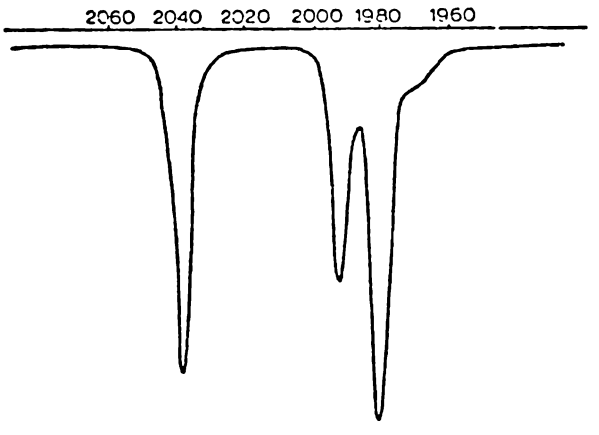

$[Fe(CO)_4SnEt_2]_2$ (59)

$[Fe(CO)_4(SnBu_2)]_2$ (146)

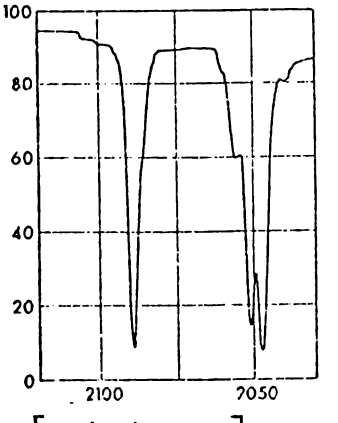

$[Fe(CO)_4GeI_2]_2$ (45)

However, this assumption is incorrect and unnecessary, as only four infrared bands or four (non-coinciding) Raman bands are expected for these D_{2h} molecules. In-phase and out-of-phase combinations of the vibrations of the individual $M(CO)_4$ units occur respectively in the Raman and in the infrared. For example, the infrared active b_1 mode in $M(CO)_4L_2$ combines in $[M(CO)_4L_2]_2$ to give the in-phase b_{3g} (Raman active only) and out-of-phase b_{2u} (infrared active only) modes (64,69,74).

(c) $M_2(CO)_6(\mu\text{-}L)_2$

Figure 1.12, page 29, illustrates the carbonyl infrared spectra of $Co_2(CO)_6(GeMe_2)_2$, $Co_2(CO)_7(GeMe_2)$ and $Fe_2(CO)_7(GeMe_2)_2$ which has $[Fe(CO)_4(GeMe_2)]_2$ impurity (20b,27). Five infrared active modes, $2a_1 + 2b_1 + b_2$ are predicted for a $Co_2(CO)_6(GeMe_2)_2$ and for terminal modes of $Fe_2(CO)_7(GeMe_2)_2$ six infrared allowed bands, $3a' + 3a''$ are predicted for terminal CO vibrations in $Co_2(CO)_7(GeMe_2)$. The similarity of all three spectra can be seen from Figure 1.12. The $M_2(CO)_7$ species have, in addition to $M_2(CO)_6$ modes, a bridging CO mode at lower frequency.

The 'theoretical' spectrum for $M_2(CO)_6(\mu\text{-}X)_2$ species is derived from ten years work over which numerous $Fe_2(CO)_6(\mu\text{-}X)_2$ and $Co_2(CO)_6(\mu\text{-}Y)_2$ complexes have been prepared, force constant calculations and ^{13}CO enrichment studies performed (69). The only ambiguity in $M_2(CO)_6(\mu\text{-}X)_2$ spectra which can't be solved *a priori*, is the order of the a_1 and b_2 modes. These assignments must be determined separately for each case studied.

1.4.3 Mass spectroscopy

The main features of $M_a(CO)_xM'_bR_y$ spectra are:

(i) parent molecular ions are typically weak (16)

(ii) a high proportion of the ion current is usually carried by fragments retaining the $M_aM'_b$ skeleton (79)

Figure 1.12

Carbonyl infrared spectra of some $M_2(CO)_6(M'R_2)_2$ species : cm^{-1}

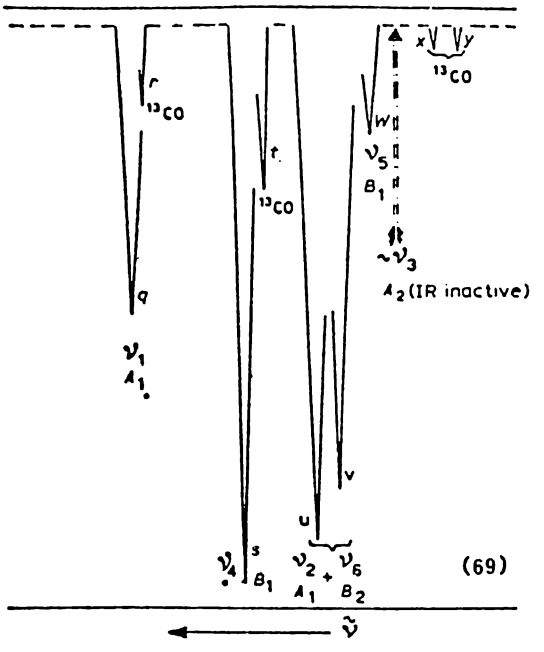

'theoretical' spectrum for $M_2(CO)_6(\mu\text{-}X_2)$ complexes in the carbonyl stretching region

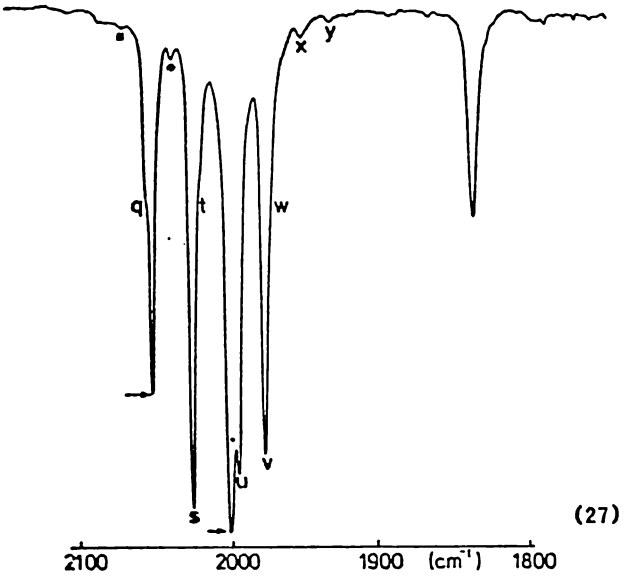

$(Me_2GeFe)_2(CO)_n$ n=7,8

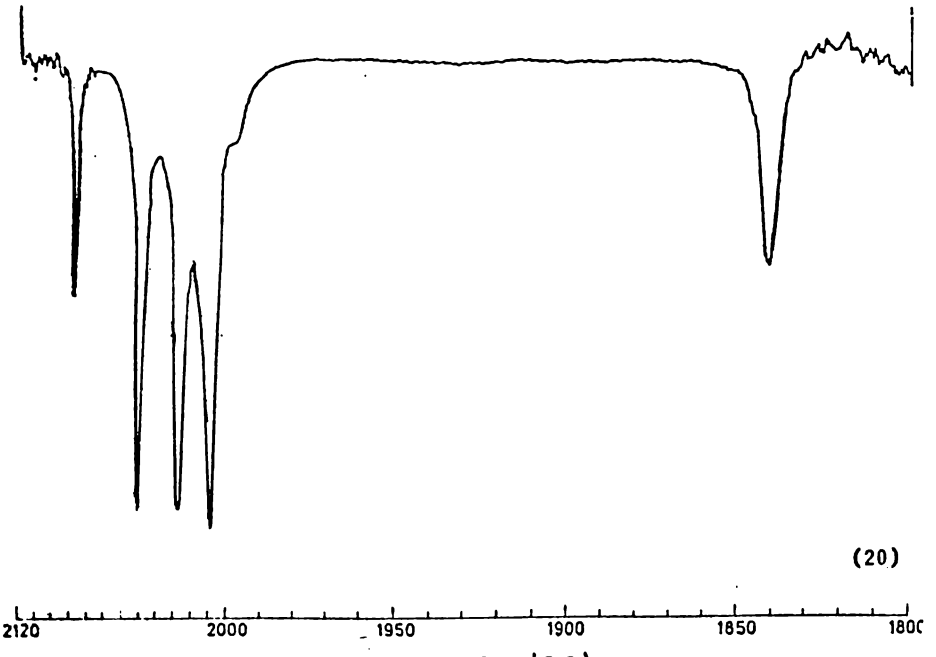

$Me_2GeCo_2(CO)_7$

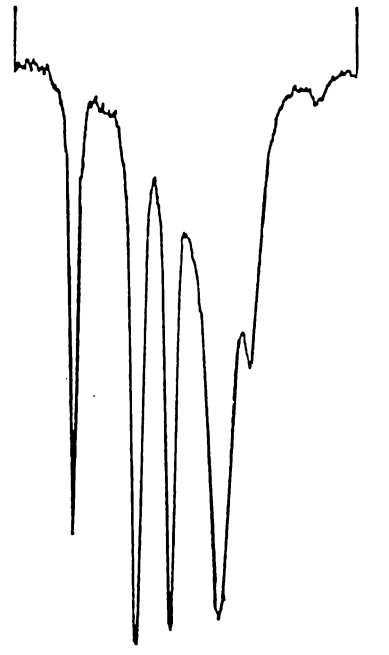

$(Me_2Ge)_2Co_2(CO)_6$

(iii) stepwise loss of CO gives a series of fragments separated by 28 *m/e* units. Similar effects are often seen from stepwise loss of R_1 or a related fragment (78).

While mass spectroscopy has been widely used to determine the molecular weight of $M_a(CO)_xM'_bM_y$ complexes (76), rarely have the series of lower molecular weight fragment ions been reported (77). The significant, although very low, vapour pressure of the $M_a(CO)_xM'_bR_y$ complexes generally enables good spectra to be recorded without heating these species. However, rearrangements of compounds may occur even under very mild conditions (31,157). For example, the highest molecular ion exhibited by $[Co(CO)_4]_2GePh_2$ is $Co_2(CO)_7GePh_2^+$ (157). It was suggested that, as for the Sn analogues, the stability of the '$Co_2(CO)_7$' containing fragment is due to the presence of a bridging carbonyl group. (*i.e.*, $[Co(CO)_4]_2M'R_2$ rearranged to give $[Co_2(CO)_7]M'R_2$ + CO in the mass spectrometer). Observation of parent ion 'plus' additional carbon monoxide has been reported. For example, $[Fe(CO)_2Cp]SnCl_2Ph$ was suggested to have a (p.m.i., + 2 CO) peak (186). In later work however, (135), such ions have been attributed to impurities or to thermal decomposition during measurement. It is not uncommon for rearrangement to occur in lower fragments. For example, hydridomanganese rearrangement ions, $Mn(CO)_5H^+$, $Mn(CO)_4H^+$, $Mn(CO)_2H^+$, $Mn(CO)H^+$, and MnH^+ are observed in the mass spectrum of $Mn(CO)_5GeH_3$. For instance, stepwise loss of CO and loss of GeH_x from $Mn(CO)_y(GeH_x)$ are metastable-supported processes (17). Doubly charged ions are occasionally observed; these are usually weak. Germanium-containing fragements have a characteristic pattern, see Figure 1.13, page 31, arising from the five

Figure 1.13

Calculated mass envelopes of some germanium containing ions

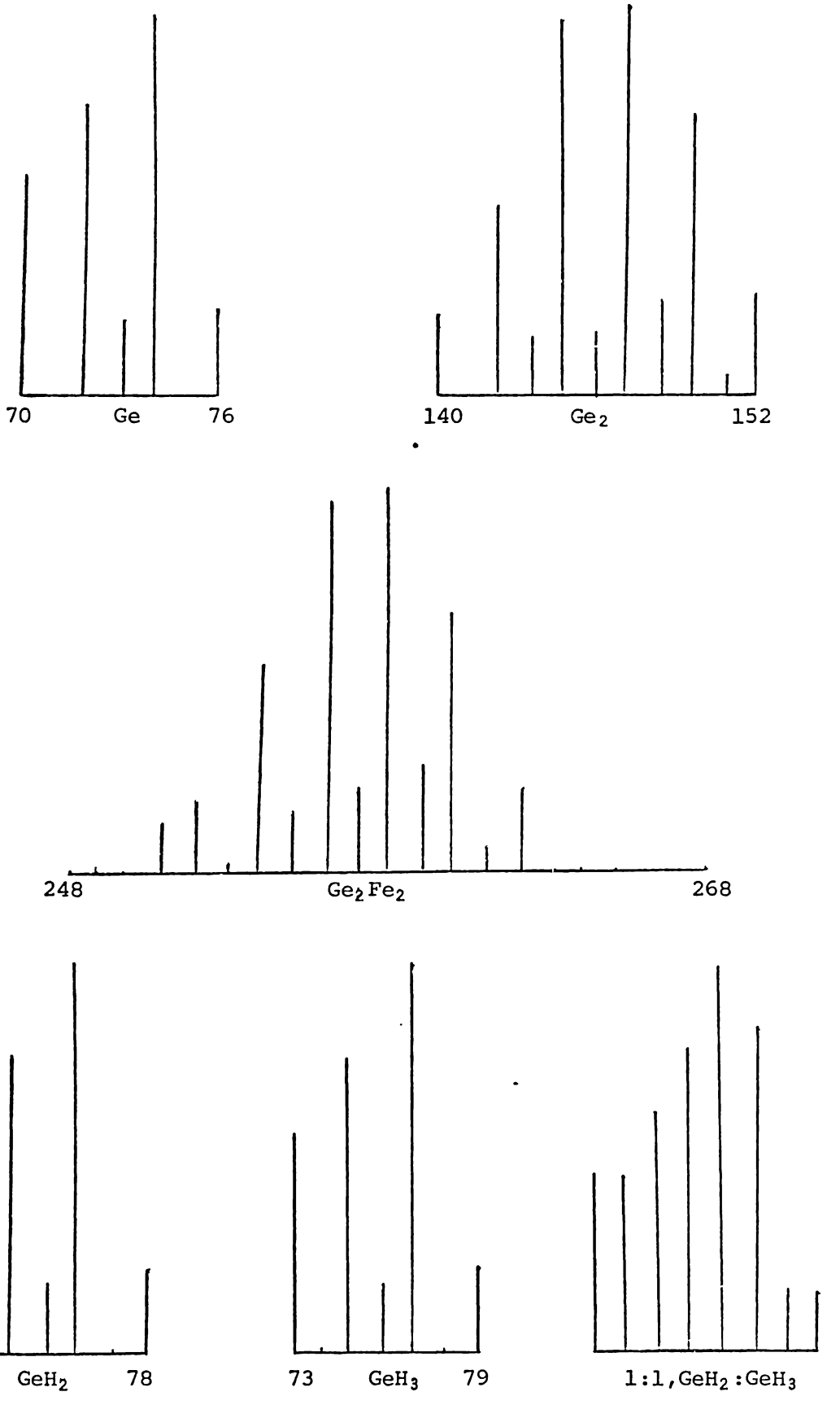

naturally occurring isotopes ^{76}Ge 7.8%, ^{74}Ge 35.6%, ^{73}Ge 7.8%, ^{72}Ge 27.4%, ^{70}Ge 20.5% . This enables fragments containing one, two or three germanium atoms to be distinguished by sight in simple complexes where fragments from R group loss and CO loss do not overlap. Sn and Ru also exhibit characteristic envelopes: (^{116}Sn 14.3% ^{117}Sn 7.6% ^{118}Sn 24%, ^{119}Sn 8.6%, ^{120}Sn 32.9%, ^{122}Sn 4.7%, ^{124}Sn 5.9%) and (^{96}Ru 5.5%, ^{98}Ru 1.9%, ^{99}Ru 12.7%, ^{100}Ru 12.6%, ^{101}Ru 17.1%, ^{102}Ru 31.6%, ^{104}Ru 18.6%) respectively. Attempts to relate fragmentation pattern to M-M' bond strength (191) are to be viewed with extreme caution since these patterns undoubtedly reflect both the different electronic and structural arrangements in these complexes.

1.4.4. Nuclear magnetic resonance spectroscopy

As proton nmr requires relatively small amounts of material (*ca* 0.01 mmol) yet, has a high degree of sensitivity towards changes in molecular composition, it is helpful for identifying compounds (30) for studying reaction rates and intermediates (75,77) and for distinguishing isomers (80,81). For example, the stereochemically-non-rigid $[Fe_2(CO)_7](SnPhMe)_2$, was found by proton nmr to undergo both bridge deformation ($\Delta G^{\ddagger} \simeq 50$ kJmol^{-1}) and iron-tin bond cleavage ($\Delta G^{\ddagger} \simeq 81$ kJmol^{-1}) in R group interchange processes (75). Overcoming the difficulties of the low natural abundance of ^{13}C and of the slow relaxation rate of ^{13}C carbonyl ligands with new techniques, has made carbon-13 nmr a very powerful analytical tool.

Fluxional processes in polymetallic complexes are ideal candidates for ^{13}C nmr studies (75,81,85 to 90). For example, non-rigid $Fe_2(CO)_7(SnBu_2)_2$ was found by carbon-13 nmr to undergo bridge deformation with simultaneous, stereospecific interchange of bridge and terminal carbonyl ligands (75).

1.4.4.1 Carbonyl carbon-13 nmr studies of $M(CO)_4(M'R_3)_2$ complexes

$M(CO)_4(M'R_3)_2$ complexes have been found by ^{13}C nmr studies to be non-rigid (56,82,83). As mentioned previously, these compounds may exist in solution as pure *cis*, pure *trans*, or as a mixture of observable amounts of *cis* and *trans* isomers, which may or may not be in rapid equilibrium at a given temperature. ^{13}C nmr studies can identify *cis* or *trans* isomers. General trends in ^{13}C nmr data of $M(CO)_4(M'R_3)_2$ complexes are as follows, (56,83):

(i) there is an upfield shift on descending the triad. The ^{13}C chemical shift for iron is in the range δ = 209-197 ppm, for ruthenium δ = 199-183 ppm and δ = 181-167 ppm for osmium.

(ii) the *trans* isomer is usually at lower field than the axial CO chemical shift of the *cis* isomer.

In *cis* isomers:

(i) the chemical shift of the carbonyls *trans* to the group IV ligand occurs at higher field than the *cis* CO's (with the exception of $Fe(CO)_4(SnMe_3)_2$)

(ii) the difference between axial and equatorial ^{13}CO shifts increases as the central atom changes from Fe to Ru to Os where $M'R_3$ is kept constant.

(iii) keeping M constant, the axial equatorial separation decreases as M' varies from Si to Ge to Sn to Pb.

(iv) in the series *cis*- $M(CO)_4(SiCl_{3-y}Me_y)_2$ for a given M, axial-equatorial separation decreases with a decrease in y.

(v) change in the $M'R_3$ ligand often causes a greater change of the axial carbonyl than in that of the equatorial carbonyl.

Thus far, it has been mentioned that $M(CO)_4(M'R_3)_2$ complexes may be 100% *cis*, *e.g.*, $Fe(CO)_4(GeMe_3)_2$, 100% *trans*, *e.g.*, $Ru(CO)_4(SnPh_3)_2$; or a mixture of the two which,

(a) are in equilibrium at room temperature,

e.g., $Fe(CO)_4(SiCl_3)_2$ 80% *cis* : 20% *trans*

(b) are not in equilibrium at room temperature,

e.g., $Ru(CO)_4(GeCl_3)_2$

1.4.4.2 Stereochemical non-rigidity in *cis*-$Fe(CO)_4(M'R_3)_2$

In *cis*-$Fe(CO)_4(M'R_3)_2$ complexes the axial and equatorial CO ligands rapidly interconvert on the nmr time scale to give one, average, signal at ambient temperatures. This process is intramolecular and proceeds *via* rapid *cis*-to-*trans*-to-*cis* isomerization which does not require an observable amount of the *trans* intermediate to be present. The activation energy for this axial-equatorial averaging process is lowest in iron compounds (ΔE = 40-50 $kJmol^{-1}$). It increases with halogen substitution, and is greater for corresponding compounds of ruthenium and osmium (ΔE = 70-80 $kJmol^{-1}$) (56).

This stereochemical non-rigidity has been linked with distortions from 90° angles at M. For example, in $Fe(CO)_4(SiMe_3)_2$ the angle between axial CO's is 141° instead of the expected 180°, and the angles between axial and equatorial CO's are *ca* 104°, 103°, 90° (82). This compound is stereochemically non-rigid. Further data are required to explore the extent of the relationship between non-rigidity and distortions from octahedral geometry about M. But, it has to be recognised that solid state and solution geometries may differ.

1.4.5 Stereochemistry of $M(CO)_4(M'R_3)_2$ complexes

As can be seen from Bonny's review (12), the $Fe(CO)_4(M'R_3)_2$ species are predominantly *cis*, the osmium analogues are predominantly *trans*, while the ruthenium complexes are somewhere in between. The abundance of each isomer usually has been evaluated from analyses of the intensities of infrared bands (see Section 1.4.2.2, page 18). However, infrared spectroscopy can not reliably detect a small percentage of *trans* isomer as, the e_u mode of the *trans* isomer is often coincident with one of the modes of the *cis* isomer. One case which illustrates this point is that of $Fe(CO)_4(SiCl_3)_2$. Infrared evidence initially led to the assignment of *cis*, C_{2v} symmetry (*c.f.* Figure 1.6, page 21). But, more recent nmr studies have shown that both the *cis* and *trans* isomers exist in equilibrium (*ca.* 80% : 20% at 35°C (56,82)).

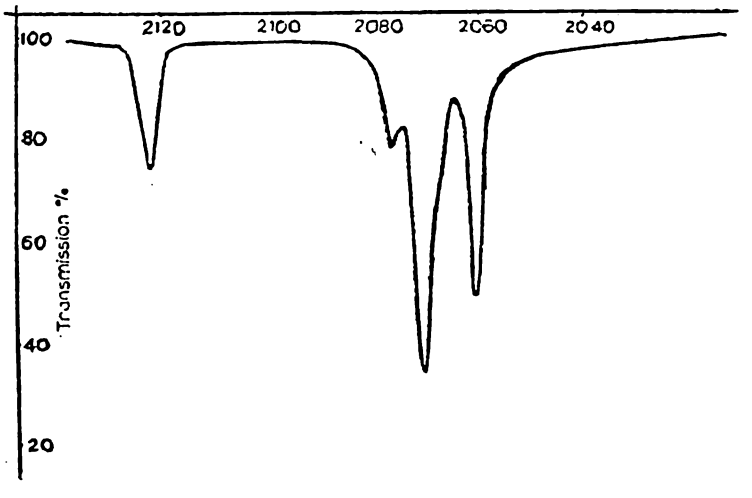

The carbonyl infrared spectrum of $Fe(CO)_4(SiCl_3)_2$: (59)

It is perhaps also worth mentioning that $M(CO)_4(M'R_3)_2$ species may well be found together with the monohydride species $M(CO)_4(H)(M'R_3)$ (irrespective of the method of preparation). The similarity of the spectra of these has also led to erroneous assignment of *cis* and *trans* isomers. For example, a product arising from reaction between $Fe_3(CO)_{12}$ and $SiCl_3H$ gave νCO bands at 2058 and 2055 cm^{-1} and was assigned as *trans*-$Fe(CO)_4(SiCl_3)_2$ (59). The appearance of two bands rather than one expected for D_{4h} symmetry was ascribed to an unspecified splitting. Others, on finding that the νCO region of $Fe(CO)_4(H)(SiCl_3)$ shows bands at 2124(m), 2069(m), 2058(s), and 2053(s) cm^{-1} have suggested that the bands earlier attributed to the *trans* isomer are more probably the two lower bands of the hydride (the two higher frequency bands being masked by bands of *cis*-$Fe(CO)_4(SiCl_3)_2$ at 2125 and 2071 cm^{-1} (92)). In the original work the species in question was found to be considerably more volatile than the *cis* isomer (59). This would also support the assignment of the hydride.

Even though the $M(CO)_4(M'R_3)_2$ species may be in equilibrium, the trend is for the $Fe(CO)_4(M'R_3)_2$ complexes to prefer C_{2v} geometry. It has been suggested that this is an electronic preference since *cis* geometry avoids *trans* carbonyl ligands from competing for π electron density of the iron (45,165). Of the iron derivatives, the only clearly 100% *trans* isomers occur for $Fe(CO)_4(GeI_3)_2$ and $Fe(CO)_4(GeBr_3)_2$. $Fe(CO)_4(GeCl_3)_2$ is a separable mixture of *cis* and *trans* (*i.e.*, not in rapid equilibrium at room temperature). $Fe(CO)_4(SiCl_2Me)_2$ and $Fe(SiCl_3)_2$ exist as 92:8 and 80:20, *cis*:*trans* mixtures respectively at ambient temperatures. The *cis* and *trans* isomers of $Fe(CO)_4(SnCl_3)_2$

have been isolated.(12) From Table 1.2, page 39, it can be seen that increasing the number of halogen substituents increases the percent of *trans* isomer in all known cases except for $Ru(CO)_4(SiF_3)_2$ and $Fe(CO)_4(SnBr_3)_2$ where the reverse applies (*i.e.*, both are 100% *cis*)

All $Fe(CO)_4(M'R_3)_2$ R = Me, Et, Bu, Pr, Ph, complexes that are known are 100% *cis*. The only data, aside from $M'Me_3$ ligands, which is known for Ru species is in the series $Ru(CO)_4(SnR_3)_2$. Here, there is a gradual change from almost totally *cis* R = Me to totally *trans* R = Ph, $PhCH_2$ (*c.f.*, Figure 1.9, page 23). $Os(CO)_4(SnMe_3)_2$ exhibits both *cis* and *trans* isomers (80:20%), but both $Os(CO)_4(SnBu_3)_2$ and $Os(CO)_4(SnPh_3)_2$ are 100% *trans*.

It would not be unreasonable to find that an increase in the activation energy of axial-equatorial averaging in *cis* species is concommittant with an increase in the percent of *trans* isomer. Although little data exists, increasing halogen substitution in *cis*-$Fe(CO)_4(M'R_3)_2$ species or changing from Fe to Ru to Os is seen to increase the activation energy barrier *e.g.*, *cis*-$Fe(CO)_4(SiMe_3)_2$ $\Delta G^{\ddagger} = 45$ kJmol^{-1} *cis*-$Fe(CO)_4(SiClMe_2)_2$ $\Delta G^{\ddagger} = 55$ kJmol. *cis*-$Fe(CO)_4(SiCl_2Me)_2$ $\Delta G^{\ddagger} = 69$ kJmol^{-1}, *cis*-$Fe(CO)_4(SiCl_3)_2$ $\Delta G^{\ddagger} = 74$ kJmol^{-1}. Compare *cis*-$Fe(CO)_4(SiMe_3)_2$ $\Delta G^{\ddagger} = 45$ kJmol^{-1} *cis*-$Ru(CO)_4(SnMe_3)_2$ $\Delta G^{\ddagger} = 74$ kJmol^{-1}, *cis*-$Os(CO)_4(SiMe_3)_2$ $\Delta G^{\ddagger} = 71.4$ kJmol^{-1} (56)

Yet another interesting observation is that $Ru(CO)_4(SiMe_3)(SnMe_3)$ exists as a mixture of *cis* and *trans* isomers whereas both $Ru(CO)_4(SnMe_3)_2$ and $Ru(CO)_4(SiMe_3)_2$ only exist in the *cis* form at ambient temperatures. Obviously, there is a very sensitive interaction between the electronic and steric effects of the group IV ligands in these transition metal carbonyl derivatives.

TABLE 1.2

Stereochemistry in some $M(CO)_4(M'R_3)_2$ Complexes

	$M'R_3$	$Fe(CO)_4(M'R_3)_2$ *cis* : *trans*	$Ru(CO)_4(M'R_3)_2$ *cis* : *trans*	$Os(CO)_4(M'R_3)_2$ *cis* : *trans*
R=Cl	$SiMe_3$	100 : 0	100 : 0	37 : 63
	$SiClMe_2$	100 : 0	100 : 0	40 : 60
	$SiCl_2Me$	92 : 8	88 : 12	both known
	$SiCl_3$	81 : 19	both known	0 : 100
	$GeMe_3$	100 : 0	100 : 0	80 : 20
	$GeCl_3$	both known	both known	0 : 100
	$SnMe_3$	100 : 0	100 : 0	80 : 20
	$SnCl_3$	both known	0 : 100	0 : 100
Other halides	SiF_3	-	100 : 0	both known
	$GeBr_3$	0 : 100	0 : 100	-
	GeI_3	0 : 100	-	-
	$GeBr_3$	100 : 0	0 : 100	0 : 100

All values are taken from reference (12), both known = *cis* and *trans* do not exist in equilibrium at ambient temperatures. These have been separated. -, not reported.

It has been noticed, that *cis*-$Fe(CO)_4(M'X_3)_2$ complexes are sometimes more soluble than their *trans* congeners in non-polar solvents (45). It has been suggested that the polarity in the *cis* isomer may be reduced by an intramolecular coordination process,

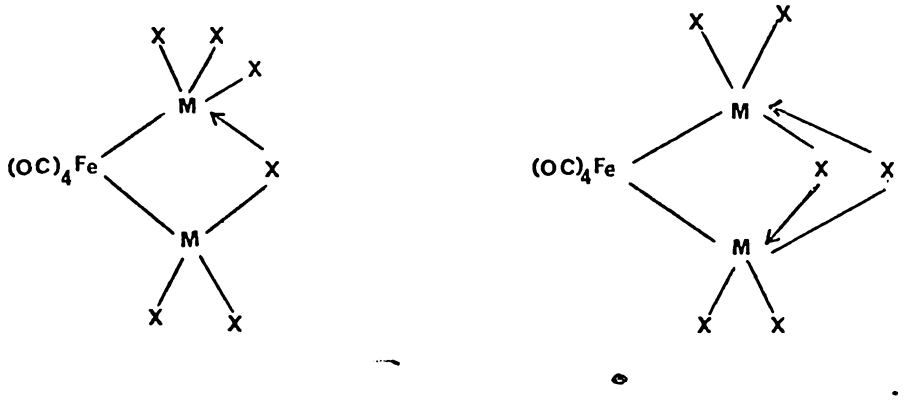

In both $Fe(CO)_4(GeCl_3)_2$ and $Fe(CO)_4(SnCl_3)_2$ where both *cis* and *trans* isomers were isolated, the less soluble, least stable, *trans* isomer was seen to isomerize readily in solution (*ca.*one hr. in CH_2Cl_2 for *trans*-$Fe(CO)_4(SnCl_3)_2$ (45)).

It has been suggested that lack of *trans* isomers in $Fe(CO)_4(M'R_3)_2$ complexes may be due to dimerisation of the *cis*-isomers. (See Section 2.3, page 52). Solutions of both *cis*-$Ru(CO)_4(SiCl_3)_2$ and *cis*-$Os(CO)_4(SiCl_3)_2$ isomerize on heating (70°, 120°C) to give mixtures of 70%:30% and 100%:0% *trans*:*cis* isomers respectively (160,188).

1.5 Bonding aspects

The type of bonding (involving a metal atom) found in $M(CO)_4M'_bR_y$ complexes ranges from pure σ bonding (*e.g.*, Ge-H) through σ with a small π contribution in M'R bonds (*e.g.*, SiF_3) to synergic bonding in MC where σ bond formation strengthens the π bonding component and *vice versa* (14,93). Most evidence to date suggests that the MM' bond is essentially a σ bonding interaction (14) unless, the MM' bond is part of a M_2M' triangle or cluster.

1.5.1 Bonding in polymetallic clusters

Multicentre bonding occurs in M_2M' units of polynuclear clusters. The most important feature of this type of bonding is that it accommodates acute MM'M angles which are found in some of these complexes (See Figure 1.3, page 5). Orbitals (Figure 1.14) constructed from detailed theoretical analyses can be extended to less symmetrical species which have similar M_2M' units (14 and references therein).

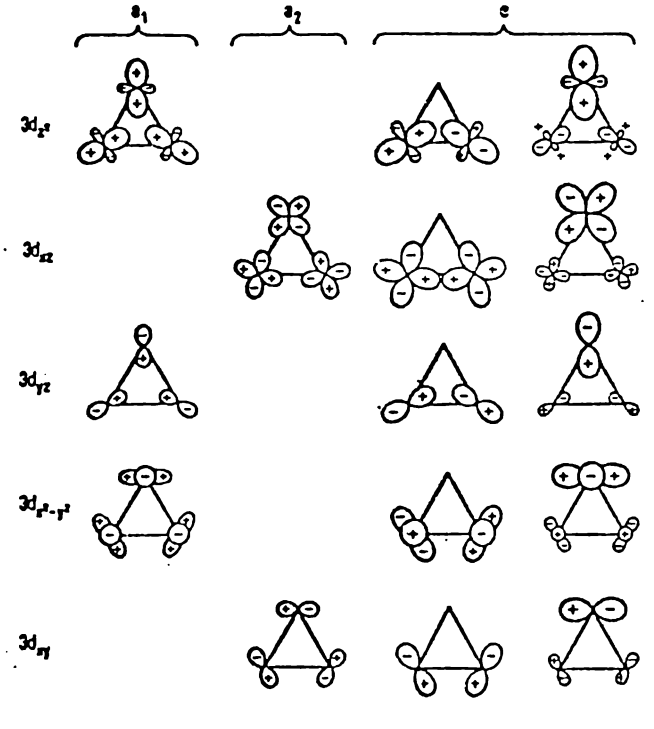

Overlapping of 3d orbitals of three Co atoms in the Co_3 triangle.

FIGURE 1.14

Orbitals involved in M_2M' multicentre bonding (155).

CHAPTER TWO

COMMENTARY ON PREPARATIVE ASPECTS

This chapter outlines in more detail some of the areas of the literature that are directly relevant to this work: aspects of salt elimination reactions; reactions of $M_a(CO)_xM'_bR_y$; self reaction studies of $M(CO)_4(M'R_3)_2$ complexes; and reactivity of metal hydride species with $Co_2(CO)_8$.

The concluding sections of this chapter outline the general experimental procedures used throughout this work.

2.1 Preparative aspects of salt elimination reactions

2.1.1 Preparation of tetracarbonylferrate (-II), $[Fe(CO)_4]^{2-}$

All the symmetrical germyl iron carbonyls prepared in this work were prepared *via* reaction of a germyl halide with $[Fe(CO)_4]^{2-}$. $[Fe(CO)_4]^{2-}$ can be prepared by a range of methods (116) to give salts with different counter ions, differing cation...anion interactions, and salts with coordinatively bound solvents: *e.g.*, $Fe(CO)_5/Na,NH_3$ (117); $Fe_3(CO)_{12}/Na,THF$ (118); $Fe(CO)_5$/alkali metal or alloys, ether (and benzophenone) (119); $Fe(CO)_5/K(s\text{-}C_4H_9)_3BH$, THF, reflux (120); $Fe(CO)_5/OH^-$ (121,122). Further reaction to give an alternative counter ion (123) may be desirable. The method of preparation adopted in this work was reaction between $Fe(CO)_5$ and sodium in liquid ammonia. There are indications that this reduction system is not simple. Hydrogen and sodium amide, but little or no CO_2, have been identified from this reaction (117). It was suggested that the following occurs,

$$Na + CO \longrightarrow Na_6(CO)_6$$

$Na_2Fe(CO)_4$ varies in colour from pale buff to brown. The colour is attributed to polynuclear anions, (122) $[Fe(CO)_4]^{2-}$ and $[Fe(CO)_4H]^-$, pale pink; $[Fe_2(CO)_8]^{2-}$ and $[Fe_3(CO)_{11}H]^-$, red; $[Fe_2(CO)_8H]^-$ yellow/brown; $[Fe_3(CO)_{11}]^{2-}$, brown. As complexes of the type $M(CO)_4(H)(M'R_3)$ (M=Fe,Ru,Os) have been isolated from reactions between $M'XR_3$ and anions prepared by sodium ammonia reduction, it has been proposed that $[M(CO)_4(H)]^-$ may also be present (125,126). The hydrido anion $[Os(CO)_4H]^-$ (deliberately generated (68)) reacts to give the products expected from $[Os(CO)_4]^{2-}$ in a salt elimination reaction (B=Base)

$$Os(CO)_4H_2 + B \longrightarrow [BH]^+[Os(CO)_4H]^-$$

$$[Os(CO)_4H]^- + SnC\ell Ph_3 \longrightarrow \textit{trans}\text{-}Os(CO)_4(SnPh_3)_2 \quad .$$

In general, reactions between group IV halides and transition metals anions are sensitive to changes in reaction procedure, for instance changes of solvent (127) or changes in counterion (128).

2.1.2. Preparation of pentacarbonylmanganate(-I), $[Mn(CO)_5]^-$

Methods for the reduction of transition metal carbonyls have been outlined.(116,129). Although it often results in contamination with small amounts of covalent mercury compounds (116,128,130), the sodium amalgam reduction is most commonly used. When

$$Mn_2(CO)_{10} + Na/Hg \xrightarrow{ether} NaMn(CO)_5$$

contamination with mercury was suspected in this work, the liquid $NaK_{2.8}$ alloy (131) was used to reduce $Mn_2(CO)_{10}$. Because the M-Ge bond has been found to be susceptible to alkaline cleavage reactions, (14,19) it is important to keep the concentration of alkali to a minimum. It has been found that it is essential to purify sodium and potassium and to use vigorously dried ether to avoid formation of oxide or hydroxide, either from the amalgam or alloy or from traces of water in the solvent(39).

2.1.3 Anomalous coupling reactions

Although coupling by salt elimination is a very widely established reaction, it cannot be relied upon unquestioningly. It has failed or given unexpected products in a number of cases.

(a) Anomalies in silicon systems

Problems often arise with the preparation of silyl transition metal carbonyls *via* salt elimination reactions (49,127,132). The lack of formation of M-Si bonds has been attributed to alternative reaction pathways; for instance, reactions of M-Si containing species with THF (a commonly used solvent), reaction with the halide ion produced in the reaction, or electrophilic attack by Si on the carbonyl oxygen of the transition metal carbonylate (127,128,132 and references therein).

$$[Co(CO)_4]^- + SiCl_4 \longrightarrow [Co(CO)_3C\text{-}O\text{-}SiCl_4]^- \qquad (127)$$

$$[Co(CO)_3C\text{-}O\text{-}SiCl_4]^- \longrightarrow Co(CO)_3C\text{-}O\text{-}SiCl_3 + Cl^-$$

$$3\ Co(CO)_3C\text{-}O\text{-}SiCl_3 \longrightarrow Co_3(CO)_9COSiCl_3 + Cl_3SiOSiCl_3? + \ldots$$

The reaction between $SiIMe_3$ or $SiBrMe_2$ and $[Fe(CO)_4]^{2-}$ does not give the expected product $Fe(CO)_4(SiMe_3)_2$ (133,134,135). Since it was known to these workers that coupling reactions between $NaMn(CO)_5$ and silicon chlorides occur successfully only in the absence of solvent or with a non-polar solvent (136) the above reaction between $SiIMe_3$ and $[Fe(CO)_4]^{2-}$ was tried not only in THF but also in "a slurry of dry, THF-free $Na_2Fe(CO)_4$ in hexane" (134). The product was the same in both cases and is now known to be $Fe_2(CO)_6(COSiMe_3)_4$, (structure *12*, p. 4) recovered in 27% yield (135)). $Fe(CO)_4(SiMe_3)_2$ has been prepared by an alternative route (49), (see Section 1.2. ., page 7). See also (199)

(b) Anomalies in the Si-Ru system

While reaction between $[M(CO)_4]^{2-}$ and monofunctional group IV halides, $M'XR_3$, yield $M(CO)_4(M'R_3)_2$ complexes, the reaction between $[M(CO)_4]^{2-}$ and difunctional group IV halides, $M'X_2R_2$, typically yield $[M(CO))_4(M'R_2)]_2$ complexes. However, reaction between $[Ru(CO)_4]^{2-}$ and SnX_2R_2 does not yield any $[Ru(CO)_4(SnR_2)]_2$ complexes (145), (both $[Fe(CO)_4]^{2-}$ and $[Os(CO)_4]^{2-}$ give the corresponding iron and osmium $[M(CO)_4(SnR_2)]_2$ analogues on reaction with SnX_2R_2 (126)). $[Ru(CO)_4(SnMe_2)]_2$ is a known compound and has been obtained from the reaction of $[Ru(CO)_4SiMe_3]^-$ with $SnC\ell_2Me_2$ (147).

$$[Ru(CO)_4(SiMe_3)]^- + SnC\ell_2Me_2 \longrightarrow [Ru(CO)_4(SnMe_2)]_2$$

(15% yield, sublimes at 80° with decomposition)

Rather than being an anomaly of the coupling reaction, the failure of the SnX_2R_2 reaction is more likely to be due to a different reaction path for ruthenium-tin systems. Supporting evidence for this comes from other reactions involving Ru and Sn. Compare for example:

(i) pyrolysis of $M(CO)_4(SnR_3)_2$. For M=Fe, $[Fe(CO)_4(SnR_2)]_2$ is the main decomposition product whereas for M=Ru and R=Me, traces of $[Ru(CO)_3(SnMe_3)(SnMe_2)]_2$ was the only species recovered (see structure *18*, p. 4, (145)).

(ii) thermal reaction between $M_3(CO)_{12}$ and $SnMe_2H_2$. Where M=Fe good yields of $[Fe(CO)_4(SnMe_2)]_2$ are recovered (together with a trace of $Fe(CO)_4(SnMe_3)_2$, believed to arise from traces of $SnMe_3H$ formed by migration of Me groups on Sn during pyrolysis). But when M=Ru very low yields of $Ru(CO)_4(SnMe_3)_2$ and $[Ru(CO)_3(SnMe_2)(SnMe_2)]_2$ (*ca* 3%) are obtained.

So, although $[Ru(CO)_4(SnMe_2)]_2$ is a stable compound the coupling reaction between $[Ru(CO)_4]^{2-}$ and SnX_2R_2 may involve a different reaction pathway.

(c) An anomalous reaction between $GeBr_2H_2$ and $Fe(CO)_4^{2-}$

No species of the type $[Fe(CO)_4]_2(GeH_2)_x$ x=1 or 2 were found in several reactions between $GeBr_2H_2$ and $Na_2Fe(CO)_4$ (RT or 0^oC, pentane (27)). The only volatiles recovered were $GeBr_2H_2$, $Fe(CO)_4(H)_2$ and/or $Fe(CO)_5$, GeH_4? . The mass spectrum of involatile residues gave polygermyl, (polyhalide?) envelopes at irregular interval spacing (*c.f.* the 28 mass unit intervals between metal carbonyl fragments). There was no indication of any germanium-containing carbonyl product. This is in contrast to the di-iodosilane coupling reactions:

$$SiI_2H_2 + NaM(CO)_4 \longrightarrow [M(CO)_x]_2SiH_2$$

$(M(CO)_x = Mn(CO)_5$, $Re(CO)_5$, $Fe(CO)_2Cp$ (138))

$$SiI_2H_2 + NaCo(CO)_4 \longrightarrow [Co(CO)_4]_2SiH_2$$

(98% yield (34))

(d) Failure to prepare $Fe(CO)_4(PbPh_3)_2$

Others (83) who have successfully prepared the *cis*-$Fe(CO)_4(SnR_3)_2$ R=Me,Et,Pr,Bu,Ph or $PhCH_2$ in yields of *ca.* 80% from reaction of the chloro or bromostannanes with $Na_2Fe(CO)_4.1.5C_4H_8O_2$ in THF at -78^oC have not been able to prepare $Fe(CO)_4(PbPh_3)_2$, a known compound, *via* this method. This was thought to be because of its ready self reaction.

$$cis\text{-}Fe(CO)_4(M'R_3)_2 \longrightarrow Fe(CO)_4(M'R_2)_2 + M'R_4$$

which occurs at or below room temperature in some of these species.

2.1.4 Preparation of unsymmetrically substituted $M(CO)_4(M'R_3)(M''R_3)$ complexes

Most of the $M(CO)_4(M'R_3)(M''R_3)$ unsymmetrically substituted species have been prepared from anions formed by cleavage of the M-M bond in $M(CO)_4(M'R_3)_2$ complexes, (see *13*, page 4), followed by a coupling reaction and salt elimination,

$$[Ru(CO)_4(GeMe_3)]_2 \xrightarrow{(i)} [Ru(CO)_4(GeMe_3)]^- \xrightarrow{(ii)} Ru(CO)_4(GeMe_3)(SnMe_3)$$

((i) Na/Hg, THF: (ii) $SnC\ell Me_3$ (44))

$Os(CO)_4(SnMe_3)(SiMe_3)$ (152), $Ru(CO)_4(GeBu_3)(SiMe_3)$, $Ru(CO)_4(SnPh_3)(SiMe_3)$, $Ru(CO)_4(SiMe_3)(SnMe_3)$ (147) have also been prepared. Iron carbonyl analogues have not been prepared *via* this route as no Fe-Fe precursors (see *13* , page 4) are known for iron. Two trichlorosilyltetracarbonyl iron derivatives, $Fe(CO)_4(SiC\ell_3)(SnC\ell_3)$ and $Fe(CO)_4(SiC\ell_3)(SnC\ell_2Ph)$ have been prepared thus: (139).

$$Et_4NC\ell + Fe(CO)_4(H)(SiC\ell_3) \longrightarrow [Et_4N]^+[Fe(CO)_4(SiC\ell_3)]^- + HC\ell$$

$$[Et_4N]^+[Fe(CO)_4(SiC\ell_3]^- + SnC\ell_4 \longrightarrow Fe(CO)_4(SiC\ell_3)(SnC\ell_3) + Et_4NC\ell$$

Unsymmetrically substituted species of the type $Fe(CO)_4(GeC\ell MeH)(GeMeH_2)$ have been prepared by partial substitution with $M'C\ell_4$ reagents (28) Unsymmetrically substituted species where the second ligand is not a group IV species are well known. Examples include the hydrides,

$$Fe(CO)_5 + SiC\ell_3H \xrightarrow{h\nu} Fe(CO)_4(H)(SiC\ell_3) + CO$$

$M(CO)_4(H)(M'R_3)$ (92,152), the halides $M(CO)_4(X)(M'R_3)$ (55) and $M(CO)_4(L)(M'R_3)$ such as alkyls like $Os(CO)_4(Me)(SiMe_3)$ (152,189).

2.2 Reactions of $M_a(CO)_xM'_bR_y$ with bases

Early studies showed that while in some cases amines cleaved M-Si bonds,

$$Co(CO)_4SiH_3 + NHMe_2 \rightarrow Co(CO)_4H + SiH_3NMe_2$$

in other cases adduct formation occurred (23b, 137). However, some of these adducts are now believed to be Lewis salts (141) of the type $[SiR_3.2B]^+[M(CO)_n]^-$ where B=base, (23a,49,138).

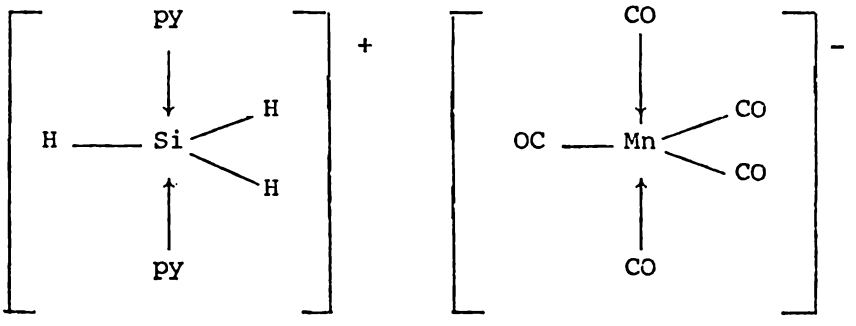

The ionic structure of $SiH_3Mn(CO)_5.2py$. (11)

The reaction of $M_a(CO)_xM'_bR_y$ complexes with bases has been utilised as a preparative route (139) to unsymmetrically substituted complexes of the type $Fe(CO)_4(SiCl_3)(SnR_3)$ and $Mn(CO)_2Cp(SiCl_3)(SnR_3)$

$$Fe(CO)_4 + nB \underset{}{\overset{k<1}{\rightleftharpoons}} [SiCl_3.nB]^+ + [Fe(CO)_4SiCl_3]^-$$

$$[Fe(CO)_4(SiCl_3)]^- + SnCl_4 \rightarrow [Fe(CO)_4(SiCl_3)(SnCl_3)] + Cl^-$$

Marks and Newman (43) have reported that Lewis bases cause facile reversible homolysis of complexes of the type $[Fe(CO)_4(M'R_2)]_2$

$$[Fe(CO)_4(M'R_2)]_2 + 2B \rightleftharpoons 2\ Fe(CO)_4 \leftarrow \overset{B}{\underset{\downarrow}{M'R_2}}$$

(B = THF, pyridine, acetone, acetonitrile, Et_2O, dimethylformamide)

Cornwell and Harrison (140) on the other hand see no reason why homolysis would be preferred to heterolysis in this case:

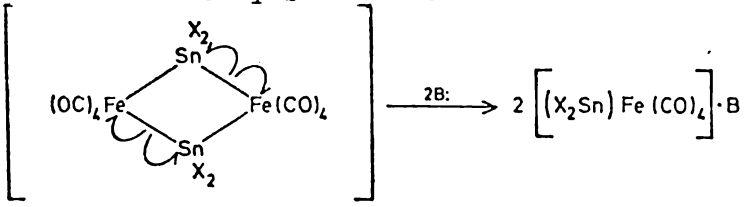

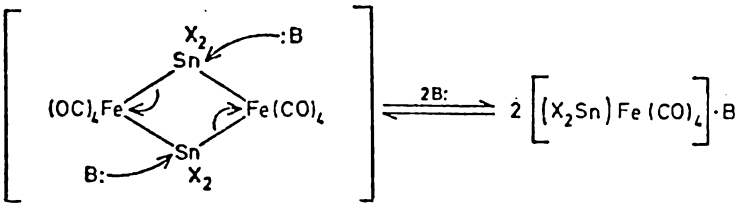

As $[Fe(CO)_4(SnX_2)]_2$ complexes can be synthesised directly from Sn(II) compounds with $Fe_2(CO)_9$ these authors proposed a mechanism involving initial formation of the monomeric species '$[Fe(CO)_4(SnX_2)]$', and its subsequent dimerisation due to the presence of acidic tin and basic iron centres. They further proposed that addition of another base B, causes competition between B and the iron for the acidic tin centre, thus giving rise to the monomer-dimer equilibrium. This then explains why strong bases such as pyridine are not easily displaced and can effectively stabilise monomers whereas weak donors are more easily displaced and both monomer and dimer are observed at room temperature. Apparently in such situations, cooling to -196°C forces the equilibrium to the more thermodynamically favoured dimer. From Mössbauer data, these authors also postulate the existence of synergic (σ donor, π acceptor) bonding in the Fe-Sn bond of the monomers. Burnham *et al.* (142) found that the following substitution (and not monomer stabilisation) occurred on reaction with phosphorus donor ligands:

$$[Fe(CO)_4(SnBu_2)]_2 + PPh_3 \longrightarrow [Fe(CO)_3(PPh_3)(SnBu_2)]_2$$

$$[Fe(CO)_4(SnBu_2)]_2 + P(OPh)_2 \rightarrow [Fe_2(CO)_7(P(OPh)_3)Sn_2Bu_4]$$

However, the phosphines are competing with CO as ligands on M. Thus, the observation does not undermine that of Marks and Newman(43), despite the comment of Burnham *et al.*(142).

In further work, Marks and Seyam (143) attempted to synthesise a stable silylene, germylene or stannylene complex with a M=M' double bond *via* the reaction,

$$R_2M'(X)—ML_n \longrightarrow [R_2M' \longrightarrow ML_n]^+ + X^-$$

However, only F abstraction from the counterion occurred.

$$Co(CO)_4(GeCl Ph_2) + AgBF_4 \longrightarrow Co(CO)_4(GeFPh_2) + AgCl + BF_3$$

Early attempts to prepare base stabilised species with four coordinate M'(II) led to decomposition in attempts to remove the base. (14 and references therein). More recently, use has been made of $M'R_2$ species (R = bulky group) to prepare genuine germylene, stannylene or plumbylene complexes, with trigonal planar M', by ligand replacement, or bridge cleavage reactions.

Schmid (144) has reported the preparation of the first base-stabilised silyene complex

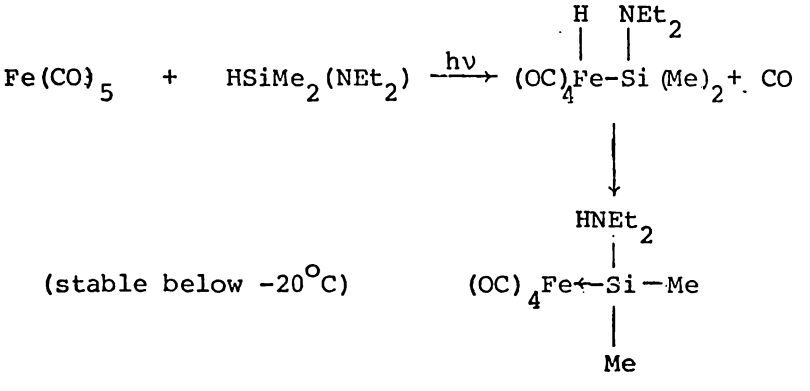

Schmid (144a) also suggests that while germylene, stannylene and plumbylene complexes can be prepared with comparative ease, silylene complexes are not stable because of the instability of divalent Si and its tendency to form four coordinate (usually di- or tri-meric) complexes where silicon bridges two metals. Sakurai *et.al*, (144b) report that they have prepared the first stable mononuclear dimethylsilandiyliron complex but reported an infrared spectron showing *four* carbonyl stretches.

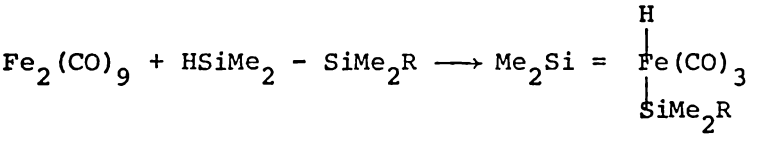

2.3 Self-reaction studies of $M(CO)_4(M'R_3)_2$ complexes

As with both the parent transition metal carbonyls and the group IV metal hydrides, the group IV transition metal carbonyls undergo condensation and cyclisation reactions. Few reactions have been studied in detail. Since self-reaction of $M(CO)_4(M'R_3)_2$ complexes are of relevance to this work, known examples will be considered individually,

see Table 2.1, page 53.

TABLE 2.1

Self reactions of some $M(CO)_4(M'R_3)_2$ complexes

No.	Compound	Products	Reaction conditions	Ref.
(i)	$Fe(CO)_4(GeMeH_2)_2$, (0.438 mmol)	$Fe(CO)_4(GeMeH_2)_2$, $[Fe(CO)_4(GeMeH)]_2$, $GeMeH_3$, CO (0.324 mmol) (0.067 mmol) (0.008 mmol)	RT, no solvent, absence of light, 25d, incondensible removed intermittently	(29)
(ii)	$Fe(CO)_4(GeMe_2H)_2$	$[Fe(CO)_4(GeMe_2)]_2$, $Fe_2(CO)_7(GeMe_2)_2$, $GeMe_2H_2$ 5% (0.19 mmol) CO/H_2 (trace)	RT, dark, 15d, gases removed intermittently	(30)
(iii)	$Fe(CO)_4(SnMe_3)_2$ (1.02 mmol)	$Fe(CO)_4(SnMe_3)_2$, $[Fe(CO)_4(SnMe_2)]_2$, $SnMe_4$, CO/H_2 (1:1 mixture .....) (0.4 mmol) (trace)	140°. 36hr, sealed tube	(146)
(iv)	$Ru(CO)_4(SiMe_3)_2$	$[Ru(CO)_4(SiMe_3)]_2$, $SiMeH_3$, $(Me_3Si)_2O$	80°, or RT - several weeks	(147)
(v)	$Ru(CO)_4(GeMe_3)_2$ (670mg, 1.48 mmol)	$[Ru(CO)_3(GeMe_2)]_3$, $Ru_2(CO)_6(GeMe_2)_3$, $GeMe_4$ (230 mg, 0.27 mmol) (5 mg, 0.008 mmol) (1.30 mmol)	140°, 16d, absence of light, intractable red-black material not identified	(44)
(vi)	$Ru(CO)_4(GeMe_3)_2$	$[Ru(CO)_3(GeMe_3)(GeMe_2)]_2$ (trace)	100°, incomplete pyrolysis	(44)
(vii)	$Ru(CO)_4(SnMe_3)_2$ (680 mg, 1.25 mmol)	$Ru(CO)_4(SnMe_3)_2$, $[Ru(CO)_3(SnMe_3)(SnMe_2)]_2$ (400 mg, 0.74 mmol) (6 mg, 0.006 mmol)	80°, 44hr, hexane 6 ml	(145)
(vii)	$Ru(CO)_4(SiMe_3)(GeBu_3)$	$Ru(CO)_4(SiMe_3)_2$, $[Ru(CO)_4(SiMe_3)]_2$, $[Ru(CO)_3(GeBu_2)]_3$?	140°	(44)
(viii)	$Os(CO)_4(GeMe_3)_2$ (540 mg, 1.0 mmol)	$[Os(CO)_3(GeMe_2)]_3$, $Os_2(CO)_6(GeMe_2)_3$ $GeMe_4$ (255 mg, 0.225 mmol) (trace) (0.93 mmol)	160°, 20 d, sealed tube	(44)

2.3.1 Self-reaction of $Fe(CO)_4(GeMe_{3-x}H_x)_2$ complexes

(i) $Fe(CO)_4(GeMeH_2)_2$ reacts mainly according to

$$2\ Fe(CO)_4(GeMeH_2)_2 \longrightarrow [Fe(CO)_4(GeMeH)]_2 + 2GeMeH_3$$

A reaction mechanism was proposed involving a germylene intermediate, formed *via* Ge-H bond scission (30).

$$Fe(CO)_4(GeMeH_2)_2 \longrightarrow '[Fe(CO)_4(GeMeH)]' + GeMeH_3$$

This was thought to then react with another $Fe(CO)_4(GeMeH_2)_2$ molecule to form $Fe(CO)_4(GeMeH)_2$ together with a second molecule of $GeMeH_3$. Reaction involving the formation of an "eight-centred" intermediate or transition state species was thought to be highly unlikely (27). It was proposed that $Fe(CO)_4(GeMeH_3)_2$ (which does not self-react under these conditions) and $Fe(CO)_4(GeMeH_2)_2$ are more stable than the analogous $Fe(CO)_4(GeMe_2H)_2$ because the GeH_2 and GeMeH groups are less effective in bridging two iron atoms (29). $Fe(CO)_4(GeMe_3)_2$ is much less reactive than any of the $Fe(CO)_4(GeMe_{3-x}H_x)_2$ complexes. This accords with the suggested reaction mechanism as the stronger Ge-C bonds are not expected to cleave under these conditions.

(ii) $Fe(CO)_4(GeMe_2H)_2$ undergoes a similar but more rapid self-reaction to produce $[Fe(CO)_4(GeMe_2)]_2$ and $GeMe_2H_2$. $Fe_2(CO)_7(GeMe_2)_2$ (5%) was thought to arise chiefly from further reaction of $[Fe(CO)_4(GeMe_2)]_2$

$$[Fe(CO)_4(GeMe_2)]_2 \longrightarrow Fe_2(CO)_7(GeMe_2)_2 + CO$$

as CO evolution was more prevalant after 95% of the $[Fe(CO)_4(GeMe_2)]_2$ had been formed.

2.3.2 Self-reaction of $M(CO)_4M'R_3)_2$ complexes, R≠H

(iii) Reaction (iii) in Table 2.1, was carried out in an attempt to understand more fully the mechanism of reaction between $Fe(CO)_5$ and $SnC\ell Bu_3$, (146).

$$Fe(CO)_5 + SnC\ell Bu_3 \xrightarrow{\text{reflux}} [Fe(CO)_4(SnBu_2)]_2 \quad (ca.\ 30\%)$$
$$+ [Fe(CO)_4]_4Sn_3Bu_4 \quad (\text{up to } 6\%)$$
$$+ [Fe(CO)_4]_4Sn \quad (0.5 \text{ to } 16\%)$$

Identification of $SnMe_4$ and $[Fe(CO)_4(SnMe_2)]_2$ were all that these workers were looking for. Since this reaction was carried out under forcing conditions (140°, 36hr), the same mechanism as was proposed for (i) could also occur here. Breaking of the relatively weak Sn-C bond is not unexpected under these conditions. A parallel was drawn here between this reaction and earlier work where reaction between $PbOHPr_3$ and $[Ca][Fe(CO)_4H]_2$ was thought to give a 1:1 molar ratio of $PbPr_4$ and $Fe(CO)_4(PbPr_2)$ (176), (the latter is now known to be $[Fe(CO)_4(PbPr_2)]_2$).

No experimental details of (iv) are given. The appearance of hexamethyldisiloxane, $SiMe_3H$ and $[Ru(CO)_4(SiMe_3)]_2$ (structure *13*, page 4), was noted in contrast to self-reaction of $Ru(CO)_4(SnMe_3)_2$ (vi).

In (V) Table 2.1 products weighed and identified from the self-reaction of $Ru(CO)_4(GeMe_3)_2$ accounted for *ca* 70% of the germanium. The yield of $GeMe_3H$ was readily obtained as it was the only volatile product. (44% based on moles of Ge). Hand sorting separated the bulk of the orange-red crystalline $[(Ru(CO)_3(GeMe_2)]_3$ from the bright yellow needles of $Ru_2(CO)_6(GeMe_2)_3$. Extraction of the residual red-black intractable

powder with hexane (100 ml) and chromatography of the red solution on silica gel separated traces of $Ru_2(CO)_6(GeMe_2)_3$ from more $[Ru(CO)_3(GeMe_2)]_3$. The remaining germanium (30%) and ruthenium (50%) presumably makes up the bulk of the red-black intractable residue or was deposited on the silica gel? Traces of $[Ru(CO)_3(GeMe_3)(GeMe_2)]_2$ were detected in another experiment where incomplete pyrolysis of $Ru(CO)_4(GeMe_3)_2$ had occurred (100°C) (44).

In (vi), $Ru(CO)_4(SnMe_3)_2$ was largely unreacted (59%) after heating in hexane at 80°C for 44 hours. The fate of the material which did react is largely unknown. Less than one percent of the initial material was recovered and identified as $[(Ru(CO)_3(SnMe_3)(SnMe_2)]_2$. Forty percent of the material was not accounted for. No details of work-up procedure were given. However, it was proposed that $Ru(CO)_4(SnMe_3)_2$ is genuinely loathe to undergo self-reaction because of the great strength of Ru-Sn bonds (*c.f.* for instance Fe-Sn bonds). These authors reflect that the only isolated product $[(Ru(CO)_3(SnR_3)(SnR_2)]_2$ requires no RuSn bonds to be be broken in its formation. (See also, Section 2.1.3, page 45).

Again, although no details are given of reaction vii in Table 2.1, (44,147), it is most interesting that an attempted distillation of $Ru(CO)_4(SiMe_3)(GeBu_3)$ (*ca.*, 140°C) afforded only the decomposition products $Ru(CO)_4(SiMe_3)_2$, $[Ru(CO)_4(SiMe_3)]_2$ and an unidentified orange complex with $\nu_{max}(CO)$ at 2042 m, 2034 w, 2012 s, 2006 w, and 1983 m, cm^{-1}. It was thought that these absorptions would be expected for the butyl analogue $[Ru(CO)_3(GeBu_2)]_3$.

(viii) After pyrolysis of $Os(CO)_4(GeMe_3)_2$, (540 mg, 1.0 mmol; 160°C, 20 d), $GeMe_4$ (0.93 mmol, 47%) was condensed away from 405 mg of orange-yellow crystalline material. Chromatography of 'almost' all the residual crystalline material with hexane afforded $[Os(CO)_3(GeMe_2)]_3$, (255 mg, 0.255 mmol, 34% based on Ge) plus, spectroscopic identification of $Os_2(CO)_6(GeMe_2)_3$. That is, at least 81% of the germanium has been recovered, together with 68% of the osmium. The unaccounted material including the unweighed $Os_2(CO)_6(GeMe_2)_3$ has an average of Ge 19%, Os 32%, and accounts for 31% by weight of the material (170 mg).

2.3.3 Comment on reactions of $M(CO)_4(M'R_3)_2$ where R=alkyl group

Products obtained from thermal or photochemical reactions where M-M bond-breaking and bond-reforming are continually occurring (187) may give rise to a range of different species. These species may represent the most thermodynamically stable configuration

c.f., $[Mo(CO)_3Cp]_2 + Co_2(CO)_8 \rightleftharpoons 2Cp(CO)_3MoCo(CO)_4$

5% 95%

Often, not all the reacted material from these reactions is recovered and identified. This could be due to the formation of intractable oliogmeric species, and/or to the decomposition and deposition of material on silica gel during chromatographic separation procedures.

Also, the products isolated from these reactions may reflect the stability of the compounds formed and/or the techniques used to separate the species. For instance, it is known that lab lighting will cause the decomposition of solutions of both $[Fe(CO)_4(Ge_2Me_4)]_2$ *20*, page 4 , and $[Fe(CO)_4]_2(GeMe_2)(Ge_2Me_4)$ *22*, page 4 , to give the air stable species $Fe_2(CO)_6(GeMe_2)_3$, *17*, page 4. (106).

2.4 Reactivity of metal hydride species, with $Co_2(CO)_8$

As M'-H in ML_nM'-H species can react further with carbonyls to yield polymetallic species, reactions of hydrides with transition metal carbonyl (especially $Co_2(CO)_8$) will be briefly discussed. A short study of the reactions of $Mn(CO)_5(GeMe_{3-x}H_x)$ with $Co_2(CO)_8$ is discussed in Chapter Six.

2.4.1 Reactions involving $M'R_3H$ and $M_a(CO)_x$

Reactions between $M'R_3H$ and $M_a(CO)_x$ are numerous (2 — 14). The 'simple' case of reaction between $M'R_3H$ and $M_2(CO)_x$ (M = Co, Mn; x = 8, 10) was initially rationalised as involving addition of M'-H across M-M followed by cleavage of the M-M bond (37,46,137,150,151).

$$SiR_3H + Co_2(CO)_8 \longrightarrow Co(CO)_4SiR_3 + Co(CO)_4H$$

$$Co(CO)_4H + SiR_3H \longrightarrow Co(CO)_4SiR_3 + H_2$$

$$2Co(CO)_4H \longrightarrow Co_2(CO)_8 + H_2$$

Reactions between $M'R_3H$ and the iron triad carbonyls are thought to involve a similar mechanism (92,125,146,147,152). The products are very dependent on reaction conditions (31,44,146).

It is interesting to compare the products obtained from reactions of $M'MeH_3$ with $Co_2(CO)_8$ as M' varies from Si to Ge to Sn.

M' = Si (153)

$$SiMeH_3 + Co_2(CO)_8 \longrightarrow Co(CO)_4(SiMeH_2) + H_2$$

(no solvent, RT, 3 hrs, 46% yield)

M' = Ge (154)

$$GeMeH_3 + Co_2(CO)_8 \longrightarrow [Co_3(CO)_{11}]GeMe + (Co(CO)_4H)$$

(1:2 mixture, benzene, RT, 80% yield)

M' = Sn (115c)

$$SnMeH_3 + Co_2(CO)_8 \longrightarrow [Co(CO)_4]_3SnMe$$

(1:1.5 ratio, RT, hexane, sealed tube, dark, quantitative yield)

Obviously the nature of the group IV metal has a great deal to do with the product formed. Nmr studies of the reaction between $GeMeH_3$ and $Co_2(CO)_8$ gives evidence for stepwise substitution through $Co(CO)_4(GeMeH_2)$, *via* $Co_2(CO)_x(GeMeH)$ species to form finally $[Co_3(CO)_{11}]GeMe$ (154). Unpublished observations (192) suggest that, in contrast, $SiMeH_3$ reacts initially to a '$[Co_2](SiMeH)$' species which disproportionates to yield the observed $Co(CO)_4(SiMeH_2)$.

It is interesting too, that the structures adopted by complexes containing one group IV metal atom and four cobalt atoms have been rationalised in terms of the size of the central atom and hence its ability to bridge Co-Co units (109,155). Thus, Si and Ge are small enough to fill the apex position of the $[Co_3]M'$ pyramid in $[Co_3(CO)_9][(Co(CO)_4]M'$ (See structure *29*, page 5).

Only Ge enters the bridging position in a cluster of the type $[Co_2(CO)_7]_2Ge$ (See Structure *33*, page 5), but, Ge, Sn and Pb all form open clusters of the type $[Co(CO)_4]_4M'$ (see Structure *31*, page 5). Attempts to form Co-Co bonded species by CO elimination in $[Co(CO)_4]_4Sn$ and $[Co(CO)_4]_4Pb$ have thus far been unsuccessful. However, terminally bonded CO's in the germanium containing complexes are readily lost to form CO bridging species *e.g.* $[Co_2(CO)_7]_2Ge$ slowly evolves CO at 50°C to form $[Co_3(CO)_9][Co(CO)_4]Ge$ (109). The reverse reaction, addition of CO to cobalt complexes with germanium bridges is also known (31,156), and typically requires considerable pressure of CO and/or elevated temperatures. This ready interconversion is not unexpected as these systems are known to be fluxional (58,86). If, as it is claimed, Sn atoms are too big to get in close enough to bridge $Co_2(CO)_7$ units, then few, if any, $[Co_2(CO)_7]SnR_2$ species would be expected to be stable. Indeed, the only species in which four coordinate tin bridges '$Co_2(CO)_7$'; $[Co_2(CO)_7]SnMe_2$, is extremely unstable (47). The six coordinate Sn species $[Co_2(CO)_7]Sn(acac)_2$ (183) exhibits an extremely acute MM'M angle 61° (13). Six coordinate tin is obviously less strained when forced to adopt a small MM'M angle in order to bridge a Co-Co unit than a four coordinate Sn will be. The known $[Co_2(CO)_7](\mu\text{-}SiR_2)$ and $[Co_2(CO)_7](\mu\text{-}GeR_2)$ complexes (see Structure *19*, page 4), are included in Table 2.2, page 62. It has been suggested that although silicon atoms are of the right size to fit into a cluster the inherently high reactivity of silicon transition metal carbonyls makes these compounds difficult to isolate and identify.

TABLE 2.2

Complexes of the type $Co_2(CO)_7(\mu\text{-}M'R_2)$

Compound	structure	reference	comments
$[Co_2(CO)_7]SiPh_2$	*19*	(36, 107)	Considerably more air sensitive than Ge analogue
$[Co_2(CO)_7][Co(CO)_4]SiPh$	*23*	(107)	Attempts to convert into $Co_3(CO)_9SiPh$ have led only to decomposition.
$[Co_2(CO)_7]SiCl_2$	*19*	(16)	Extracted in C_6H_{14} after attempts to sublime it failed at 40°C. The mass spectrum was recorded at 100°C
$[Co_2(CO)_7]SiMe_2$	*19*	(54)	Impossible to isolate because of its lability and low volatility.
$[Co_2(CO)_7][Mn(CO)_5]SiCl$	*23*	(16)	Slight decomposition was noticed if it was left for long periods of time
$[Co_2(CO)_7]GePh_2$	*19*	(51, 157)	Stable, mpt 78-80°C
$[Co_2(CO)_7]GeMe_2$	*19*	(58)	Thermally unstable, rapidly decomposes at 25°C, air sensitive.
$[Co_2(CO)_7][Co(CO)_4]GeMe$	*23*	(154, 158)	Thermolysis at 80°C leads to CO loss and formation of $Co_3(CO)_9GeMe$
$[Co_2(CO)_7][Co(CO)_4]GePh$	*23*	(107)	mpt 77-78°C (decomposition)
$[Co_2(CO)_7]_2Ge$	*33*	(109)	Slowly loses CO at 55°C to form $[Co_3(CO)_9][Co(CO)_4]Ge$
$[Co_2(CO)_7]SnMe_2$	*19*	(47)	Exceedingly unstable

2.4.2 Reactions between $M'_2R_{6-x}H_x$ and $M_a(CO)_x$

In reactions between $M'_2R_{6-x}H_x$ and $M_a(CO)_x$, the products obtained may result from both M'-M' and M'-H cleavage. This often results in quite complex reaction mixtures (54).

$$Si_2Me_4H_2 + x\ Co_2(CO)_8 \xrightarrow{R.T}$$

$Co(CO)_4(Si_2Me_4H)$, $[Co(CO)_3(\mu\text{-}SiMe_2)]_2$, $Co_2(CO)_6(\mu\text{-}CO)(\mu\text{-}SiMe_2)$,

$Co_2(CO)_8(Si_2Me_4)$, $Co_4(CO)_{12-x}(SiMe_2)_x$ x=1,2,

$(OC)_4Co(SiMe_2)_yOCCo_3(CO)_9$ y=1,2.

Most of the work to date has focused on the isolation and identification of the more abundant lower molecular weight complexes in these systems.

2.4.3 Reactions between M-M'-H and $M_a(CO)_x$

The few mixed group IV metal, transition metal carbonyl complexes which appear in the literature, tend to give reasonable yields of predicted species.

$$[Mn(CO)_5][Co(CO)_4]SiCl_2H + Fe_3(CO)_{12} \longrightarrow \textit{39}, + H_2 + CO$$

(see Structure *39*, page 5, (16))

(hexane, RT, rapid reaction 49% yield)

$$[Mn(CO)_5]GePh_2H + Co_2(CO)_8 \longrightarrow [Mn(CO)_5][Co(CO)_4]GePh_2$$

(25°C, high yield, (21)).

OVERVIEW

Examples of polymetallic complexes of the type $M_a(CO)_xM'_bR_y$ appear at random in the literature. There is as yet no clear route to the formation of specific $M_a(CO)_xM'_bR_y$ complexes. Thermal and photochemical reactions between M-M and $M'R_3H$ species have given rise to a number of the mixed metal polynuclear clusters (12). But, it appears that one is unable to predict the type of complex which will result from these reactions. This is probably because M-M, M'-M' and M-M' bond cleavage and reformation occurs continuously under forcing reaction conditions.

A good illustration of this is:

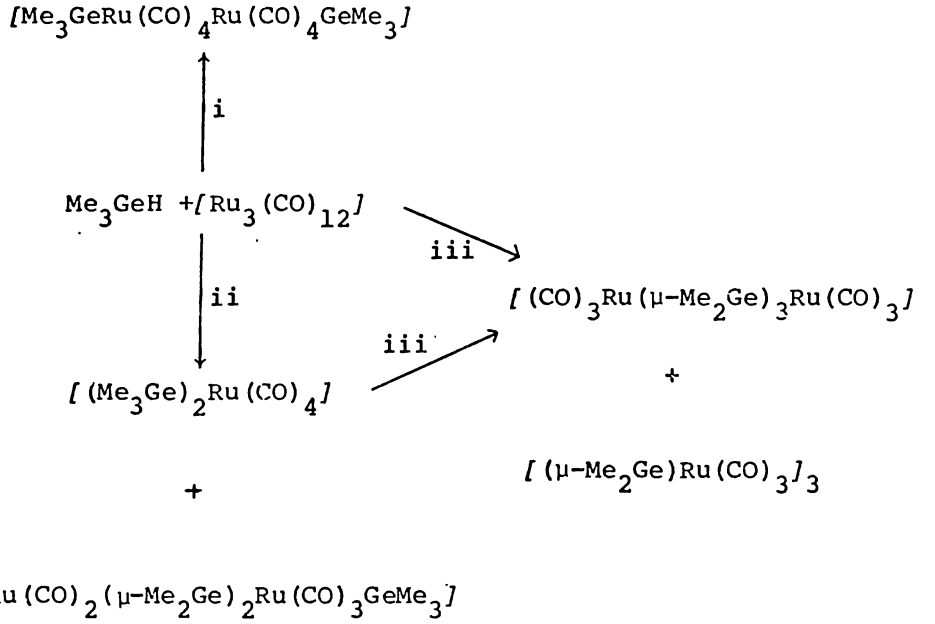

i, photolysis, $-H_2$: ii 80-100° in hexane, $-H_2$: iii 160° Si,Sn and Os species similarly: ii also yields $(Me_3M')OsH(CO)_4$

Products isolated from such mixtures thus favour presumably the most thermodynamically stable arrangement of atoms. Understandably, product yields may be low.

One method for the formation of polynuclear clusters might possibly be by controlled reactions between M-M'-H species and other carbonyls at ambient temperatures. Perhaps, reasonable yields of predictable products will arise in such reactions. Lack of hydride precursors could be a problem as in the case of Sn-H derivatives. However, if the halide derivatives could be prepared then these may be reduced with *e.g.*, $NaBH_4$ (32) or $(i\text{-}Bu)_2AlH$ (21)

$$[Fe(CO)_2Cp]GeCl_2 + NaBH_4 \longrightarrow [Fe(CO)_2Cp]GeH_2$$

(55% yield (32))

$$[Mn(CO)_5]_2SnCl_2 + 2(i\text{-}Bu)_2AlH \longrightarrow [Mn(CO)_5]_2SnH_2$$

(good to excellent yields (21))

In contrast, if no reaction occurred under mild conditions, (see Section 1.2.2, page 7) then it may be necessary to do the reverse. Rather than heating or irradiating the reactants it may be more advisable to halogenate the functional hydrogen; *via* exchange reactions with covalent halides (28,40,159) and then couple the M-M'-X species to carbonyl anions. (See Section 1.2.1, page 6).

2.5 Experimental Procedures

2.5.1 General techniques

Most of the compounds presented in this thesis were handled by a conventional vacuum line fitted with greased taps and mercury manometers. A rotary oil pump usually gave sufficient vacuum (*ca.*, 10^{-2} mmHg) but a mercury diffusion pump was required for the handling of the methylgermyl iron carbonyls. Separation of a reaction mixture was effected by fractional distillation, the mixture being allowed to vapourise and condense in a series of adjacent traps kept at successively lower temperatures by constant temperature slush baths (166). Slush baths commonly used include, carbon tetrachloride $CC\ell_4$, -23°C, Chlorobenzene $C_6H_5C\ell$, -45°C, Chloroform $CHC\ell_3$ -63°C, ethylacetate $C_2H_5COOCH_3$, -83°C, n-propanol C_3H_7OH, -127°C, propanol-ethanol mixtures,<-127°C. The last trap, a liquid nitrogen trap, -196°C was left open to the pump during a fractionation.

Involatile materials were initially manipulated in a glove box flushed with a stream of nitrogen which was slowly evaporating from a dewar of liquid nitrogen. Later, it was found that traces of oxygen in the nitrogen was one cause of decomposition in germyl iron carbonyls.

Better anaerobic conditions were obtained using a plastic bag flushed with oxygen-free nitrogen, cylinders of which were of variable quality (although the N.Z.I.G, specification for OFN is 10 ppm oxygen, up to 1000 ppm O_2 has been detected by other workers at this university (177e)).

Vacuum manipulation was used where ever possible and was far superior even to conventional nitrogen line and schlenk tube techniques, for the very air sensitive germyl iron carbonyls.

2.5.1.1 Glassware

Pyrex glassware was used throughout. All glassware was treated with *aqua regia* before final rinsing (at least eight cycles). Reaction vessels and U-traps were either ovened at *ca*, 500°C or flame annealed under vacuum before use.

Non standard items of glassware used in this work are shown in Figure 2.1

Figure 2.1 A, shows the reduction-coupling reaction vessel in which the unsymmetrical germyl iron carbonyls were made.

Figure 2.1 B, shows a U-tube with attached nmr tube. These tubes were inserted between the reaction vessel and vacuum pump after unreacted material and solvent had been pumped out of the reaction vessel.

Products of low volatility were collected at the bottom of the U-tube using liquid nitrogen. When sufficient sample had collected in the tube, the taps were closed and the sample was allowed to warm up and run into the bottom of the nmr tube. Any sample adhering to the walls of the nmr tube was condensed into the nmr tube by repeated lowering of the liquid nitrogen level allowing the product to condense into the cold zone. The nmr tube was then sealed off from the U-tube at the constriction just below the middle of the U.

Figure 2.1 C. This vessel was used as a weighing vessel. Samples were condensed into this tube in a similar manner to that described above.

Figure 2.1 D, shows the nmr tube breaker. Throughout most of this work, starting materials were checked for purity using nmr. The checked samples were then opened under vacuum using this apparatus. Standard nmr tubes were made from 0.5 mm o.d. pyrex tubing.

Figure 2.1

Non-standard items of glassware

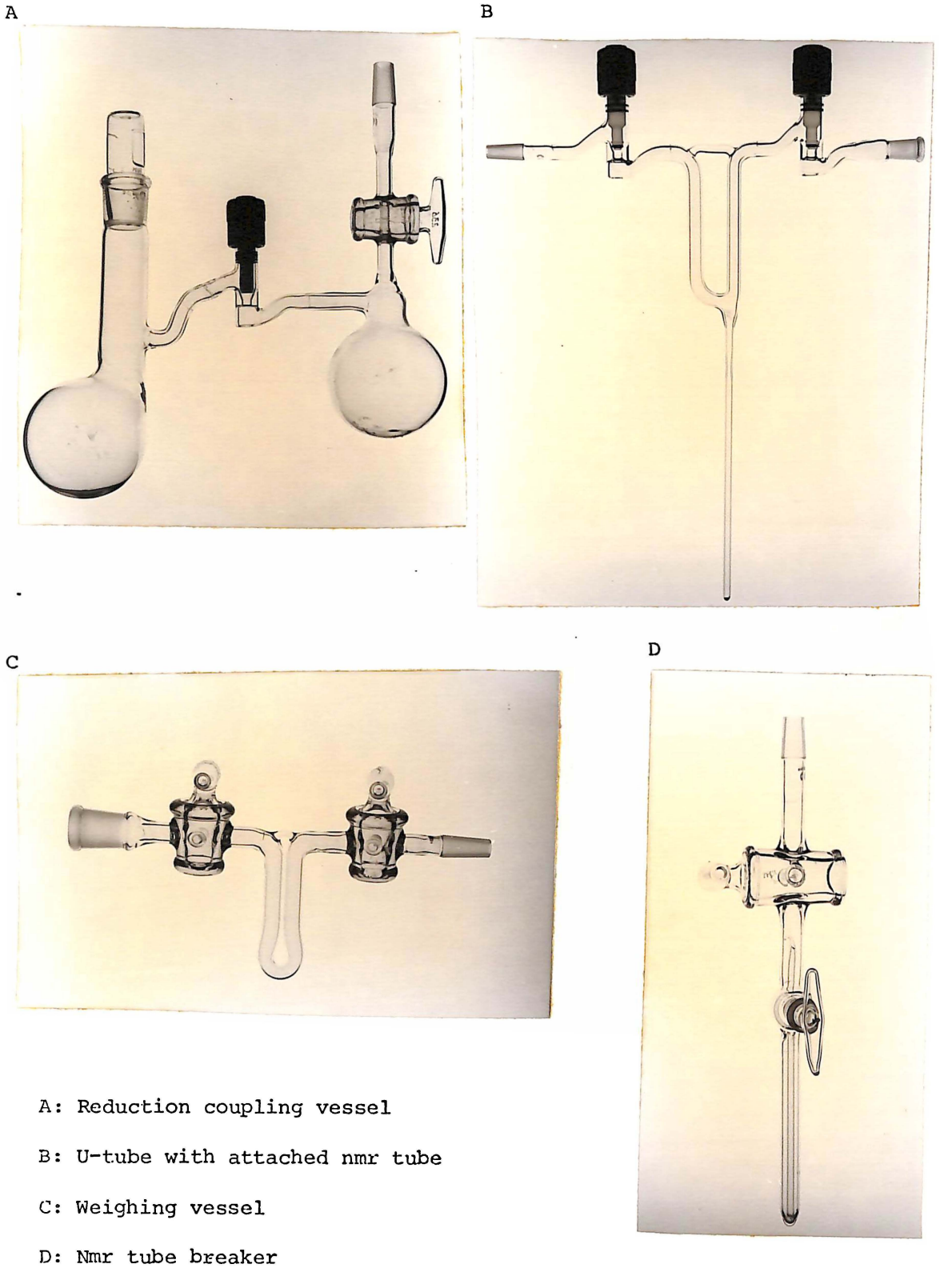

A: Reduction coupling vessel

B: U-tube with attached nmr tube

C: Weighing vessel

D: Nmr tube breaker

2.5.1.2 Solvents

Solvents were dried in the following ways; hexane, cyclohexane pentane and benzene were dried over sodium wire or $LiAlH_4$. Diethyl ether Et_2O, tetrahydrofuran THF and di-n-butyl ether were distilled under a nitrogen atmosphere from sodium/benzophenone $C_6H_5COC_6H_5$. Dichloromethane was distilled from phosphorus pentoxide P_4O_{10}, under an atmosphere of nitrogen. Ammonia was dried over sodium and kept as a gas in a 20 litre storage facility on the vacuum line.

2.5.1.3 Sodium and potassium amalgams and alloys

Throughout this work the sodium or potassium used was first purified by melting under vacuum and pouring the molten sodium or potassium away from impurities. This procedure was found to be necessary since traces of ethoxide or hydroxide are responsible for cleavage of germanium transition metal bonds (19). One percent by weight, sodium amalgams were prepared under N_2 by adding purified sodium to mercury which had been cleaned up using dilute acid and alkali rinses followed by vacuum distillation (177d). Sodium-Potassium alloy was freshly prepared before each reaction. Typically, Na,(10 mmol), K,(30 mmol) were melted together in a schlenk tube under nitrogen (131). The alloy was destroyed immediately after use with propanol under a nitrogen atmosphere.

Spectroscopic techniques

2.5.2.1 Vibrational spectra

Routine infrared spectra were run on a Shimadzu IR-27G or a Beckman IR 20A spectrophotometer. Detailed spectra were run on a Perkin Elmer 180. Gas phase spectra were run in 10 cm pathlength gas cells with kBr windows. Solution spectra were recorded in conventional KBr solution cells 0.1 mm pathlength and solids were recorded as nujol mulls. During this work the calibration of the PE 180 and wave number marker were checked against DCl in the CO region and found to be calibrated to within ± 0.2 cm^{-1}. The spectra reported here were not run under high resolution conditions, but are believed to be accurate to within ± 1 cm^{-1}.

Raman spectra were recorded at Auckland University on a J.A.S.C.O. R300 spectrometer using the green line (488 nm) of an argon ion 'control' laser operating at 25 mW. The samples were recorded in nmr tubes and required careful aligning (achieved using plasticine). Spectra reported here have been corrected for the 7 cm^{-1} calibration error.

The relative intensities reported in this work are taken from peak heights from interpolated baselines.

2.5.2.2 Mass spectroscopy

Mass spectra were recorded on a Varian CH5 spectrometer (with the electron beam of 70 eV) at the Ruakura Agricultural Research Centre. Samples were introduced into the spectrometer either *via* a gas inlet or *via* the solid insertion probe. During this work it was found that it was imperitive to keep both of the inlets as cool as possible. It was also found necessary to turn the ion source temperature as low as possible for sensitive samples. Air sensitive compounds of low volatility had to be protected by a nitrogen atmosphere during the insertion procedure. Again, an oxygen-free nitrogen-flushed plastic bag was employed to meet this requirement. A number of modifications were made to the mass spectrometer, particularly involving change to computer control. This, and the inexperience of the operator, has led to difficulties with all mass spectra run on compounds prepared in this research

2.5.2.3 Nuclear magnetic resonance spectroscopy

All spectra were run on a Jeol C-60HL spectrometer. Most samples were recorded in sealed tubes at 29°C. All starting materials were checked for purity by nmr before use. Benzene was used regularly as the solvent and reference Tetramethylsilane TMS was not employed as a reference since it overlaps with the resonance of methylgermyl protons, ($Ge-CH_3$). Chemical shift values reported here are calibrated with respect to benzene at 2.76τ. Carbon-13 facilities were not available.

2.6 Starting materials

2.6.1 Pentacarbonyliron(0) $Fe(CO)_5$

Commercial grade $Fe(CO)_5$ (Merck-Schuchard) was crudely purified by pumping away incondensible carbon monoxide and condensing the $Fe(CO)_5$ away from any $Fe_2(CO)_9$ into a separate tube. Because of its instability (toward heat and light) and toxicity $Fe(CO)_5$ was stored in a vacuum tight tube in a cool, dark, well-ventilated fume cupboard.

Any residues which could have contained $Fe(CO)_5$ were destroyed with bromine in alkali.

2.6.2 Decacarbonyldimanganese(0) $Mn_2(CO)_{10}$ and Octocarbonyldicobalt(0) $Co_2(CO)_8$

$Mn_2(CO)_{10}$ and $Co_2(CO)_8$ were obtained from Pressure Chemical Company, and were used directly.

2.6.3 Monogermane, GeH_4

A suspension of GeO_2 (10 g, 100 mmol), NaOH (20 g), $NaBH_4$ (18 g, 500 mmol) and H_2O (200 ml) was typically stirred for several hours to disperse the solid GeO_2. The suspension was then added dropwise to a 50% H_3PO_4 solution. H_2, GeH_4, Ge_2H_6, Ge_3H_8..., form instantly and boil ('bump') out of solution. There was sufficient hydrogen gas evolved to carry over Ge_3H_8. The volatile material passed over $CaCl_2$ into traps cooled to $-10^{\circ}C$ and $-196^{\circ}C$ (*ca*, four of these). Once all the GeO_2 had reacted, the

volatiles were recombined and fractionated through -45^{o}, -83^{o}, -120^{o} -196^{o} traps. GeH_4 (*ca* 70% yield) was identified by its infrared spectrum. Ge_2H_6 (*ca* 10 to 15%) and Ge_3H_8 were also obtained. This was a modification of the Drake, Jolly synthesis (167).

2.6.4 Methylgermane, $GeMeH_3$

$GeMeH_3$ was prepared by treatment of $GeCl_3Me$ (obtained from Laramie Chemicals, and which contained $GeCl_2Me_2$, 20%) with $LiAlH_4$ in Bu_2O. Hours of slow fractionations using propanol and propanol-ethanol slush baths resulted in head fractions of $GeMeH_3$ free from $GeMe_2H_2$ and $GeMe_3H$ impurities. Both nmr (168) and *ir* (169) were used to determine purity.

2.6.5 Dimethylgermane, $GeMe_2H_2$

$GeMe_2H_2$ was prepared by reaction of $GeCl_2Me_2$ with $LiAlH_4$. Batches of $GeCl_2Me_2$ (Laramie Chemcials, Lot 98) were found to contain up to 20% $GeCl_3Me$ impurity. The percent of each component was determined from the ratio of methyl protons in the nmr of a newly opened vial of $GeCl_2Me_2$. Again, nmr (168) and *ir* (169) spectra were used to determine purity.

In retrospect, it is probably less time-consuming to:

(i) prepare $GeCl_4$ (177a) then react this with MeMgI in stoichiometric amounts to try to achieve a relatively clean sample of the chloride before reduction is attempted.

(ii) Reduce GeH_4 in sodium ammonia and react the anion with MeI (177c).

2.6.6 Bromogermane $GeBrH_3$

$GeBrH_3$ was prepared by leaving bromine with GeH_4 (*ca*, 1:10 ratio) in a suspension of solid propanol in liquid nitrogen for 24 hours. The temperature warms up from -196° to -127°C during this time and permits this highly exothermic reaction to take place in a controlled fashion. (170a). An alternative method, (170b) that of reacting small portions of bromine with a large excess of GeH_4 at room temperature gives a poor yield of $GeBrH_3$; and $GeBr_2H_2$, and $GeBr_3H$ are also found in these reactions. $GeBrH_3$ was identified by its *ir* (171), nmr (172) and vapour pressure (148).

2.6.7 Bromomethylgermane, $GeBrMeH_2$ and Bromodimethylgermane, $GeBrMe_2H$

$GeXMe_2H$ was prepared according to the following equations (170, 173).

$$GeMe_2H_2 + Br_2 \longrightarrow GeBrMe_2H + GeBr_2Me_2 + HBr$$

$$GeMe_2H + HBr \longrightarrow GeBrMe_2H + H_2$$

$$GeMe_2H_2 + SnCl_4 \longrightarrow GeClMe_2H + HCl + SnCl_2$$

$GeXMeH_2$ was prepared in a similar manner. Reaction products were identified by infrared (174) and nmr (173) spectra.

2.6.8 Group IV metal chlorides, $M'Cl_4$ and hydrogen Chloride, HCl

HCl was prepared in the vacuum line by the reaction of concentrated H_2SO_4 on NaCl. Traces of HCl were crudely removed from Group IV chlorides by taking the middle cut of a sample. $SiClMe_3$ (bpt. 57°C) was freed from $(Me_3Si)_2O$ (bpt 100°C) by distillation under nitrogen.

2.6.9 Preparation of sodiumpentacarbonylmanganate (-I) $[NaMn(CO)_5]$

$NaMn(CO)_5$ was usually prepared in the reduction-coupling vessel, see Figure 2.1 A, page 68. Having evacuated the right-hand side of the reaction vessel, excess of 1% sodium amalgam, a solution of $Mn_2(CO)_{10}$ in Et_2O (*ca*, 20-50 ml) and a magnetic follower were placed in the left-hand side of the vessel in the glove box. The vessel was then removed from the glove box, the nitrogen pumped out of the left-hand side of the vessel and the solution stirred for one to three hours. The pale-green anion solution was then decanted away from the amalgam into the right-hand side of the vessel, the ether condensed back onto the amalgam, and any further anion decanted into the right-hand side of the vessel. The ether and any unreacted carbonyl were then pumped away leaving the white carbonyl anion (plus traces of amalgam) in the right-hand side of the reaction vessel ready for coupling.

2.6.10 Preparation of disodiumtetracarbonylferrate (-II), $[Na_2Fe(CO)_4]$

Typically, a deficit of $Fe(CO)_5$ (*ca* 8 mmol) was condensed into a *ca*, 0.1 moleℓ^{-1} solution of sodium (*ca*, 20 mmol) in ammonia. The mixture was then left at -45°C for 20 minutes. By this time, (sometimes with a little shaking) the blue colour was discharged, leaving a brown suspension. The solution was frozen with liquid nitrogen, incondensible gases were pumped away, and ammonia allowed to evaporate leaving a pale pink-to-brown $Na_2Fe(CO)_4$. The last traces of ammonia were removed by pumping the solid product at room temperature for 18 hours.

Experimental observations

In order to secure a good yield from the salt elimination reaction, the following points about the $Na_2Fe(CO)_4$ preparation were surmised:

(i) Contamination by oxygen-containing species (*e.g.*, Na_xO_y,) should be minimised.

(ii) Sodium ammonia solutions of concentrations less than 0.1 moleℓ^{-1} are preferable to more concentrated solutions.

(iii) Less than the stoichiometric quantity of $Fe(CO)_5$ (*ca* 0.8 times) is sufficient to react completely with the available sodium (as shown by the discharge of the intense blue colour).

$$0.8\ Fe(CO)_5 + 2Na \longrightarrow 0.8Na_2Fe(CO)_4 + \text{'}0.8CO\text{'}$$

(iv) As soon as the blue colour is discharged, the ammonia and any unreacted $Fe(CO)_5$ should be removed as quickly as possible.

(v) Long pumping times should be used to ensure complete removal of ammonia.

CHAPTER THREE

PREPARATION OF KNOWN SYMMETRICALLY SUBSTITUTED GERMYL IRON CARBONYLS VIA SALT ELIMINATION REACTIONS

$Fe(CO)_4(GeH_3)_2$, $Fe(CO)_4(GeMeH_2)_2$, $Fe(CO)_4(GeMe_2H)_2$, $Fe(CO)_4(GeMe_3)_2$, have been prepared. Apart from $Fe(CO)_4(GeMe_2H)_2$ these symmetrically substituted complexes have been used as starting materials to prepare unsymmetrical complexes of the type $Fe(CO)_4(GeMe_{3-x}H_x)(GeMe_{3-y}H_y)$. The preparation and spectra of the symmetrically substituted species are compared with literature data. The spectra of $[Fe(CO)_4(GeMeH)]_2$ and $[Fe(CO)_4(GeMe_2)]_2$ where these have arisen adventitiously from self reaction of $Fe(CO)_4(GeMeH_2)_2$ and $Fe(CO)_4(GeMe_2H)_2$ are also noted. Suggestions for the assignment of the unexpected product from reaction between $Fe(CO)_4^{2-}$ and $GeBr_2H_2$ are offered.

In this chapter, each reaction will be considered separately, experimental details will be given first, discussion and analysis of spectra will follow in later sections.

3.1 Experimental

3.1.1 Preparation of tetracarbonyldigermyliron, $[Fe(CO)_4(GeH_3)_2]$

Typically, $Na_2Fe(CO)_4$ (prepared as in section 2.6.10 from Na 365mg, 15.88 mmol, $Fe(CO)_5$ 1617mg, 8.25 mmol), $GeBrH_3$ (1307mg, 8.36 mmol) and pentane (4 ml) were allowed to react at room temperature with intermittent shaking for 20 minutes. The volatiles were then removed and fractionated. Unreacted $GeBrH_3$ and pentane were condensed back into the reaction vessel. After a further 20 minutes the volatiles were pumped out of the reaction vessel and roughly fractionated through traps at -196^{o}, -127^{o}, -63^{o}. Refractionation of the head fraction using -127^{o} and -196^{o} baths separates traces of pentane from GeH_4 (0.6 mmol). Slow refractionation of the lowest fraction using -45^{o} and -63^{o} baths maximises the product yield (2.70 mmol, 65%) while ensuring complete removal of $Fe(CO)_4H_2$. The -127^{o} fraction containing unreacted $GeBrH_3$ and pentane was recycled and used in other $Fe(CO)_4(GeH_3)_2$ preparations.

Table 3.1, page 79, outlines experimental conditions for similar $Fe(CO)_4(GeH_3)_2$ preparations. The first three entries in Table 3.1 are preparations by other workers.

TABLE 3.1

Experimental conditions for the preparation of $Fe(CO)_4(GeH_3)_2$

a $Fe(CO)_5$ (mmol)	b GeH_3X (mmol)	c Reaction time (min.)	d Yield (mmol)	Yield percent	$Fe(CO)_4(H)(GeH_3)$	ref
8.25	4.23	15	0.77	37%	9%	(26)
11.1	9.0	3	1.44	32%	obs.	(27)
1.69	3.79	25	0.59	34.9%*	obs.	(175)
4.8	7.14	7	1.7	48%	obs.	*
7.44	7.29	12	1.47	40%	-	(f)*
8.25	8.36	20	2.70	65%	-	(e)(f)*
9.44	14.0	30	3.81	54%	-	(e)(f)*
7.87	11.49	30	3.98	69%	-	(e)(f)*

(a) In all cases $Na_2Fe(CO)_4$ was prepared by Na/NH_3 reduction using this quantity of $Fe(CO)_5$

(b) X = Br : except (26) where X = Cl

(c) Reaction temperature = RT, solvent = Pentane (2-5ml) : except (26) where T = 0°C, solvent = butane (4 ml).

(d) Yield is based on GeH_3X used: except (175) where unreacted $Fe(CO)_5$ was recovered from the NH_3 and, in this case, an excess of GeH_3X was used.

(e) In these reactions unreacted GeH_3Br and pentane which had been fractionated away from the less volatile $Fe(CO)_4(GeH_3)_2$ was re-introduced to the reaction vessel and allowed to react for a further 20 minutes. The total yield from these reactions is quoted.

(f) nmr of the GeH_3Br used shows that these samples are free of HBr and GeH_2Br_2 impurity

* This work

obs. $Fe(CO)_4(H)(GeH_3)$ was observed.

3.1.2 Reaction of $Na_2Fe(CO)_4$ with a mixture of $GeBrH_3$ and $GeBr_2H_2$

In a trial run, a tail fraction containing $GeBr_2H_2$ as well as $GeBrH_3$, was reacted with $[Fe(CO)_4]^{2-}$ under the usual conditions. From infrared evidence, new species were present in the less volatile fractions but several attempts to isolate single components were unsuccessful. Reaction and/or self decomposition of the species in this mixture was evident as involatile yellow and orange material was being deposited from components initially trapped at -22° and -45°. Nmr analysis of the least volatile fraction which remained undecomposed showed that it was mostly $Fe(CO)_4(GeH_3)_2$ accompanied by a small amount of an iron hydride species. (17.6τ in benzene solution, *cf.* $Fe(CO)_4H_2$ 20.00 in C_6H_6 and $Fe(CO)_4(H)(GeH_3)$ 19.87 in $CDCl_3$ and C_6D_6 (27,26)). A cyclohexane extract of the involatile material in the -22° trap had infrared bands at 2108 w, 2080 s, 2049 m, 2034 vs, 2028 sh, 2020 sh, and 605 w cm^{-1}. A similar extract from the involatile material in the -45° trap showed infrared bands at 2091 w, 2080 s, 2049 w, 2036 s, and 604 w cm^{-1}. The nmr spectrum of a benzene solution of the involatile material in the second trap gives single peaks at 5.00τ , 5.95τ 6.51τ , (6.58 sh), 6.89τ (GeH_4)

3.1.3 Attempted preparation of $[Fe(CO)_4(GeH_2)]_2$

Na, (230 mg, 10 mmol) was placed in a trap and $Fe_2(CO)_9$, (2053 mg, 5.64 mmol) was placed in a side arm of the trap. $NH_{3(\ell)}$ (1 mole) was condensed onto the Na to give a blue solution. $Fe_2(CO)_9$ was then tipped onto the solution by rotating the bent side arm of the trap. The mixture was allowed to react for 15 minutes at -45^{o}. During this time the pressure built up. The tap adaptor lifted slightly to release excess gas. During the reaction, the solution changed to a deep brown-black colour. The NH_3 was evaporated off leaving a pale grey-orange solid and a few lumps of unreacted $Fe_2(CO)_9$. $GeBr_2H_2$, (6.75 mmol) with some $GeBrH_3$ impurity (*ca.*0.07 mmol) and pentane (10 ml) were added. The reaction vessel was left at room temperature for 30 minutes with intermittent shaking. Effervescence was noticed throughout this period. Volatiles were pumped out of the reaction vessel, crudely fractionated, and unreacted $GeBr_2H_2$ and pentane were condensed back and left to react overnight. Refractionation of the volatiles showed very little GeH_4, pentane and unreacted $GeBr_2H_2$ and $GeBrH_3$, $Fe(CO)_4(GeH_3)_2$, $Fe(CO)_4(H)(GeH_3)$ and a small amount of an unidentified fraction exhibiting νCO and δGeH frequencies. The least volatile fractions were combined in benzene and their ^1H nmr spectrum examined. The resulting thick yellow solution gave singlets at 3.59τ , 4.89τ , 5.86τ , 6.49τ $(Fe(CO)_4(GeH_3)_2$, and 6.86τ (GeH_4)

The residues left in the reaction vessel were extracted with C_6H_{12} (25 ml). Infrared values obtained from both C_6H_{12} and CS_2 solution are tabulated along with those obtained from section 3.1.2., see page 80 . No signal was obtained from a benzene solution of the orange residue . The mass spectrum of the residue is tabulated in Table 3.2 page 82. Reaction of a small amount of the orange material with nitric acid followed by addition of $AgNO_3$, gives a white precipitate.

TABLE 3.2

Mass spectrum of the orange residues obtained from section 3.1.3

Fragment ion assignment	envelope m/e	relative intensity	envelope *maxima*
$Fe_3(CO)_6Ge_3Br_3H_2^+$	804-788	vw	798
$Fe_3(CO)_5Ge_3Br_3H_x^+$	778-758	wm	770
$Fe_3(CO)_4Ge_3Br_3H_x^+$	748-730	w	742
$Fe_3(CO)_3Ge_3Br_3H_x^+$	720-706	wm	714
$Fe_3(CO)_2Ge_3Br_3H_x^+$	694-678	wm	686
$Fe_3(CO)Ge_3Br_3H_x^+$	666-650	w	658
$Fe_3Ge_3Br_3H_x^+$	640-622	w	632
$Fe_3(CO)_5Ge_3BrH_x^+$	616-596	m	610
$Fe_3(CO)Ge_3Br_2H_x^+$	588-564	m	574
$Fe_3(CO)_6Ge_3H_x^+$	564-548	w	556
$Fe_3(CO)_5Ge_2BrH_x^+$	540-532	w	536
$Fe_3(CO)_5Ge_3H_x^+$	532-518	m	528
$Fe_3(CO)_4Ge_3H_x^+$	512-490	wm	498
$Fe_3(CO)_3Ge_3H_x^+$	476-464	wm	470
$Fe_3(CO)_2Ge_3H_x^+$	448-436	m	442
$Fe_3(CO)Ge_3H_x^+$	421-407	m	415
$Fe_3(CO)_5GeH_x^+$	362-350	m	356
$Fe(CO)Ge_2H^+$	235-223	s	231

Weak ions were also observed at 195-189 w $GeFe(CO)_2H^+$, 181-175 w $GeBrC_2H_x^+$, 169-163 w $GeBrCH_x^+$. Strong envelopes were found at 157-149 $GeBrH_x^+$, 141-133s ?, 130-119 ?, 113-109 s Fe_2H^+, 100-93 $GeCH_x^+$. Very weak doubly-charged ions occurred at 236-230 vw $Fe_3Ge_3Br_3^+$, 226-221 vvw $Fe(CO)_3Ge_2Br_2^+$, 201-194 vw $Fe(CO)Ge_2Br_2H_2^+$

3.1.4 Preparation of $Fe(CO)_4(GeH_3)_2$ using $Na_2(Fe(CO)_4$ prepared *via* sodium amalgam reduction in THF.

$Fe(CO)_5$ (2107 mg, 10.75 mmol) was condensed onto excess 1% Na/Hg and THF (25 ml) and left stirring for 12 hours. Material (0.6 mmol) incondensable at -196°C was removed and the solution stirred a further 6 hours. Incondensable gases (0.2 mmol) were again removed and the orange-red solution was stirred for a further 48 hours. No further incondensable gas was evolved. The solution was then decanted from the amalgam. Volatiles were removed and the anion (pale yellow) was pumped for 18 hours. $GeBrH_3$, (1138 mg, 7.32 mmol) together with pentane (5 ml) was then introduced to the anion and the mixture was shaken for 10 minutes. The solution turned orange in colour. Incondensable (0.3 mmol), GeH_4 (0.2 mmol), pentane and $GeBrH_3$, $Fe(CO)_4(GeH_3)_2$ (541 mg, 1.67 mmol, 48%) and a less volatile oily yellow material were recovered. The tail fraction of $Fe(CO)_4(GeH_3)_2$ was, however, never totally freed from the yellow oil. White involatile solid remained in the reaction vessel. The gas phase infrared spectrum of the slightly volatile yellow material, although weak, showed three CO stretching modes at 2056 m, 2038 s, 2018 m cm^{-1}. This fraction was unstable under the infrared conditions used with the stretches initially doubling up, giving 2054, 2051 w; 2036, 2033 m; 2017, 2010 m cm^{-1}. The sample then decomposed completely.

Orange solid remaining in a trap which had previously contained the yellow oil gave absorptions at 2101 m, 2089 w, 2046 s, 2029 s, 2021 sh, 2008 s, 1995 m and 639 sh, 620s, 603 sh, cm^{-1} in C_6H_{12}. A very, very weak spectrum of the reaction vessel residues gave absorptions in C_6H_{12} at approximately 2066 m, 2020 vs and 1997 m cm^{-1}.

3.1.5 Characterisation of $Fe(CO)_4(GeH_3)_2$

In all cases $Fe(CO)_4(GeH_3)_2$ was identified by its characteristic infrared spectrum in the gas phase. Table 3.5, page 97, compares values from routine scans ($\pm$ 3 cm^{-1}) obtained in this work with those previously reported.

3.2 Discussion of some aspects arising from salt elimination reactions between $GeBr_xH_{3-x}$ / $Na_2Fe(CO)_4$

3.2.1 Comment on $Na_2Fe(CO)_4$ preparation with respect to further reaction with $GeXR_3$

(a) The sodium in liquid ammonia reduction

Key observations referring to the preparation of $Na_2Fe(CO)_4$ have been listed, Section 2.6.10, page 76. These observations seem reasonable in light of results obtained by other workers.

(i) It has been found that it is necessary to purify sodium prior to use to avoid alkali cleavage of M-Ge bonds.(19).

(ii) Less concentrated $Na/NH_{3(\ell)}$ solutions may help to avoid possible side reactions occurring (117)

e.g., $Na + CO \longrightarrow Na_6(CO)_6$

(iii) The reaction between Na and $Fe(CO)_5$ in $NH_{3(\ell)}$ is not stoichiometric (117,145). As $Fe(CO)_5$ is solid at -45^{o} condensing this in a fine film across the top of the frozen Na/NH_3 solution presumably helps avoid polynuclear anions.

(iv) Halting the reaction immediately the reduction has been effected may stop further side reactions from continuing.

(v) Removal of the last traces of NH_3 may help avoid side reactions occurring later on (125,126).

(b) Preparation by sodium amalgam in THF

As has been noted by other workers this method of reduction is slow (118,119). The pale colour of the anion indicates that polynuclear anions are not present. (See Section 2.1.1). The occurrence of the unexpected, and as yet unidentified, yellow oil, suggests that the THF has not been completely removed. (*cf.* Nicholson (192b) has found that after pumping on $Co(CO)_4^-$ for 2 hours at 50°C the sodium salt (similarly prepared from Na/Hg in THF) appears to be $NaCo(CO)_4.2THF$.) Another interesting feature is that no $Fe(CO)_4H_2$ was observed among the volatile products of the subsequent coupling reaction with $GeBrH_3$. This is in contrast to reactions where the anion was prepared by Na/NH_3 reduction where $Fe(CO)_4H_2$ was always observed. Reduction of $Ru_3(CO)_{12}$ or $Os_3(CO)_{12}$ in Na/NH_3 solution is thought to give rise to both $M(CO)_4H^-$, and $M(CO)_4^{2-}$, M = Ru, Os. (125,126). The absence of $Fe(CO)_4(H)(GeH_3)$ was also noted. This suggests that $Fe(CO)_4(H)_2$ arising from the coupling reaction, is actually an artifact of the anion preparation. Aside from the slow reduction and minor contamination by the less volatile material; $Na_2Fe(CO)_4.xTHF$ (?) appears to couple with $GeBrH_3$ to give a comparable yield (*ca.* 48% of $Fe(CO)_4(GeH_3)_2$.

3.2.2 Observations in $GeBrH_3/Na_2Fe(CO)_4$ reactions - Na/NH_3 reduction

It seemed odd that $Fe(CO)_4(SiH_3)_2$ could be prepared in up to 70% yield (23) *via* reaction between $SiIH_3$ and $Na_2Fe(CO)_4$ whereas the analogous reaction between $GeCℓH_3$ (26) or $GeBrH_3$ (27,175) and $Na_2Fe(CO)_4$ gave yields of the order 30% to 40% (see Table 3.1). But this work shows that there is no inherent difference or anomaly causing this. Indeed, yields of up to 69% $Fe(CO)_4(GeH_3)_2$ have been obtained by ostensibly the same reaction followed in previous reports.

A good deal of the $Fe(CO)_4(GeH_3)_2$ prepared in this work was obtained from reactions using recycled $GeBrH_3$ and pentane, hence, yields could not be accurately determined. However, useful observations were also gleaned from these 'batches'.

(i) Where unreacted GeH_4 was separated from the pentane and measured, it accounted for less than 10% of the total germanium used.

(ii) $Fe(CO)_4H_2$ was always observed where Na/NH_3 reduction had been used to reduce $Fe(CO)_5$, (No traces of $Fe(CO)_4H_2$ were observed in the volatile fraction from the coupling reaction between $GeBrH_3$ and $Na_2Fe(CO)_4$ where $Fe(CO)_4^{2-}$ had been prepared by sodium amalgam reduction.)

(iii) No C_6H_{12} soluble material was recovered from extraction of reaction residues where $Fe(CO)_4(H)(GeH_3)$ was not found in among the volatile components.

(iv) $Fe(CO)_4(H)(GeH_3)$ was not observed in preparations where the $GeBrH_3$ used had less than 1% HBr or $GeBr_2H_2$ impurity.

(v) Where more than 1% $GeBr_2H_2$ was used, both $Fe(CO)_4(H)(GeH_3)$ and higher molecular weight involatile carbonyl containing species were recovered.

(vi) In reactions where unreacted $GeBrH_3$ and pentane were added back into the reaction vessel for further reaction, the bulk of the $Fe(CO)_4(GeH_3)_2$ obtained had been synthesised in the first 15 to 20 minutes reaction time, *e.g.*, see Table 3.1, page 79, the yield 65% was actually made up of 3 reactions, the first 20 minutes yielding 51%, the second 20 minutes yielding 14% while the third 20 minutes yielded a barely detectable quantity.

From these experiments, it can be seen that yields from the coupling reactions are very sensitive to reaction conditions. An attempt will now be made to rationalise the above observations:

(i) Typically, little monogermane (*ca.*, 3%) was recovered from reactions, where the anions had been prepared from both Na/NH_3 and Na/Hg reductions. Its formation presumably is the result of a minor reaction path.

(ii) The presence of $Fe(CO)_4H_2$ may indicate $[Fe(CO)_4H]^-$ anions from the sodium ammonia reductions, although, one would also expect $Fe(CO)_4(H)(GeH_3)$. But, this is not always observed.

The two pieces of evidence which have led previous workers to suspect the occurrence of $[M(CO)_4H]^-$ species in sodium ammonia reductions are:

(a) The 8 infrared bands and 4 Raman bands of an aqueous solution of the cream coloured solid from Na/NH_3 reduction of $Os_3(CO)_{12}$ clearly indicates that the product is not solely $NaOs(CO)_4H$ or $Na_2Os(CO)_4$.

(b) The occurrence of 'substantial amounts' of $Os(CO)_4H(M'R_3)$ in reactions with a 1:1 ratio of $[Os(CO)_4]^{2-}$: $M'XR_3$ as opposed to 'minor formation' of $Os(CO)_4H(M'R_3)$ in reactions where a 1:2 ratio of $[Os(CO)_4]^{2-}$: $M'XR_3$ gave some authors (126) the impression that $[Os(CO)_4H]^-$ may well account for this. However, on looking more closely at the actually experimental details which were used, it would appear that there is not a consistent basis for comparison. Indeed, these authors conclude that "either $NaOs(CO)_4H$ or $Na_2Os(CO)_4$ and probably both, are formed on sodium reduction of $Os_3(CO)_{12}$ in liquid ammonia."

(iii) No involatile polymetallic, molecular species such as $[Fe(CO)_4(GeH_2)]_2$ can have been produced. (*cf.* Self reaction of the $Fe(CO)_4(GeMe_xH_y)_2$ complexes.)

(iv) Although it is a negative observation, it would appear that $Fe(CO)_4(H)(GeH_3)$ occurs only in reactions where HBr or $GeBr_2H_2$ are known contaminants, or at least, not specifically eliminated. HCℓ is known to react with $Fe(CO)_4(GeH_3)_2$ to give $Fe(CO)_4(H)(GeH_3)$ (26) and also germanium substituted species, *e.g.*, $Fe(CO)_4(GeCℓH_2)(GeH_3)$ (27) It seems probable therefore, that both $Fe(CO)_4(H)(GeH_3)$ and the concomitant involatile orange residues obtained can be interpreted as involving reactions with HBr.

(v) $GeBr_2H_2$ while seemingly innocuous, is known to be unstable at room temperature with respect to HBr elimination (148). An intermediate "$Fe(CO)_x(Ge_bBr_yH_z)$" species may also decompose to give HBr. Traces of HX in the reagents used in example (ii) above may have been partly responsible for the presence of $Os(CO)_4(H)(M'R_3)$.

(vi) It has been previously reported (26) that longer reaction times lead to the formation of more $Fe(CO)_4H_2$ and lowered yields of germyl iron species.

3.2.3 Contrasting the reactions $Na_2Fe(CO)_4$ and $GeBrH_3$ (Na/Hg reduction) and $Na_2Fe(CO)_4$ and $GeBrH_3$ (Na/NH_3 reduction)

In contrast to reactions where Na/NH_3 reduction was used to prepare $Na_2Fe(CO)_4$, no $Fe(CO)_4H_2$ (nor $Fe(CO)_4(H)(GeH_3)$) was observed from the coupling reaction where $Na_2Fe(CO)_4$ had been prepared by sodium amalgam reduction. It would therefore seem that $[Fe(CO)_4H]^-$ and/or traces of $NaNH_2$? may in some way be responsible for the formation of $Fe(CO)_4H_2$ in the sodium ammonia preparations. It is curious that $Fe(CO)_4(H)(GeH_3)$ is not concomitant with the presence of $Fe(CO)_4H_2$. As traces of unidentified yellow subliming material are less easily removed than $Fe(CO)_4H_2$, sodium ammonia is the preferred method for reducing $Fe(CO)_5$.

3.3 The nature of involatile orange solid from reactions involving $GeBr_2H_2$

3.3.1 The mass spectrum of the involatile orange material formed in reactions with $GeBr_2H_2$

The mass spectrum of the orange reaction residues from the preparation described in Section 3.1.3, page 81, is summarised in Table 3.2, page 82. The highest molecular weight envelope is ascribed to $Fe_3(CO)_6Ge_3H_3Br_3^+$. Envelopes arising from stepwise loss of CO are observed. Another series of lower molecular weight ion envelopes is attributed to ions of the type $Fe_3(CO)_{6-x}Ge_3H_y^+$ X = 0 to 5. It is difficult to formulate a reasonable compound if the $Fe_3(CO)_6Br_3H_3^+$ ion is the parent ion. However, it is reasonable to postulate a trimeric species $[Fe(CO)_3(\mu\text{-}GeBrH)]_3$ where P^+ and $(P\text{-}nCO)^+$ (n=1,2,3) are too weak to be observed.

A characteristic feature of the mass spectrum of many $M_a(CO)_xM'_bR_y$ species are low-intensity parent ions: for example, for many $[M(CO)_4M'R_2]_2$ species P^+ is missing or very much weaker than $(P\text{-}CO)^+$. This feature is not uncommon, also, for the parent $M_a(CO)_x$ species (193), see Figure 3.1

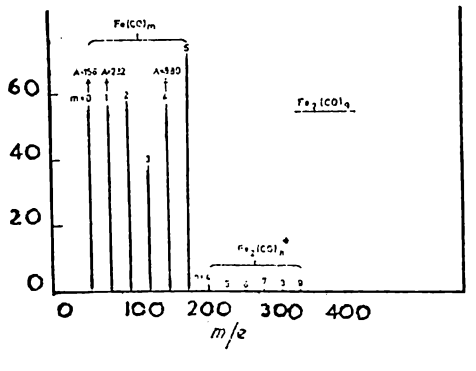

FIGURE 3.1

The mass spectrum of $Fe_2(CO)_9$

Parent molecular ions are known for $[M(CO)_3(M'R_2)]_3$ compounds (44,108b). Fragmentation patterns were not included in these reports.

Alternative assignments of the mass spectrum are less convincing. Thus, if the compound is formulated as $Fe_2(CO)_8Ge_3Br_3H_3$, the parent ion is observed (as the resolution used does not distinguish Fe from two CO). However, the observation of the fragment ions corresponding to the loss of seven or eight carbonyl groups would be expected. In the spectrum obtained in this work, loss of only six CO groups from the highest molecular weight ion was observed. Another possibility is the addition of, for example, CO to a lower molecular weight parent ion, (*e.g.*, $Fe_2(CO)_6(GeBrH)_3$) during the mass spectroscopic handling. The existence of $(P + nCO)^+$ has been claimed but is rare (186) and not well substantiated. Such a process is not known to have occurred in any of the numerous metal carbonyl derivatives prepared in this department and run on the same mass spectrometer. A third alternative, loss of a $M'R_y$ group *e.g.*, from a higher molecular species such as $Fe_3(CO)_xGe_4Br_yH_x^+$? is thought to be equally unlikely as the metal-metal skeleton usually remains intact. Indeed, $M_aM'^+_b$ is commonly found as the base peak in $M_a(CO)_xM'_bR_y$ mass spectra.

However, even if it is granted that $[Fe(CO)_3(GeBrH)]_3$ is the most reasonable species to ascribe to the observed mass spectrum, this may not have been the original product. As the spectrum was obtained only after the sample had been heated above 100°C, the possibility of rearrangement in the mass spectrometer source cannot be ruled out. Indeed, on further heating, the pressure rose and the highest apparent mass observed dropped to *ca.*, $m/e \simeq 500$. In a third stage of heating, ions from new species appeared with an apparent mass, m/e >800

and an extensive series of envelopes at $m/e \doteq 12$ units apart. Despite the warnings implicit in these latter observations, the trimer is regarded as the best choice as a tentative attribution.

3.3.2 The infrared spectrum of the orange solid

The most striking features of the infrared spectrum of the orange residues are the values for the νCO modes. These frequencies fall between those of Fe-GeH_x species and those of Fe-$GeBr_2$ species.

It is well known that replacement of R groups by halogens on M' shifts the νCO bands to higher energy. This evidence tends to support the mass spectral assignment of -GeBrH moieties as opposed to -GeH_2 or -$GeBr_2$. The values in Table 3.3, page 93 , show some variation among different samples, suggesting the presence of extra minor components. However, the characteristic features are bands at 2035 cm^{-1}, 2080 cm^{-1} and 2050 cm^{-1}, decreasing in intensity in that order, together with the mode at 604 cm^{-1}. A weaker band near 2090 cm^{-1} is also probable, though not observed in sample a.

If we compare these values with those expected for the various formulae suggested in the discussion of mass spectra above, two significant points emerge. The first is that the average CO stretching frequency lies between the values expected for Fe-GeH_x species and those for Fe-$GeBr_2$ compounds, thus the frequencies are compatible with monobromo groups such as μ-(GeBrH). Secondly, the number of modes is compatible with those predicted for all the possible molecules, Table 3.4 page 94.

TABLE 3.3

Infrared spectra of involatile orange residues obtained in reactions between $GeBr_2H_2$ and $Na_2Fe(CO)_4$

A C_6H_{12}	B C_6H_{12}	C C_6H_{12}	D CS_2	$[Fe(CO)_4(GeBr_2)]_2$ C_6H_{12} e
2108 w				
		2096 vw	2093 sh	
	2091 w	2092 m	2091 m	2093 vs
		2086 vw	2085 w	
2080 s	2080 s	2082 vs	2080 s	
		2060 sh		2058 s,sh
				2054 s,sh
2049 m	2049 w	2052 s	2049 s	2052 vs
2034 vs	2035 vs	2035 vs	2035 vs	
2028 sh		1989 m		
2020 sh				
605 w	604 w	604 m	604 s	

A Involatile in -22° trap see section 3.1.2., B Involatile in -45° trap see section 3.I.2
C Extraction of reaction vessel residues, section 3.1.3. D Reaction vessel residues in C redissolved in CS_2
e reference (45)

TABLE 3.4

Predicted number of CO stretching modes for candidates of the orange residues

Proposed formula	Structural type	Symmetry group	Predicted infra-red modes
$[Fe(CO)_3(GeBrH)]_3$	*24*	C_{3v}	$3a_1 + 3e$
$Fe_2(CO)_8(GeBrH_x)_3$	linear	C_{2v} or less	7 - 8 modes
$Fe_2(CO)_8(GeBrH)_3$	*22*	C_{2v} or less	up to 8 modes
$Fe_2(CO)_6(GeBrH)_3$	*17*	ψ-D_{3h}, true C_s	up to 6 modes
$Fe_2(CO)_6(GeBrH)_2(GeBrH_2)_2$	*18*	C_{2v} or less	up to 6 modes

The relatively simple spectrum would be unexpected for possible linear octacarbonyl formulations. We also note that other trimers, $[M(CO)_3(M'R_2)]_3$ in the literature show three strong and two weaker bands:

$[Os(CO)_3(GeMe_2)]_3$: 2052 s, 2043 w, 2014 s, 2008 w, 1984 s, (108b)

$[Os(CO)_3(SiMe_2)]_3$: 2054 s, 2039 w, 2016 vs, 2008 w, 1984 s (108b)

$[Ru(CO)_3(GeMe_2)]_3$: 2046 s, 2038 w, 2017 s, 2011 w, 1986 m (44)

$[Ru(CO)_3(GeBu_2)]_3$: 2042 m, 2034 w, 2012 s, 2006 w, 1983 m (44)

3.3.3 Parallels with literature data

Other physical comparisons can be drawn between the major component of the orange residue, $[Fe(CO)_3(GeBrH)]_3$?, and compounds of the type suggested in Table 3.4, page 94. For instance, the ruthenium and osmium species $[M(CO)_3(M'R_2)]_3$ are all reported to be robust (44,108b), whereas $Fe_2(CO)_8(GeBrH)_3$, *22*, is known to be very unstable (106). Few linear structures are known. (*cf.* structure *26* and *27*, page 5). None of this type are known by this author for iron, although attempts have been made to prepare these (21,68).

Taking this stability into consideration, the fact that only two bands, (are perhaps?) unseen in the infrared and that it is very common to find very weak parent envelopes in mass spectra of these compounds, the most reasonable suggestion for the identity of the bulk of the orange involatile material is $[Fe(CO)_3(GeBrH)]_3$. As can be seen in Section 2.1.3, salt elimination reactions do not always yield the product which was aimed for. Attempts to synthesise cobalt, molybdenum, tungsten, and iron species of the type $[M(CO)_x]_2SnH_2$, and $[M(CO)_x]_3SnH$ by the reaction,

$$[M(CO)_x]_2Sn\,Cl_2 + 2(i\text{-}Bu)_2AlH \longrightarrow [M(CO)_x]_2SnH_2 \qquad (21)$$

were unsuccessful. The manganese analogues however, have been prepared in good yield *via* this method. So even though Aylett has successfully prepared $[Mn(CO)_5]_2SiH_2$ and $[Co(CO)_4]_2SiH_2$ derivatives *via* salt elimination of $M(CO)_x^-$ with SiI_2H_2, the iron congeners $[Fe(CO)_4]_2(GeH_2)_x$ may be unstable with respect to further reaction. That this is seen to be the case in these reactions is evident from the deposition of involatile

material in the -22^{o} and -45^{o} traps during fractionation of the volatile material from reactions between $Fe(CO)_4^{2-}$ and $GeBr_2H_2$.

It is not inconceivable that further reaction of a species of the type $Fe(CO)_xGeBr_yH_z$ may be initiated by the ready elimination of HBr, (*cf.* $GeMe_xH_{3-x}$ elimination in $Fe(CO)_4(GeMe_{3-x}H_x)_2$ species.)

Although $Fe(CO)_4(GeH_3)_2$ is stable with respect to self condensation reaction at room temperature, heating at $55^{o}C$ for several days is reported (27) to give, as well as unreacted starting material, $[Fe(CO)_4(GeH_3)]_2$, $[Fe(CO)_3(GeH_2)]_3$ (and possibly $FeGe_3O_2H_2^+$, $Fe_2Ge_2O_3H_2^+$ or Ge_4O^+ ?). Evidence for these species was by mass spectroscopy since no proton nmr signals of the brown solid were observed, and the infrared spectrum was dominated by unreacted $Fe(CO)_4(GeH_3)_2$. From the shape of the envelopes, a series of ions attributed to $Fe_3(CO)_nGe_3^+$ (n = 6 to 0) was observed. The apparent absence of hydrogen is not unexpected in these envelopes as H loss is concomittant with loss of several CO groups in germyl transition metal carbonyl derivatives.

3.4 The vibrational spectrum of $Fe(CO)_4(GeH_3)_2$

Infrared spectra have been reported for $Fe(CO)_4(GeH_3)_2$ in the gas phase (26,27) and in cyclohexane solution (27), while Raman spectra have been measured in the solid phase (27) and in solution (26). Data from these studies together with gas phase infrared data collected in this work is given in Table 3.5, page 97, (see also Figure 1.7, page 22).

TABLE 3.5

The vibrational spectrum of $Fe(CO)_4(GeH_3)_2$ (cm^{-1})

Infrared				Raman	Assignment
(a)	(b)	(c)	(d)	(e)	
		2110.7wsh			combination ?
2101s	2100s	2100.1s	2091.5s	2099s**	νCo_{ax} (a_1)
			2084.5w,sh		$\nu^{13}CO_{ax}$
2060s,sh		2083-2058w,br	2072-2042w,br		νGeH
			2033m,br,sh		νCO_{eq} (a_1)
		2047.7sh R		**	
2042vvs	2046-vvs(f) -2041	2044.6vvs Q 2041.5sh P	2024.3vs	2042 vs	νCo^{+}_{ax} (b_2)
		2024 w,sh			
2022vs	2020vs	2020.5vs	2008.5vvs	2023s,sh**	νCO_{eq} (b_1)
		1995vw ?	1987.6w		$\nu^{13}CO$
	1983w	1983w	1974.2w		$\nu^{13}CO$
1954w					
890w				890w** 870vw**	δGeH_3 ($2b_1+b_2$)
838R)	)				
835Q)vs	833)vs		827s		δGeH_3 (a_1)
831P)	)				
812R)	)				
809Q)vs	808)vs		801s		δGeH_3 (a_1)
805P)	)				
728w	726w		744w,br		$\delta FeCO$ or δGeH_3
628vs	627vs		625.7vs		$\delta FeCO$ (a_1)
			529vw,br		ρGeH_3
			435w	436vs,p*	νFeC (a_1)
		229w		229vs,p*	$\nu GeFe$ (a_1)
		216m		216m *	$\nu GeFe$ (b_1)
				105vvs*	$\delta CFeC$ $\delta CFeGe$

See Figure 1.7, page 22 , νCO region (27)
(a) reference (26), gas phase
(b) this work, routine scan ($\pm 3 cm^{-1}$)
(c) reference (27), gas phase, region 900-400 cm^{-1} not re-examined.
(d) reference (27), C_6H_{12} solution.
(e) Raman values recorded in C_6H_{12}* (26) or as a solid** (27).
(f) very intense, unresolved.

The 2000 cm^{-1} region

The νCO modes in Table 3.5 are as expected for a *cis* derivative (see Section 1.4.2.2, page 18) : note the different labels compared with reference (26) where the x and y axes were reversed. Shoulders around 2060 cm^{-1} have been assigned as the νGeH modes in $Fe(CO)_4(GeH_3)_2$ by comparision with the assignment of bands at 2070 - 2055 cm^{-1} in $Co(CO)_4(GeH_3)$ (30) which were established by comparison with $Co(CO)_4(GeD_3)$. In spectra of the germyl carbonyls, $Mn(CO)_5(GeH_3)$ (31), $Re(CO)_5(GeH_3)$ (50) $Co(CO)_4(GeH_3)$ (30), $Fe(CO)_4(H)(GeH_3)$ and $Fe(CO)_4(GeH_3)_2$ (26) the Type-A gas phase contours show rotational structure with a prominent Q branch and noticeably weak P branch. They have polarised Raman counterparts and are assigned as totally symmetric vibrations (31). This rotational fine structure is also seen in silyl derivates, *e.g.* the νSiH, three νCO, and two νSiH_3 all show type-A contours; the *maxima* of these absorptions all having shoulders both to higher frequency and to lower frequency of *ca* 4 cm^{-1}. The ρSiH_3, δMCO, and νMCO modes do not show this fine structure in $Fe(CO)_4(SiH_3)_2$ (23a).

GeH_3 deformation modes

In related molecules, the GeH_3 deformations were assigned as follows: for $Mn(CO)_5(GeH_3)$, 885 sh, 887 m, (a' + a") and 818 s (a'); for $Re(CO)_5(GeH_3)$ 885 w,br, (a' + a") and 817 s (a'); and for $Co(CO)_4(GeH_3)$, 881 w (e) and 810 vs (a_1). In each case, the strong band in the 820-810 cm^{-1} region corresponds to the symmetric deformation of the GeH_3 unit. If the δGeH_3 modes in $Fe(CO)_4(GeH_3)_2$ are independent of one another, then the GeH_3 deformations would be expected to be similar to those of the monosubstituted germyl carbonyls. If, however, the δGeH_3 modes interact, five infrared active modes would be predicted,

$2a_1 + 2b_1 + b_2$. These modes would arise from the in-phase and out-of-phase combinations of the GeH_3 deformations. Perhaps the best eivdence for the interaction of the δGeH_3 modes is the two strong bands in the 820 cm^{-1} region with clear type-A contours. (Figure 3.2).

FIGURE 3.2

Routine scan of the 950-770 cm^{-1} region in $Fe(CO)_4(GeH_3)_2$

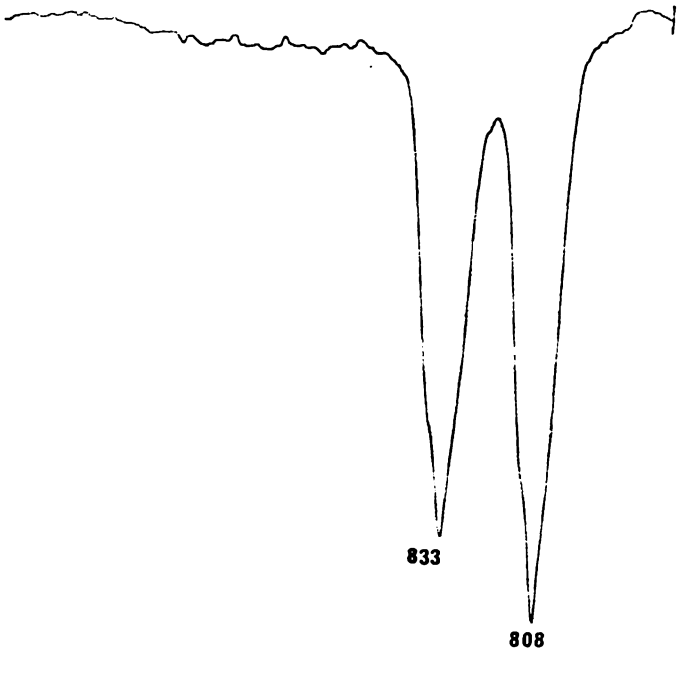

These are assigned as the in- and out-of-phase combinations of the symmetric GeH_3 deformations.

Aylett (23a) on observing two δSiH_3 at 924 and 898 cm^{-1} in $Fe(CO)_4(SiH_3)_2$ comments that these modes are split almost symmetrically about 913 cm^{-1}, the δSiH_3 value in $Fe(CO)_4(H)(SiH_3)$. This is approximately the same situation as in the germyl analogues, where the symmetric deformation in $Fe(CO)_4(H)(GeH_3)$ occurs at 821 cm^{-1}. The gas phase

infrared spectrum of $Fe(CO)_4(GeH_3)(SiH_3)$ (173) is also very interesting in this region. Bands occurring at 962 vw, 954 vw and 831 w, 822 mw, 807 mw have been attributed to the δSiH_3 and δGeH_3 modes respectively. Another interesting observation made by Aylett *et al.*, (23a) was that in disilyl compounds with a large angle between the Si groups *e.g.*, $(SiH_3)_2O$ 144°, and $(SiH_3)_2$ NH, 128°, only one strong band is assigned to the silyl deformation, while compounds with a smaller angle *e.g.*, $(SiH_3)_2S$ 97°, and $(SiH_3)_2Se$ 97°, show two strong bands of nearly equal intensity. In compounds of the type $M(CO)_4(M'R_3)_2$ the M'MM' angles are typically in the range *ca.* 112°-90° (12,82,83). Symmetric in-phase and out-of-phase $\delta M'H_3$ deformations are therefore not an unreasonable assignment of the two type-A contour bands in compounds of the type $M(CO)_4(M'H_3)_2$

FeCO deformations and FeC stretches

For C_{2v} geometry the δFeCO and νFeC modes are predicted to be $2a_1 + 2a_2 + 2b_1 + 2b_2$ ($6ir$, $8R$, $2R$p) and $2a_1 + b_1 + b_2$ ($4ir$, $4R$, $2R$p) respectively. As only two or possibly three absorptions appear in this region (*ca* 750-350 cm^{-1}) out of the expected ten modes, assignment of these bands will not be pursued. δMnCO and νMnC modes have been assigned to the 672 m, 663 vs, cm^{-1} and 474 m, 410 w cm^{-1} modes in $Mn(CO)_5(GeH_3)$ and $Mn(CO)_5(GeD_3)$ (17) respectively.

In $Fe(CO)_4(GeH_3)_2$ two strong bands have been assigned as: 628 cm^{-1} δFe(CO) a_1, 436 cm^{-1} νFeC a_1, a weak band at 728 cm^{-1} was assigned as δFeCO.

Fe-Ge Stretches

For a *cis* complex, two νFeGe fundamentals are predicted, $a_1 + b_1$ ($2ir + 2R$, one Rp). For a *trans* D_{4h} complex $a_{1g} + a_{2u}$ would be predicted (*i.e.*, one *ir* + one *R*p and no coincidences). As the two infrared bands assigned as νFeGe are coincident with two Raman bands, one of which is polarised, this is further evidence for C_{2v} geometry. Stobart (26) mentions that the a_1 mode is at higher frequency (229 cm^{-1} *cf.* b_1 at 216 cm^{-1}) and this is the reverse order of the νM'-M' stretches in polysilanes and germanes.

Little data exists for transition metal carbonyls. Stobart cites one example where the a_1 mode is higher than the b_1: $Fe(CO)_4(HgX)_2$, and mentions that in other cases the reverse applies (26).

3.5 Preparation of Bis(methylgermyl)tetracarbonyliron(0), $Fe(CO)_4(GeMeH_2)_2$

3.5.1 Experimental details

$Na_2Fe(CO)_4$, (Na 371mg, 16.16 mmol: $Fe(CO)_5$ 1289 mg, 6.57 mmol), $GeBrMeH_2$, (1980 mg, 11.68 mmol), and pentane (5 ml) were allowed to react at room temperature for 20 minutes. Incondensible (0.04 mmol) and other volatile products were pumped out of the reaction vessel. Unreacted $GeBrMeH_2$ and pentane were reintroduced to the reaction vessel. After a further 20 minutes the reaction vessel was pumped for two hours. The product which was still in the reaction vessel, was then transferred into a U-tube (using the diffusion pump to maintain a lower vacuum) and weighed. $Fe(CO)_4(GeMeH_2)_2$, 855 mg, 2.46 mmol, was recovered (42% yield) $GeMeH_3$ (*ca* 1.41 mmol) was found together with unreacted $GeBrMeH_2$ and pentane. C_6H_{12} extraction of residues in the reaction vessel gave $[Fe(CO)_4(GeMeH)_2]_2$. Identification of all species was by infrared spectroscopy.

3.5.2 Characterisation of $Fe(CO)_4(GeMeH_2)_2$

The infrared data of $Fe(CO)_4(GeMeH_2)_2$ prepared in this work is tabulated along with data from previous reports (29,178) of this compound; Table 3.6, page 103. The vibrational spectrum of $Fe(CO)_4(GeMeH_2)_2$ reported by Bonny (29), looks suspiciously similar to that of $Fe(CO)_4(GeH_3)_2$ in the νCO region. Recent work by Jager (178) gives alternative vibrational data, see Table 3.6. Data obtained in this work compares well with that of Jager (178).

It appears that the spectra of $Fe(CO)_4(GeMeH_2)_2$ and $Fe(CO)_4(GeH_3)_2$ may have been confused by Bonny. Further comment will be made on the validity of the alternative vibrational data in Section 5.5.2.

TABLE 3.6

The vibrational spectrum of $Fe(CO)_4(GeMeH_2)_2$ cm^{-1}

Infrared					Raman	Assignment †
gas (29)	gas this work	gas (178)	C_6H_{12} (178)	solid (178)	liquid (29)	
2119m,sh						)
	2089m	2090(5)	2082(6)	2084(7)	2086m,p	) νCO_{ax}, a_1
2101s						)
			2051sh(1)			) νGeH ?
2042vs					2040w,sh	)
	2030vs	2031(10)	2015(9)	2021(10)	2014s	) νCO_{ax} b_2 +
						νCO_{eq} a_1
2020m						)
	2007s	2007(9)	1996(10)	1986(10)	2009vs	) νCO_{eq} b_1
1985w,sh	1985w	1992(1)	1977			$\nu^{13}CO$
		1972	1962	1954		$\nu^{13}CO$
873sh	876w	879(2)	874(2)	873(2)		δGeH_2 a_1
			857(1)	858(2)		δGeH_2 b_1 ?
846)	842)	843(3)	838(1)	839(2)		)
837)vs	836)m					) ρCH_3 + δGeH_2 b_1
829)	831	833(4)	823(2)	823(2)		)
					700vvw	
683m	693w	684(1)	690	687(2)		) GeH_2 wag,
					658vvw	)
639w	643w	643(2)	639	651(2)		) in) out) of phase
	615m	617(4)	613(3)	620(4)	620vw	$\delta FeCO$ a_1
					591m,p	
580s	583w	583(2)	579(1)	585(2)	583m	νGeC a_1+ b_1
535vw	*no.*	542		539	539m	) $\delta FeCO$, ρGeH
		525				) $\nu FeCO$ a_1
485vw			477	488vw	490vw,p	)
440vw			454		448 m,p	) $\delta HGeMe$
			409,388	415vvw		
					225s,p	) $\nu FeGe$ a_1
					210s	) $\nu FeGe$ b_1
					113vs,sh	)
					103vvs	) $\nu CFeGe, \delta C_2Fe$
					58vw	$\delta FeGe_2$

(29 See reference (29)

* $Fe(CO)_4(GeMeH_2)_2$ was unstable in gas cells which had been previously used for recording $M(CO)_xGeR_y$ species.

(178) See reference (178), here the intensity of the strongest absorption is (10) other values are labelled with respect to this peak.

no. Region not observed.

† Assignment as in (178)

page 214 , along with comparison of vibrational data from other $Fe(CO)_4(GeMe_{3-x}H_x)(FeMe_{3-y}H_y)$ species.

The proton nmr spectrum of $Fe(CO)_4(GeMeH_2)_2$ in benzene consists of a quartet centred at 6.13τ and a triplet at 9.51τ , $^3J_{HGeCH}$=3.4 hz. This is compared with data from other workers in Table 3.7, page 104.

TABLE 3.7

Nmr data of $Fe(CO)_4(GeMeH_2)_2$

τCH_3 (ppm)	τGeH_x (ppm)	$^3J_{HH}$ (H_3)	Solvent	reference
9.31	6.18	3.75	CS_2 + 2%C_6H_6	(178)
9.27	6.22	3.8	CS_2	(29)
9.28	6.21	3.8	CS_2	(178)
9.51	6.13	3.4	C_6H_6	this work

The mass spectrum of $Fe(CO)_4(GeMeH_2)_2$ was not recorded in this work, but has been reported elsewhere (29,178).

3.5.3 Characterisation of $[Fe(CO)_4(GeMeH)]_2$ recovered by extraction of reaction vessel residues

$[Fe(CO)_4(GeMeH)]_2$ was characterised spectroscopically.

The mass spectrum, though weak because of instrumental difficulties, agrees with previous observations (26) as shown in Table 3.8, page 106.

A poor ^1H nmr spectrum was observed, probably because of traces of paramagnetic impurity, but broad signals occurred in the appropriate Ge-H and Ge-Me regions.

For the infrared spectrum, data are available from two previous workers (27,148) and are compared with experimental values obtained in this work, Table 3.9, page 107. The carbonyl stretching region is shown in Figure 3.3, page 108.

The vibrational spectrum of $[Fe(CO)_4(GeMeH)_2]_2$

Bonny (29) found two sets of signals in the ^1H nmr spectra of his sample of $[Fe(CO)_4(GeMeH)]_2$, which he attributed to the C_{2v} (both Me groups on same side of ring) and C_{2h} isomers present in a 3:1 ratio. However, neither electronic nor mechanical coupling between the two $Fe(CO)_4$ moieties is likely to be significantly changed by the relative orientation of the GeMeH units. Thus, the observed frequencies of the two isomers may be very close in energy, and the in-phase modes which are allowed for the C_{2v} isomer may be very weak. Thus the observed spectra may not be distinguishable from those expected from GeR_2 species such as $[Fe(CO)_4(GeMe_2)]_2$ (43,72), of D_{2h} symmetry.

TABLE 3.8

The mass spectrum of $[Fe(CO)_4(GeMeH)_2]_2$

assignment	Apparent mass, m/e	relative intensity y=2		apparent mass m/e	relative intensity y=1	
		a	(26)		a	(26)
$Fe_2Ge_2(CO)_8Me_yH_x^+$	520-508	-	w	504-494	-	vw
$Fe_2Ge_2(CO)_7Me_yH_x^+$	490-480	s	vs	476-466	-	vw
$Fe_2Ge_2(CO)_6Me_yH_x^+$	464-450	m	s	447-437	-	w
$Fe_2Ge_2(CO)_5Me_yH_x^+$	434-422	m	s	420-406	-	vw
$Fe_2Ge_2(CO)_4Me_yH_x^+$	406-394	m	s	390-378	-	vw
$Fe_2Ge_2(CO)_3Me_yH_x^+$	378-364	s	vvs	363-352	-	w
$Fe_2Ge_2(CO)_2Me_yH_x^+$	350-338	s	vvs	335-325	-	w
$Fe_2Ge_2(CO)Me_yH_x^+$	322-308	w	ms	310-297	vw	mw
$Fe_2Ge_2Me_yH_x^+$	294-282	s	vs	299-266	vs	vvs
Other fragments include;						
$Fe_2Ge_2^+$	264-250	vs	vvs			
$FeGe_2Me^+$	220-210	w	ms			
$FeGe_2^+$	206-198	w	ms			
Fe_2Ge^+	188-182	vw	w			
$GeC_2H_2^+$	107-100	w	m			
$GeCH_2^+$	91-84	w	mw			

(26) also showed additional vw ions including doubly-charged species and a vvw, br, *ca* 431 metastable ion attributed to the process $Fe_2(CO)_7Ge_2Me_2H_2^+ \rightarrow Fe_2(CO)_6Ge_2Me_2H_2^+ + CO$

a This work

TABLE 3.9

The infrared spectrum of $[Fe(CO)_4(GeMeH)]_2$: cm^{-1}

This work C_6H_{12}	(.178) C_6H_{14}	(27) C_6H_{12}	Assignment
	2088		$Fe(CO)_4(GeMeH_2)_2$
2067 w	2068 (1)	2067 vw	νGeH ?
		2063 vvw	
2060 s	2060 (9)	2060 vs	νCO_{ax}, b_{1u}
	2046 vw	2055 vw,sh	$\nu^{13}CO$, νGeH ?
	2036 vvw	2035 vw,br	
2022 mw	2023 (2)	2022 mw	νCO b_{2u} ?
		2018 vw	
2012 sh	2012 sh (9)	2012 vs	
2008 vs	2009(10)	2008 vvs	νCO_{ax}, b_{3u}
		2002 vw,sh	
1977 br,sh	1997 br,sh	1981 vvw	νCO_{eq}, b_{1u} ?
1972 vw	1973 vw	1972 vw	$\nu^{13}CO$
	n.o.	662 w	
622		623 m	
613		613 ms	δFe CO
603		603 mw	
n.o.		523 vw, 514 vw	

(178) See reference (178)

(27) See reference (27)

n.o. region not observed

Assignments are based on D_{2h} symmetry in the νCO region

Figure 3.3

The carbonyl infrared spectrum of $[Fe(CO)_4(GeMeH)]_2$, C_6H_{12} : cm^{-1}

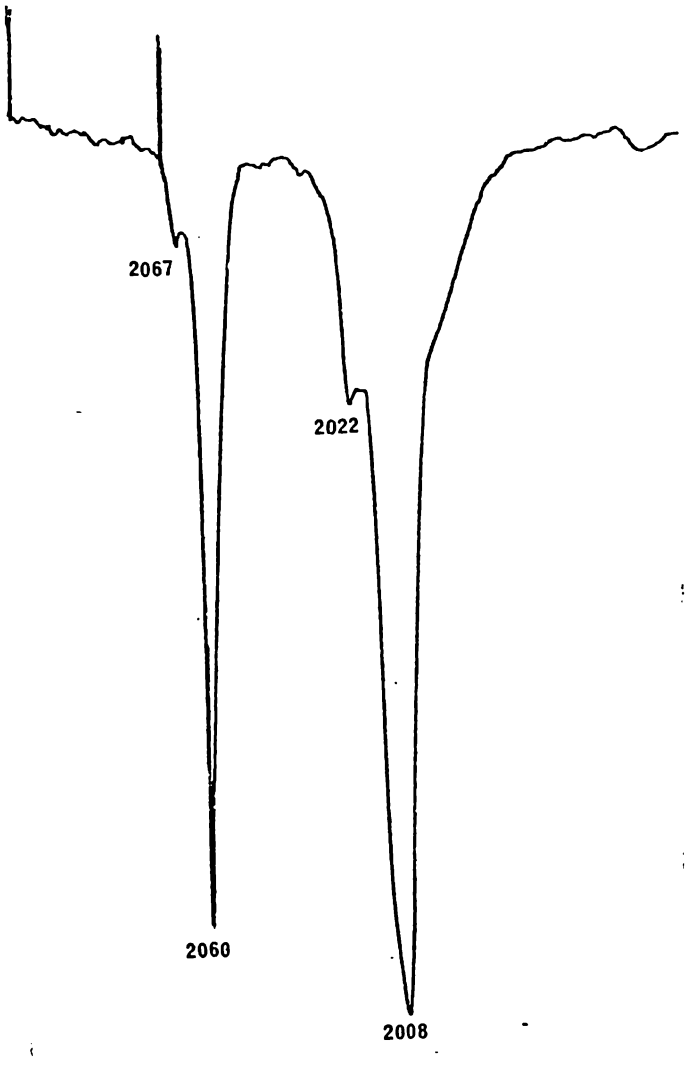

With these factors in mind, the data from this study shown in Table 3.9, page 107, must be interpreted cautiously. The values compare well with those found for D_{2h} molecules, and thus give no evidence for a mixture of isomers nor can a choice of one isomer versus the other be justified. Observations, in this work also match those reported by Jager (178), allowing for slight contamination of his sample by $Fe(CO)_4(GeMeH_2)_2$. Bonny's data (27), Table 3.9, page 107, clearly indicates a substantial number of additional *maxima*, all of which are very weak. These would be compatible with the presence of a second isomer.

Unfortunately, the ^1H nmr spectrum of the sample from this work was poorly resolved so supporting evidence is not available. However, the most justified conclusion from the infrared data is that while Bonny's sample does give evidence for isomers, these preparations and Jager's (178) seem to produce a sample which is predominantly of the C_{2h} isomer only. These samples differ only slightly in origin - Bonny's arose from the self-reaction of pure $Fe(CO)_4(GeMeH_2)_2$ while this sample comes from the original preparation.

3.5.4 Review of the $Fe(CO)_4(GeMeH_2)_2$ preparation

This preparation is interpreted as,

$$2GeBrMeH_2 + Fe(CO_4^{2-} \rightarrow Fe(CO)_4(GeMeH_2)_2 \quad \ldots 1$$

(42% recovered)

$$2Fe(CO)_4(GeMeH_2)_2 \longrightarrow 2GeMeH_3 + [Fe(CO)_4(GeMeH)]_2 \quad \ldots 2$$

(11% $GeMeH_3$ recovered)

where the percentage figures are based on the original amount of $GeBrMeH_2$, (some was unreacted but could not be measured since it was recovered mixed with a large amount of pentane). If the yield of the dimer is taken as stoichiometric with the yield of $GeMeH_3$, then 64% of the original Ge is accounted for. This compares well with typical yields of 20% and 40% $Fe(CO)_4(GeMeH_2)_2$ reported previously (29,178). The maximum yield reported 56% (178) was secured by intermittently pumping the product out of the reaction vessel, fractionating the product mixture and re-introducing unreacted $GeBrMeH_2$ and pentane back into the reaction vessel. The total reaction time was 4½ hours. It was noted (29,178), that the rate of product formation decreases as the reaction proceeds.

Yields of the $-GeMeH_2$ derivative are lower than those of $Fe(CO)_4(GeH_3)_2$, but this is to be understood not as a function of the inappropriate synthetic route, but as an inherent characteristic of the product which, unlike the GeH_3 compound, undergoes self-reaction; see equation ...2. Because of the self-reaction of $Fe(CO)_4(GeMeH_2)_2$ optimisation of yields requires minimum reaction vessel residence time of the product together with maximum reaction time. Purity of starting materials is also very important. It may also help (27) to reduce exposure to light.

3.6 Preparation of bis(dimethylgermyl)tetracarbonyliron(0), $Fe(CO)_4(GeMe_2H)_2$

3.6.1 Experimental details

$Na_2Fe(CO)_4$, (Na 418 mg, 18.18 mmol; $Fe(CO)_5$ 1572 mg, 8.02 mmol), $GeC\ell Me_2H$, (2123 mg, 15.25 mmol) and $CH_2C\ell_2$ (10 ml) were shaken for 20 minutes at room temperature. Incondensible gases (0.05 mmol), $GeMe_2H_2$, $CH_2C\ell_2$ and $GeC\ell Me_2H$ were pumped out of the reaction vessel. After pumping (diffusion pump) the reaction vessel for 6 hours, $Fe(CO)_4(GeMe_2H)_2$, (486 mg, 1.29 mmol, *ca* 17% yield) was condensed into a U-tube trap held at -196°C.

An attempt was made to transfer the product to an nmr tube attached to a U-tube (see Figure 2.1, page 68). However, $GeMe_2H_2$ appeared to be the major component of the volatile material condensing into the *nmr* tube trap, and an orange solid had precipitated out of solution in the weighed trap. The nmr spectrum of this sample, after most of the $GeMe_2H_2$ had been pumped away, showed that a doublet centred at 9.66τ was rapidly decomposing while a broad multiplet centred around 6.34τ increased. Peaks at 9.55τ, 9.50τ, and 9.24τ were also evident. The peak due to $Fe(CO)_4(GeMe_2)_2$ was very minor. The solvent used was benzene.

The reaction vessel residues were extracted with $CH_2C\ell_2$ (15 ml), the $CH_2C\ell_2$ was pumped off and the remaining green solid was pumped on. More colourless-to-yellow oily product was obtained, (about a third as much again as the above).

The above manipulations were performed on a warm, sunny day. Attempts to exclude light from the product were not extensive. However the blinds were closed, no artificial lighting was on, and the reaction vessel and traps were wrapped in aluminium foil and dust cloths.

Extraction of the green solid that did not sublime, was identified as $[Fe(CO)_4(GeMe_2)]_2$ by its infrared spectrum.

3.6.2 Preparation of $[Fe(CO)_4(GeMe_2)]_2$

$Na_2Fe(CO)_4$ (Na 261 mg, 11.38 mmol), $GeCl_2Me_2$ (950 mg, 5.47 mmol) and THF (*ca.*, 15 ml) were reacted at room temperature. The volatile material was removed in vacuo and the orange-green residue was extracted with C_6H_{12} (*ca.* 25ml). No further purification was made. The product was characterised by its infrared spectrum. See Table 3.10, page 113. and Figure 3.4, page 114; mass spectrum, see Table 3.12, page 121, and a singlet in the nmr spectrum at 8.90τ in benzene.

3.6.3 Characterisation of $Fe(CO)_4(GeMe_2H)_2$

3.6.3.1 The ^1H nmr spectrum

$Fe(CO)_4(GeMe_2H)_2$ was most clearly identified by the strong doublet centred on 9.41τ and the weaker heptet centred around 5.83τ, $^3J_{HGeCH}$ = 3.2 Hz relative intensities 6:1, in benzene. (*cf.* 9.36τ, 6.02τ, $^3J_{HGeCH}$ = 3.4Hz in CS_2 (30)). $GeMe_2H_2$ and $[Fe(CO)_4(GeMe_2)]_2$ (8.90τ in benzene *cf.* 8.85τ in CS_2 : C_6H_6 solution (30) and 8.7τ in C_6H_6 (43)) and a small shoulder at *ca* 9.55τ were also present in these samples.

TABLE 3.10

The infrared spectrum of $[Fe(CO)_4(GeMe_2)]_2$, cm^{-1}

This work cyclohexane	(72) n-hexadecane	(43) hydrocarbon	(26) cyclohexane	tentative assignment
2060 sh		2061 s	2057 vw,sh[c]	
2052 vs	2053		2053 vs	νCO_{ax}, b_{1u}
			2048 vw,sh	$\nu^{13}CO_{ax}$, in-phase
2040 w			2030 vw,br,sh	
2025 w			2025 w,sh[c]	
			2009 w,sh	
		2007 vs		
2001 vvs	2000		2001 vvs	νCO_{ax}, b_{3u}
1988 m	1987[b]			νCO_{ax}, b_1
			1999 w,sh[c]	
			1993 w,sh	
1977 vw			1978 w	)
1963 vw			1964 w	) $\nu^{13}CO$
			1949 w	) out-of-phase
			796 mw	ρCH_3
no.	628 w[a]			
	620 vs		625 ms	$\delta FeCO$
	600 vs			
	554		614 s	
	514 w			
	470 m, 460 mw			
	430		430 vw,br	νFeC

See references (72), (43), (26).

a KBr disc. Note also, that $Fe(CO)_4(GeMe_2)_2$ is sensitive to aerial decomposition.

b Increased with time.

c Absorptions attributed to $Fe_2(CO)_7(GeMe_2)_2$

no Region not observed.

Figure 3.4

The carbonyl infrared spectrum of $[Fe(CO)_4(GeMe_2)]_2$: cm^{-1}

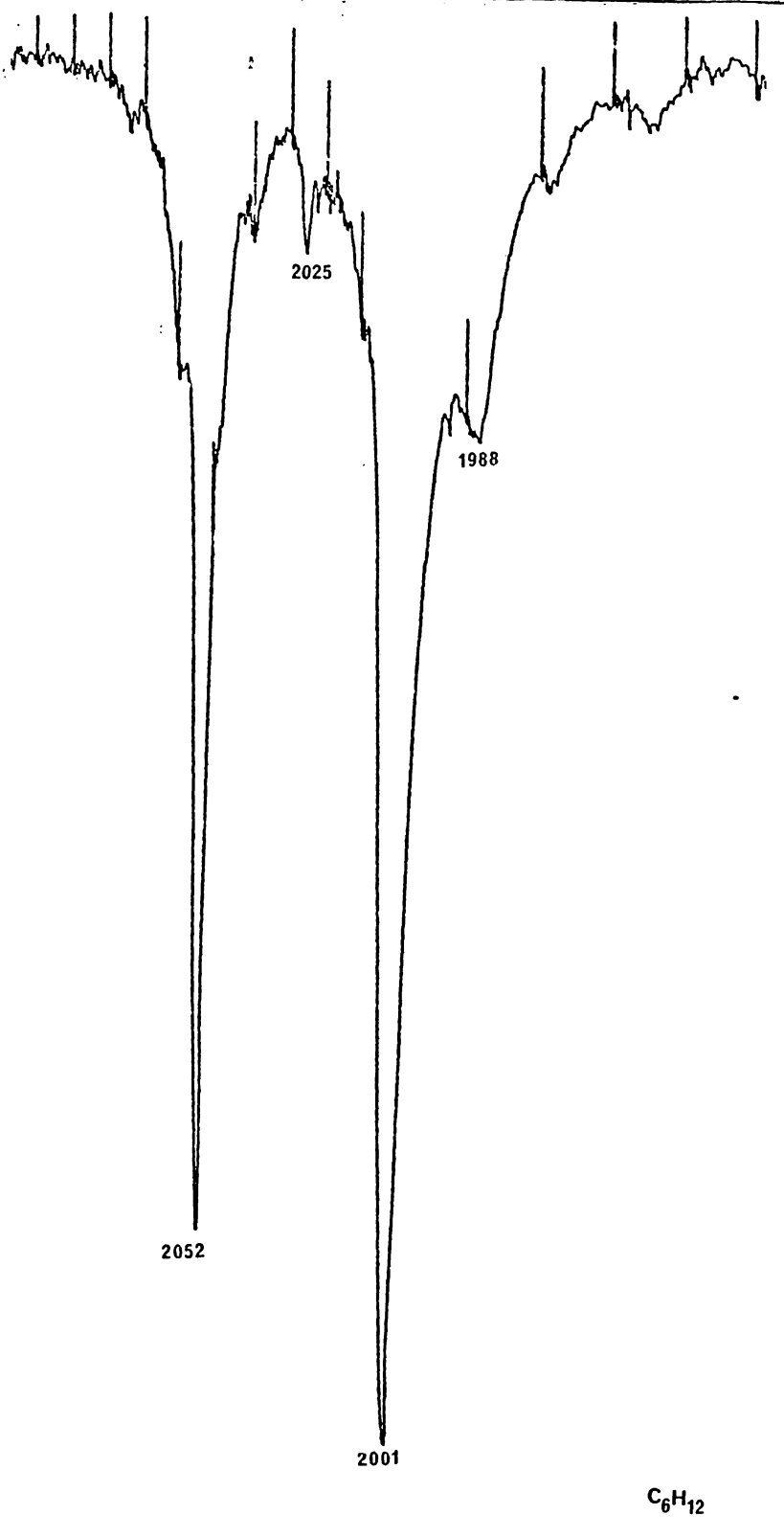

Samples for infrared solution and nmr studies were prepared simultaneously under nitrogen. The nmr samples were stored at -196° while the infrared spectra were being recorded.

3.6.3.2 The infrared spectrum of $Fe(CO)_4(GeMe_2H)_2$

The carbonyl stretching region of the infrared was recorded in hexane and appears to be a mixture of $Fe(CO)_4(GeMe_2H)_2$ and $[Fe(CO)_4(GeMe_2)]_2$, see Figure 3.5, page 116. Table 3.10, page 113, compares cumulated infrared data for $[Fe(CO)_4(GeMe_2)]_2$ from previous work with values obtained in this work. The values for the νCO region after subtraction of the νCO of $[Fe(CO)_4(GeMe_2)]_2$ occur at 2073 s, 2007 vs, and 1988 vs in hexane. These are thought to be the a_{11} (*ax*), and $a_{12} + b_2$ and b_1 (*eq* ,) νCO modes of an isomer containing C_{2v} symmetry.

These observations contrast with the previous report (30) that gas phase and solution phase spectrum for this compound could not be obtained due to its ready self reaction. However, "by condensing the sample directly on to a KBr plate cooled by liquid nitrogen, it was possible to observe the infrared spectrum of the solid free from any reaction product apart possibly, from $GeMe_2H_2$" (30). Figure 3.6, page 118 shows the actual νCO region obtained. Table 3.11, page 117, lists data from other regions obtained (30). However, this spectrum is so complex that comparison with the solution spectrum obtained in this work is meaningless. It is not unexpected to find extra modes arising from crystal effects. Further, it was suggested that different conformational isomers may have been frozen out in this case (27). See also

Figure 3.5

The carbonyl infrared spectrum of $Fe(CO)_4(GeMe_2H_2)$ together with $[Fe(CO)_4(GeMe_2)]_2$: cm^{-1}

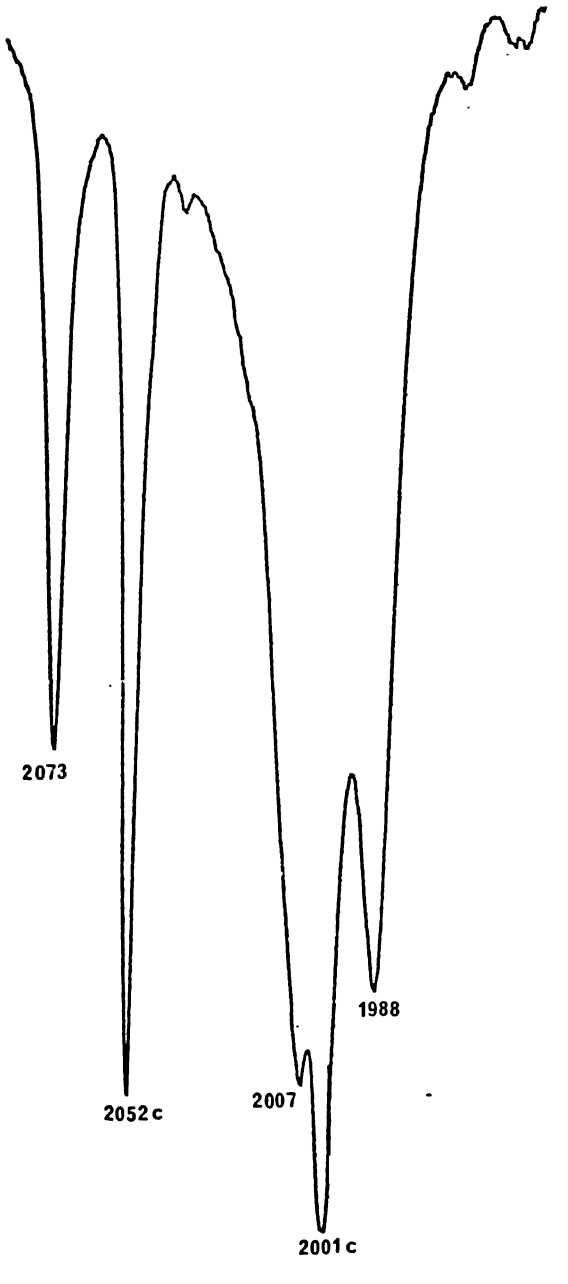

c = absorptions due to $[Fe(CO)_4(GeMe_2)]_2$

TABLE 3.11

The infrared spectrum of $Fe(CO)_4(GeMe_2H)_2$ cm^{-1}

C_6H_{14} solution this work [a]	annealed solid reference (30) [b]	Tentative assignment [c]
	2095 mw	)
	2083 vw,sh	)
	2077s, sh	)
2073 m, a,	2074s	) νGeH)
2052 vs*	2055w	))
2025 w,sh*	*ca* 2025 s,br	) νCO
2007 $s,a_{12} + b_2$		)
		)
		)
2001 vvs*	1991 vs	)
		)
1988 $ms*b_1$	1977 br,vvs	)
	1962 mw,sh	)
		)
	1942 w	) $\nu^{13}CO$
	875 w	)
	ca 852 vw,sh	) ρCH_3
	842 m	)
	823 w	)
	795vw,750br,	) GeH deformations
	725 w	)
	695-675 w	
	643 w	)
623s*	623vw,sh	) δFeCO
614vs*	609vs	)
	586w,sh	) νGeC
	574 m	)
	534vw	
	444vw	) νFeC

a See Figure 3.5, page 116 and Figure 3.4, page 114.
b See Figure 3.6, page 116
c Assignment is as for reference (30).
* Absorptions due to $[Fe(CO)_4(GeMe_2)]_2$ occur at these positions.

Figure 3.6

The carbonyl infrared region of $Fe(CO)_4(GeMe_2H)_2$; solid film (27,30)

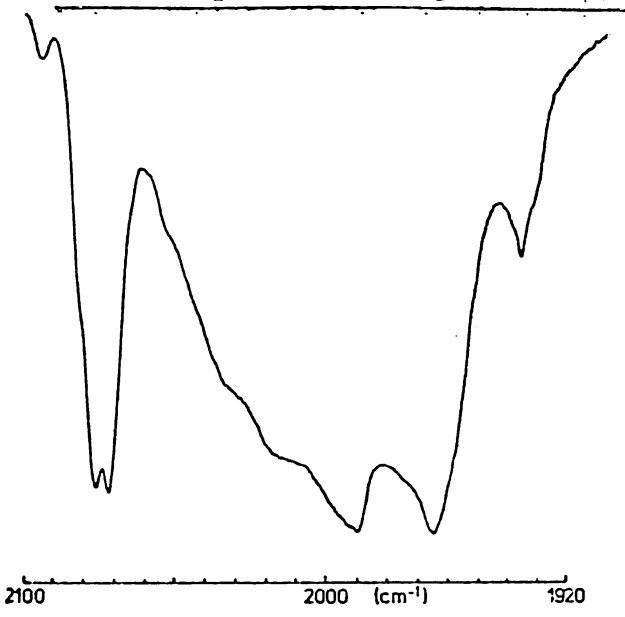

A; Un-annealed sample at *ca* -196° (27)

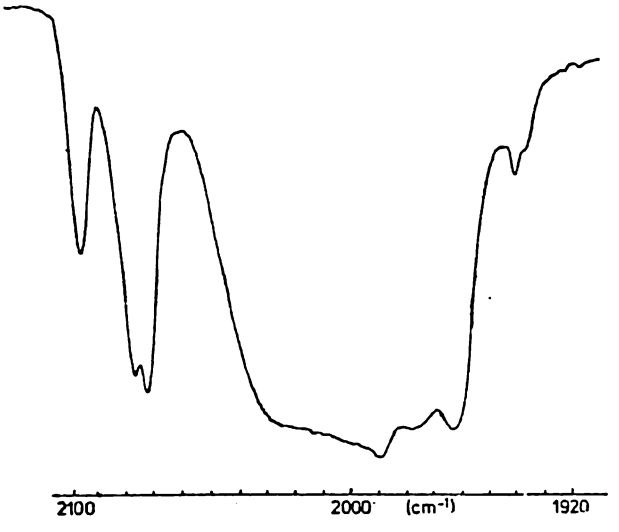

B; Another un-annealed sample of $Fe(CO)_4(GeMe_2H)_2$ in the 2000 cm^{-1} region (27)

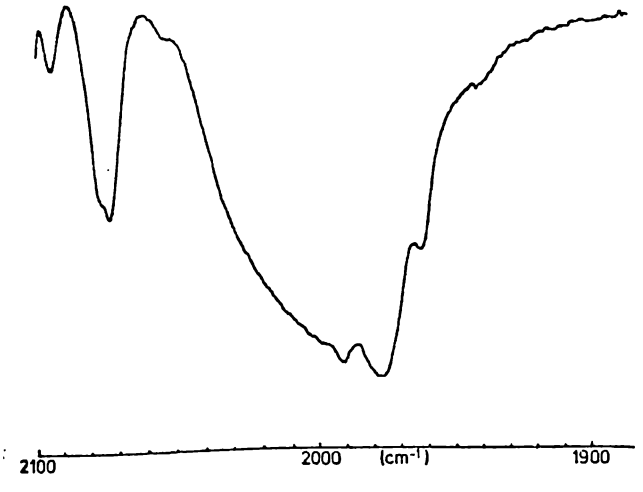

C; The infrared spectrum recorded in the 2000 cm^{-1} region for a sample of $Fe(CO)_4(GeMe_2H)_2$ which had warmed from -196°C and then been re-frozen (27)

section 5.5.2. page 214, where data from symmetric and unsymmetrically substituted species, has been collated.

3.6.4 Comment on the preparation and handling of $Fe(CO)_4(GeMe_2H)_2$

From this one experiment, at least 20% yield of $Fe(CO)_4(GeMe_2H)_2$ was obtained by reacting $Na_2Fe(CO)_4$ and $GeC\ell Me_2H$ in dichloromethane. In contrast, Bonny (30) found only two successful runs yielding on one occasion 6% and on another 8%, out of a large number of attempts where $Na_2Fe(CO)_4$ and $GeBrMe_2H$ were allowed to react in pentane. An alternative solvent (but not a weakly-basic solvent, see Section 2.2, page 49) was sought for this reaction since it was clearly obvious that the corresponding $Na_2Fe(CO)_4$ and $GeC\ell Me_3$ or $SiC\ell Me_3$ formed suspensions rather than solutions in hydrocarbons. As $CH_2C\ell_2$ was seen to solve this problem in the $Na_2Fe(CO)_4/GeC\ell Me_3$ system, it was tried here. There were initial fears that $CH_2C\ell_2$ may take part in the reaction, since $CC\ell_4$ and $CHC\ell_3$ chlorinate Ge-H in most metal carbonyl derivatives. However, as the average yield from reaction in pentane was around zero to one percent, it was thought that it was well worth the risk. There was no indication of Ge-Cℓ species in this run. It should be noted here too, that the reactions between $Na_2Fe(CO)_4$ and $GeBrH_3$ and $GeBrMeH_2$ are also probably surface reactions because these systems are not homogeneous either. One suggestion for low product yield could be lack of reaction. In the numerous attempts to prepare $Fe(CO)_4(GeMe_2H)_2$ (30) it is not stated whether unreacted $GeBrMe_2H$ is recovered from these preparations. Certainly unreacted halogermanes were always obtained (even when a marked deficit was used) after reaction with $Na_2Fe(CO)_4$ in this work.

Initially, it was thought that $Fe(CO)_4(GeMe_2H)_2$ might be more stable once it was in a clean tube, away from reaction residues. This however, was not the case, as an attempt to condense the product into an nmr tube resulted in the precipitation of an orange solid in the bulk sample and the evolution of $GeMe_2H_2$. If the product had been undergoing self-reaction in the reaction vessel at a similar rate as it did in the weighed tube, then this author surmises that the amount of product initially made would be well in excess of 60%. The rapid rate of decomposition in the U-tube may have been accelerated by having the sample in a confined area. As a neat liquid sample, self-reaction may be faster than when the product is splattered around the walls of the reaction vessel.

3.6.5 The infrared spectrum of $[Fe(CO)_4(GeMe_2)]_2$

Values found in this work agree well with those found by other workers, see Table 3.10, page 113. The νCO region has been assigned as previously reported (59), although a different set of axes has been chosen in this work (see Figure 1.11, page 27).

3.6.6 The mass spectrum of $[Fe(CO)_4(GeMe_2)]_2$

The major portion of the ion current in the mass spectrum of $[Fe(CO)_4(GeMe_2)]_2$ is carried by fragments of the type $Fe_2(CO)_nGe_2Me_4^+$, see Table 3.12, page 121. The series of ions $Fe_2(CO)_nGe_2Me_3^+$ is also evident but the series $Fe(CO)_nGeMe_2^+$ is represented only in the case when $n = 3$.

TABLE 3.12

The mass spectrum of $[Fe(CO)_4(GeMe_2)]_2$

tentative assignment	apparent mass m/e	relative intensity y=0		aparent mass m/e	relative intensity y=1	
		a	b		a	b
$Fe_2(CO)_8Ge_2Me_{4-y}^+$	546-536	vvvw	w	531-521	-	w
$Fe_2(CO)_7Ge_2Me_{4-y}^+$	520-504	s	vs	504-494	vw	m
$Fe_2(CO)_6Ge_2Me_{4-y}^+$	492-478	s	svs	476-465	w	m
$Fe_2(CO)_5Ge_2Me_{4-y}^+$	462-451	m	m	448-436	w	mw
$Fe_2(CO)_4Ge_2Me_{4-y}^+$	436-420	m	s	420-408	-	w
$Fe_2(CO)_3Ge_2Me_{4-y}^+$	408-394	vs	vvs	392-376	-	w
$Fe_2(CO)_2Ge_2Me_{4-y}^+$	380-364	s	s	364-352	-	w
$Fe_2(CO)Ge_2Me_{4-y}^+$	352-336	s	s	335-325	m	w
$Fe_2Ge_2Me_{4-y}^+$	324-310	s	s	308-294	m	m
$Fe_2Ge_2Me_{2-y}^+$	292-280	m	m	278-264	s	vs
$FeGe_2Me_{2-y}^+$	236-222	vw	w	221-208	m	ms
$Fe(CO)GeMe_{1-y}^+$	174-168	-	vvw	162-154	-	vw
$FeGeMe_{1-y}^+$	147-138	-	mw	133-126	-	w
$Fe_2Ge_2^+$	264-250	s	s			
$Fe(CO)_3GeMe_2^+$	246-240	m	mw			
$FeGe_2^+$	206-196	w	mw			
$FeGeMe_3^+$	202-194	m	m			
Fe_2Ge^+	188-180	m	m			

Several week ions occur at lower m/e values, *e.g.* $GeMe_2^+$, $GeMe_3^+$, $Fe_2/Fe(CO)_2^+$, $GeMe^+$, $Fe(CO)^+$, $FeMe^+$,

(a) This work, pre-recorded and stored on computer file.
(b) See reference (27) recorded directly.
(c) Note that H loss from Me groups also occurs especially in lower molecular weight ions from which CO has already been eliminated.

3.7 Preparation of bis(trimethylgermyl)tetracarbonyliron(o) $Fe(CO)_4(GeMe_3)_2$

3.7.1 Experimental detail

$Fe(CO)_4(GeMe_3)_2$ was prepared by the salt elimination route as previously described for $Fe(CO)_4(GeMe_xH_y)_2$ species. Specific details of experimental conditions are listed in Table 3.13.

TABLE 3.13

Experimental conditions for the preparation of $Fe(CO)_4(GeMe_3)_2$

$Fe(CO)_5$ (mmol)	$GeClMe_3$ (mmol)	Reaction time (mins)[c]	Percent yield*
9.8	24.7	15	[a]
7.44	21.6	20	>50%[b]
7.69	18.6	15	48%
10.6	14	45	70%

* yields were proportional to sublimation time.

a Yield not measured. Handling problems and oxygen contamination meant that the white sublimed product turned brown and oily the instant the sublimation probe was withdrawn from the reaction vessel in the nitrogen flushed glove box.
b First sublimation only recorded.
c RT, CH_2Cl_2 (10-15 ml)

After reaction, the volatile products were pumped out of the reaction vessel. Little incondensible gas (*ca.* 0.02 mmol) was observed. The least volatile species included $Fe(CO)_5$ together with traces of unidentified species which were not stable in the infrared conditions used.

Extraction of the residues in the reaction vessel with $CH_2C\ell_2$ (*ca*, 30 ml), gave $Fe(CO)_4(GeMe_3)_2$ as wine-coloured through to brown-coloured solutions. Sublimation of the oily wine/brown coloured extract after the solvent was removed yielded white crystals of $Fe(CO)_4(GeMe_3)_2$. Traces of oxygen in handling the product gave initially a green tinge to the white crystals; on further contamination a brown oil appeared where the crystals had been. On trying to transfer the product into an nmr tube attached to a U-tube (using the diffusion pump) it was noticed that traces of a white involatile air stable solid was formed, and yellow $Fe(CO)_5$ was produced.

The intractable air stable white solid remaining was insoluble in C_6H_{12} and $CH_2C\ell_2$, and may be an oxide species.

3.7.2 Characterisation of $Fe(CO)_4(GeMe_3)_2$

$Fe(CO)_4(GeMe_3)_2$ was initially identified by its infrared spectrum. Table 3.14, page 125, compares values obtained in this work with those obtained by others. Figure 3.7, page 126, shows the carbonyl stretching region of the infrared spectrum of $Fe(CO)_4(GeMe_3)_2$. Clearly, again the solution spectra gave more easily interpreted information than the spectrum of an un-annealed low-temperature film (181).

Although early samples of $Fe(CO)_4(GeMe_3)_2$ decomposed in the mass spectrometer, a mass spectrum was eventually recorded where the temperature of the ion source had been turned as low as possible and the water cooling on the probe turned back on, see Table 3.15, page 127. Assignments of spectra are as for (181) and follow the general pattern for these complexes.

$Fe(CO)_4(GeMe_3)_2$ shows up as a singlet at 9.43τ in benzene (*cf.* 9.39τ in CS_2 (181)).

3.7.3 Reviewing the $Fe(CO)_4(GeMe_3)_2$ preparation

$Fe(CO)_4(GeMe_3)_2$ has been made (181) in 9% yield by reaction of $[Fe(CO)_4]^{2-}$ and $GeC\ell Me_3$ in pentane. Unreacted $GeC\ell Me_3$, $(Me_3Ge)_2O$, $GeMe_3H$, $Fe(CO)_5$ and $Fe(CO)_4(H)(GeMe_3)$ were also identified in the reaction (181). In this work a more polar solvent, $CH_2C\ell_2$ and longer reaction times are thought to be major factors resulting in the greatly improved yields. Once prepared, $Fe(CO)_4(GeMe_3)_2$ can be kept in daylight at room temperature under nitrogen for several months without any obvious signs of decomposition. $Fe(CO)_4(GeMe_3)_2$ is however, rapidly decomposed by even a trace of oxygen. The low volatility and decomposition under high vacuum precludes vacuum line manipulation of this compound.

TABLE 3.14

The vibrational spectrum of $Fe(CO)_4(GeMe_3)_2$; cm^{-1}

Infrared				Raman	Assignment
this work C_6H_{12}	this work nujol	a C_5H_{12}	(181)c Solid	(181)b Liquid	e
			2970vw	2980 mw,br	)
					) νCH
			2910 w	2908 w,br	)
			2089 w		)
					) νCO
			2061 w,sh		)
2065 s	2068 m	2067 s	2056 s	2067 w,p	νCO a_1
			2046 w,sh		$\nu^{13}CO$
			2013 mw		)
					) νCO
			1995 mw		)
					)
			1981 w		)
2003 s	2003 m	2005 s	1971 mw		νCO_{ax} b_2 (a_{12})
2000 m	2000 sh	2000 m,sh	1953vbr,sh		νCO_{eq} a_{12}(b_2)
1980 vs	1980 s	1983 vs	1941 vs		νCO_{eq} b_1
1946 vw	1946 vw		1918 w		$\nu^{13}CO$ out-of-phase
			1242 vw,sh	1245 vw,sh	)
					) δCH_3 Symmetric
			1226 w	1232 w	)
	819 m		832 vw,sh		)
					)
	809 m		829 mwbr		)
					) ρCH_3
	737 w		819 w,sh		)
					)
	712 w		755 w,br		)
622	623 s		624 w,sh	627 w,p	$\delta FeCO$ a_1
615	615 vs		615 s		$\delta FeCO$
			595 w		
	586 w		585 vw	587 s	νGeC
	554 m		558 w		νFeCO
			544w, 512 w,	445 ms,p	νFeC a_1
				200 vs[d]	νFeGe a_1, b_1
				105 vvs	δCGeFe, δCFeGe, δGeFeGe

a Data from reference (181) GRAHAM, W.A., JETZ, W., Unpublished work.

b Data for a liquid sample at ambient temperature. Note: In this work even slight O_2 contamination resulted in $Fe(CO)_4(GeMe_3)_2$ changing from a white crystalline solid to a brown oil.

c Data obtained using a conventional cold cell; sample held at *ca.*-196°C

d A change was noted in the contour of this band during polarisation studies consistent with the superposition of the a_1 and b_1 νGeFe modes.

e Assignment is as given in reference (181)

Figure 3.7

The carbonyl infrared stretching region of $Fe(CO)_4(GeMe_3)_2$, C_6H_{12} : cm^{-1}

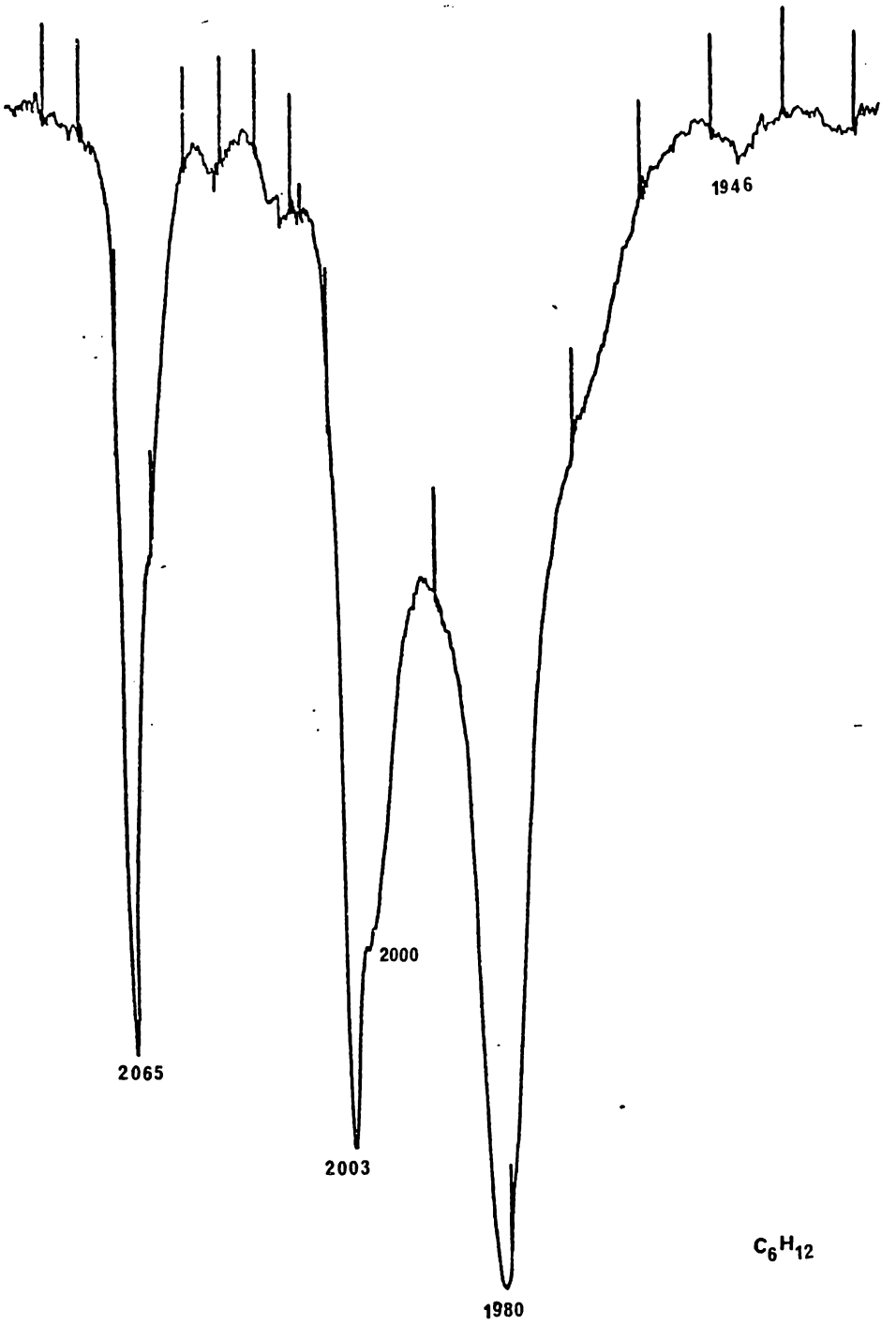

TABLE 3.15

The mass spectrum of $Fe(CO)_4(GeMe_3)_2$

fragment assignment	y = 0			y = 1		
	apparent mass m/e	this work	(181)	apparent mass m/e	this work	(181)
$FeGe_2(CO)_4Me_{6-y}^+$	410-396	w	mw	395-381	m	s
$FeGe_2(CO)_3Me_{6-y}^+$	380-370	-	vvw	367-353	w	ms
$FeGe_2(CO)_2Me_{6-y}^+$	352-342	vvw	w	339-325	w	ms
$FeGe_2(CO)Me_{6-y}^+$	326-314	w	m	311-299	w	ms
$FeGe_2Me_{6-y}^+$	298-284	s	svs	285-271	vs	m
$FeGe(CO)_4Me_{2-y}^+$	274-266	vs	vvs	259-253	w	m
$FeGe_2Me_{2-y}^+$	232-225	w	m	220-208	s	s
$FeGe(CO)Me_{2-y}^+$	191-182	m	ms	177-166	m	ms
$FeGeMe_{2-y}^+$	163-152	vs	vs	147-136	s	svs
$GeMe_{3-y}^+$	122-115	vs	vvs	107-100	w	m
$GeMe^+$	91-85	m	ms	77-70	vw	mw
Other fragments include:						
$FeGe_2Me_4^+$	265-260	-	mw			
$FeGe(CO)_3Me_2^+$	246-238	s	vs			
$FeGe_2^+$	206-196	m	ms			
$GeMe_4^+$	133-126	m	ms			

(181) See reference (181)

H loss from Me groups also occurs, but to a limited extent until most of the CO groups are lost.

CHAPTER FOUR

THE PREPARATION OF UNSYMMETRICALLY SUBSTITUTED GERMYLIRONCARBONYL COMPLEXES

The unsymmetrically substituted methyl germyl iron carbonyls have been prepared *via* the following reaction:

$$Fe(CO)_4(GeR_3)_2 + [Mn(CO)_5]^- \longrightarrow [Fe(CO)_4(GeR_3)]^- + Mn(CO)_5(GeR_3) \quad \ldots(4.1)$$

$$[Fe(CO)_4(GeR_3)]^- + GeXR_3 \longrightarrow Fe(CO)_4(GeR_3)(GeR'_3) \quad \ldots(4.2)$$

(R_3, R'_3 are different combinations of H and Me)

One attempt (178) to prepare $Fe(CO)_4(GeMeH_2)(GeH_3)$ by equations ...(4.1) and (4.2) yielded 75% of the expected $Mn(CO)_5(GeMeH_2)$ but only traces of $Fe(CO)_4(GeMeH_2)(GeH_3)$. Spectroscopic studies showed mostly $Mn(CO)_5(GeH_3)$, $Fe(CO)_4(H)_2$, $Fe(CO)_4(H)(GeH_3)$ and $Fe(CO)_4(GeH_3)_2$ as volatile products.

In this chapter, the preparation and characterisation of the mixed-substituted species $Fe(CO)_4(GeMeH_2)(GeH_3)$, $Fe(CO)_4(GeMe_2H)(GeH_3)$ and $Fe(CO)_4(GeMe_2H)(GeMeH_2)$ are outlined. Self-reaction studies of $Fe(CO)_4(GeMeH_2)(GeH_3)$ and $Fe(CO)_4(GeMe_2H)(GeH_3)$ are viewed (*c.f.* section 2.3, page 52). Halogenation of the monomethylgermyl(germyl)- and dimethylgermyl(germyl)-tetracarbonyliron species have been looked at in ^1H nmr studies section 4.3 and 4.5.3 and 4.5.4. Each compound and its reaction(s) will be treated separately.

4.1. Methylgermyl(germyl)tetracarbonyliron(0), $Fe(CO)_4(GeMeH_2)(GeH_3)$

4.1.1 Preparation of $Fe(CO)_4(GeMeH_2)(GeH_3)$

$NaMn(CO)_5$, (prepared from $Mn_2(CO)_{10}$ 731 mg, 1.87 mmol), $Fe(CO)_4(GeH_3)_2$, (1271 mg, 3.98 mmol), and Et_2O (4 ml) were allowed to react at room temperature for 20 minutes. The volatile components of the mixture were pumped out of the reaction vessel leaving a white-orange residue. Fractionation of the volatile components of the reaction gave $Fe(CO)_4(GeH_3)_2$ (37 mg, 0.1 mmol), $Mn(CO)_5(GeH_3)$ (929 mg, 3.44 mmol, 92%) and Et_2O. $GeBrMe_2H$, (599 mg, 3.53 mmol) and pentane (1687 mg) were condensed onto the white-orange $[Fe(CO)_4(GeH_3]^-$ and allowed to react at room temperature for 15 minutes with intermittent shaking. The more volatile components of the greenish reaction mixture were removed under vacuum (*ca.* 2 hr, 10^{-2} mmHg). A U-trap was then weighed and connected into the vacuum line directly in front of the reaction vessel. This trap was kept at -196° and the reaction vessel was pumped a further 4 hours using the diffusion pump to maintain a lower vacuum. $Fe(CO)_4(GeMeH_2)(GeH_3)$, (699 mg, 2.10 mmol) and $Fe(CO)_4(GeH_3)_2$ (*ca.* 121 mg, 0.38 mmol) made up the colourless oily liquid which condensed into this trap. Another U-trap was weighed and connected into the vacuum line in front of the reaction vessel. Another 214 mg, 0.64 mmol of $Fe(CO)_4(GeMeH_2)(GeH_3)$ was recovered (*i.e.*, *ca.* 78% yield based on $Fe(CO)_4(GeH_3)_2$ used and 80% yield based on $Mn(CO)_5(GeH_3)$ recovered). Extraction of the pale yellow residues in the reaction vessel with C_6H_{12} gave bands at 2067 ms, 2063 s, 2026 s,sh, 2017 vs, 2011 vs, and 642 m, 619 s, cm^{-1}. Fractionation of the more volatile components from the reaction showed $GeMeH_3$, pentane, and a little $Mn(CO)_5(GeH_3)$, $Fe(CO)_4(H)(GeMe_xH_{3-x})$ X = 0, 1, and $Fe(CO)_4(GeMeH_2)(GeH_3)$,

(all identified by their infrared spectra).

In this and similar experiments essentially quantitative yields (*c.a.* 90%) of $Mn(CO)_5(GeH_3)$ were recovered from reactions starting with $Fe(CO)_4(GeH_3)_2$. In one preparation where $Fe(CO)_4(GeMeH_2)_2$ was reacted with $[Mn(CO)_5]^-$ (*i.e.*, followed by coupling with $GeBrH_3$) the recovery of $Mn(CO)_5(GeMeH_2)$ was 61% based on $Mn_2(CO)_{10}$ used.

A deficit of $[Mn(CO)_5]^-$ was always used.

Brown involatile, intractable solid is formed when the product is briefly exposed to air. This reaction appears to be an all-or-none reaction, as $Fe(CO)_4(GeMeH_2)(GeH_3)$ condensed away from the brown solid behaves in exactly the same manner as product which has not been exposed to air.

4.1.2 Characterisation of $Fe(CO)_4(GeMeH_2)(GeH_3)$

The proton nmr spectrum of $Fe(CO)_4(GeMeH_2)(GeH_3)$ shows a triplet at 9.49τ, a singlet at 6.47τ, and a quartet at 6.11τ $^3J_{HGeCH}$ = 3.4 Hz in the ratio 3 : 3 : 2.

The mass spectrum, obtained *via* gas sampling, is tabulated. See Table 4.1, page 131. A weak parent ion, $Fe(CO)_4(GeMeH_2)(GeH_3)^+$ is observed together with two series of ions; the more intense stronger series, $(P\text{-}nCO)^+$ indicating that CO loss is the favoured decomposition process. The weaker series is attributed to the less favoured methyl loss fragmentation and results in ions of the type $[P\text{-}Me\text{-}nCO]^+$

The infrared spectrum, see Table 4.2, page 138, is consistent with the formulation of this compound, see Section 1.4.2.2.

A ^{13}C nmr facility (JEOL FX90Q) was installed in this Department, right at the end of the period of this work. The first carbonyl spectrum to be recorded on this facility was that of $Fe(CO)_4(GeMeH_2)(GeH_3)$. This was recorded with some difficulty, as a neat liquid in a 5 mm o.d.

TABLE 4.1

Mass spectrum of $Fe(CO)_4(GeMeH_2)(GeH_3)$

Fragment Assignment	Apparent Mass *m/e*	Relative intensity	Envelope *maxima*
$Fe(CO)_4Ge_2MeH_x^+$	340-323	w	333
$Fe(CO)_4Ge_2H_x^+$	325-308	w	318
$Fe(CO)_3Ge_2MeH_x^+$	312-295	s	304
$Fe(CO)_3Ge_2H_x^+$	297-280	w	290
$Fe(CO)_2Ge_2MeH_x^+$	284-267	ms	276
$Fe(CO)_2Ge_2H_x^+$	269-252	m	262
$Fe(CO)Ge_2MeH_x^+$	256-239	s	248
$Fe(CO)Ge_2H_x^+$	241-224	m	230
$FeGe_2CH_x^+$	228-211	s	216
$FeGe_2H_x^+$	213-196	vs	202
$Fe(CO)_2GeH_x^+$	190-182	m	186
$Fe(CO)GeMeH_x^+$	176-169	m	174
$Fe(CO)GeH_x^+$	162-154	m	158
$FeGeCH_x^+$	150-141	m	146
$FeGeH_x^+$	134-126	m	130
$GeCH_xO^+$	108-102	w	106
$GeCH_x^+$	93-82	s	88
GeH_x^+	79-70	s	74
$Fe(CO)_4^+$, m; $Fe(CO)_3^+$, s; $Fe(CO)_2^+$, s; $Fe(CO)^+$, w.			

nmr tube suspended inside a 10 mm o.d. tube of $CDC\ell_3$ as lock sample. The carbonyl carbon region of this spectrum shows three signals of chemical shift values, 206.9, 205.6, and 205.1 in parts per million downfield from TMS. The former signal was clearly larger than the other two which were approximately the same height. The $^{13}CH_3$ signal was at -2.8 ppm. The middle line of the 13-C resonance of $CDC\ell_3$ is taken as 77.1 ppm downfield from TMS.

4.1.3 Weighed decomposition study

$Fe(CO)_4(GeMeH_2)(GeH_3)$, (98 mg, 0.29 mmol) was left at room temperature in the dark for 122 days. CO and/or H_2 (*ca.* 0.04 mmol) was pumped out of the weighed vessel. $GeMeH_3$ (*ca.* 9 mg, 0.09 mmol) and GeH_4 (*ca.* 0.7 mg, 0.01 mmol) condensed out of the reaction vessel at 0^oC. The remaining volatile material (56 mg, 0.17 mmol) was unreacted $Fe(CO)_4(GeMeH_2)(GeH_3)$. C_6H_{12} extraction of the orange-red oil remaining gave an infrared spectrum with absorptions at 2067 m,sh, 2063 s, 2060 ms, 2024 m, 2018 s, 2010 vs, 2008 s cm^{-1}.

4.1.4 Decomposition of $Fe(CO)_4(GeMeH_2)(GeH_3)$ in benzene

$Fe(CO)_4(GeMeH_2)(GeH_3)$, (78 mg, 0.23 mmol) was sealed together with benzene in a standard nmr tube and the self-reaction of this compound was followed by changes in the ^1H nmr. Table 4.3, page 144, lists the products obtained from the nmr profile of the decomposition reaction.

4.1.5 The reaction of $Fe(CO)_4(GeMeH_2)(GeH_3)$ with $SiCl_4$

Benzene, $Fe(CO)_4(GeMeH_2)(GeH_3)$ (33 mg, 0.1 mmol) and $SiCl_4$ (*ca.* 16 mg, 0.1 mmol) were sealed together. Reaction between $SiCl_4$ and methylgermyl(germyl)tetracarbonyliron(0) was followed by proton nmr spectroscopy. The course of this reaction is shown in Table 4.5, page 151.

4.1.6 The reaction between $Fe(CO)_4(GeMeH_2)(GeH_3)$ and CCl_4

Reaction between $Fe(CO)_4(GeMeH_2)(GeH_3)$, (85 mg, 0.26 mmol) and CCl_4 (26 mg, 0.17 mmol) in benzene was followed by ^1H nmr. Initially the solution was layered and the signals from $Fe(CO)_4(GeMeH_2)(GeH_3)$ were very broad. After *ca.* one hour the signals of the pale yellow solution had settled down and the quartet and triplet of the GeH and Me signals in the starting material were resolved. A summary of the changes as this reaction proceeded is given in Table 4.6, page 156.

4.1.7 Reaction between $Fe(CO)_4(GeMeH_2)(GeH_3)$ and HCl

$Fe(CO)_4(GeMeH_2)(GeH_3)$ and HCl (0.1 mmol) were allowed to react in benzene solution at room temperature for 84 days, during which time products from this reaction were monitored by nmr spectroscopy. The reaction sequence is reported in tabular form. See Table 4.7, page 159.

4.2 Discussion

4.2.1 Discussion of the preparation

The reaction

$$Fe(CO)_4(GeH_3)_2 + [Mn(CO)_5]^- \longrightarrow [Fe(CO)_4(GeH_3)]^- + Mn(CO)_5(GeH_3)$$

is found to yield $Mn(CO)_5(GeH_3)$ in near quantitative yields. In the alternative reaction,

$$Fe(CO)_4(GeMeH_2)_2 + [Mn(CO)_5]^- \longrightarrow [Fe(CO)_4(GeMeH_2)]^- + Mn(CO)_5(GeMeH_2)$$

only 61% of $Mn(CO)_5(GeMeH_2)$ was recovered. This drop in yield is thought to reflect the more sensitive nature of the reacting species, $Fe(CO)_4(GeMeH_2)_2$, see Section 2.3.1. The unsymmetrically substituted product, was prepared in up to 70% yield together with some $Fe(CO)_4(GeH_3)_2$ and/or $Mn(CO)_5(GeH_3)$, *via* the reaction

$$[Fe(CO)_4(GeH_3)]^- + GeBrMeH_2 \longrightarrow Fe(CO)_4(GeMeH_2)(GeH_3)$$

$Fe(CO)_4(GeH_3)_2$ and/or $Mn(CO)_5(GeH_3)$ being the more volatile, only contaminates the head fraction of the product: later fractions are free from these contaminant(s). The infrared spectrum of the reaction vessel residues gives evidence for octacarbonyl species, $Fe_2(CO)_8(GeR_2)_2$ (see Sections 4.2.4, 4.2.5).

While the bulk of the sample shows no evidence for contamination by any impurities, the tail fraction from these preparations contains a closely similar species whose ^1H nmr spectrum shows a triplet at 9.51 or 9.45τ, singlet at 6.50 or 6.47τ, and a quartet at 6.12 or 6.07τ, ^3J = 3.2 or 3.8 Hz in benzene. The intensity ratio appears to be 3 : 3 : 2, see Figure 4.1, page 135.

A curious thing is that where this extra species appears, it forms approximately 50% of the sample. Disproportionation of $Fe(CO)_4(GeMeH_2)(GeH_3)$ to give $Fe(CO)_4(GeMeH_2)_2$ and $Fe(CO)_4(GeH_3)_2$ is one possible explanation for this, compare:

Figure 4.1

The nmr spectrum of a tail fraction of $Fe(CO)_4(GeMeH_2)(GeH_3)$.

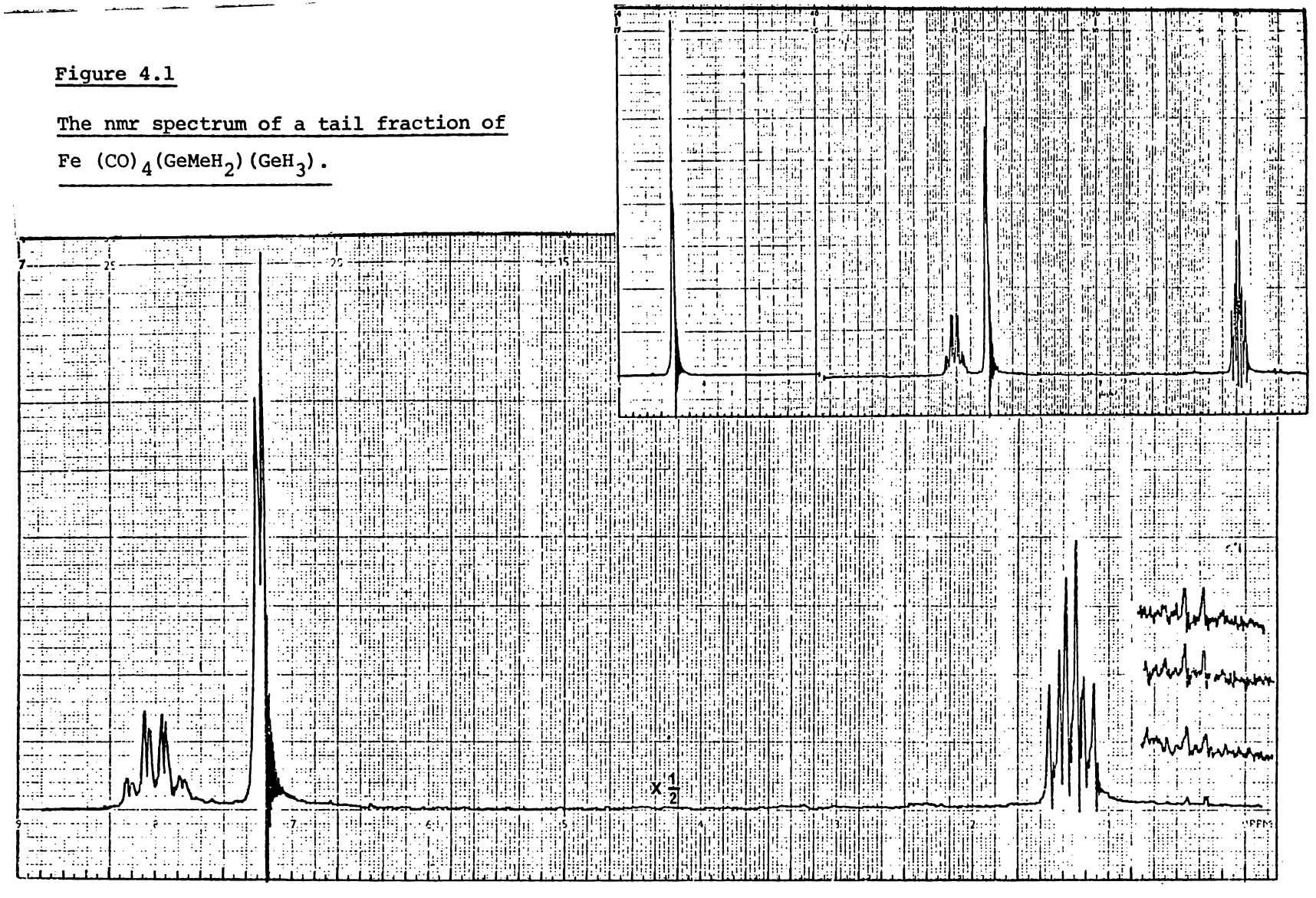

Compound	CH (τ)	GeH(τ)	^3J (Hz)
$Fe(CO)_4(GeMeH_2)(GeH_3)$ [a]	9.49	6.48 6.11	3.4
$Fe(CO)_4(GeMeH_2)_2$ [a]	9.51	6.13	3.4
$Fe(CO)_4(GeH_3)_2$ [b]		6.50	
$Fe(CO)_4(H)(GeH_3)$ [c]		6.65	

a C_6H_6 this work. b, C_6D_6 see reference (27).

c, $CDC\ell_3$ see reference (26).

This disproportionation could not have occurred during the preparation, as fractionation of $Fe(CO)_4(GeH_3)_2$ from $Fe(CO)_4(GeMeH_2)_2$ would have given various mixtures of the two in all the samples condensed out of the reaction vessel. It is, however, possible that some fairly involatile contaminant remained to catalyse the disproportionation in the tail fraction.

Another explanation compatible with the closely similar nmr spectra is that the unidentified species is an isomer of the parent compound. While assignment of this species as *trans*-$Fe(CO)_4(GeMeH_2)(GeH_3)$ is possible, it is noted that no other *trans*-$Fe(CO)_4(M^tR_3)_2$ species (where R = alkyl or aryl) are known.

As mentioned previously, $Ru(CO)_4(SiMe_3)_2$ and $Ru(CO)_4(SnMe_3)_2$ are both *cis* while $Ru(CO)_4(SnMe_3)(SiMe_3)$ exists as a mixture of both *cis* and *trans* isomers.

4.2.2 Vibrational spectra of $Fe(CO)_4(GeMeH_2)(GeH_3)$

The vibrational spectrum of $Fe(CO)_4(GeMeH_2)(GeH_3)$ is listed in Table 4.2, page 138. Figure 4.2, page 139, illustrates the gas phase infrared region. Assignments have been made following discussion in Section 1.4.2.2. Parallels between the infrared spectra of $Fe(CO)_4(GeR_3)_2$ R=Me,H species are drawn in Section 5.5.2, page 214.

The Raman spectra of $Fe(CO)_4(GeMeH_2)(GeH_3)$ were recorded on material from the least volatile fraction of the preparation.

Infrared spectra of the Raman sample were recorded after the Raman spectra had been recorded. These spectra are similar to the bulk of the sample, although small shoulders in the νCO region had appeared, 2099, 2012 cm^{-1}, and subtle changes in the intensity of the 836 cm^{-1} *maxima* were evident.

The vibrational spectra of $Fe(CO)_4(GeMeH_2)(GeH_3)$, as can be seen from Table 4.2, page 138, is compatible with the assignment of this compound as a *cis*-$Fe(CO)_4(GeR_3H_{3-x})(GeH_3)$ species. Three prominent νCO modes in the infrared spectrum are assigned as 2094 s, νCO_{ax} a_{11}, 2034 vvs, a_{12} + b_2 modes, 2012 vs, νCO_{eq} b_1 (cm^{-1}), see Figure 4.2, page 139. The strong Raman polarised band at 2091 cm^{-1} supports the a_{11} assignment of the highest frequency νCO mode.

νCH and ρCH_3 occur as expected. The ρCH_3 and δGeH_3 modes coincide in the 900-830 cm^{-1} region. The symmetric δGeH_3 deformation is observed at 811 cm^{-1}. The GeH_2 wagging mode occurs at 691 cm^{-1}. The strong characteristic δFeCO mode which is seen in iron carbonyls of this type occurs at 627 cm^{-1}. Other modes include the νGeC (a_1 + b_1) at 589 (R_p) and 619 cm^{-1}, ρGeH_x 534 cm^{-1}, νFeC 445 (a_1) cm^{-1} and νGeFe 227 cm^{-1} (R_p). While only one νGeFe mode was also observed in *cis*-$Fe(CO)_4(GeMe_3)_2$, two νFeGe modes are expected for a *cis*-$Fe(CO)_4(GeR_3)_2$ species.

TABLE 4.2

The vibrational spectrum of $Fe(CO)_4(GeMeH_2)(GeH_3)$ cm^{-1}

Infrared gas	Raman[a]		Assignment
	C_6H_6	neat liquid	
	2942 s,p	2987 w, p	) νCH
	2913 m	2917 w	)
2094 s	2090 vs	2091 s, p	) a_{11} *(ax)*
2034 vvs			) νCO $a_{12} + b_{2}$?
(2017 sh)	2023 vvs	2023 vvs	)
2012 vs			) b_1 *(eq)*
		1243 w	) δCH_2
		1059 s	
	875 m	883 m	)
852 w			)
			) ρCH_3
843) m			)
836) ms			) +
832) m			) δGeH
815) ms			)
811) m	813 w	813 w	) δGeH_3
807) wm			)
	743 vw	739 vs	δFeCO?
691 w		703 w	GeH_2 wag
627 s			δFeCO
619 sh			νGeC
581 w	588 m	589 m,p	νGeC symmetric
		566 m	
n.o	537 w	534 vs	ρGeH_x
	440 m,p	445 s,p	νFeC a_1
	225 m	227 s(p)	νGeFe a_1+b_1

a - Values corrected for the calibration error.

n.o - Region not observed.

Figure 4.2

The carbonyl infrared spectrum of $Fe(CO)_4(GeMeH_2)(GeH_3)$, cm^{-1}

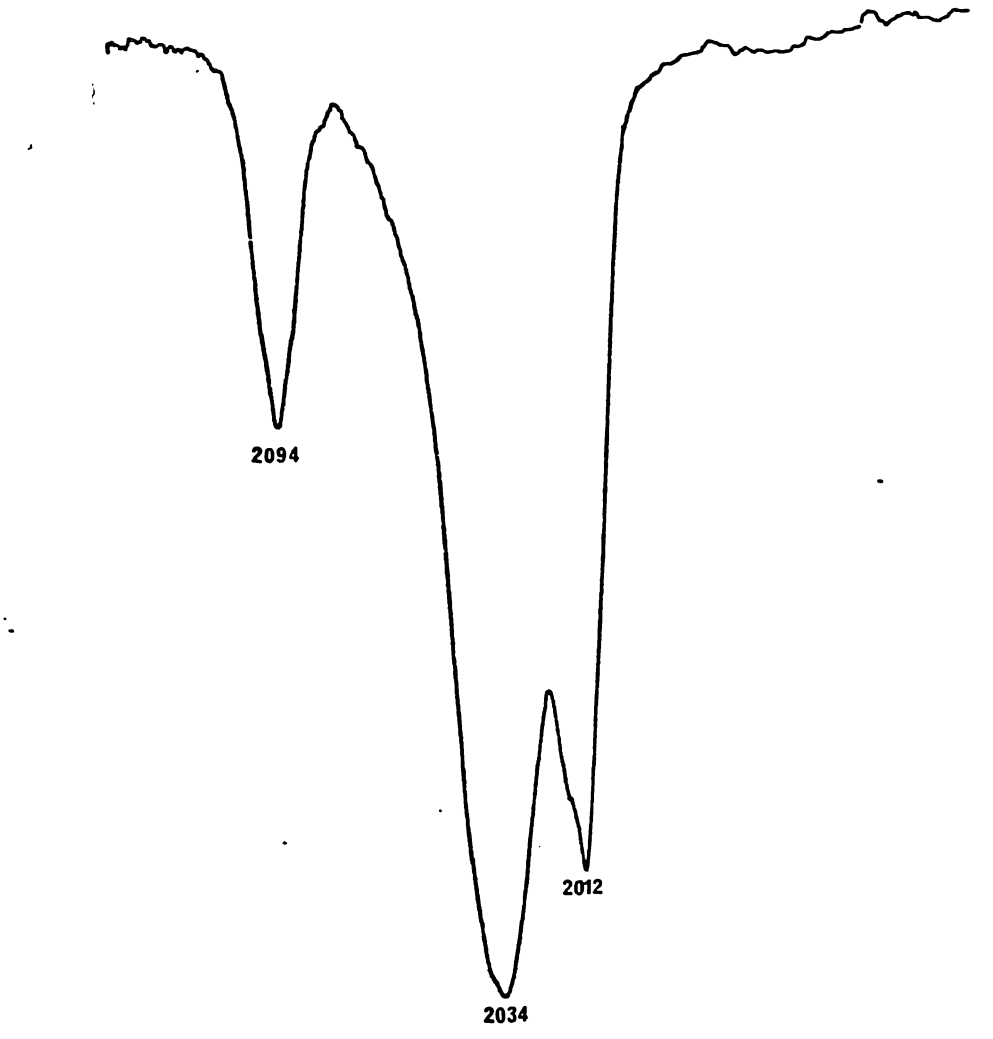

It is quite possible that the $a_1 + b_1$ νFeGe modes are coincident in this species. Indeed, the partial decrease in the intensity of the 227 cm^{-1} mode on polarisation studies suggests that there is an a_1 component in this *maxima*. Both $Fe(CO)_4(GeH_3)_2$ and $Fe(CO)_4(GeMeH_2)_2$ exhibit two νGeFe; 229 vs p, 216 m, cm^{-1} (26), and 225 s p, 210 s cm^{-1} (29) respectively.

4.2.3 Carbon-13 nmr spectrum of $Fe(CO)_4(GeMeH_2)(GeH_3)$

The larger ^{13}CO signal at 206.9 ppm was assigned to the two CO groups *cis* to the germanium ligands (*i.e.*, axial CO's) and the 205.6 and 205.0 signals to the two CO groups *trans* to the germanium (*i.e.*, equatorial CO's). These chemical shift values compare well with literature values for other $Fe(CO)_4(M'R_3)_2$ species, all of which to date have fallen in the range 209-197 ppm. Assignment of the equatorial carbonyl carbon resonances at higher field than axial CO resonance is also consistant with data of compounds of this type.

The methyl carbon resonance at -2.8 ppm is found in the same region as other trimethyl analogues, $Fe(CO)_4(SiMe_3)_2$ 7.50 ppm, $Fe(CO)_4(GeMe_3)_2$ 7.34 ppm, $Fe(CO)_4(SnMe_3)_2$ -3.29 ppm (56).

Multinuclear nmr facilities open up the prospect of much more detailed studies, possibly adding ^{73}Ge and ^{17}O experiments to ^{13}C and ^{1}H work. Compounds like $Fe(CO)_4(GeMe_xH_y)_2$, which are liquids, at room temperature, are very convenient for such work.

4.2.4 Weighed self-reaction study

After being left in the dark for 122 days, 43% of the 0.29 mmol sample of neat $Fe(CO)_4(GeMeH_2)(GeH_3)$ had reacted. The reaction stoichiometry was as follows:

$$Fe(CO)_4(GeMeH_2)(GeH_3) \longrightarrow GeMeH_3 + GeH_4 + CO/H_2$$

(0.12 mmol) (0.09 mmol) (0.01 mmol) (0.04 mmol)

+ solid products

(32 mg, by difference).

Thus the principal reaction may be formulated as in equation (4.3),

$$2Fe(CO)_4(GeMeH_2)(GeH_3) \longrightarrow 2GeMeH_2 + [Fe(CO)_4(GeH_2)]_2 \quad ...(4.3).$$

This is similar to the self-reaction of $Fe(CO)_4(GeMeH_2)_2$ to give $GeMeH_3$ and $[Fe(CO)_4(GeMeH)]_2$ (29) and is also consistent with the observation (27) that $Fe(CO)_4(GeH_3)_2$ shows little tendency to self-react at room temperature. The small amount of incondensable gas suggests a slow further reaction, perhaps to $Fe_2(CO)_7(GeR_2)_2$ species as found earlier (29).

The alternative condensations of equations (4.4) and (4.5) can also be envisaged:

$$2Fe(CO)_4(GeMeH_2)(GeH_3) \longrightarrow 2GeH_4 + [Fe(CO)_4(GeMeH)]_2 \quad ...(4.4)$$

$$\longrightarrow GeH_4 + GeMeH_3 + [Fe(CO)_4]_2(GeMeH)(GeH_2) \quad ...(4.5)$$

The 32 mg of solid product would correspond to 0.062-0.065 mmol of octacarbonyl (depending on the number of methyls) so equations (4.3) to (4.5) are all compatible with the mass balance. If they occurred to the extent (4.3)>>(4.5)>(4.4), this would give the observed 9:1 ratio of $GeMeH_3$: GeH_4. The infrared spectrum of the solid product may also be assigned on the basis of the three octacarbonyls of equations (4.3) to (4.5). (See Section 5.6).

Carbonyl stretching frequencies (cm^{-1})		compound
2067 s	2017 vs	$[Fe(CO)_4(GeH_2)]_2$
2064 s	2012 vs	$[Fe(CO)_4]_2(GeMeH)(GeH_2)$
2060 s	2008 vs	$[Fe(CO)_4(GeMe_2)]_2$

The relative intensities suggest a greater predominance of the mixed-bridge species than is compatible with the hydride ratio.

One further reaction equation (4.6) must not be dismissed in the light of the non-condensation of $Fe(CO)_4(GeH_3)_2$ (27):

$$2Fe(CO)_4(GeMeH_2)(GeH_3) \longrightarrow GeMeH_3 + [Fe(CO)_4(GeHe_3)]_2(GeMeH) \quad ...(4.6)$$

In this case, 32 mg would equate with 0.056 mmol of product. This would enhance the proportion of $GeMeH_3$, give a carbonyl-stretching region similar to the other species, and reflect the observed reluctance to eliminate GeH_4 between two GeH_3 groups. It could further react with starting material in analogous reactions to give longer chains.

The overall mass balance and most of the observations could thus be reconciled if approximately 10% of the reaction yields GeH_4 by following equations (4.5) and/or (4.4) while the rest gives $GeMeH_3$ by dividing evenly between equations (4.3) and (4.6).

4.2.5 The self-reaction of $Fe(CO)_4(GeMeH_2)(GeH_3)$ in benzene

The changes in the proton nmr spectrum of a solution of $Fe(CO)_4(GeMeH_2)(GeH_3)$ in benzene are listed in Table 4.3, page 144, and illustrated in Figure 4.3, page 145. The self-reaction is very slow and 70% of the starting material remains after 84 days.

Up to this time, only two products are apparent, $GeMeH_3$ and a species giving a doublet at 8.98τ, ^3J = 3.4 Hz, values characteristic of a (μ-GeMeH)Fe_2 species. The ratio of the 8.98τ doublet to $GeMeH_3$ probably increases from about 1:4 to 1:2 as reaction proceeds (though the accuracy of intensity measurements of very weak signals is low). Thus, both reactions (4.3) and (4.6) may be occurring slowly over the first 80 days. If the 8.98τ doublet is due to $[Fe(CO)_4(GeH_3)]_2GeMeH$, then the GeH_3 resonance would also be expected.

The GeH_3 environment however, would be very similar to the starting material, and the GeH quartet of the species would probably coincide with the 6.11τ region and would not be expected to be strong enough to detect. When it became possible to run the spectrum at 90 MHz a second component in the GeH_3 region, separated by about (0.01 ppm) from the parent material and of approximately the correct intensity for a signal from $[Fe(CO)_4(GeH_3)]_2(GeMeH)$ became apparent. However, this also occurs in the same region as the GeH_3 quartet from $GeMeH_3$ so assignment of this peak is not firm. At the higher field, weak signals under the quartet at 6.11τ were also clear. These may include both the GeH resonance of the μ-(GeMeH) group and the signals from the μ-(GeH_2) group of $[Fe(CO)_4(GeH_2)]_2$ formed *via* equation (4.3)

TABLE 4.3

Nmr study of the decomposition of $Fe(CO)_4(GeMeH_2)(GeH_3)$ in benzene

TIME days a	Intensity of methyl signal (%)		
	$Fe(CO)_4(GeMeH_2)(GeH_3)$ b	$GeMeH_3$ c	Product d
1	100		
7	100	Infinitesimal	
11	99.5	0.5	Infinitesimal
16	96.5	3	0.5
22	90	8	2
54	85	11	3
84[e,f]	70	20	10

a - The benzene solution was observed to change from colourless to yellow within 5 days of reaction. No further physical changes were observed. See Figure 4.3,

b - $Fe(CO)_4(GeMeH_2)(GeH_3)$, triplet 9.49τ, singlet 6.47τ, quartet 6.11τ. ^3J = 3.4 Hz, intensity ratio 3 : 3 : 2.

c - $GeMeH_3$ occurs at 9.97τ quarter, and *ca.*6.51τ quartet ^3J = 3.8 Hz. (The quartet of $GeMeH_3$ occurs under the GeH_3 signal of $Fe(CO)_4(GeMeH_2)(GeH_3)$

d - Product peaks occur at *ca.* 8.98τ doublet ^3J = 3.4 Hz, and *ca.* 8.95τ doublet?, the latter signal has about a quarter the intensity of the former.

e - GeH_4, 6.9τ (1%) occurs after 84 days.

f - Opened after a further 15 days at room temperature and 24 hours at 35°C.

Figure 4.3

Nmr spectra from the decomposition of $Fe(CO)_4(GeMeH_2)(GeH_3)$

(Continued over page)

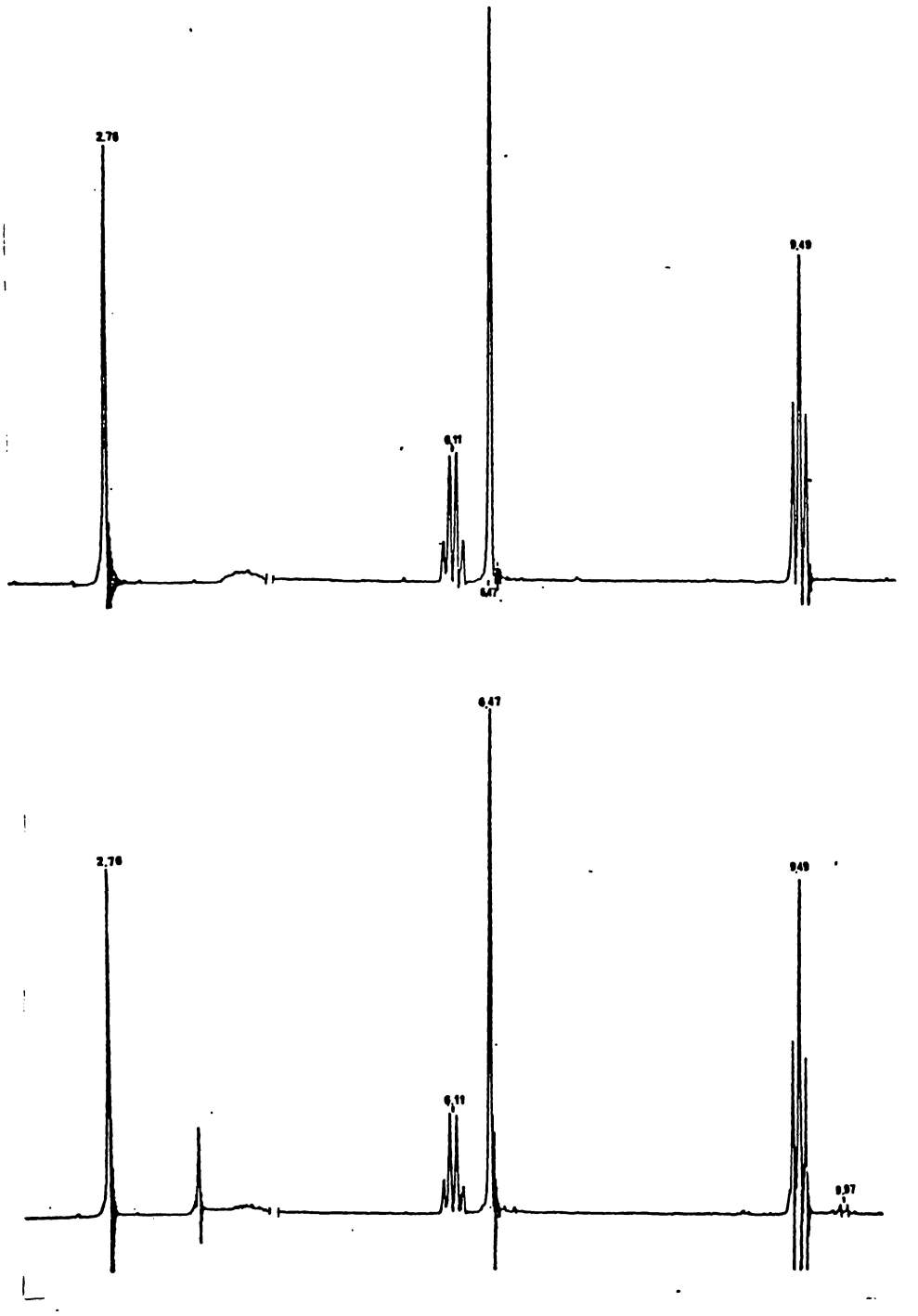

Figure 4.3 (Continued)

Nmr spectra from the decomposition of $Fe(CO)_4(GeMeH_2)(GeH_3)$.

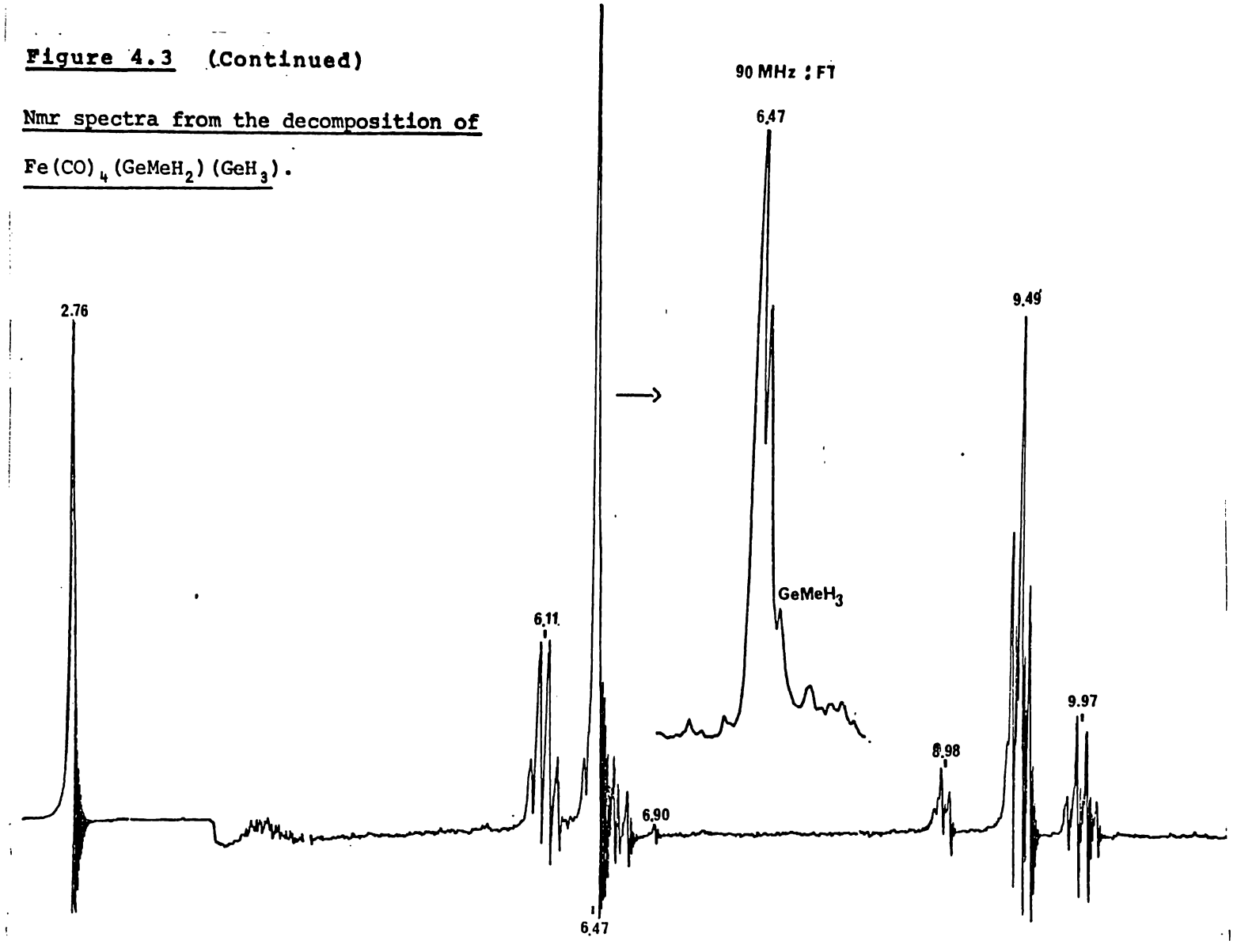

The formation of a little GeH_4, together with the appearance of a second weak GeMeH doublet? at *c.a* 8.95 τ, ^3J = 4.5 Hz?, became clear after about 100 days of reaction. These could arise from equations (4.4) or (4.5), or might reflect formation of a longer chain species by a reaction analogous to (4.6). Either way, this is a very minor process.

Thus, the reaction in solution, as followed by ^1H nmr, appears to follow the same equations as the reaction of the pure compound. However, the proportion of GeH_4 formed in solution is much lower, showing that reactions (4.4) and/or (4.5) are much less significant.

After 100 days, the involatile products of the reaction were isolated as a yellow oil which deposited orange crystals after three hours. The mass spectrum of this material shows strong series of peaks for the families $[Fe_2(CO)_nGe_2Me_x]^+$ n = 0 to 8 and x = 2, 1 and 0. Since Me loss is a relatively minor process (compare for example Tables 3.8 and 3.10, pages 106 and 113), this suggests a mixture of the three species $[Fe(CO)_4(GeMeH)]_2$, $[Fe(CO)_4]_2(GeMeH)(GeH_2)$ and $[Fe(CO)_4(GeH_2)]_2$ The infrared spectrum Figure 4.4, page 147, also suggests that $[Fe(CO)_4]_2(\mu\text{-}GeMeH)(\mu\text{-}GeH_2)$ was formed.

Finally, it should be noted that an attempt to run the mass spectrum of the solids from the reaction of neat $Fe(CO)_4(GeMeH_2)(GeH_3)$ was not very successful as the probe was too hot, but ions were observed which indicated a $[Fe(CO)_4Ge]_2Ge$ species together with an indication of Fe_3Ge_3 species.

Figure 4.4

An infrared spectrum of a mixture of $Fe(CO)_4(GeMe_{2-x}H_x)(GeMe_{2-y}H_y)$ species, cm^{-1}

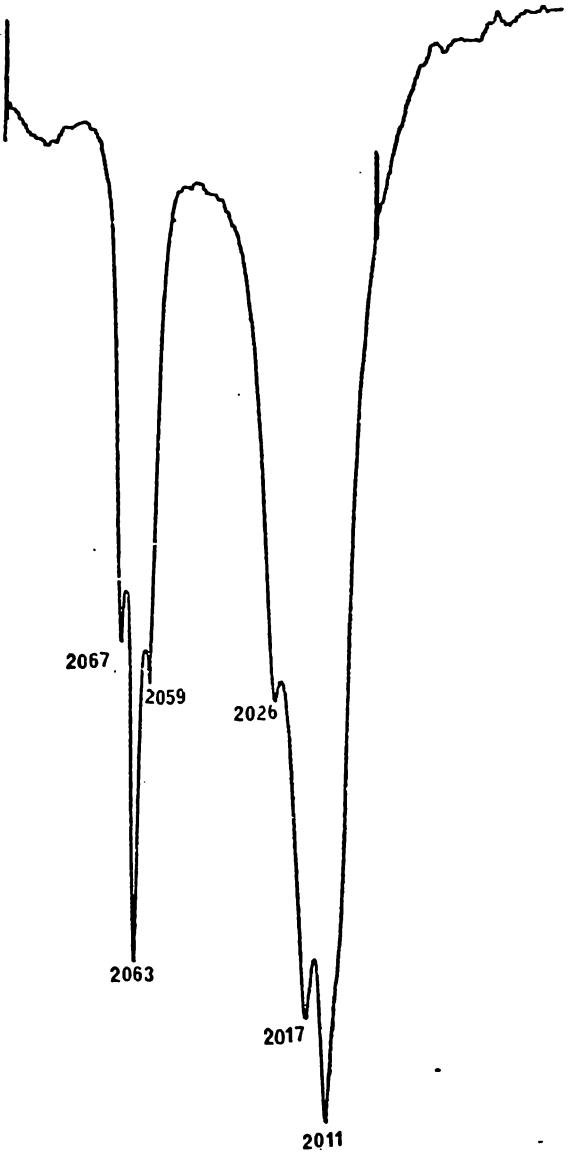

4.3 Nmr studies of reactions between $Fe(CO)_4(GeMeH_2)(GeH_3)$ and covalent halides

Bonny found that $Fe(CO)_4(GeMeH_2)_2$ (27,28), reacted with mild reagents such as $SiC\ell_4$ to give stepwise halogenation at alternative germanium atoms. The more reactive hydrogen halides substituted and then cleaved the Fe-Ge bonds. In the $Fe(CO)_4(GeH_3)_2$ system, however, the dichlorogermyl species $Fe(CO)_4(GeC\ell H_2)_2$ was not observed. Instead, the monochloro species very slowly reacted, with precipitation, to form GeH_4, $[Fe(CO)_4(GeH_2)]_2$, $[Fe(CO)_4]_2(GeC\ell_2)(GeC\ell H)$, $[Fe(CO)_4(GeC\ell H)]_2$ and higher molecular weight species. (evidence from infrared and mass spectroscopic studies (27)).

It was postulated that while the reaction

$$2Fe(CO)_4(GeH_3)_2 \xrightarrow{X} [Fe(CO)_4(GeH_2)]_2 + 2GeH_4 \quad ...(4.7).$$

did not occur in clean samples, this reaction was catalysed by $SiC\ell_4$. No $GeC\ell H_3$ was formed in this reaction either. Bonny (27) further postulated the reactions:

$$Fe(CO)_4(GeH_3)_2 + Fe(CO)_4(GeC\ell H_2)(GeH_3) \rightarrow [Fe(CO)_4]_2(GeC\ell_2)(GeC\ell H) + 2GeH_4 \quad ...(4.8)$$

$$[Fe(CO)_4(GeH_2)]_2 + SiC\ell_4 \rightarrow [Fe(CO)_4]_2(GeC\ell_2)(GeC\ell H) + SiC\ell_3H \quad ...(4.9)$$

$$2Fe(CO)_4(GeC\ell H_2)(GeH_3) \rightarrow [Fe(CO)_4]_2(GeC\ell_2)(GeC\ell H) + GeC\ell H_3 + GeH_4 \quad ...(4.10)$$

as possible sources of $[Fe(CO)_4]_2(GeC\ell_2)(GeC\ell H)$.

In the digermanyl iron species, $Fe(CO)_4(Ge_2H_5)_2$ the alpha-hydrogens were preferentially halogenated in a very slow reaction, leaving the GeH_3 protons unchanged (175). The main product was $Fe(CO)_4(GeC\ell HGeH_3)(Ge_2H_5)$. In the mixed species $Fe(CO)_4(Ge_2H_5)(GeH_3)$ substitution occurred preferentially at the GeH_3 group and the reaction was somewhat faster. Then the elimination reaction followed,

$$Fe(CO)_4(Ge_2H_5)(GeH_3) + SiC\ell_4 \longrightarrow Fe(CO)_4(GeC\ell H_2)(Ge_2H_5) \quad ...(4.11a)$$

$$Fe(CO)_4(GeC\ell H_2)(Ge_2H_5) \longrightarrow [Fe(CO)_4(GeC\ell H)]_2 + 2Ge_2H_6 \quad ...(4.11b)$$

Products identified from previous reactions (27,28) between $Fe(CO)_4(GeH_3)_2$ and $Fe(CO)_4(GeMeH_2)_2$ and covalent halides have been very helpful in assigning products in this work. Table 4.4.1 page 150, lists this data.

4.3.1 Reaction with $SiC\ell_4$

The course of the reaction of methylgermyl(germyl)tetracarbonyl-iron(0) and $SiC\ell_4$ is shown by Table 4.5, page 151. Figure 4.5, page 152, illustrates the nmr spectrum at several points in the reaction.

Identification of products

$Fe(CO)_4(GeC\ell MeH)(GeH_3)$ As Table 4.4.1 shows the changes in methyl chemical shift and coupling constant are as expected for chlorine substitution at the $GeMeH_2$ group. The relative intensity of the GeH_3 resonance also matches this formulation. Further, the shift upfield of the GeH_3 resonance on monosubstitution at $GeMeH_2$ parallels the changes observed in other species but is unexpectedly large. Thus, the unsubstituted GeH resonance shifts upfield from the starting material by 0.02τ in $Fe(CO)_4(GeC\ell H_2)(GeH_3)$ (27) and by 0.11τ in $Fe(CO)_4(GeC\ell MeH)$-$(GeMeH_2)$ (28) while this system shows a shift of 0.24τ. The upfield shift is ascribed to the induced and anisotropic field of the Ge-Cℓ bond

TABLE 4.4.1

Nmr parameters of some germanium hydride and chloride species

Compound	Chemical Shift values (τ)	Coupling Constant (H_3)	Solvent	Ref.
GeH_4	6.85		C_6H_{12}	(172)
$GeMeH_3$	9.71, 6.55	4.22	CS_2	(173)
$GeMe_2H_2$	9.71, 6.27	3.95	$CC\ell_4$	(174a)
$GeC\ell H_3$	4.77		CS_2	(27)
$GeC\ell MeH_2$	9.27, 4.70	2.9	CS_2	(173b)
$GeC\ell Me_2H$	9.2, 4.45	2.7	$CC\ell_4$	(174a)
$GeC\ell_2H_2$	3.42		CS_2	(27)
$GeC\ell_2MeH$	8.86, 3.26	1.2	CS_2	(173b)
$GeC\ell_2Me_2$	8.86		$CC\ell_4$	(174)
$GeC\ell_3H$	2.82		CS_2	(27)
$Fe(CO)_4(H)(GeH_3)$	6.55			(27)
$Fe(CO)_4(H)(GeC\ell MeH)$	20.48, 9.10, 4.12	3.0	CS_2	(28)
$Fe(CO)_4(H)(GeC\ell H_2)$	20.04, 4.32		CS_2	(27)
$Fe(CO)_4(GeH_3)_2$	6.50		C_6D_6	(26)
$Fe(CO)_4(GeMeH_2)_2$	9.30, 6.20	3.9	CS_2	(29)
$Fe(CO)_4(GeMe_2H)_2$	9.36, 6.02	3.4	CS_2	(30)
$Fe(CO)_4(GeC\ell H_2)(GeH_3)$	4.40		CS_2	(26)
$Fe(CO)_4(GeC\ell MeH)(GeMeH_2)$	9.26, 8.84, 6.24	3.8	CS_2	(28)
$Fe(CO)_4(GeC\ell_2Me)(GeC\ell MeH)$	8.75, 8.50, 4.13	2.6	CS_2	(28)
$Fe(CO)_4(GeC\ell_2Me)_2$	8.38		C_6H_6	(28)
$[Fe(CO)_4(GeH_2)]_2$	6.65		CS_2	(27)
$[Fe(CO)_4(GeMeH)]_2$	8.84, 8.81, 3.4	3.4	CS_2	(29)
$[Fe(CO)_4(GeMe_2)]_2$	8.85		CS_2	(30)
$[Fe(CO)_4(GeC\ell Me)]_2$	8.44		C_6H_6	(28)
$Fe(CO)_4(H)_2$	19.98		CS_2	(27)
H_2	5.4		CS_2	(27)

TABLE 4.5

Nmr data from reaction between $Fe(CO)_4(GeMeH_2)(GeH_3)$ and $SiCl_4$

TIME (days)	COLOUR	Relative intensity of signal*				
		$Fe(CO)_4(GeMeH_2)(GeH_3)$ a	$Fe(CO)_4(GeClMeH)(GeH_3)$ b	$GeClMeH_2$ c	$GeMeH_3$ d	GeH_4 e
4	none	100	trace			
7	"	99	1			
10	"	97	3	trace		
15	"	92	4	4		
29	pale yellow	79	12	9		
47	pale yellow	68	17	3	12	2
91	yellow-orange	53	20	2	24	5

* Relative proportions calculated as a percent of the total signal (all but 'e' based on relative intensity of methyl resonances.) see Figure 4.5.

a $Fe(CO)_4(GeMeH_2)(GeH_3)$, 9.49τ triplet, 6.47τ singlet, 6.11τ quartet, intensity ratio 3 : 3 : 2 ^3J = 3.4 Hz

b $Fe(CO)_4(GeClMeH)(GeH_3)$ 9.08τ doublet, 6.70τ singlet, intensity ratio *ca.* 1 : 1 ^3J = 2.5 Hz, quartet of GeClMeH is obscured by ^{13}CH satelites from benzene.

c $GeClMeH_2$, 9.77τ triplet, *ca.* 4.98τ quartet, intensity ratio 1.57 : 1, ^3J = 2.7 Hz.

d $GeMeH_2$, 9.97τ quartet, ^3J = 3.8 Hz, GeH_3 quartet expected at *ca.*6.47τ lies under starting material.

e GeH_4, 6.90τ singlet.

Figure 4.5

Nmr spectra at 4, 29, 47 and 91 days during reaction of $Fe(CO)_4(GeMeH_2)(GeH_3)$ with $SiCl_4$

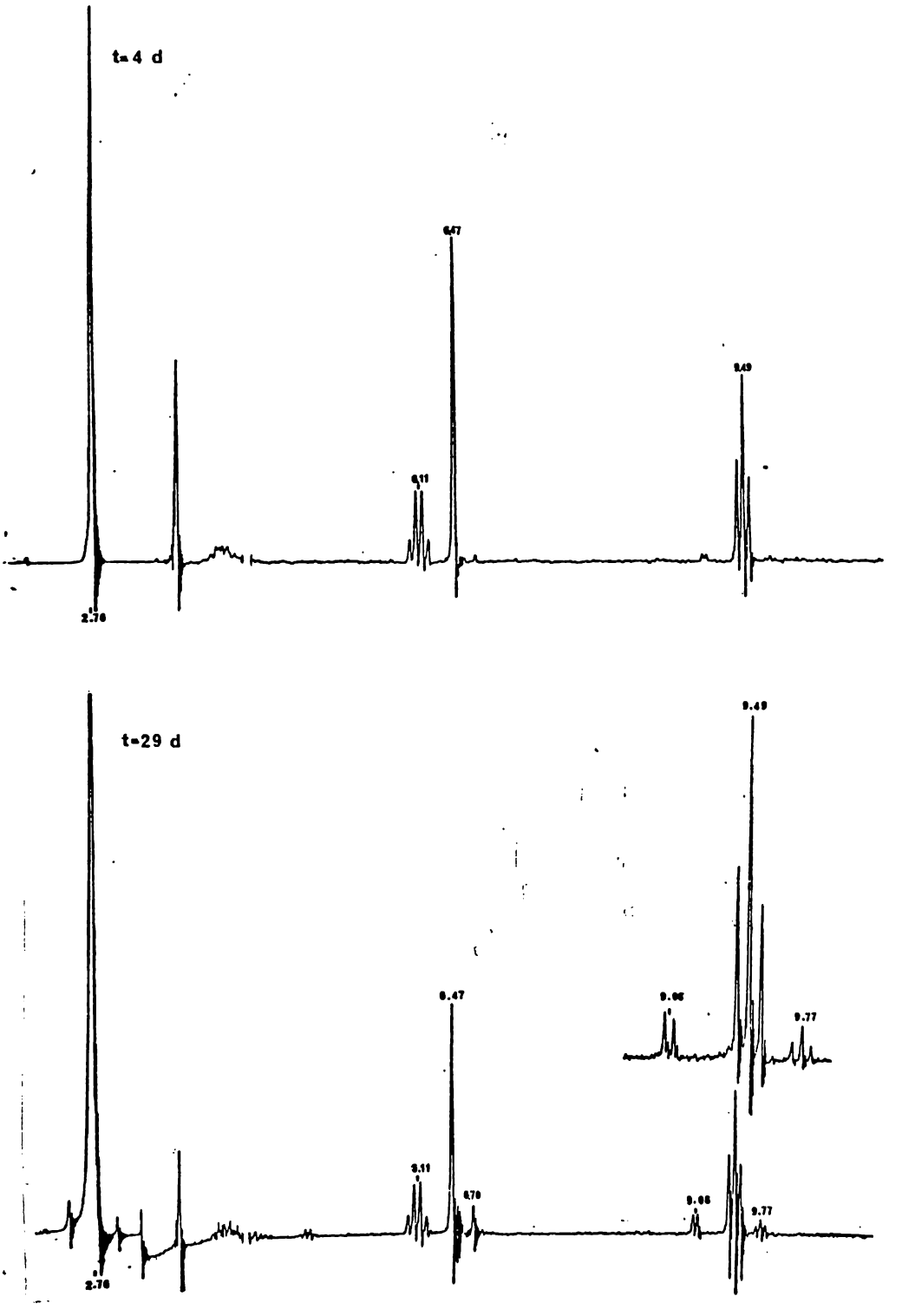

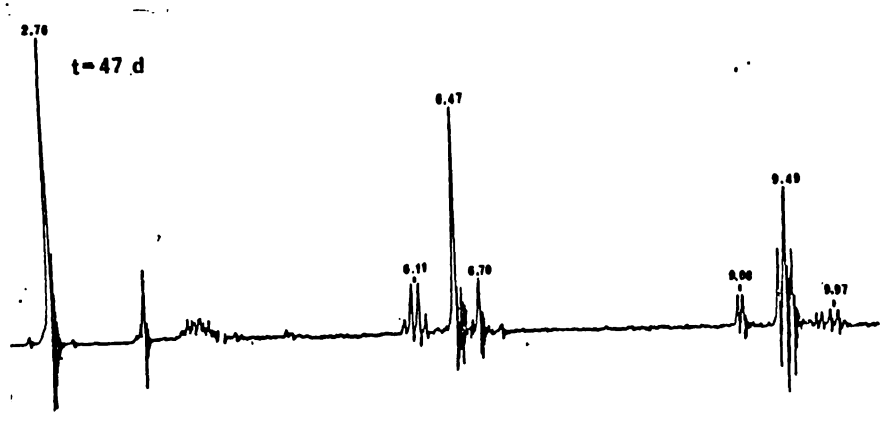

Figure 4.5 (Continued)

Nmr spectra of 4, 29, 27 and 91 days during reaction of $Fe(CO)_4(GeMeH_2)(GeH_3)$ with $SiCl_4$

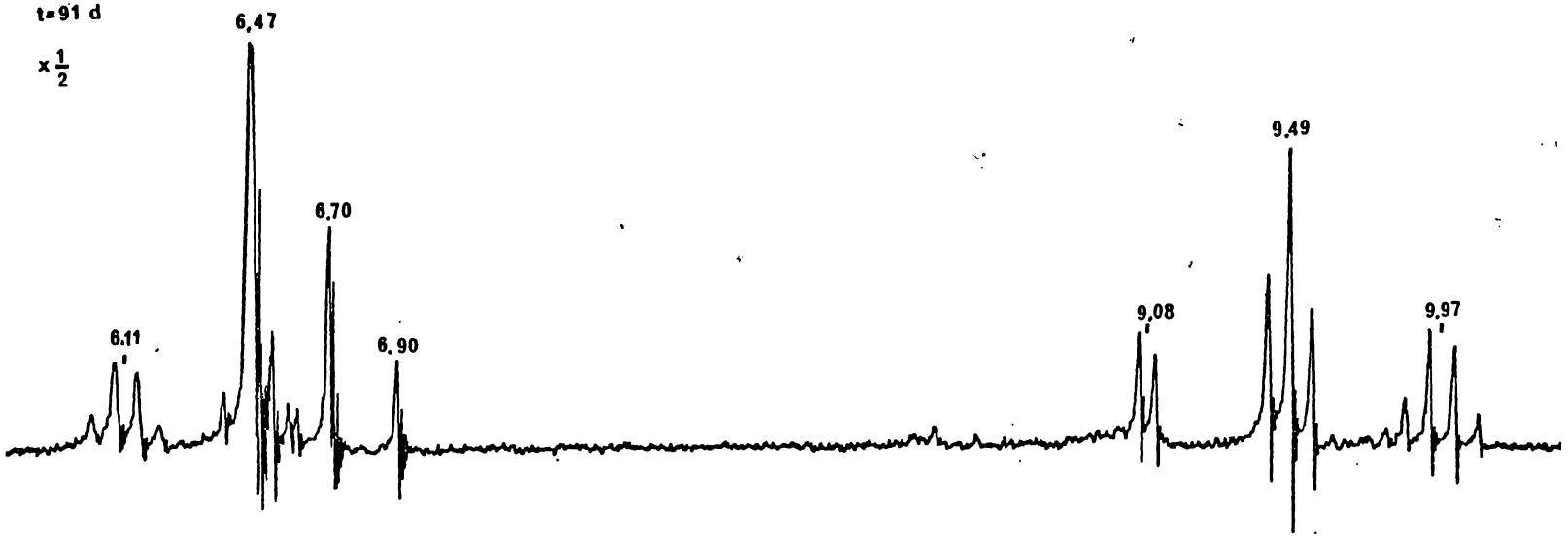

and the difference in its effect in the three compounds probably reflects the degree to which rotational isomers holding the Ge-H close to Ge-Cℓ predominate with different degrees of methyl substitution.

$GeC\ell MeH_2$ The signal intensities, coupling constant, and multiplicities all indicate a $GeC\ell MeH_2$ species, but the chemical shift values differ substantially from those in the literature (Table 4.4), albeit in different solvents. Bonny (27) assigned signals at 9.63τ triplet, 4.98τ quartet, ^3J = 3.0 Hz (C_6H_6) to $GeC\ell MeH_2$ from reaction of $SnC\ell_4$ and $GeMeH_3$. He also attributed signals at 9.78τ, 5.05τ, ^3J = 3.0 Hz in CS_2 solution arising from reaction of $Fe(CO)_4(GeMeH_2)_2$ with $HC\ell$ to $GeC\ell MeH_2$. Overall, it is probably not inconsistent to identify the observed signals 9.77τ and 4.98τ ^3J = 2.7 Hz with $GeC\ell MeH_2$.

$GeMeH_3$ and GeH_4 Both are identified by comparison with values obtained in benzene solution, from preparations of these gases. Note that the given proportions of these, especially of GeH_4, are only indicative as some will be present in the gas phase.

The reaction sequence

Clearly, the first step in the reaction between $Fe(CO)_4(GeMeH_2)(GeH_3)$ and $SiC\ell_4$ is

$$Fe(CO)_4(GeMeH_2)(GeH_3) + SiC\ell_4 \longrightarrow Fe(CO)_4(GeC\ell MeH)(GeH_3) \quad ...(4.12)$$

with presumably formation of $SiC\ell_3H$ whose signal is obscured by the benzene. This parallels the results (27,28) for $Fe(CO)_4(GeH_3)_2$ and $Fe(CO)_4(GeMeH_2)_2$ where monosubstitution occurred and was faster for the methyl species. Note, however, that the overall rate of reaction was much slower than found previously, (27,28), perhaps reflecting the absence of traces of reactive impurities (*e.g.*, $HC\ell$) in this system.

In the next stage, it is suggested that reaction (4.13) occurs,

$$2Fe(CO)_4(GeC\ell MeH)(GeH_3) \longrightarrow 2GeC\ell MeH_2 + [Fe(CO)_4(GeH_2)]_2 \quad ...(4.13)$$

$[Fe(CO)_4(GeH_2)]_2$ has a resonance at 6.71τ, which would coincide with the GeH_3 resonance of $Fe(CO)_4(GeC\ell MeH)(GeH_3)$. Reaction (4.11a) resembles (4.12) in paralleling the relative reactivity of $Fe(CO)_4(GeH_3)_2$ and $Fe(CO)_4(Ge_2H_5)_2$ but the elimination of chlorohydride in (4.13) contrasts with (4.11b).

In the later stages of the reaction, $GeC\ell MeH_2$ declines in relative amount and $GeMeH_3$ builds up to eventually exceed $Fe(CO)_4(GeC\ell MeH)(GeH_3)$. Smaller amounts of GeH_4 also appear. Both these hydrides could appear from the self-reaction of $Fe(CO)_4(GeMeH_2)(GeH_3)$. GeH_4 is most likely to arise from the reaction analogous to (4.10). However, $GeMeH_3$ is probably also formed from $GeC\ell MeH_2$, possibly by the reaction

$$Fe(CO)_4(GeMeH_2)(GeH_3) + GeC\ell MeH_2 \longrightarrow GeMeH_3 + Fe(CO)_4(GeC\ell MeH)(GeH_3) \quad ...(4.14)$$

Despite the uncertainties about the later stages of the reaction, two major characteristics are very clear,

(i) the reaction of $SiC\ell_4$ with $Fe(CO)_4(GeMeH_2)(GeH_3)$ is very slow

(ii) the initial step is monosubstitution at $GeMeH_2$.

4.3.2 Reaction with $CC\ell_4$

The initial stages of this reaction are similar to (although faster than) those of the $SiC\ell_4$ reaction *i.e.*, $Fe(CO)_4(GeC\ell MeH)(GeH_3)$ is formed by chlorine exchange (see Table 4.6, page 156 and Figure 4.6 page 157). After three days, white-orange solid has been precipitated. (Note that dichlorides are typically less soluble than their hydride congers (27)). At this stage too, both $GeMeH_3$ and GeH_4 are apparent, together with $GeC\ell Me\ H_2$. This implies that more than one process to form octacarbonyl species is occurring. Processes which account for small signals (such as 6.77τ and 8.35τ ?) include,

$$2Fe(CO)_4(GeC\ell MeH)(GeH_3) \longrightarrow [Fe(CO)_4(GeH_2)]_2 + 2GeC\ell MeH_2 \quad ...(4.15)$$

$$2Fe(CO)_4(GeMeH_2)(GeH_3) \longrightarrow [Fe(CO)_4(GeH_2)]_2 + 2GeMeH_3 \quad ...(4.16)$$

$$2Fe(CO)_4(GeC\ell MeH)(GeH_3) \longrightarrow [Fe(CO)_4(GeC\ell Me)]_2 + 2GeH_4 \quad ...(4.17)$$

The identity of the major product(s)? which are precipitating from solution can not be determined by nmr. The possible formation of small amounts of dichlorosubstituted tetracarbonyl can not be overlooked. It may be that these species more rapidly undergo germane elimination and cyclization than the monosubstituted species,

$Fe(CO)_4(GeC\ell MeH)(GeH_3)$. Candidates for $Fe(CO)_4(GeC\ell_2Me)(GeH_3)$ and $Fe(CO)_4(GeC\ell MeH)(GeC\ell H_2)$ could be 8.38τ singlet, 6.77τ or 6.32τ, 5.78τ singlet and 8.70τ doublet, 4.49τ singlet. Thus the processes

$$2Fe(CO)_4(GeC\ell_2Me)(GeH_3) \longrightarrow [Fe(CO)_4(GeC\ell_2)]_2 + 2GeMeH_3 \quad ...(4.18)$$

$$Fe(CO)_4(GeC\ell MeH)(GeC\ell H_2) \longrightarrow [Fe(CO)_4(GeC\ell Me)]_2 + 2GeC\ell H_3 \quad ...(4.19)$$

could account for signals at 8.46τ singlet and 4.45τ or 4.49τ.

TABLE 4.6

Nmr study of the reaction between $Fe(CO)_4(GeMeH_2)(GeH_3)$ and $CC\ell_4$

Reaction time days a	COMMENT	$Fe(CO)_4(GeMeH_2)(GeH_3)$ (A)	$Fe(CO)_4(GeC\ell MeH)(GeH_3)$ (B)	$GeC\ell MeH_2$ (C)	$GeMeH_3$ (D)	GeH_4 (E)	$GeH_2C\ell_2$ (F)	Minor Me Products (G)	Minor GeH Products (H)
1	Initially paragmagnetic and colourless. Slowly turns yellow	98	2						
2	Orange in colour	92	5	2	1				s, s, s
3	White-orange solid has been precipitated	80	11	3	4	1	1		s, s, s
5	Ditto	73	12	3	7	2	1	s, d	s, s, s
22	Ditto	61	16	4	7	7	1	s, d	d, s, s
31	Ditto	48	18	3	15	9	3	d, s, d	d, s
40	Ditto	47	13	2	17	14	3	d, s, d	br, s, s?
88	Signals of starting material now appear to be doubled	27	6	3	26	21	16	d, s, d	s,

Relative proportions calculated as a mole percent of the total signal (based on intensity of methyl resonances where applicable).

a - See also Figure 4.6, (A), $Fe(CO)_4(GeMeH_2)(GeH_3)$, 9.49τ, triplet, 6.47τ singlet, 6.11τ quartet, ^3J = 3.4 Hz, intensity ratio 3 : 3 : 2, (B), $Fe(CO)_4(GeC\ell MeH)(GeH_3)$, 9.07τ, doublet, 6.70τ, singlet, ^3J = 2.6 Hz, intensity ratio *ca.*1 : 1, quartet of $GeC\ell MeH$ is under the benzene. (C) $GeC\ell MeH_2$?, 9.69τ, triplet, 4.91τ, quartet, ^3J = 2.6 Hz, intensity ratio approximately 1 :<1 (difficult to determine because of weak signals and overlap of $GeMeH_3$ signals). (D), $GeMeH_3$, 9.93τ, quartet, ^3J = 3.8 Hz, GeH quartet underlies the starting material, (E) GeH_4, 6.90τ, (F) $CH_2C\ell_2$, 5.54τ,(measured separately in benzene), (G), small signals accounting initially for less than 2% of the methyl signal occur at s = singlet, 8.35τ, d = doublet 8.70τ. After 31 days, small signals of not more than 4% of the methyl signal occur at d = doublet 8.35τ, s = singlet 8.46τ, d = doublet? 8.70τ. (H), Small signals of less than 1% of the total methyl proton intensity occur as follows: s = singlet 4.49τ, s = singlet 5.78τ, s = singlet 6.77τ, ($CH_3C\ell$?). After 22 days a peak at 4.45τ, makes the s = 4.49τ appear to be a doublet. Both peaks broaden and diminish in the latter stages of the reaction.

Figure 4.6

Nmr spectra from the reaction between $Fe(CO)_4(GeMeH_2)(GeH_3)$ and CCl_4

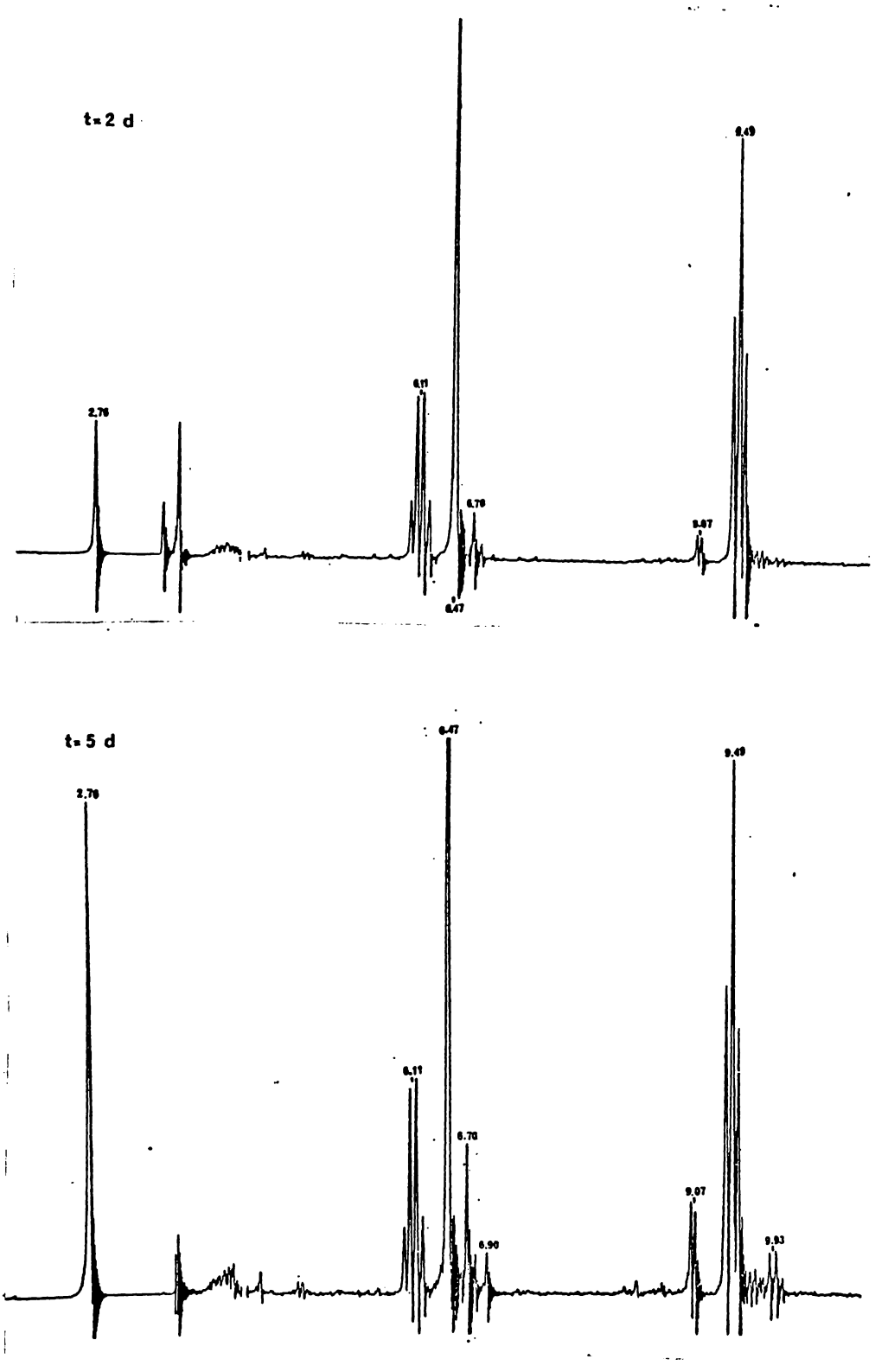

Figure 4.6 (Continued)

Nmr spectra from the reaction between $Fe(CO)_4(GeMeH_2)(GeH_3)$ and CCl_4

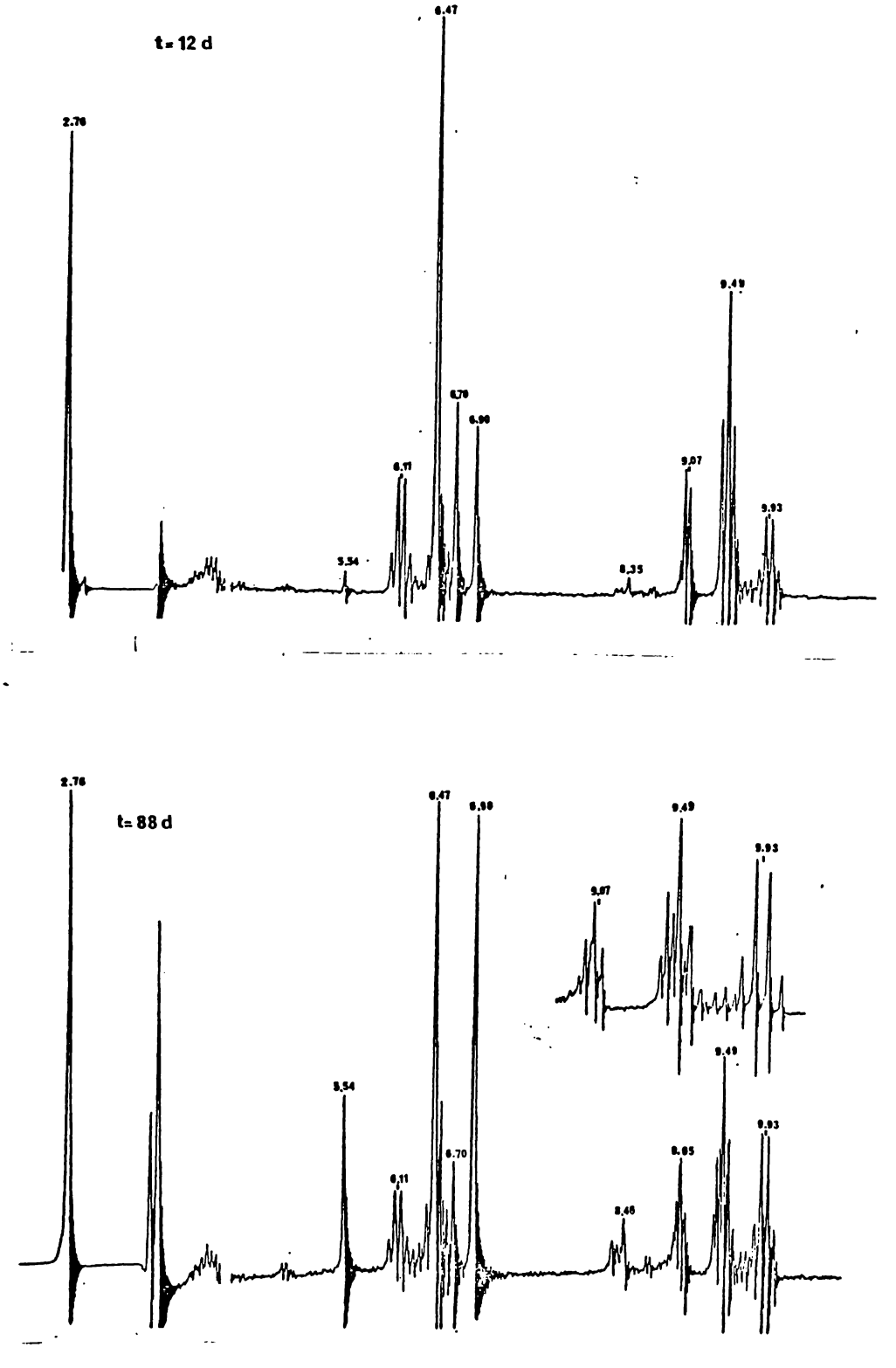

4.3.3 Reaction with HCℓ

Table 4.7, page 159 lists the species observed on reaction of $Fe(CO)_4(GeMeH_2)(GeH_3)$ with HCℓ in benzene.

Identification of signals

Assignments have been made in comparison with species previously recorded in this work and in (27);

$Fe(CO)_4(H)(GeCℓH_2)$ — 4.38τ, 20.74τ, C_6H_6 (*c.f.* 4.32τ, 20.04τ, CS_2 (27)).

$Fe(CO)_4(H)(GeCℓMeH)$ — 9.10τ doublet, ^3J = 2.5 Hz, 20.56τ singlet, C_6H_6 (*c.f.* 9.10τ doublet, ^3J = 3.0 Hz, 20.48τ singlet (27)).

$GeCℓH_3$ — 5.37τ, (*c.f.* 4.77 CS_2 (27)). Note, that the 5.37τ obtained by Bonny was assigned as H_2. (*c.f.* this work where H_2 is assigned as 5.7τ (see Section 6.4.1)).

$Fe(CO)_4(H)(GeH_3)$ — 6.57τ singlet, 20.10τ singlet (*c.f.* 6.55τ and 6.59τ CS_2 (27)).

$Fe(CO)_4(H)(GeCℓ_2Me)$ — 8.78τ singlet, 20.24τ singlet. This signal could alternatively be assigned as an octacarbonyl signal but this would mean that a hydride signal would not be assigned.

No attempt will be made to assign the latter stages of this reaction which is more complex, and from which solid has precipitated.

TABLE 4.7

Data from reaction between $Fe(CO)_4(GeMeH_2)(GeH_3)$ and HCℓ

TIME days	Relative intensity of signal (mole percent)[a]							
	$Fe(CO)_4(GeMeH_2)(GeH_3)$	HCℓ	$GeCℓMeH_2$	$Fe(CO)_4(H)(GeCℓMeH)$	$GeCℓH_3$	$Fe(CO)_4(H)(GeCℓH_2)$	$Fe(CO)_4(H)(GeH_3)$	$Fe(CO)_4(H)(GeCℓ_2Me)$
	c	d	e	f	g	h	i	j
1	73	[61]	10	4	5	5	3	
2	44	[45]	19	10	12	12	3	
3[b]	28	[44]	25	14	15	14	3	
4	16	[9]	28	16	19	18	4	
6	11	[3]	32	16	19	18	3	1
12	2		39	15	23	18		3
22			29	18	27	21		4
40			37	14	25	17		8
84[k]			25	8			3	

a - See Figure 4.7

b - Solution has turned pale yellow in colour.

c - $Fe(CO)_4(GeMeH_2)(GeH_3)$, 9.49τ triplet, 6.47τ singlet, 6.11τ multiplet, intensity ratio 3 : 3 : 2, ^3J = 3.4 Hz

d - HCℓ 9.8τ

e - $GeCℓMeH_2$, 9.77τ triplet, 4.95τ quartet, ^3J = 2.7 Hz, intensity ratio 3 : 2.

f - $Fe(CO)_4(H)(GeCℓMeH)$, 9.10τ doublet, ^3J = 2.5 Hz, 20.56τ singlet

g - $GeCℓH_3$?, 5.37τ singlet.

h - $Fe(CO)_4(H)(GeCℓH_2)$, 4.38τ singlet, 20.74τ singlet.

i - $Fe(CO)_4(H)(GeH_3)$, 6.57τ singlet, 20.10τ singlet.

j - $Fe(CO)_4(H)(GeCℓ_2Me)$?, 8.78τ singlet, 20.24τ singlet.

k - Large changes are manifest in the spectrum after 84 days reaction. Orange solid has precipitated. Signals occur as follows: 5.39τ quartet, ^3J = 4.5 Hz? I = 6, GeH_4, 6.89τ, I = 16, 8.52τ doublet? ^3J = 5.4 Hz? I = 6, 9.00τ singlet, I = 11, 8.94τ doublet, ^3J = 2.2 Hz I = 8, 9.27τ singlet I = 1, 9.60τ singlet, I = 13 9.59τ singlet, I = 4.

Figure 4.7

Nmr spectra obtained during reaction of $Fe(CO)_4(GeMeH_2)(GeH_3)$ and HCl

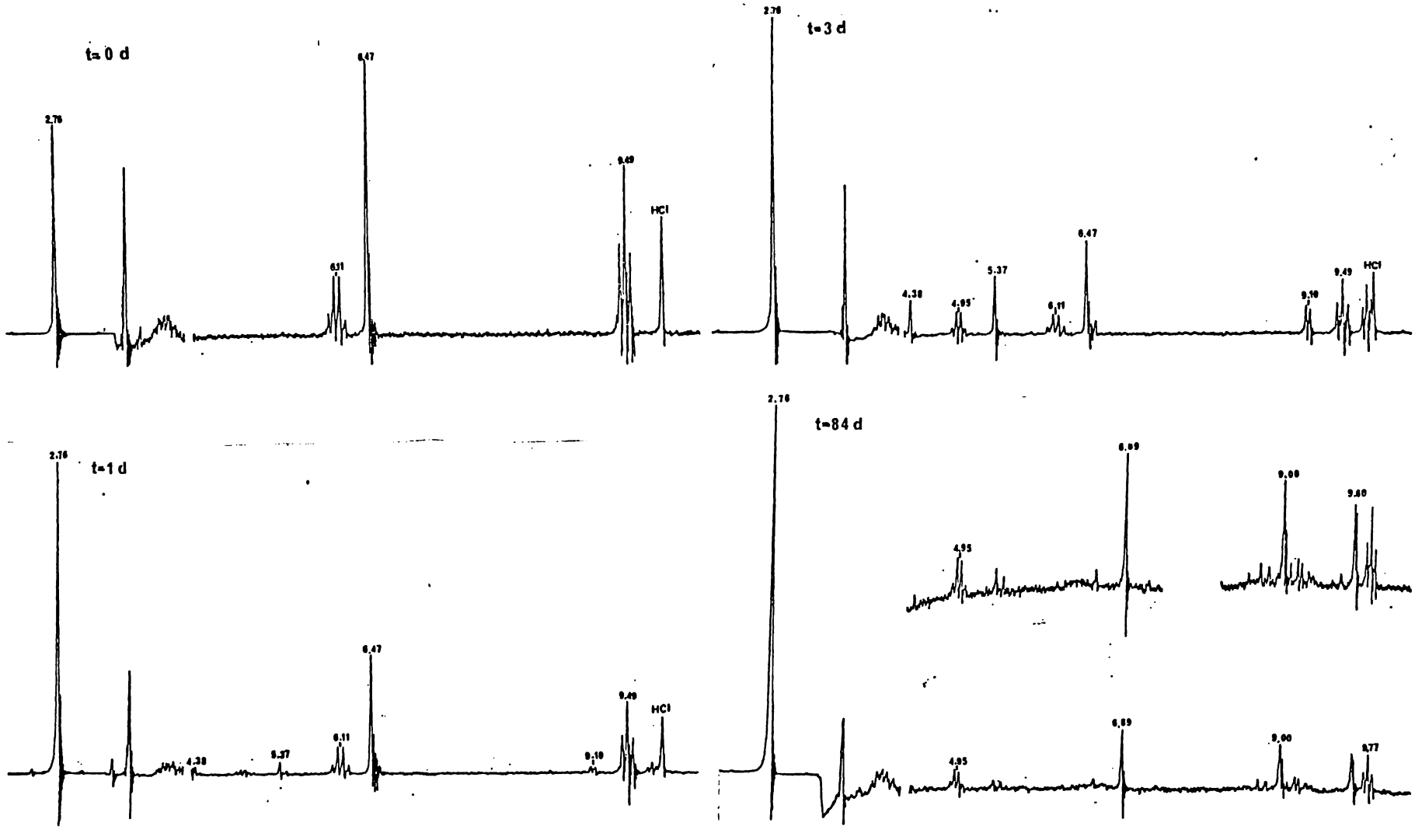

Figure 4.7 (Continued)

Nmr spectra obtained during reaction of $Fe(CO)_4(GeMeH_2)(GeH_3)$ and HCl

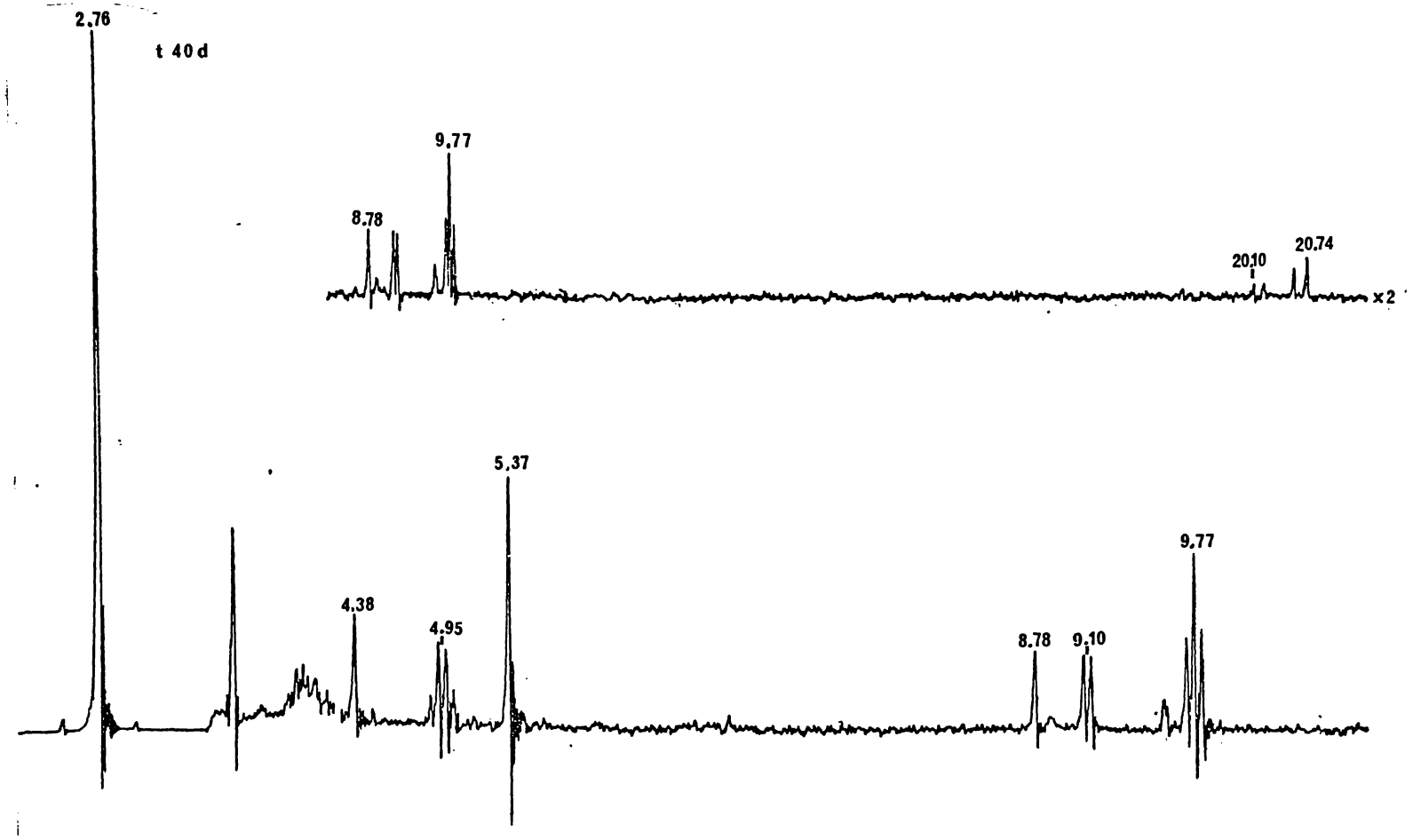

The reaction

The major products identified from the reaction between HCℓ and $Fe(CO)_4(GeMeH_2)(GeH_3)$ involved Ge-Fe cleavage to give the iron hydride species, $Fe(CO)_4(H)(GeCℓMeH)$, $Fe(CO)_4(H)(GeCℓH_2)$ and $Fe(CO)_4(H)(GeH_3)$, together with $GeCℓMeH_2$, $GeCℓH_3$ and presumably H_2 (gas phase). No sign of chlorine substitution alone was evident, but either chlorine substituion must have occurred initially, followed by a rapid cleavage reaction or cleavage must have been followed by rapid chlorine substitution.

Scheme (i)

$$\begin{array}{ccc} Fe(CO)_4(GeMeH_2)(GeH_3) & \xrightarrow[-H_2]{+HCℓ} & \{Fe(CO)_4(GeCℓMeH)(GeH_3)\} \\ \Big\downarrow {\scriptstyle +HCℓ \atop -GeCℓH_3} & & \Big\downarrow {\scriptstyle +HCℓ \atop -GeCℓH_3} \\ \{Fe(CO)_4(H)(GeMeH_2)\} & \xrightarrow[-H_2]{+HCℓ} & Fe(CO)_4(H)(GeCℓMeH) \end{array}$$

Scheme (ii)

$$\begin{array}{ccc} Fe(CO)_4(GeMeH_2)(GeH_3) & \xrightarrow[-GeCℓMeH_2]{+HCℓ} & Fe(CO)_4(H)(GeH_3) \\ \Big\downarrow {\scriptstyle +HCℓ \atop -H_2} & & \Big\downarrow {\scriptstyle +HCℓ \atop -H_2} \\ \{Fe(CO)_4(GeMeH_2)(GeCℓH_2)\} & \xrightarrow[-GeCℓMeH_2]{+HCℓ} & Fe(CO)_4(H)(GeCℓH_2) \end{array}$$

The compounds in { } were unseen and therefore either do not occur or exist for a very short time only. The amount of $GeCℓH_3$ arising in the initial stages of this reaction was roughly equal to the amount of $Fe(CO)_4(H)(GeCℓMeH)$ which had formed. Likewise, the $GeCℓMeH_2$ was roughly equal to the amount of $Fe(CO)_4(H)(GeH_3)$ and $Fe(CO)_4(H)(GeCℓH_2)$ initially formed. This latter process (scheme (ii)) is preferred under

these conditions to Scheme (i) (*c.a.*, 2 : 1 preference). Cleavage, followed by chlorination would appear to be the major pathway in Scheme (ii) since the intermediate species in Scheme (ii), $Fe(CO)_4(H)(GeH_3)$ is observed. This pathway, contrasts with Bonny's scheme (27,28), where chlorine substitution followed by cleavage was postulated for reactions between HCℓ and $Fe(CO)_4(GeRH_2)_2$ R = Me, H.

Reaction was seen to continue after HCℓ had been depleted. After six days, $Fe(CO)_4(H)(GeCℓ_2Me)$ had formed. The corresponding $Fe(CO)_4(H)(GeCℓ_2H)$ would not be seen in these reaction conditions as its signal is expected to lie under the solvent, C_6H_6, resonance. $Fe(CO)_4(H)(GeH_3)$ also reacted out after six days. Its apparent appearance after 84 days coincided with a catastrophic change in the reaction products; numerous weak singlets appeared, solid precipitated and GeH_4, together with $GeCℓMeH_2$, and new peaks at 9.60τ singlet, 8.94τ doublet ^3J = 2.2 Hz, 9.00τ singlet, 8.52τ doublet? ^3J = 5.4 Hz? and 5.39τ quartet ^3J = 4.5 Hz ? made up the bulk of the material in the solution phase.

Numerous schemes could be proposed for the formation of new, condensed and/or more highly chlorinated species, but too many unknowns and ambiguities occur in the latter stages to allow any valid selection. Bonny has found evidence for higher molecular weight species (mass spectrum) in these systems *e.g.* $[Fe_3(CO)_{12}(Ge_2Cℓ_4Me_2)]^+$ in the $Fe(CO)_4(GeMeH_2)_2$ system (28).

4.4 Dimethylgermyl(germyl)tetracarbonyliron(0) $Fe(CO)_4(GeMe_2H)(GeH_3)$

4.4.1 Preparation of $Fe(CO)_4(GeMe_2H)(GeH_3)$

$NaMn(CO)_5$ (from $Mn_2(CO)_{10}$, 553 mg, 1.41 mmol) plus $Fe(CO)_4(GeH_3)_2$, (1218 mg, 3.82 mmol) were reacted in Et_2O (3 ml) for 35 minutes at room temperature. The volatile material was pumped out. The nmr spectrum of the least volatile fraction showed unreacted $Fe(CO)_4(GeH_3)_2$ and $Mn(CO)_5(GeH_3)$ in a ratio of 1 : 3. The involatile material remaining in the reaction vessel was an orange colour. $GeCl Me_2H$, (699 mg, 2.87 mmol) and pentane (3 ml) were then condensed into the reaction vessel. After 10 minutes at room temperature the volatile material $GeMe_2H_2$ and pentane was pumped out of the reaction vessel. The diffusion pump was required to obtain a sufficiently low vacuum to move the product. Infrared spectra showed a little $Mn(CO)_5(GeH_3)$ but the nmr spectrum indicated that the major components were $Fe(CO)_4(GeH_3)_2$ and the product. Some of the product was condensed into an nmr tube. Intensities showed $Fe(CO)_4(GeH_3)_2$ (*ca.*, 90 mg, 0.3 mmol) contaminant while $Fe(CO)_4(GeMe_2H)(GeH_3)$ (*ca.*, 5.3 mg, 1.6 mmol) made up the bulk of this sample. The nmr spectrum of following fractions showed no $Fe(CO)_4(GeH_3)_2$. Product yield was 1.96 mmol, (69% of $GeCl Me_2$ used, 70% based on Mn used).

4.4.2 Self-reaction followed by proton nmr

$Fe(CO)_4(GeMe_2H)(GeH_3)$ (18 mg, 0.05 mmol) was sealed, together with benzene. No $Fe(CO)_4(GeH_3)_2$ impurity was observed. The starting material was characterised by the methyl doublet centred around 9.49τ, only five inner lines of the GeH heptet are usually observed, these are centred on 5.84τ ^3J = 3.2 Hz, and the GeH_3 singlet is centred at 6.48τ.

The average intensity ratio is 6.1 : 3 : 1 respectively. The products which formed on the self-reaction of $Fe(CO)_4(GeMe_2H)(GeH_3)$ were monitored by nmr spectroscopy and are listed in Table 4.10, page 170.

4.4.3 The infrared spectrum of $Fe(CO)_4(GeMe_2H)(GeH_3)$

$Fe(CO)_4(GeMe_2H)(GeH_3)$ (*ca.* 4 mg, 0.01 mmol) was then condensed into a gas cell from the bulk sample in the weighed U-tube. Note that no $Fe(CO)_4(GeH_3)_2$ is thought to be in this sample as it was not seen in the previous fraction. $GeMe_2H_2$ formed during the transfer operation was removed before recording the spectrum. Initially, the spectra were weak, broad and the carbonyl-stretching region showed extra shoulders *ca.* 2099 m sh, 2091 m, 2044 sh, 2040 s, 2034 sh, 2025 s, 2021 s, 2018 sh cm^{-1}. On warming up the carbonyl infrared region had settled down to 2099 m, 2094 m, 2060 sh, 2044 sh, 2042 vs, 2040 vs, 2039 sh, 2024 sh, 2020 s, cm^{-1}. The lower region maintained its initial profile. The sample was unstable over long periods in the gas cell. GeH_4, CO, and a trace of $Fe(CO)_5$ and possibly $GeMe_2H_2$ were all that was left of the sample after it had been left in the gas cell for 24 hours. Other samples showed a similar pattern of events.

4.4.4 The Raman spectrum of $Fe(CO)_4(GeMe_2H)(GeH_3)$

$Fe(CO)_4(GeMe_2H)(GeH_3)$, (47 mg, 0.14 mmol) was sealed together with benzene. A proton nmr spectrum of this sample was recorded before the Raman spectrum was run. The sample was stored at -196°C both before and after the Raman spectrum was recorded. The ^1H nmr spectrum of the sample taken after the Raman measurement showed that the $GeMe_2H_2$ had increased by 12% (from 3% to 15%) during the recording of the Raman spectrum. Octacarbonyl species were also present. The Raman spectrum is tabulated in Table 4.9, page 168. No absorptions due to $GeMe_2H_2$ were observed. Octacarbonyl bands are also thought to be too weak to be observed.

4.4.5 Reaction with $CC\ell_4$

$Fe(CO)_4(GeMe_2H)(GeH_3)$ (12 mg, 0.035 mmol), benzene and $CC\ell_4$ (7 mg, 0.04 mmol) were sealed in an nmr tube. The reaction between $CC\ell_4$ and $Fe(CO)_4(GeMe_2H)(GeH_3)$ was monitored by nmr spectroscopy. Details of this reaction are given in Table 4.11, page 173.

4.4.6 Reaction with $HC\ell$

$Fe(CO)_4(GeMe_2H)(GeH_3)$ (21 mg, 0.06 mmol) was sealed together with benzene and $HC\ell$ (3 mg, 0.09 mmol). Nmr spectroscopic details of this reaction profile are given in Table 4.12, page 178.

4.5 Discussion

The most convincing evidence for the product identity is obtained from ^{1}H nmr spectrum. Apart from the neat, head fraction of product which shows some $Fe(CO)_4(GeH_3)_2$ impurity, the main fractions show only a multiplet (inner five lines of a heptet), 5.84τ, a singlet 6.48τ, and a doublet 9.49τ $^{3}J_{HGeCH}$= 3.2 Hz, with an intensity ratio 1 : 3 : 6 in benzene.

The mass spectrum of $Fe(CO)_4(GeMe_2H)(GeH_3)$ is given in Table 4.8, page 167. It accords well with the mass spectrum of other $Fe(CO)_4(GeMe_xH_{3-2})_2$ spectra recorded in this work; namely, it exhibits a weak parent ion; successive loss of CO; and methyl and hydrogen loss are minor processes until most of the CO's are lost. An unusual feature was the occurrence of two fragment ions corresponding to an apparent mass, *m/e* 178-169 m $Fe(CO)GeH_x^+$? and 122-113 vs, $GeMeCH_xO^+$? which occurred in only one sample.

4.5.1 Vibrational spectra

Vibrational spectra of $Fe(CO)_4(GeMe_2H)(GeH_3)$ are reported in Table 4.9, page 168.

The infrared active carbonyl-stretching bands are indicative of a *cis*-$Fe(CO)_4L_2$ species. The major absorptions are assigned to 2091 m νCO_{ax} (A_{11}), 2040 vs νCO (a_{12} + b_2) and 2021 s νCO_{eq} b_1 cm^{-1} This region shows more shoulders and weak structure than gas phase structure of other $Fe(CO)_4(GeR_3)_2$ species, reflecting perhaps the low stability of the compound. The 900-800 cm^{-1} region shows a range of infrared *maxima* for methyl rocks and GeH_x deformations.

TABLE 4.8

The mass spectrum of $Fe(CO)_4(GeMe_2H)(GeH_3)$

Fragment assignment	Envelope *m/e*	Relative Intensity	Envelope *maxima*
$Fe(CO)_4Ge_2Me_2H_x^+$	354-338	vvw	345
$Fe(CO)_4Ge_2MeH_x^+$	339-323	vw	331
$Fe(CO)_3Ge_2Me_2H_x^+$	326-310	m	318
$Fe(CO)_3Ge_2MeH_x^+$	311-295	vw	304
$Fe(CO)_2Ge_2Me_2H_x^+$	298-282	sm	290
$Fe(CO)_2Ge_2MeH_x^+$	283-267	w	275
$Fe(CO)Ge_2Me_2H_x^+$	270-254	s	262
$Fe(CO)Ge_2MeH_x^+$	255-239	m	244
$FeGe_2Me_2H_x^+$	242-226	s	234
$FeGe_2CH_x^+$	227-211	s	214
$FeGe_2H_x^+$	212-196	vs	202
$Fe(CO)_2GeH_x^+$	191-182	ms	186
$Fe(CO)GeCH_x^+$	178-169	*[m]*	176
$Fe(CO)GeH_x^+$	163-154	s	158
$FeGeCH_x^+$	148-138	m	144
$FeGeH_x^+$	136-126	s	130
$GeMeCH_xO^+$	122-113	*[vs]*	118
$GeCH_xO^+$	107-98	m	105
$GeCH_x^+$	92-82	s	89
GeH_x^+	79-70	m	74
$Fe(CO)_4^+$ 168 s, $Fe(CO)_3^+$ 140 s, $Fe(CO)_2^+$ 112 s, $Fe(CO)^+$ 84 s.			

Gas sampling, *[ ]* = occurred in one sample only

TABLE 4.9

Vibrational spectra of $Fe(CO)_4(GeMe_2H)(GeH_3)$

Infrared gas	Raman C_6H_6	Tentative Assignment
2099 m		)
2094 m	2084 vs	) $\nu CO_{(ax)}$ a_{11}
2060 sh		) νGeH?
2042 vs		)
2040 vs		) νCO $a_{12} + b_2$?
2039 sh		)
2024 sh		)
2020 s	2018 vvs	) νCO b_{1} $(e.g)$
	882) m	)
	865)	)
850 br,sh		) δGeH_x
840) m		) +
836) s		) ρCH_3
833) m		)
821 w		)
817) w		)
811) m		)
807) s	808 m	) δGeH_3 (sym)
805 w,sh		)
728 w		$\delta FeCO$
662 wm		δGeH
628 s		$\delta FeCO$
	573 s	νGeC
n.o.	537 mw	ρGeH_3
	440 s	νFeC
	229 s	$\nu GeFe$

a = No polarisation data recorded, no bands observed from $GeMe_2H_2$ (169).

As for $Fe(CO)_4(GeMeH_2)(GeH_3)$, the symmetric GeH_3 deformation is distinguished as a distorted type A band with the Q branch at 807 cm^{-1}, matching a medium intensity Raman band at 808 cm^{-1}. The weak feature at 662 cm^{-1}, which does not appear in the spectrum of the $GeMeH_2$ analogue, is assigned as δGeH. The characteristic νFeC and δFeCO modes appear in their expected regions and the GeFe stretches are found as a single strong Raman band at 229 cm^{-1}. Unfortunately, polarisation measurements were not made, but this coincidence of the two GeFe modes parallels that for the monomethyl analogue.

4.5.2 Self-reaction of $Fe(CO)_4(GeMe_2H)(GeH_3)$

A colourless solution of $Fe(CO)_4(GeMe_2H)(GeH_3)$ in benzene was seen to decompose slowly in the dark at room temperature. Refer to Table 4.10, page 170. $GeMe_2H_2$, (9.89τ triplet, 6.18τ, heptet, $^3J_{HGeCH}$ = 3.5 Hz) was observed as the major decomposition product together with $[Fe(CO)_4(GeH_2)]_2$ (6.71τ singlet) and a small amount of material at 8.99τ, singlet. This is precisely where bridging $GeMe_2$ methyl signals come. However, if $[Fe(CO)_4(GeMe_2)]_2$ was formed, GeH_4 would also be expected, (*c.f.* equation 4.3, page 141). GeH_4 is observed (in minor amounts) only later in the reaction. A shoulder on the GeH_3 signal at 6.51τ is difficult to differentiate from the ringing of the GeH_3 until the later stages of the reaction where the GeH_3 has receded and the new signal 6.51τ is now seen to be genuine, and to be in *c.a.* a 1:1 ratio with the $GeMe_2$ singlet. A scheme which explains the lack of GeH_4, formation of a $GeMe_2$ bridging species and the singlet at 6.51τ is; (4.20) *c.f.* (4.6).

$$2Fe(CO)_4(GeMe_2H)(GeH_3) \longrightarrow [Fe(CO)_4(GeH_3)]_2GeMe_2 + GeMe_2H_2 \quad ...(4.20)$$

TABLE 4.10

Self-reaction study of
$Fe(CO)_4(GeMe_2H)(GeH_3)$ in solution

TIME days	Relative intensity of signal (mole percent)[a]			
	$Fe(CO)_4(GeMe_2H)(GeH_3)$	$GeMe_2H_2$	$[Fe(CO)_4(GeH_2)]_2$	$[Fe(CO)_4(GeH_3)]_2(GeMe_2)$
	c	d	e	f
0[b]	100			
1.5	71	22	6	1
3	65	24	8	3
6	56	29	10	3
35[i]	24	50	20	7

a - The mole percent is calculated using methyl intensity where possible. See also Figure 4.8.

b - The colourless solution had turned yellow within 1.5 days.

c - $Fe(CO)_4(GeMe_2H)(GeH_3)$, 9.49τ doublet, 6.48τ singlet, 5.41τ heptet, ^3J = 3.2 Hz, intensity ratio 6 : 3 : 1.

d - $GeMe_2H_2$, 9.89τ triplet, 6.18τ heptet, ^3J = 3.5 Hz,

e - $[Fe(CO)_4(GeH_2)]_2$, singlet 6.71τ.

f - $[Fe(CO)_4(GeH_3)]_2(GeMe_2)$, singlet 9.00τ, singlet 6.51τ, this peak is close to the singlet of the starting material and it is difficult to determine at what stage this signal appears. At 35 days there is no mistaking this peak for 'ringing' associated with the parent material as these signals are of comparable height.

i - Signals less than 1% intensity occur at 6.56τ, $Fe(CO)_4(H)(GeH_3)$? 6.90τ, GeH_4 and 8.91τ, were just discernable at this stage.

Figure 4.8

Nmr spectra from the self-reaction of $Fe(CO)_4(GeMe_2H)(GeH_3)$

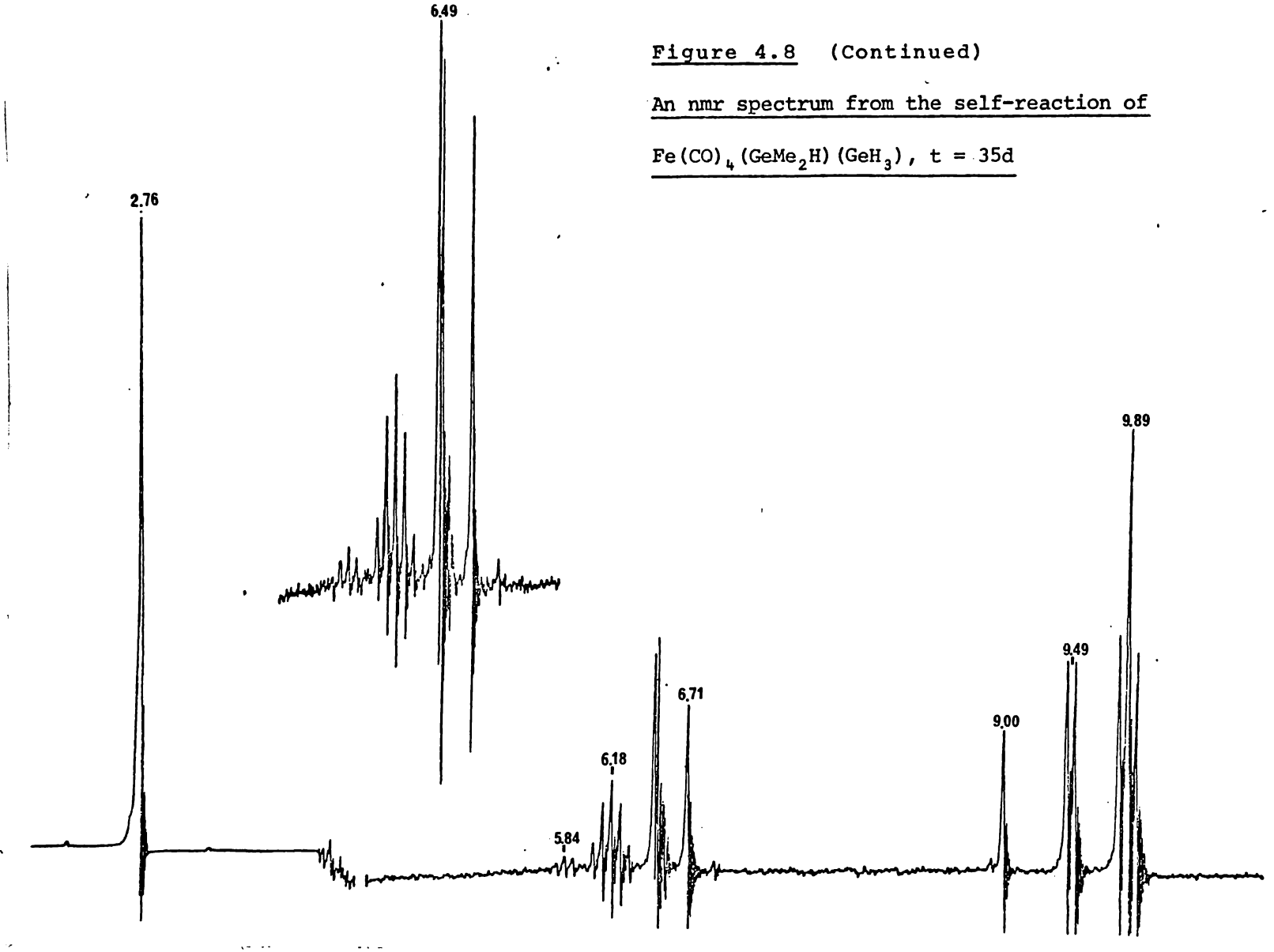

Figure 4.8 (Continued)

An nmr spectrum from the self-reaction of

$Fe(CO)_4(GeMe_2H)(GeH_3)$, t = 35d

This type of scheme was also proposed in the $Fe(CO)_4(GeMeH_2)$-(GeH_3) case where a barely perceptible amount of GeH_4 occurs and then only in the latter stages of the reaction. In the $Fe(CO)_4(GeMeH_2)(GeH_3)$ case resonance of the GeH_3 protons in $GeMeH_3$ and $[Fe(CO)_4(GeH_3)]_2(GeMeH)$ occur in the region of the GeH_3 protons of $Fe(CO)_4(GeMeH_2)(GeH_3)$, thus doubts about these signals were raised until the 90 MHz facility became available. Here, although formation of the proposed intermediate species occurs to a lesser extent, assignment of $[(Fe(CO)_4(GeH_3)]_2(GeMe_2)$ is more firm. While it is difficult to determine the absolute intensity of different signals especially of weaker signals and signals which are very close together, the percent of $GeMe_2H_2$ would appear to be accounted for by the sum of the two processes, (4.20) and (4.21).

$$2Fe(CO)_4(GeMe_2H)(GeH_3) \longrightarrow [Fe(CO)_4(GeH_2)]_2 + 2GeMe_2H_2 \quad \ldots(4.21)$$

4.5.3 Reaction between $Fe(CO)_4(GeMe_2H)(GeH_3)$ and $CC\ell_4$

Reaction between dimethylgermyl(germyl)tetracarbonyliron(0) and $CC\ell_4$ was more rapid than for the analogous unsymmetrically substituted monomethylgermyl(germyl)tetracarbonyliron(0) species (see Table 4.11, page 173). In this reaction too, competition with the self-reaction;

$$Fe(CO)_4(GeMe_2H)(GeH_3) \longrightarrow GeMe_2H_2 + [Fe(CO)_4(GeH_2)]_2 + [Fe(CO)_4(GeH_3)]_2(GeMe_2) \quad \ldots(4.22)$$

is evident. $GeMe_2H_2$, $[Fe(CO)_4(GeH_2)]_2$ and $[Fe(CO)_4(GeH_3)]_2(GeMe_2)$ undoubtedly arise chiefly from this reaction.

Chlorine-substitution was also rapid, but no simple derivative such as $Fe(CO)_4(GeC\ell Me_2)(GeH_3)$ was seen. Thus, halogenation

TABLE 4.11

Nmr reaction between $Fe(CO)_4(GeMe_2H)(GeH_3)$ and $CC\ell_4$

TIME days	Relative intensity of signal (mole percent)								
	$Fe(CO)_4(GeMe_2H)(GeH_3)$ a	$GeMe_2H_2$ b	$GeC\ell Me_2H$ c	$[Fe(CO)_4(GeH_3)]_2(GeMe_2)$ d	$[Fe(CO)_4]_2(GeC\ell_2)(GeH_2)$ e	$[Fe(CO)_4(GeH_2)]_2$ f	GeH_4 g	$[Fe(CO)_4]_2(GeMe_2)(GeC\ell_2)$ h	$[Fe(CO)_4]_2(GeMe_2)(GeC\ell H)$ i
1[j]	86	5	4	3	2				
2	65	8	15	3	9				
5	30	11	36	3	15	2	2		
20	12	12	50	5	8	8	3	1	2
34[k]	-	15	55	7	2	10	5	3	3

a $Fe(CO)_4(GeMe_2H)(GeH_3)$, 9.49τ doublet, 6.48τ singlet, 5.84τ, septet, ^3J = 3.2 Hz, intensity ratio, 6 : 3 : 1.

b $GeMe_2H_2$, 9.89τ triplet, 6.18τ multiplet, ^3J = 3.5 Hz, intensity ratio 3 : 1., c, $GeC\ell Me_2H$, 9.72τ doublet, 4.62τ , multiplet, ^3J = 2.2 Hz, intensity ration 6 : 1.,

d $[Fe(CO)_4(GeH_3)]_2(GeMe_2)$, 9.03τ singlet, 6.51τ singlet,

e $[Fe(CO)_4]_2(GeC\ell_2)(GeH_2)$?, 6.59τ, singlet. f, $[Fe(CO)_4(GeH_2)]_2$, 6.71τ singlet, g, GeH_4, 6.90τ singlet, h, $[Fe(CO)_4]_2(GeMe_2)(GeC\ell_2)$? 9.29τ singlet, i, $[Fe(CO)_4]_2(GeMe_2)(GeC\ell H)$?, 9.07τ singlet, 5.61τ singlet, j, After one day the solution appears slightly yellow

k, After thirty-four days, the solution is orange in colour, and a trace of unreacted $Fe(CO)_4GeMeH_2)(GeH_3)$ is seen.

See also Figure 4.9.

Figure 4.9

Nmr spectra from reaction between $Fe(CO)_4(GeMe_2H)(GeH_3)$ and CCl_4

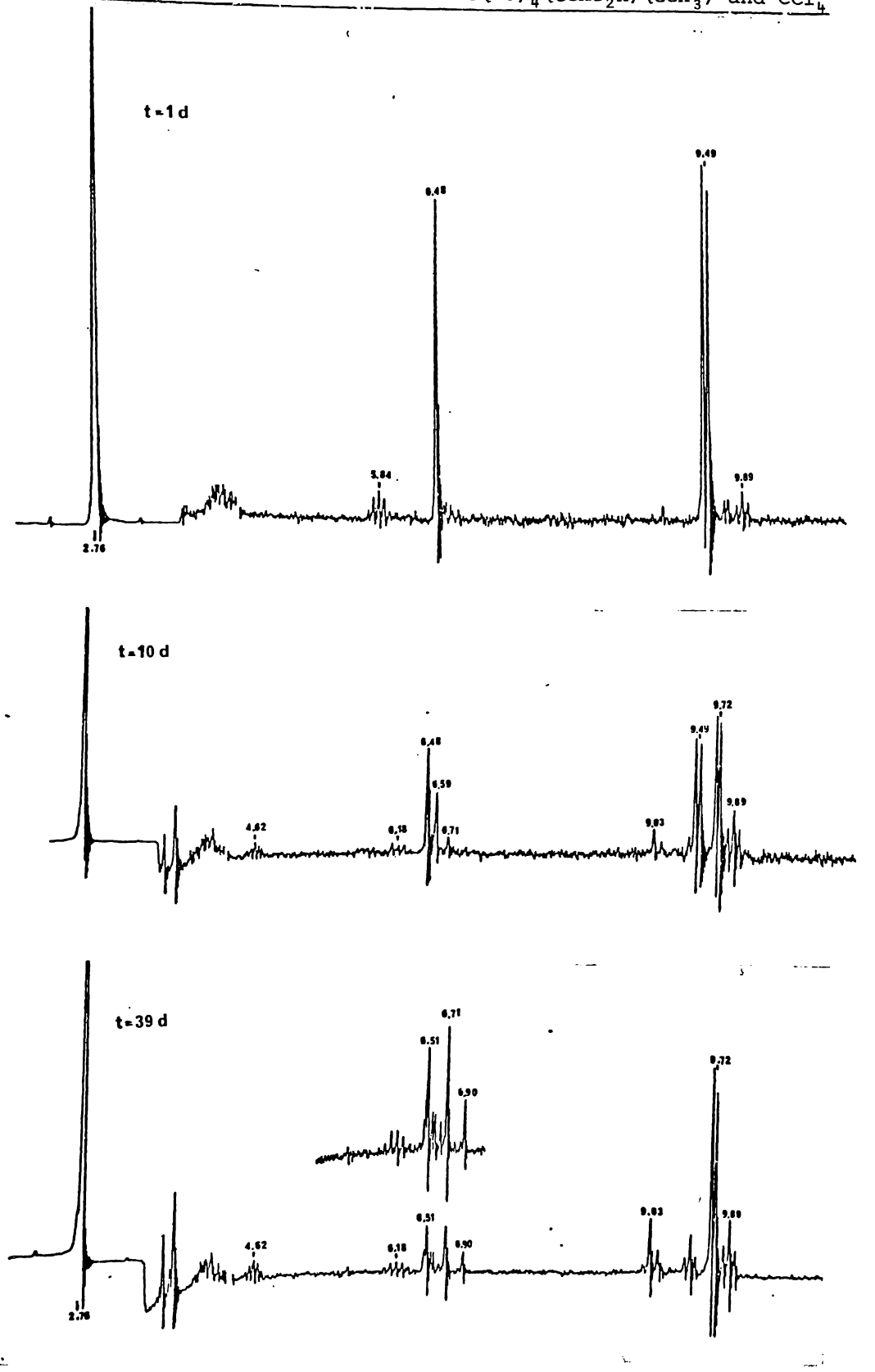

must be followed by rapid condensation, thus accounting for the $GeC\ell Me_2H$ observed. Thus, reactions such as (4.23) are suggested.

$$2Fe(CO)_4(GeC\ell Me_2)(GeH_3) \longrightarrow 2GeC\ell Me_2H + [Fe(CO)_4(GeH_2)]_2 \quad ...(4.23)$$

However, the proportion of $[Fe(CO)_4(GeH_2)]_2$ is far below that of $GeC\ell Me_2H$ throughout the reaction. Indeed, if the sum of $GeMe_2H_2$ and $GeC\ell Me_2H$ is taken, then the proportion of condensed products indicated by equations (4.22) and (4.23) are never seen. This strongly indicates:

i) that the new species giving the singlet at 6.59τ is a condensed product - most reasonably $[Fe(CO)_4]_2(\mu\text{-}GeC\ell_2)(\mu\text{-}GeH_2)$ and,

ii) that further species with weak or non-existent ^1H signals also occur. The latter would include μ-$GeC\ell H$ and μ-$GeC\ell_2$ groups.

Thus to account for the observed distribution of products, it is proposed that equation (4.22) is significant, equation (4.23) may occur to a minor extent, and equation (4.24), involving rapid initial poly-substitution, is dominant.

$$Fe(CO)_4(GeMe_2H)(GeH_3) + nCC\ell_4 \longrightarrow Fe(CO)_4(GeC\ell Me_2)(GeC\ell_nH_{3-n})$$

$$\Big\downarrow -GeC\ell Me_2H$$

$$[Fe(CO)_4(GeC\ell_yH_x)]_2$$

For combinations of x = 2,1,0 : y = 2,1,0.

...(4.24)

No signals from μ-$GeC\ell H$ species were positively identified but these would be weak.

Weak singlets in the methyl region, arising late in the reaction can be ascribed to species with μ-$GeMe_2$ groups arising by minor paths

similar to (4.24). Further halogenation of products such as $[Fe(CO)_4]_2(GeC\ell_2)(GeH_2)$ can also be expected at later stages of the reaction. Such a step could also give μ-$GeMe_2$ species *via* equations of the type (4.25).

$$[Fe(CO)_4(GeH_4)]_2(GeMe_2) \longrightarrow [Fe(CO)_4(GeH_3)](\mu\text{-}GeMe_2)[Fe(CO)_4(GeC\ell_yH_x)]$$

$$\downarrow -GeH_4$$

$$[Fe(CO)_4]_2(\mu\text{-}GeMe_2)(\mu\text{-}GeC\ell_yH_x)$$

$$x = 2,1,0: \quad y = 0,1,2 \qquad \ldots(4.25)$$

These suggestions for routes *via* polyhalogenation are in accord with earlier observations (27,28), on species like $Fe(CO)_4(GeMeH_2)_2$ where very carefully controlled conditions were required to identify mono-halo products. For example, a reaction system using $CC\ell_4$ as solvent which rapidly produced a precipitate analysed as a mixture of tri- and tetra-chlorides.

One further aspect of this reaction is the effect of the $CC\ell_4$ on the self-condensation reaction (4.22). Judged by the low proportion of $[Fe(CO)_4(GeH_2)]_2$ and the relatively large amount of $[Fe(CO)_4(GeH_3)]_2$-$GeMe_2$ in the early stages, the course of (4.22) is perturbed and accelerated compared with (Section 4.52) by the presence of $CC\ell_4$ or of the chloro-substituted products. The apparent perturbation of the self-reaction sequence is also observed in the reaction between $Fe(CO)_4(GeH_3)_2$ and $SiC\ell_4$ (see Section 4.3, (27)). These curious processes are not improbable in light of the self-reaction mechanisms proposed in Section 5.7.1 .

4.5.4 Reaction with hydrogenchloride

The reaction between $Fe(CO)_4(GeMe_2H)(GeH_3)$ and $HCl_{(g)}$ was very similar to that of $Fe(CO)_4(GeMeH_2)(GeH_3)$, see Table 4.12, page 178. Here again, the germylchlorides $GeClMe_2H$ and $GeClH_3$, together with the iron hydride species $Fe(CO)_4(H)(GeClMe_2)$, $Fe(CO)_4(H)(GeH_3)$ and $Fe(CO)_4(H)(GeClH_2)$, accounted for the initial products formed. These species presumably arise *via* similar processes (*c.f.*, scheme (i) and (ii)).

Scheme (iii)

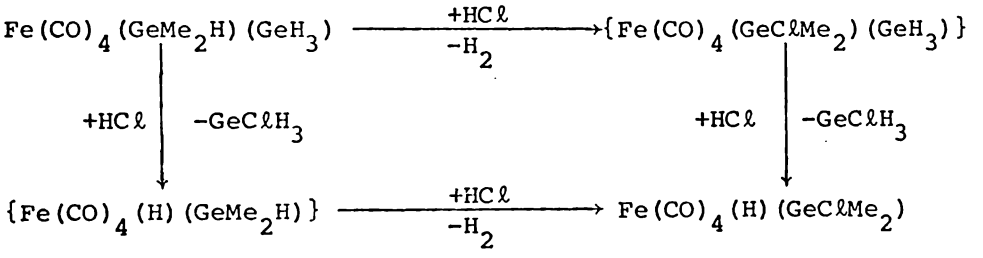

Scheme (iv)

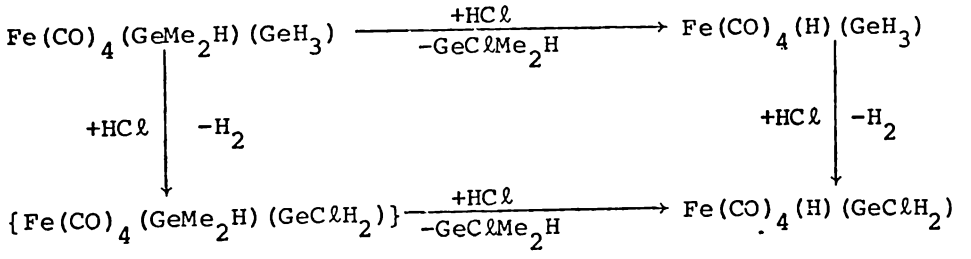

where compounds in { } are not observed.

TABLE 4.12

Nmr study of the reaction between $Fe(CO)_4(GeMe_2H)(GeH_3)$ and HCℓ

TIME (days)	Relative intensity of signal (mole percent)									
	$Fe(CO)_4(GeMe_2H)(GeH_3)$	HCℓ	$GeCℓMe_2H$	$Fe(CO)_4(H)(GeCℓMe_2)$	$Fe(CO)_4(H)(GeH_3)$	$GeCℓH_3$	$Fe(CO)_4(H)(GeCℓH_2)$	GeH_4	$GeCℓ_2Me_2$	$[Fe(CO)_4(GeH_2)]_2$
a	b	c	d	e	f	g	h	i	j	k
1	83	[72]	11	1	4	<1	n.o.			
2	48	[42]	20	8	5	8	11			
5	29	[24]	26	11	9	12	12			
16	1		41	15	22	7	11	2	<1	<1
34 [1]	-		41	13				13	23	6

a, Changes from colourless through pink (1d) to orange (34d). see also Figure 4.10; b, $Fe(CO)_4(GeMe_2)(GeH_3)$, 9.49τ doublet, 6.48τ singlet, 5.84τ multiplet, intensity, 6 : 3 : 1, ^3J = 3.4 Hz; c, HCℓ 9.89τ singlet; d, $GeCℓMe_2H$, 9.71τ doublet, 4.63τ multiplet, ^3J = 2.2 Hz; e, $Fe(CO)_4(H)(GeCℓMe_2)$, 9.10τ singlet, 20.54τ singlet; f, $Fe(CO)_4(H)(GeH_3)$, 6.58τ singlet, 20.45τ singlet; g, $GeCℓH_3$, 5.40τ; h, $Fe(CO)_4(H)(GeCℓH_2)$, 4.42τ singlet, 20.84τ singlet; i, GeH_4, 6.91τ singlet; j, $GeCℓ_2Me_2$, 9.46τ singlet; k, $[Fe(CO)_4(GeH_2)]_2$ 6.71; l, New singlets (intensity <2) at 4.58τ, 5.47τ, 6.64τ, 6.75τ, 8.60τ.

Figure 4.10

Nmr spectra obtained during reaction of $Fe(CO)_4(GeMe_2H)(GeH_3)$ and HCl

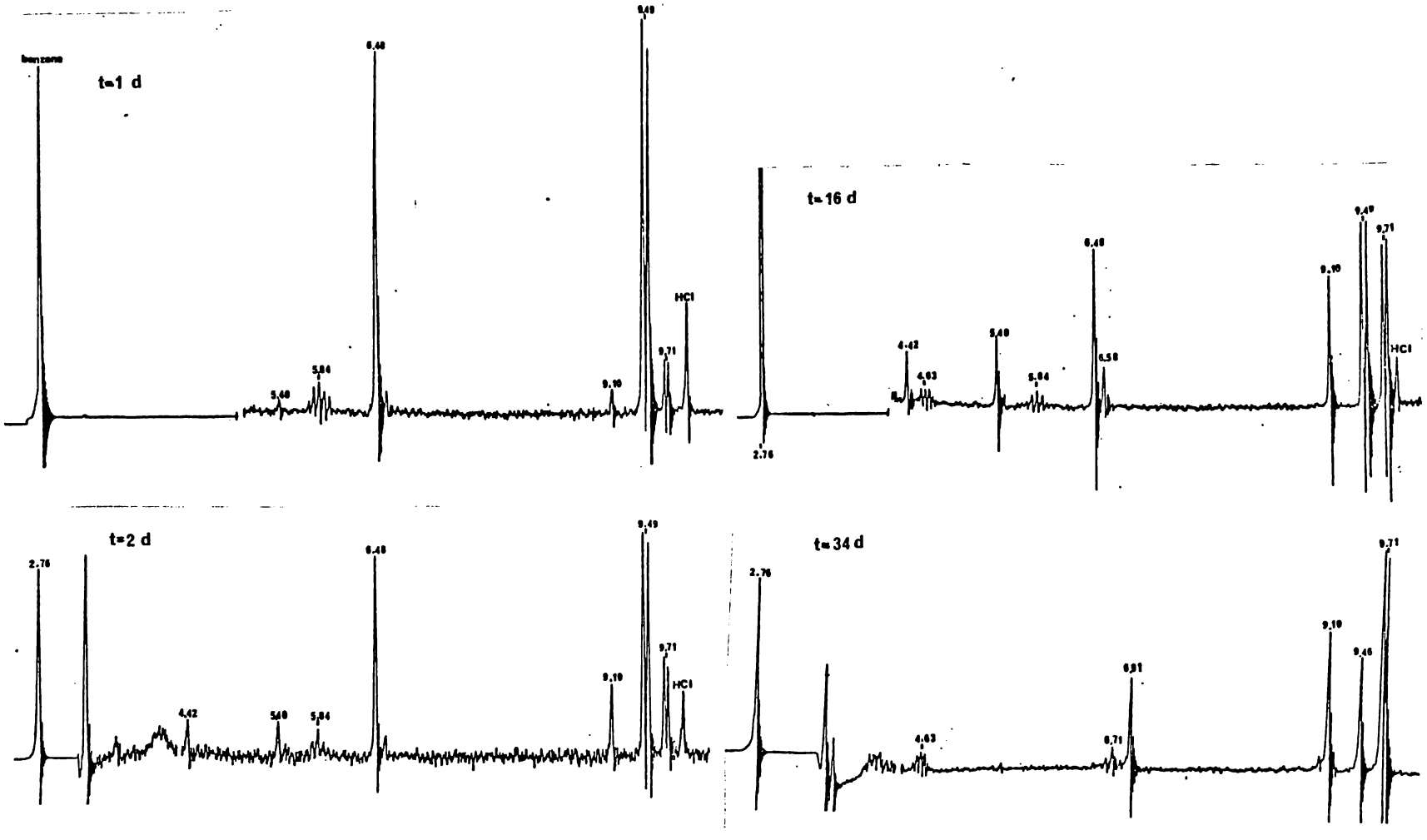

Again, no chlorine substituted $Fe(CO)_4(GeMe_2H)(GeH_3)$ species were observed, and Scheme (iv) would appear to indicate the dominant process, since $GeCl Me_2H$ is the dominant hydride seen and in this case the unsubstituted $Fe(CO)_4(H)(GeH_3)$ is also observed. This reaction differs from that of the monomethyl congener, however, in that the amount of $GeCl Me_2H$ appearing is not approximately equal to the amount of $Fe(CO)_4(H)(GeCl H_2)$ plus $Fe(CO)_4(H)(GeH_3)$ observed. Perhaps in this case $Fe(CO)_4(H)(GeCl_2H)$ and even $Fe(CO)_4(H)(GeCl_3)$ was formed (the GeH signal would be obscured by the massive solvent peak). The amount of $GeCl H_3$ does, however, initially match the amount of $Fe(CO)_4(H)(GeCl Me_2)$ observed. While the initial stages in the reactions between the monomethylgermyl(germyl) and dimethylgermyl(germyl)-tetracarbonyliron occur at similar rates, further reaction of the initial products in the dimethylgermyl system is more rapid.. If GeH_4 is taken as a very rough guide of the extent at which condensation processes are occurring then for example, 13 mole percent GeH_4 in 34 days for the dimethyl system clearly indicates more further reaction than 16 mole percent GeH_4 at 84 days in the monomethylgermyl(germyl)-tetracarbonyliron system. $GeCl_2Me_2$ is also evident in relatively large quantities in this sytesm, whereas, no $GeCl_2MeH$ was observed in the $Fe(CO)_4(GeMeH_2)(GeH_3)/HCl$ reaction. This too, indicates that $Fe(CO)_4(GeMe_2H)(GeH_3)$ is more reactive than $Fe(CO)_4(GeMeH_2)(GeH_3)_2$ on reaction with HCl.

4.5.5 Summary of reactions between $Fe(CO)_4(GeMe_{3-x}H_x)(GeM_{3-y}H_y)$ and covalent halides

In summary, it can be seen that reactions with $SiC\ell_4$ and $CC\ell_4$ result in preferential halogenation of the methyl substituted group. No evidence is seen for stepwise halogenation at alternate germanium groups. Rather, the chloro and methyl substituted species have a propensity for reacting further to form higher molecular weight species. (*c.f.* reaction between $[Fe(CO)_4]^{2-}$ and $GeBr_2H_2$, Section 3.3).

Hydrogenchloride is seen to :

(a) act as a chlorinating agent,

and (b) cause fission of the Fe-Ge bonds.

While it is not definite which process occurs first, or whether, in fact, one process occurs before the other, results in this work tend to support the mechanism: (b) followed by (a).

There also appears to be a preference for cleavage of the methyl substituted germane as opposed to the competing process, cleavage of a $Fe\text{-}GeH_3$ (or $Fe\text{-}GeC\ell H_2$) moiety.

Table 4.4.2, page 182, lists nmr data relevant to reactions involving covalent halides obtained in this work. The paucity of data precludes any major generalisations about changes in chemical shift values on chlorine substitution, suffice those already mentioned. Assignments given in this work were gleaned chiefly from previous nmr data (especially 27,28), reaction data (27,28), the intensities of the signals, chemical shift data and coupling constants. Certainly, product species showing multiplicities were more readily identifiable because of

(i) the multiplicity of the signal and

(ii) the sensitivity of the coupling constant to chlorine substitution.

TABLE 4.4.2

Nmr parameters of different compounds in benzene solution

Compound	Chemical Shift (τ)			Coupling Constant (Hz)
GeH_4			6.90 s	
$GeMeH_3$	9.93 q		6.47 q	3.8
$GeMe_2H_2$	9.89 t		6.18 h	3.5
$GeMe_3H$	9.83 d		5.89 m	3.2
$GeClH_3$			5.37 s	
$GeClMeH_2$	9.70 t		4.91 q	2.6
$GeClMe_2H$	9.72 d		4.62 m	2.2
CH_2Cl_2			5.54	
HCl	9.8 s			
H_2			5.7 s	
$Fe(CO)_4(H)(GeH_3)$	20.10 s		6.57 s	
$Fe(CO)_4(H)(GeClH_2)$	20.74 s		4.38 s	
$Fe(CO)_4(H)(GeClMeH)$	20.56 s		9.10 d	2.5
$Fe(CO)_4(H)(GeCl_2Me)$	20.24 s		8.78 s	
$Fe(CO)_4(H)(GeClMe_2)$	20.54 s		9.10 s	
$Fe(CO)_4(GeMeH_2)(GeH_3)$	9.49 t	6.47 s	6.11 q	3.4
$Fe(CO)_4(GeMeH_2)_2$	9.51 t		6.13 q	3.4
$Fe(CO)_4(GeMe_2H)(GeH_3)$	9.49 d	6.48 s	5.84 h	3.2
$Fe(CO)_4(GeClMeH)(GeH_3)$	9.07 d		6.70 s	2.6
$[Fe(CO)_4(GeH_2)]_2$			6.71 s	
$[Fe(CO)_4(GeMeH)]_2$	8.99 d			3.4
$[Fe(CO)_4(GeMe_2)]_2$	9.00 s			
$[Fe(CO)_4(GeH_3)]_2(GeMe_2)$	9.03 s		6.51 s	
$[Fe(CO)_4]_2(GeMe_2)(GeClH)$?	9.07 s		5.61 s	
$[Fe(CO)_4]_2(GeCl_2)(GeMe_2)$?	9.29 s			
$[Fe(CO)_4]_2(GeCl_2)(GeH_2)$?			6.59 s	

All values were obtained in this work.

4.6 Dimethylgermyl(monomethylgermyl)tetracarbonyliron(0), $Fe(CO)_4(GeMe_2H)(GeMeH_2)$

4.6.1 Preparation of $Fe(CO)_4(GeMe_2H)(GeMeH_2)$

It took 20 hours to condense $Fe(CO)_4(GeMeH_2)_2$, (600 mg, 1.73 mmol), under mercury diffusion pump vacuum into the double reaction vessel containing $NaMn(CO)_5$ (from $Mn_2(CO)_{10}$, 401 mg, 1.03 mmol). Et_2O (2 ml) was then introduced into the reaction vessel and the reaction mixture was allowed to warm to room temperature. After intermittent shaking for ten minutes the solution had turned from green to red in colour.

Following fractionation, $Mn(CO)_5(GeMeH_2)$ (264 mg, 0.92 mmol, 53%), was recovered. $GeXMe_2H$ (326 mg, *ca.* 2.02 mmol, X = Cℓ, Br) and pentane (4 ml) were then left to react for 12 minutes with the orange-red material in the reaction vessel. No incondensable gases were evolved. $GeMe_2H_2$, $GeMeH_3$ (trace), pentane and $Mn(CO)_5(GeMe_xH_{2-x})$ were evident in the volatile material that condensed out of the reaction vessel. The colourless, oily product, together with traces of mercury, was pumped into a U-trap. White subliming solid was also observed which was less volatile than the oily product. Reaction vessel residues were extracted with hexane (25 ml), the hexane was removed in vacuo and more white solid sublimed onto a cold finger from the orange-red solid. This was found to be a mixture of octacarbonyls, $[Fe(CO)_4(GeMeH)]_2$, $[Fe(CO)_4]_2(GeMe_2)(GeMeH)$ and $[Fe(CO)_4(GeMe_2)]_2$ from from infrared and mass spectra.

$GeMe_2H_2$, ($GeMeH_3$?), $Mn(CO)_5(GeMeH_2)$ and ($Mn(CO)_5(GeMe_2H)$?) were recovered in the volatile fraction, together with unreacted $GeXMe_2H$ and pentane.

4.6.2 Discussion

$Fe(CO)_4(GeMe_2H)(GeMeH_2)$ was not prepared pure but it was possible to identify its spectroscopic characteristics. Not all the $Mn(CO)_5(GeMe_{2-x}H_x)$ was removed, so the most volatile fractions - those giving the mass spectrum and the gas phase infrared spectrum, were contaminated. Indeed, the mass spectrum was dominated by $Mn(CO)_nGeMeH^+$ (or $Fe(CO)_4(Me)(GeMe_2H)^+$?) ions and gave no useful information.

When the bulk product was handled for ^1H nmr and solution infrared measurements minor contamination by similar species was noticed.

Despite these problems, the strongest resonances in the ^1H nmr spectrum (Figure 4.11, page 185), can be assigned to the product as follows:

$GeMeH_2$, triplet 9.38τ, quartet 6.07τ ^3J = 3.4 Hz

$GeMe_2H$, doublet 9.44τ, multiplet 5.80τ ^3J = 3.2 Hz

The ratio of GeH intensity to Me proton intensity is 1:3.3 (benzene)

The extra weak signals, heptet *ca.* 5.81τ, ^3J = 3.2 Hz, quartet 6.04τ ^3J = 3.4 Hz and shoulders on the methyl signals do not indicate the presence of:

$Mn(CO)_5(GeMe_2H)$, triplet 9.50τ, quartet 6.21τ, ^3J = 3.8 Hz (C_6H_6)

or

$Mn(CO)_5(GeMe_2H)$, doublet 9.39τ, heptet 5.83τ, ^3J = 3.6 Hz (C_6H_6)

Figure 4.11

The ^{1}H nmr spectrum of $Fe(CO)_4(GeMe_2H)(GeMeH_2)$

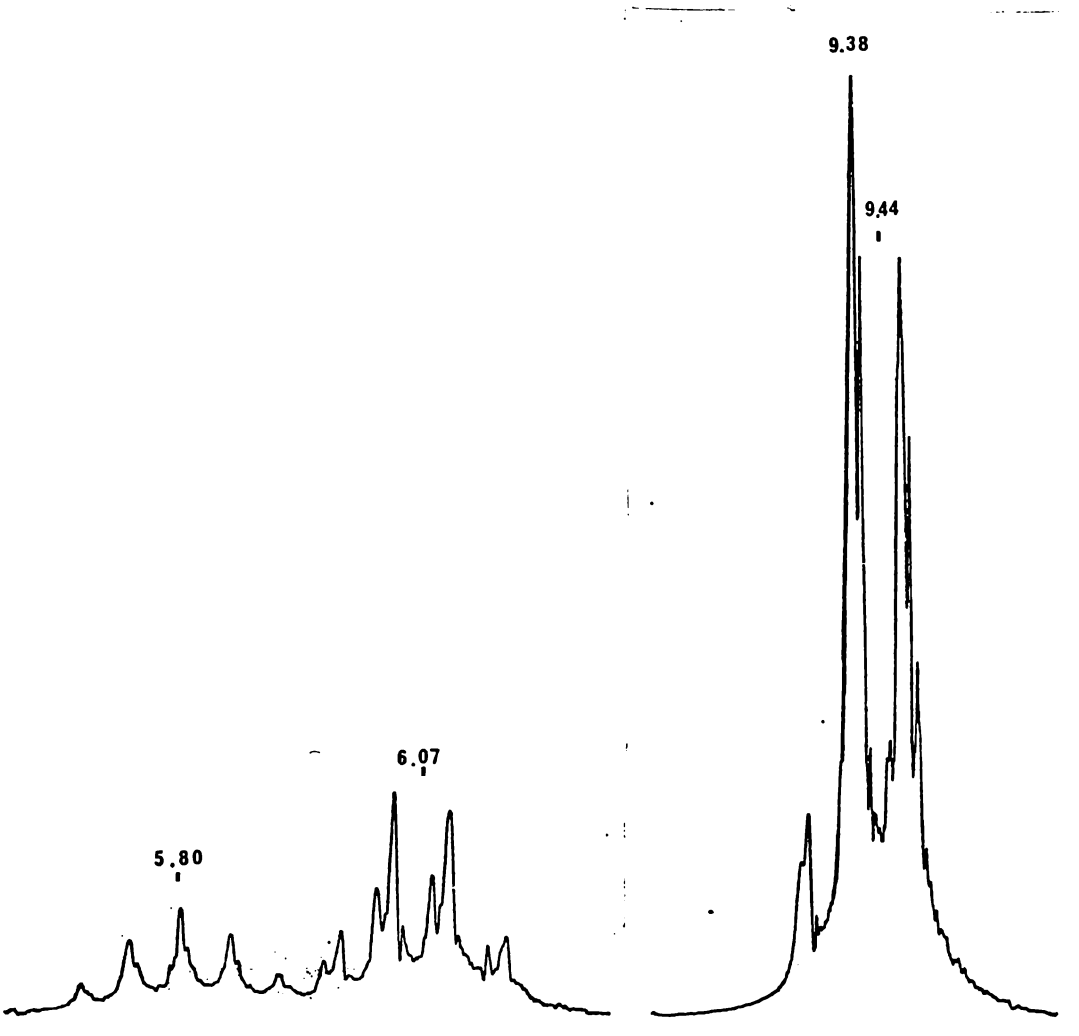

but, may possibly indicate both of the symmetric species

$Fe(CO)_4(GeMeH_{3-x})_2$ (n = 1,2).

$Fe(CO)_4(GeMeH_2)_2$ triplet 9.51τ, quartet 6.13τ, ^3J = 3.4 Hz

$Fe(CO)_4(GeMe_2H)_2$ doublet 9.41τ, heptet 5.83τ, ^3J = 3.2 Hz

$GeMe_2H_2$ (and a little $GeMeH_3$) were found together with octacarbonyl species on transference of sample material.

In a further experiment, a portion of the neat liquid was divided into two under nitrogen. One portion was used for a ^1H nmr measurement and the other was used for measuring the infrared spectrum in cyclohexane and in hexane. A fairly rapid scan gave carbonyl stretches at 2077 m, 2058 w, 2010 s, 1998 sh, 1991 vs cm^{-1} (C_6H_{12}/C_6H_{14}). Octacarbonyl impurity is thought to be contributing the 2058 band and some intensity to the strong band at *ca.*1998 cm^{-1}. The sample was pipetted out of the solution cell after the infrared spectrum had been recorded and was put in an nmr tube. The solvent was pumped off and benzene added. Both samples (*i.e.* that exposed to infrared spectral conditions and that which was not) showed two strong singlets in the nmr at 8.59τ and 5.63τ along with the $Fe(CO)_4(GeMe_2H)(GeMeH_2)$ signals. The chemical shift values recorded in this work for octacarbonyl species in benzene are:

$[Fe(CO)_4(GeH_2)]_2$ singlet 6.71τ

$[Fe(CO)_4(GeMeH)]_2$ doublet 8.99τ ^3J = 3.4 Hz

$[Fe(CO)_4(GeMe_2)]_2$ singlet 8.89τ

The new singlets are thus spurious peaks arising from the handling technique. (*c.f.* $Fe(CO)_4(GeMe_3)_2$, Section 3.7.3). Involatile white-yellow solid which was left after transferring $Fe(CO)_4(GeMe_2H)(GeMeH_2)$ under high vacuum gives a mass spectrum which is compatible with the possible condensation product $[Fe(CO)_4]_2(\mu\text{-}GeMe_2)(\mu\text{-}GeMeH)$ but a mixture of $[Fe(CO)_4(\mu\text{-}GeMe_2)]_2$ and $[Fe(CO)_4(\mu\text{-}GeMeH)]_2$ cannot be ruled out. The infrared spectrum of this material is shown in Figure 4.12, page 188 . Absorption *maxima* occur at 2059 sh, 2056 s, 2053 s, 2021 wsh, 2016 wsh, 2006 vs, *ca.* 2003 sh, 2001 vs, 1991 msh, 1970 vw, 1964 vw, 624 m, 613 s cm^{-1}.

This material is thought to be a mixture of two or three different methylgermylsubstituted octacarbonyls, $\mu\text{-}(GeMe_2)_2$ $\mu\text{-}(GeMe_2)(GeMeH)$ and $\mu\text{-}(GeMeH)_2$ (see Section 5.6.)

Self-reaction

The proton nmr of one sample of $Fe(CO)_4(GeMe_2H)(GeMeH_2)$ in benzene showed signals from $GeMe_2H_2$ (*ca.* 10%) a trace of $GeMeH_3$ and overlapping signals from various octacarbonyls, 8.91τ w, 8.94τ s, 8.98τ m, 9.00τ m, after three hours. From these observations, it is tentatively suggested that reactions:

$$2Fe(CO)_4(GeMe_2H)(GeMeH_2) \longrightarrow 2GeMe_2H_2 + [Fe(CO)_4(GeMeH)]_2 \quad \ldots(4.26)$$

$$2Fe(CO)_4(GeMe_2H)(GeMeH_2) \longrightarrow 2GeMeH_3 + [Fe(CO)_4(GeMe_2)]_2 \quad \ldots(4.27)$$

$$2Fe(CO)_4(GeMe_2H)(GeMeH_2) \longrightarrow GeMe_2H_2 + GeMeH_3 + [Fe(CO)_4]_2(GeMe_2)(GeMeH) \quad \ldots(4.28)$$

are all possible with (4.26) the fastest. Further study of purer samples would be needed to put these conclusions on a firm basis. Undoubtedly self-reaction of contaminating species $Fe(CO)_4(GeMe_{3-n}H_n)_2$ will also occur in these samples. The neat sample of this material(s) showed no sign of self-reaction in two hours in contrast to samples in benzene solution.

Figure 4.12

The carbonyl infrared spectrum of the octacarbonyl product(s) from condensation of $Fe(CO)_4(GeMe_2H)(GeMeH_2)$, C_6H_{12}, cm^{-1}

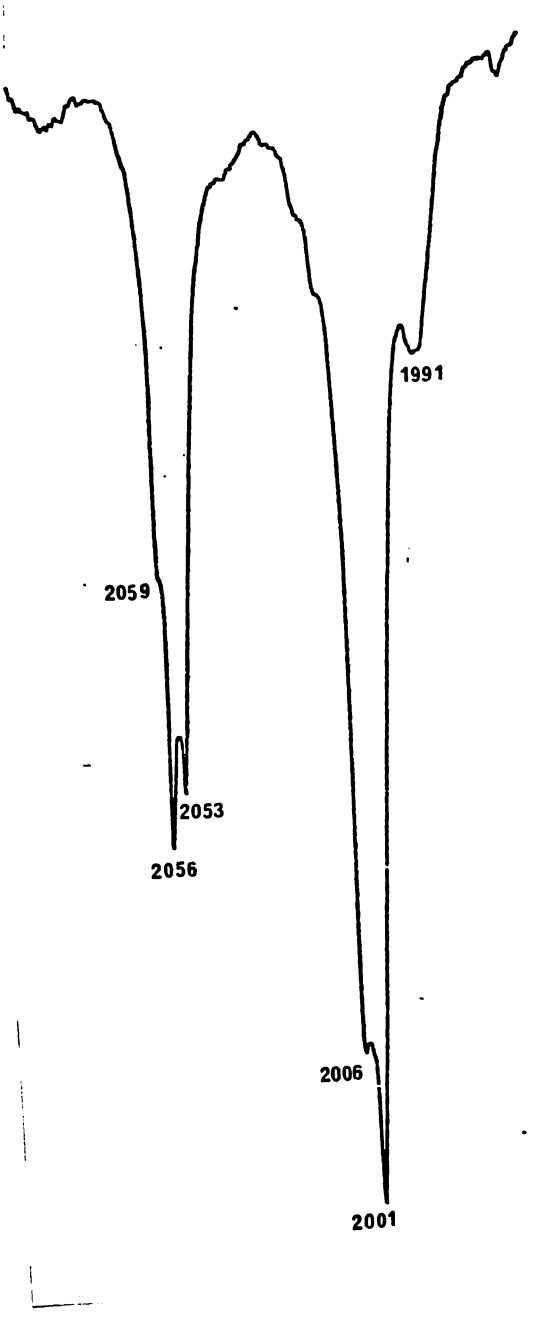

CHAPTER FIVE

PREPARATION OF TRIMETHYLGERMYL IRON CARBONYL COMPOUNDS AND SURVEY OF THE PROPERTIES OF $Fe(CO)_4(GeMe_{3-x}H_x)(GeMe_{3-y}H_y)$

In this chapter, the preparation and properties of $Fe(CO)_4(GeMe_3)(GeMe_{3-x}H_x)$ are discussed briefly, together with data obtained from their decomposition. The concluding sections briefly outline and summarise the characteristics of compounds of the type $Fe(CO)_4(GeMe_{3-x}H_x)(GeMe_{3-y}H_y)$.

This work was initiated by the quest for a preparative route to the formation of a new species, $[Fe(CO)_4(GeH_2)]_2$ found in *ca.* 10% in Bonny's reactions between $[Fe(CO)_4(GeH_3)]^-$ and $GeC\ell Me_3$ (27).

Unlike $[Fe(CO)_4(GeMe_2)]_2$, $[Fe(CO)_4(GeH_2)]_2$ is not a product of the coupling reaction between $[Fe(CO)_4]^{2-}$ and $GeBr_2H_2$ (Section 3.3) and nor is it formed significantly in the self-reaction of $Fe(CO)_4(GeH_3)_2$ (27). Bonny's reaction stoichiometry was as follows:

$$\underset{(0.57\ \text{mmol})}{Fe(CO)_4(GeH_3)_2} + \underset{(0.29\ \text{mmol})}{[Mn(CO)_5]^-} \xrightarrow[20\ \text{min}]{Et_2O}$$

$$[Fe(CO)_4(GeH_3)]^- + \underset{(0.28\ \text{mmol})}{Mn(CO)_5(GeH_3)} + \underset{(0.04\ \text{mmol})}{CO} + \underset{(0.002\ \text{mmol})}{H_2}$$

$$[Fe(CO)_4(GeH_3)]^- + \underset{(0.78\ \text{mmol})}{GeC\ell Me_3} \xrightarrow[5\ \text{min}]{Et_2O} \underset{(0.06\ \text{mmol})}{GeH_4} + \underset{(0.045\ \text{mmol})}{CO/H_2}$$

$$\underset{(0.13\ \text{mmol})}{Mn(CO)_5(GeH_3)} + \underset{(0.11\ \text{mmol})}{(Me_3Ge)_2O} + \underset{(\text{not determined})}{GeMe_3H/Et_2O} + \underset{(0.07\ \text{mmol})}{[Fe(CO)_4(GeH_2)]_2}$$

The involatile $Fe(CO)_4(GeH_2)_2$ was found in a trap held at -10°. $Fe(CO)_4(GeMe_3)(GeH_3)$ was postulated as an intermediate in this reaction. (27).

5.1 Trimethylgermyl(germyl)tetracarbonyliron(0), $Fe(CO)_4(GeMe_3)(GeH_3)$

5.1.1 Preparation of $Fe(CO)_4(GeMe_3)(GeH_3)$

After 30 minutes at room temperature, $Fe(CO)_4(GeH_3)_2$ (94 mg, 2.94 mmol), $NaMn(CO)_5$ (from $Mn_2(CO)_{10}$ 584 mg, 1.49 mmol), and Et_2O (2 ml) had changed from green to a red coloured oily mixture. The volatile components were removed; Carbon monoxide and/or hydrogen (*ca.* 0.07 mmol), GeH_4 (*ca.* 0.2 mmol), Et_2O, a trace of $Fe(CO)_4(GeH_3)_2$ or $Fe(CO)_4(H)(GeH_3)$, and $Mn(CO)_5(GeH_3)$ (675 mg, 2.50 mmol; *ca.* 84% yield based on the manganese used). The red $NaFe(CO)_4(GeH_3)$ containing residue was left at room temperature for 12 hours. A small amount of GeH_4, $Mn(CO)_5(GeH_3)$ and Et_2O were observed after this time, (Et_2O having leaked through the teflon tap of the double reaction vessel). $GeC\ell Me_3$ (449 mg, 2.93 mmol), and Et_2O (676 mg) were introduced to the reaction vessel. A brown solution formed after 30 minutes reaction at room temperature. No incondensable gases were observed. GeH_4 (*ca.* 0.15 mmol) Et_2O and $GeMe_3H$ (and $GeC\ell Me_3$?), $Mn(CO)_5(GeH_3)$ (*ca.* 1.5 mg, 0.006 mmol) and $Fe(CO)_4(GeH_3)_2$ (*ca.* 3 mg, 0.01 mmol) condensed out of the reaction vessel and were identified after fractionation. $Fe(CO)_4(GeMe_3)(GeH_3)$ (2100 mg, 0.58 mmol), contaminated with traces of mercury), had condensed into a U-trap held at -196° (*ca.* 10^{-5} mm Hg) after pumping on the reaction vessel for 3 hours. The yield based on the $Mn(CO)_5(GeH_3)$ recovered is 23%. $[Fe(CO)_4(GeH_2)]_2$ was extracted from the reaction vessel residues with C_6H_{12}.

5.1.2 Characterisation of $Fe(CO)_4(GeMe_3)(GeH_3)$

The proton nmr spectrum of $Fe(CO)_4(GeMe_3)(GeH_3)$ was run in benzene, just above the melting point of the solution to minimise decomposition. It shows a singlet at 9.45 τ and a singlet at 6.53 τ in intensity ratio 3:1 (average = 3.06:1).

The mass and vibrational spectra are also consistent with the formulation $Fe(CO)_4(GeMe_3)(GeH_3)$ but could only be acquired with difficulty because of the very ready self-reaction. They are detailed below in Section 5.1.5, and Section 5.1.6.

5.1.3 Self-reaction of the neat liquid

(a) Colourless, oily, $Fe(CO)_4(GeMe_3)(GeH_3)$, (77.2 mg, 0.214 mmol) was left in a U-trap under vacuum, in the dark, at room temperature for 64 hours. At this time an orange red solid precipitated out of the oily starting material. Negligible incondensable gas (H_2 and/or CO), GeH_4 (0.3 mg, 0.004 mmol) $GeMe_3H$ (14.8 mg, 0.125 mmol), $Fe(CO)_4(GeMe_3)(GeH_3)$ (27.5 mg, 0.075 mmol, weight by difference) $[Fe(CO)_4(GeH_2)]_2$, (34.6 mg, 0.07 mmol) were separated by their volatility differences, and identified by infrared and mass or nmr spectroscopy.

(b) In another trial run from a different preparation which retained a trace of Et_2O, $Fe(CO)_4(GeMe_3)(GeH_3)$ (155.2 mg, 0.43 mmol) was left in the dark at room temperature for 16 hours. Incondensable, H_2 and/or CO (*ca.* 0.1 mmol), $GeMe_3H$ and Et_2O (39 mg), $Fe(CO)_4(GeMe_3)(GeH_3)$ (28 mg, 0.077 mmol, weight by difference), and $[Fe(CO)_4(GeH_2)]_2$ (88 mg, 0.18 mmol), were recovered.

5.1.4 Self-reaction in solution

A colourless solution of $Fe(CO)_4(GeMe_3)(GeH_3)$ in benzene was warmed up to 7°C and the ^1H nmr spectrum was recorded. After 30 minutes at this temperature incipient self-reaction is evident from the change in colour of the solution (yellow). After 60 minutes over which time the temperature was increased from 7°C to 17°C peaks due to the methyl protons of $GeMe_3H$, (doublet 9.82 τ, multiplet 5.89 τ, ^3J = 3.2 Hz), $[Fe(CO)_4(GeH_2)]_2$ (singlet, 6.71 τ) and a small unidentified singlet at 9.72 τ were measurable. At this stage, the reacting system was warmed to room temperature. The 9.72 τ signal may be due to $(Me_3Ge)_2O$: it remained unaltered throughout the experiment.

The 6.71 τ signal ascribed to $[Fe(CO)_4(GeH_2)]_2$ became more prominent as the starting material was consumed. However, its intensity does not indicate the quantity of product since much of this was precipitated. Further changes are therefore best shown by the intensities of methyl signals which are given in Table 5.1, page 197.

Figure 5.1, page 198 , illustrates the nmr spectrum at various intervals during this reaction.

The singlets which appear at 42 hours *ca.* 2 Hz to the low frequency side of the parent singlets appear to increase in intensity as the reaction proceeds, *viz.*,

TIME	Signal intensity as a percent of the parent signal	
	9.47 τ	6.49 τ
42 hours	15%	30%
30d	30%	45%
43d	50%	50%
170d	parent material and these peaks too small to obtain data for	

5.1.5 Mass spectroscopic data

The mass spectrum of $Fe(CO)_4(GeMe_3)(GeH_3)$ was obtained *via* the gas sampling inlet. The inlet heater and temperature of the ion source were both turned as low as possible. The sample had to be intermittently pumped on to remove $GeMe_3H$ which formed throughout this procedure. After several attempts, satisfactory scans were obtained. See Table 5.2, page 200.

5.1.6 The infrared spectrum of $Fe(CO)_4(GeMe_3)(GeH_3)$

$Fe(CO)_4(GeMe_3)(GeH_3)$ was found to be unstable in the gas phase and in solution. However, gas phase data could be obtained transiently as the sample warmed up after being condensed into a cold-finger gas cell. The spectra from various runs under slightly differing conditions were all relatively rapid scans. The spectrum was changing with time in each of the samples in the same manner, but different runs caught the product at different stages of self-reaction. A balance was required between the increase in intensity as the sample warmed up and the self-reaction of $Fe(CO)_4(GeMe_3)(GeH_3)$. The spectrum which best met these two criteria is illustrated in Figure 5.2, page 203, together with the same sample after 60 minutes in the gas cell. The actual frequencies recorded in these spectra are given in Table 5.3, page 202, along with the vibrational data for $Fe(CO)_4(H)(GeH_3)$ which appears to be the material that $Fe(CO)_4(GeMe_3)(GeH_3)$ is initially forming. There was no sign of any $GeMe_3H$ or GeH_4 in these gas phase decompositions of $Fe(CO)_4(GeMe_3)(GeH_3)$ in the infrared cell. Both the carbonyl-stretching modes and the 900-500 cm^{-1} region of the infrared spectrum of the decomposition product, strongly indicate that this product is in fact $Fe(CO)_4(H)(GeH_3)$. At this stage, it is not known what is happening to the $GeMe_3$ groups. During these studies, the walls of the gas cell were seen to become slightly

orange in colour. This suggests that octacarbonyl and/or polymetallic species were forming on the cell walls. Solid film spectra obtained by 'blowing' solid material out of the inlet onto the cooled KBr plate in the centre of the gas cell with nitrogen gas typically showed very broad, irregular peaks. As mentioned previously, this is thought to be an artefact of the technique rather than a property of the compound in question.

No Raman spectrum could be obtained as a dense orange deposit formed on the wall of the sample tube the instant that the sample was placed in the laser beam.

5.2. Discussion

5.2.1 Discussion of the preparation of $Fe(CO)_4(GeMe_3)(GeH_3)$

Typically, 20% yield was obtained from reactions of the type described in Section 5.1.1. Yields of the $GeMe_3H$ formed, and the amount of $GeC\ell Me_3$ used were not determined as these were not fractionated away from the Et_2O solvent. This yield contrasts with Bonny's previous report (27) of the same reaction, where no $Fe(CO)_4(GeMe_3)(GeH_3)$ was recovered. Similar reaction conditions were used in this work. But, in retrospect, Et_2O was a poor choice of solvent, since it is well known that this solvent can catalyse the formation of $[Fe(CO)_4(M'R_2)]_2$ species from $Fe(CO)_4(M'R_3)_2$ precursors. (See Section 2.2). While the exchange reaction between $[Mn(CO)_5]^-$ and $Fe(CO)_4(GeH_3)_2$ requires a basic solvent to proceed, a non-basic solvent (*e.g.*, hydrocarbon) for the proceeding coupling reaction between $[Fe(CO)_4(GeH_3)]^-$ and $GeC\ell Me_3$ could contribute to improved $Fe(CO)_4(GeMe_3)(GeH_3)$ yields.

5.2.2 Self-reaction of $Fe(CO)_4(GeMe_3)(GeH_3)$

5.2.2.1 Weighed self-reaction studies

If $Fe(CO)_4(GeMe_3)(GeH_3)$ undergoes the following self-reaction in the dark,

$$2Fe(CO)_4(GeMe_3)(GeH_3) \longrightarrow [Fe(CO)_4(GeH_2)]_2 + 2GeMe_3H$$

then for a reaction where 0.14 mmol of $Fe(CO)_4(GeMe_3)(GeH_3)$ are known to have reacted the expected yield of $GeMe_3H$ and $[Fe(CO)_4(GeH_2)]_2$ are 0.14 mmol and 0.07 mmol respectively.

The experimental data from this work does not deviate markedly from this expected product yield. Compare with the experimental values of:

$$Fe(CO)_4(GeMe_3)(GeH_3) \longrightarrow [Fe(CO)_4(GeH_2)]_2 + GeMe_3H + GeH_4 + CO/H_2$$

(0.14 mmol) (0.07 mmol) (0.13 mmol) (0.004 mmol) (negligible)

In another trial which was known to contain a trace of Et_2O, the above reaction seems to have been accelerated. Compare 64% decomposition in the ether-free reaction above in 64 hours at room temperature with 82% reaction after 16 hours at room temperature in the presence of Et_2O. This latter reaction had a material balance,

$$Fe(CO)_4(GeMe_3)(GeH_3) + (Et_2O) \longrightarrow [Fe(CO)_4(GeH_2)]_2 + (GeMe_3H + Et_2O) + H_2/CO$$

(0.36 mmol) (0.18 mmol) (*ca.* 0.34 mmol) (0.1 mmol)

Enhanced rate of self-reaction where Et_2O is a known contaminant is not unexpected in view of the base catalysed reaction studies carried out previously on $[M(CO)_4(M'R_2)]_2$ species. (Section 2.2).

5.2.2.2 Nmr monitored self-reaction studies

As Table 5.1, page 197, shows, the principal changes were the steady disappearnce of $Fe(CO)_4(GeMe_3)(GeH_3)$ and its replacement by $GeMe_3H$. This change is near to quantitative (*ca.* ± 5%) as judged by the intensities of the methyl signals. The GeH product signals include both $GeMe_3H$ and a singlet from the product $[Fe(CO)_4(GeH_2)]_2$ but these changes are not quantitative since product precipitates. Thus, the basic reaction is:

$$2Fe(CO)_4(GeMe_3)(GeH_3) \xrightarrow{\text{benzene}} [Fe(CO)_4(GeH_2)]_2 + 2GeMe_3H$$

Further significant features were seen somewhere between 20% and 45% reaction where a second signal appeared within 3 Hz of the GeH_3 and $GeMe_3$ signals of the starting material. Intensities were difficult to determine because of the small separation but the extra signal at 6.49 τ appeared to be about 30% of the GeH intensity and that at 9.52 τ was about 15% of the GeMe at 45% reaction. These secondary signals decreased as the starting material was consumed, but increased in proportion making 40%-50% of the total at 90% reaction. A second feature was the appearance of a small amount of GeH_4 from the half-way stage. Other very minor peaks also appeared in the latter stages of this reaction.

The explanation of the peaks to low frequency of the GeH_3 and $GeMe_3$ resonance is not clear. They are unlikely to be due to instrumental effects since only two resonances were affected, and these signals persisted even when the total intensity was very small. Two suggestions for these peaks are: a) resonances from the *trans* isomer

b) resonance from $Fe(CO)_4(GeH_3)_2$ (6.50 τ, C_6D_6 (26) and $Fe(CO)_4(GeMe_3)_2$, (9.43 τ, C_6H_6, this work), formed *via* a disproportionation reaction.

TABLE 5.1

Nmr data from the self-reaction of $Fe(CO)_4(GeMe_3)(GeH_3)$ in solution

Reaction Time	COMMENT	Relative intensity (%)[a]	
		$Fe(CO)_4(GeMe_3)(GeH_3)$	$GeMe_3H$
0.75 hr	Yellow solution	87	12
5.5 hr	Orange solution, precipitate	79	20
42 hr	Increased precipitate, orangered solution	54[b]	45
30 d	GeH_4 observed (6.90τ) (*ca*. 6% of $GeMe_3H$)	18	82
43 d	Other small signals are just visible.[c]	12	88
170 d	GeH_4 is now *ca*. 5% of the $GeMe_3H$	0.5	99.5

a Determined from intensities of CH_3 resonances.

b Decreased intensity reveals very weak peaks at 9.47τ and 6.49τ.

c 9.37 τ singlet, 6.43 τ singlet, 6.23 τ singlet, these signals are all very small, together with spinning side-bands and ^{13}C bands off $GeMe_3H$ they make up less than 1% of the total intensity.

Figure 5.1

Nmr spectra obtained from the self-reaction of $Fe(CO)_4(GeMe_3)(GeH_3)$ in solution

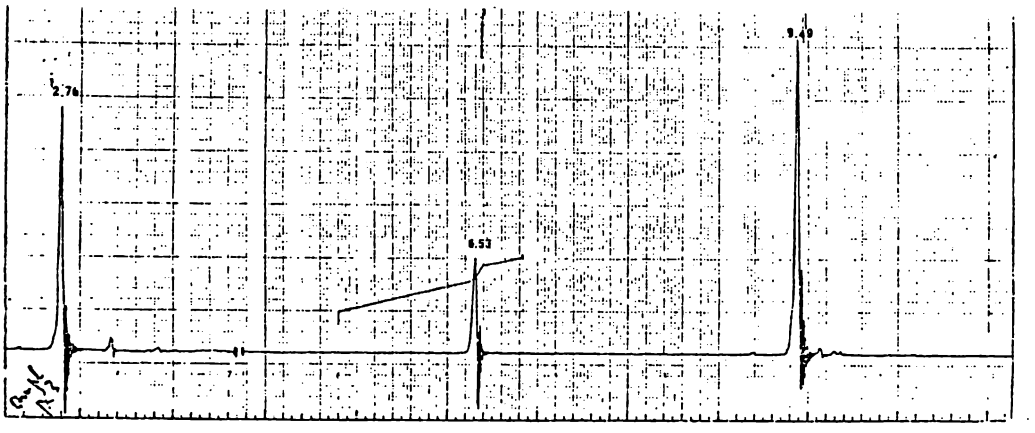

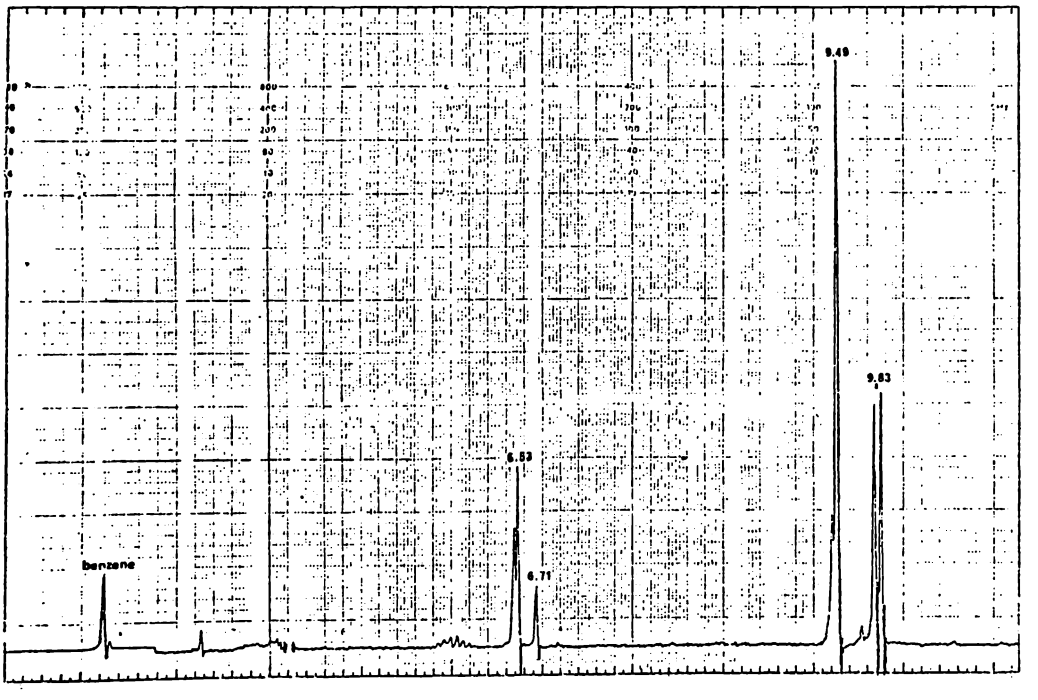

Figure 5.1 (Continued)

Nmr spectra obtained from the self-reaction of $Fe(CO)_4(GeMe_3)(GeH_3)$ in solution

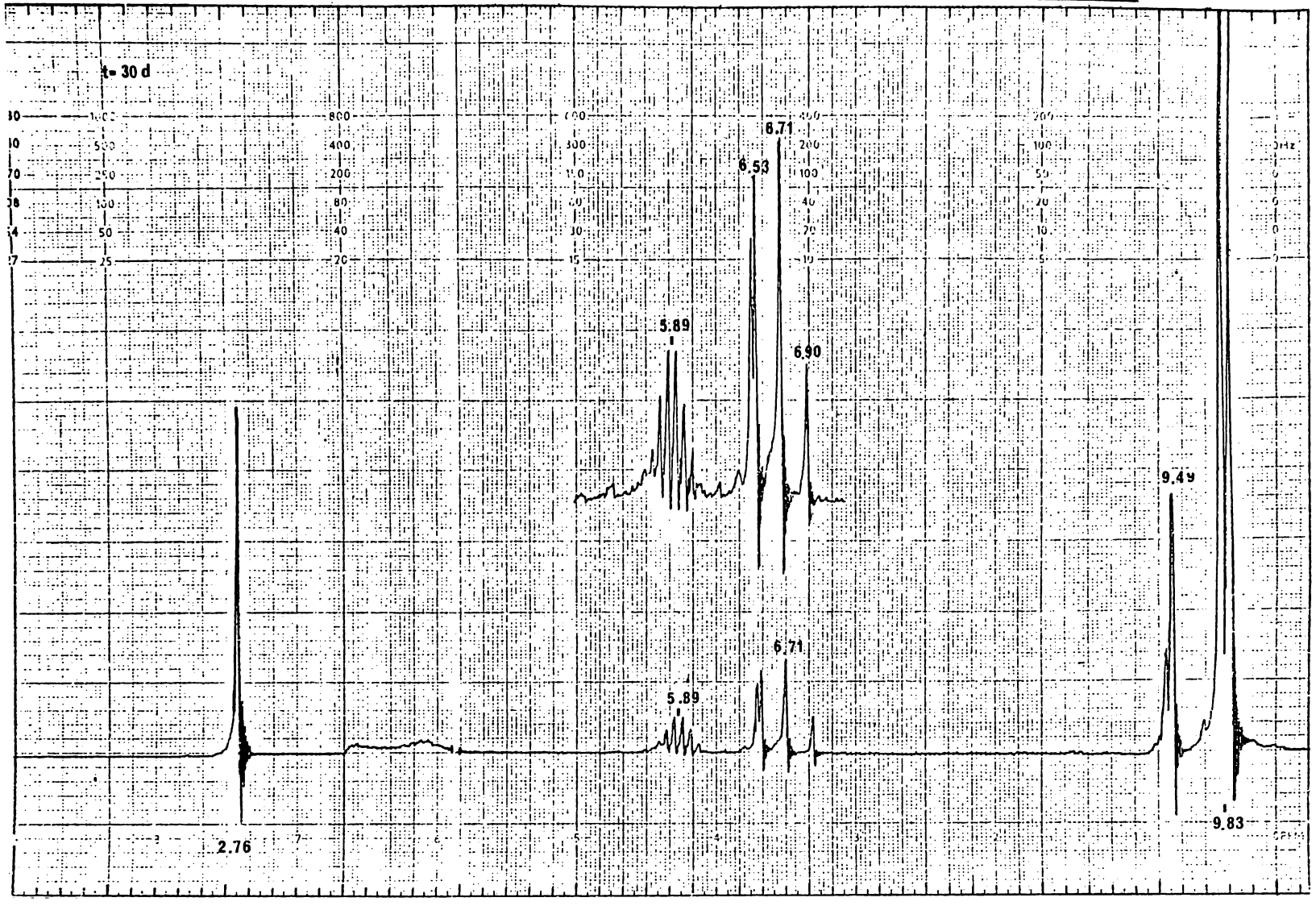

If either process is basically a very slow equilibrium, the second species may: (i) either react directly or transform back to give final products

and (ii) only be found because its transformation was catalysed by the initial reaction products.

Against the interpretation as *trans* isomer is the apparent difference in relative intensities of the new GeH and GeMe resonances. This difference would not preclude the interpretation as disproportionation, as the $GeMe_3$ species may react further to give insoluble products.

While the appearance of GeH_4 in the latter stages might be a consequence of (i) or (ii) above, further slow neutral molecule elimination reactions may occur, *e.g.*,

$$[Fe(CO)_4(GeH_2)]_2 + Fe(CO)_4(GeMe_3)(GeH_3) \longrightarrow GeH_4 + Fe_3(CO)_nGe_3H_x \text{ (or other more complex species)}$$

or $2[Fe(CO)_4(GeH_2)]_2$

Such further condensation reactions could also account for the very weak signals seen at the last stages of the reaction.

5.2.3 The mass spectrum of $Fe(CO)_4(GeMe_3)(GeH_3)$

Despite the experimental difficulties involved the mass spectrum of $Fe(CO)_4(GeMe_3)(GeH_3)$ was obtained. This spectrum shows the typical features expected for compounds of this type; weak parent ion, stepwise loss of CO as the dominant fragmentation process, and little fission of the metal-metal skeleton. The very strong base peak, $GeMe_3^+$, reflects the ready cleavage of this moiety from $Fe(CO)_4(GeMe_3)(GeH_3)$. However, as $GeMe_3H$ was undoubtedly present from decomposition before ionisation of $Fe(CO)_4(GeMe_3)(GeH_3)$, little can be gleaned from the mass spectrum about the propensity of this molecule to cleave the Fe-$GeMe_3$ bond on ionisation as compared with other molecules of the type $Fe(CO)_4(GeMe_{3-x}H_x)(GeMe_{3-y}H_y)$.

TABLE 5.2

The mass spectrum of $Fe(CO)_4(GeMe_3)(GeH_3)$

Fragment Assignment	Apparent mass *m/e*	Relative intensity	Envelope *maxima*
$Fe(CO)_4Ge_2Me_3H_x^+$	368-353	vvw	362
$Fe(CO)_4Ge_2Me_2H_x^+$	353-338	vw	347
$Fe(CO)_3Ge_2Me_3H_x^+$	340-325	m	332
$Fe(CO)_3Ge_2Me_2H_x^+$	325-310	vw	317
$Fe(CO)_2Ge_2Me_3H_x^+$	312-297	w	304
$Fe(CO)_2Ge_2Me_2H_x^+$	297-282	ms	292
$Fe(CO)Ge_2Me_3H_x^+$	284-269	m	278
$Fe(CO)Ge_2Me_2H_x^+$	269-254	m	262
$FeGe_2Me_3H_x^+$	256-241	w	244
$FeGe_2Me_2H_x^+$	241-226	vs	232
$FeGe_2MeH_x^+$	226-211	s	214
$FeGe_2H_x^+$	211-196	vs	204
$Fe(CO)_2GeH_x^+$	191-182	m	186
$FeGeMe_3^+$	177-171	mw	176
$Fe(CO)GeH_3^+$	163-154	s	158
$FeGeCH_x^+$	147-141	m	144
$FeGeH_x^+$	135-126	s	130
$GeMe_3^+$	121-115	vvs	119
$GeCH_xO^+$	107-98	m	105
$GeCH_x^+$	92-82	m	89
GeH_x^+	79-70	w	74
$Fe(CO)_4^+$ 168 s, $Fe(CO)_3^+$ 140 s, $Fe(CO)_2^+$ 112 s, $Fe(CO)^+$ 84 s, $FeGe(CO)_2H_x^{2+}$ 95.5-91 vw, $FeGe_2MeH_x^{2+}$ 113-106 vw			

5.2.4 The infrared spectrum of $Fe(CO)_4(GeMe_3)(GeH_3)$

Apart from the substantial phase shift in the carbonyl region, the solid film and the initial gas phase spectra of $Fe(CO)_4(GeMe_3)(GeH_3)$ are in reasonable concord. (See Table 5.3, page 202). The spectrum shows four carbonyl infrared stretching modes which is consistent with C_{2v} geometry (Figure 5.2, page 203). These modes have been assigned as follows: 2085 m νCO_{ax} a_{11}, 2036 s and 2023 s νCO $b_1 + a_{12}$, 2004 vs cm^{-1} νCO b_2. The low frequency region is also very weak initially. A weak, broad shoulder at 829 cm^{-1} is assigned to the anti-symmetric deformation and/or CH_3 rock, while the stronger mode at 817 cm^{-1} is ascribed to the symmetric GeH_3 deformation. The strong characteristic FeCO deformation occurs at 624 cm^{-1}.

The proclivity of $Fe(CO)_4(GeMe_3)(GeH_3)$ to react under infrared conditions necessitated relatively fast scans and hence the accuracy of the peak *maxima* is thought to be ± 2 cm^{-1}.

Within 10 minutes of warming up in the gas cell, extensive decomposition was observed. After 60 minutes, there was very little sign of any $Fe(CO)_4(GeMe_3)(GeH_3)$. The curious thing is that the decomposition product was not $GeMe_3H$ (the volatile decomposition product observed in the nmr and weighed decomposition reaction studies), but $Fe(CO)_4(H)(GeH_3)$. The hydride species $M(CO)_4(H)(M'R_3)$, is known to be in equilibrium with the octacarbolyl $[M(CO)_4(M'R_2)]_2$ in some systems. (See Section 1.4). It is conceivable that $Fe(CO)_4(H)(GeH_3)$ is an intermediate in the self-reaction of $Fe(CO)_4(GeMe_3)(GeH_3)$. As a rapidly reacting species in such a system it would not be surprising that this is not seen in nmr spectra. However, if the reaction was proceeding in the same manner as in the liquid and solution phases, $GeMe_3H$ would also be expected to be observed in the infrared spectra. The gradual disappearance of the $Fe(CO)_4(H)(GeH_3)$ after several hours could be

TABLE 5.3

Infrared studies of $Fe(CO)_4(GeMe_3)(GeH_3)$ cm^{-1}

$Fe(CO)_4(GeMe_3)(GeH_3)$				$Fe(CO)_4(H)(GeH_3)$	Tentative Assignment
Solid	Gas, t=0	Gas, t=20 min	Gas, t=60 min	gas (26)	
			2114)	2115 s	)
		2110 wm	2110) m		)
			2106)		)
					)
2079 m	2085 m	2084 wm	2085 w		) νCO , a_{11}
				2052)	)
		(2048 sh)	2048 sh	2049) vvs	)
		2045 vs	2044 vs	2043)	) νCO
		2039 vs	2039 vs	2039 vvs	)
	2036 s				) νCO a_{12}/b_1
					)
2005 sh,br	2023 s				) νCO b_1/a_{12}
				2018 w	)
1977 vs,br	2004 vs	2004 ms	2004 wm		) νCO b_2
1958 sh				1970 w	)
878 w				900 w	)
	829 sh	835sh,br			)
824 m		823).	823)	825)	) $\delta GeH_3+\rho CH_3$
		820)ms	820) m	821) vs	)
	817 s	818)	817)	818)	)
		754) w	754 w,br	755 m	) $\delta FeCO$
743 w		749)			
				732)	)
		727 m	727 ms	728) vs	) δFeH
				726)	)
666vw,br	666vw,br	665w,br	667vw,br		
	624 s	625 ms	625 ms	623 vs	) $\delta FeCO$
614 s					
		597 w	597 wm	596 s	) δFeH
		572 w	572 w	570 m	) $\delta FeCO$
557 m					
534 vw					) ρGeH_3
				550 w,br	
				468 w	) νFeC

Figure 5.2

The gas phase carbonyl infrared region of $Fe(CO)_4(GeMe_3)(GeH_3)$: cm^{-1}

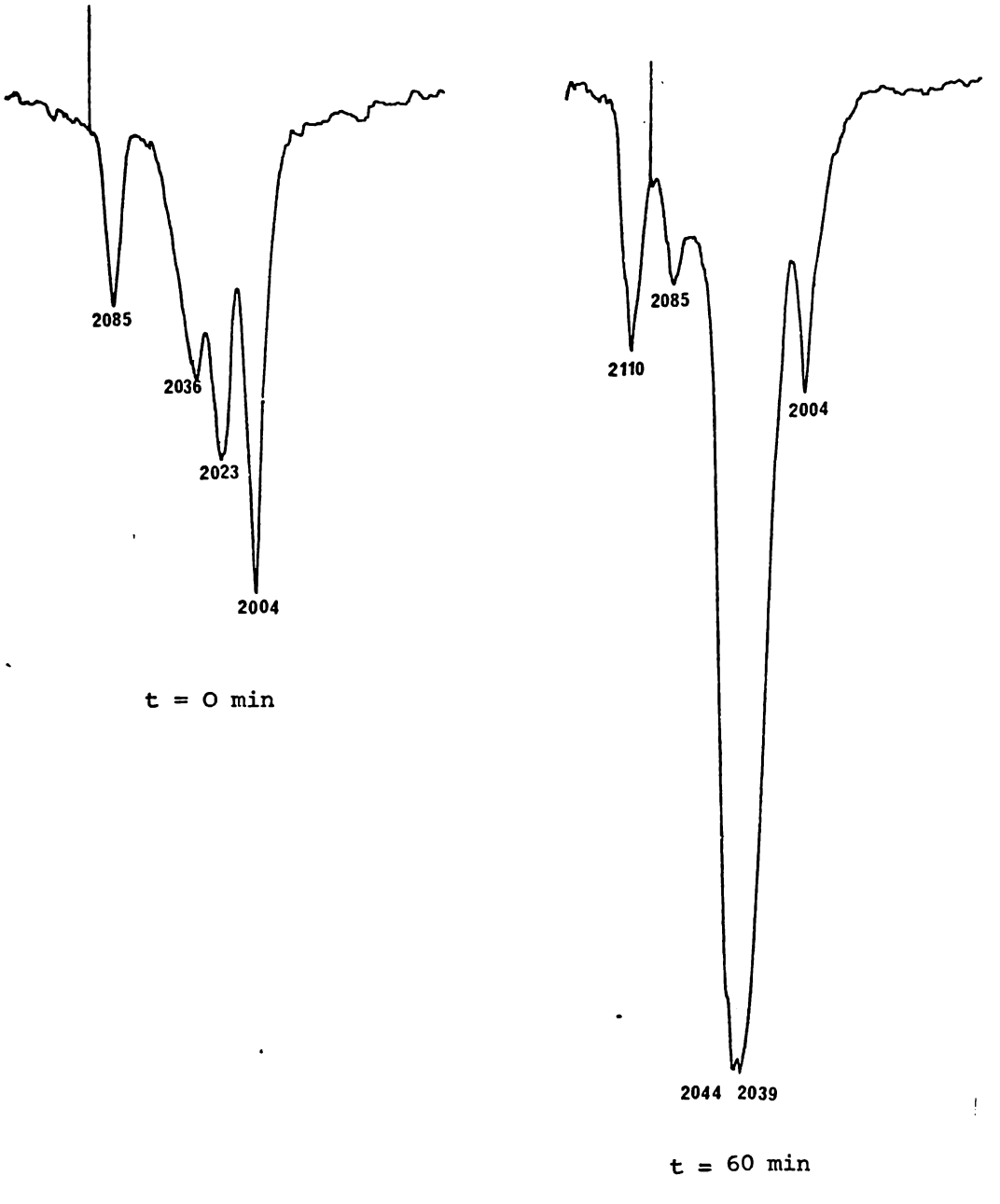

explained by the following equation:

$$2Fe(CO)_4(H)(GeH_3) \longrightarrow [Fe(CO_4(GeH_2)]_2 + 2H_2$$

The gas cell does indeed become coated with an orange film as the reaction proceeds. While the reason for the different fate of $Fe(CO)_4(GeMe_3)(GeH_3)$ under infrared conditions remains an enigma, several suggestions for the alternative reaction path are:

(i) Photocatalysed reaction.

Previous reactions have been carried out in the absence of light.

(ii) Thermal reaction.

Whereas previous reactions have been carried out at *ca.* 20°C, the temperature of the infrared cell cavity is *ca.* 29°C.

(iii) Reaction with apiezon or at the surface of the gas cell or KBr windows.

5.2.5 Characterisation of $[Fe(CO)_4(GeH_2)]_2$

Figure 5.3, page 205, illustrates the infrared carbonyl stretching frequency region of $[Fe(CO)_4(GeH_2)]_2$. Table 5.4, page 206, lists the infrared data and compares it with that obtained by Bonny (27).

Figure 5.3

The carbonyl infrared spectrum of $[Fe(CO)_4(GeH_2)]_2$, cm^{-1}

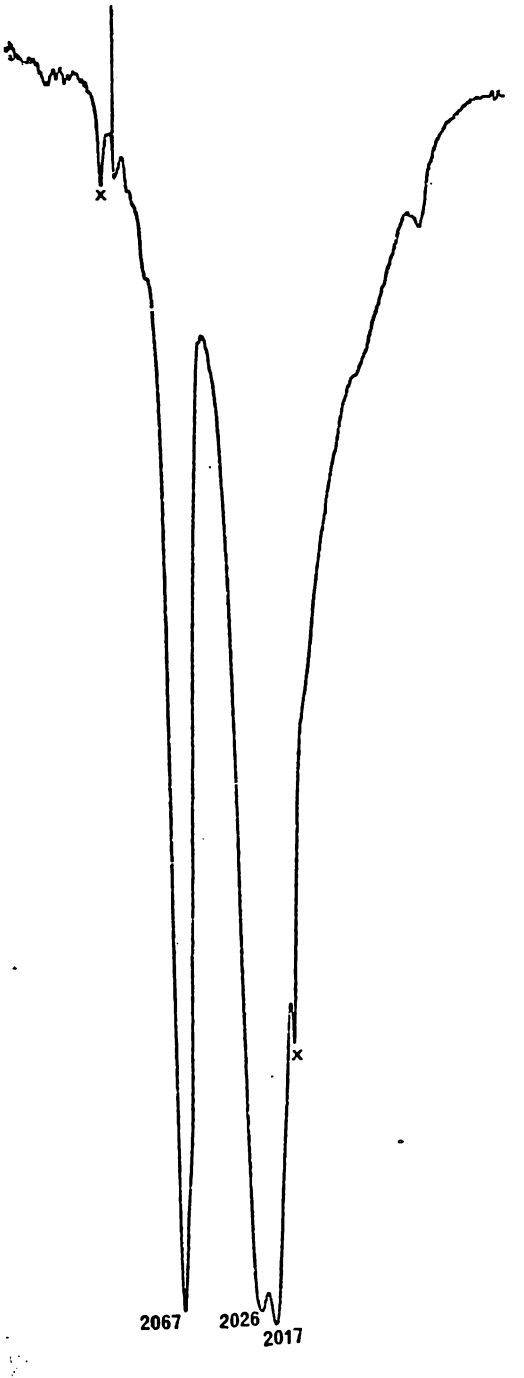

TABLE 5.4

Infrared spectra of $[Fe(CO)_4(GeH_2)]_2$, cm^{-1}

solution		infrared	Tentative Assignment
C_6H_{12} (9)	$CH_2C\ell_2$ (a)	C_6H_{12} (b)	
2067 vs	2066 vs	2067 vs	) νCO_{ax} b_{1u}
		2063 vw, sh	)
		2045 vw, br	) νCO
2026 vs		2026 s	) $\nu CO_{e.g.}$ b_{2u}
2017 vs	2015 vs	2017 vvs	) b_{3U} + b_{1u}
		1999 w	)
1981 sh		1981 w, br	
1964 w,			
n.o.	n.o.	830 vw, sh	) δGeH_x
		800 w	)
682 m		683 mw	)
			)
618 s	618 m	618 mw, sh	) $\delta FeCO$
609 vs	609 s	609 ms	)

n.o. Region not observed.

a This work

b Reference (27)

The carbonyl-stretching region of the infrared spectrum is not unlike that of $[Fe(CO)_4(GeI_2)]_2$. See Figure 1.11, page 27. This similarity precludes the possibility of a linear 'FeGe' species which would be expected to exhibit a more complex carbonyl spectrum. Assignments of νCO bands are described and compared with νCO modes in other $[Fe(CO)_4]_2(GeR_2)(GeR'_2)$ species in Section 5.6, page 219.

The mass spectrum of $[Fe(CO)_4(GeH_2)]_2$ is tabulated in Table 5.5, page 207.

TABLE 5.5

The mass spectrum of $[Fe(CO)_4(GeH_2)]_2$

Fragment Assignment	Apparent mass *m/e*	Relative Intensity a	Relative Intensity b
$Fe_2(CO)_8Ge_2H_x^+$	490-480	vvw	w
$Fe_2(CO)_7Ge_2H_x^+$	462-450	m	s
$Fe_2(CO)_6Ge_2H_x^+$	432-420	w	m
$Fe_2(CO)_5Ge_2H_x^+$	404-392	w	m
$Fe_2(CO)_4Ge_2H_x^+$	374-364	w	ms
$Fe_2(CO)_3Ge_2H_x^+$	348-336	m	s
$Fe_2(CO)_2Ge_2H_x^+$	318-308	wm	ms
$Fe_2(CO)Ge_2H_x^+$	290-280	w	m
$Fe_2Ge_2H_x^+$	262-252	m	vs

Very weak ions occured at 354-350 $Fe_2(CO)_6GeH_x^+$,
297-293 $Fe_2(CO)_4GeH_x^+$
272-268 $Fe_2(CO)_3GeH_x^+$
$Fe(CO)_4^+$ or $Fe_2(CO)_2^+$ 168 m,
150 ? s, and
$Fe(CO)_2^+$ or Fe_2^+ 112 w, were also also observed in this work.

a This work

b See reference (27).

As with the methyl substituted octacarbonyls the ion showing loss of one CO ($Fe_2(CO)_7Ge_2H_4^+$) is very much stronger than the parent ion. It is possible that these $[Fe(CO)_4(GeR_2)]_2$ species are undergoing the rearrangement; $[Fe(CO)_4(GeR_2)]_2 \xrightarrow{-CO} Fe_2(CO)_7(GeR_2)_2$ in the mass spectrometer.

$[Fe(CO)_4(GeH_2)]_2$ shows a single peak at 6.71τ in benzene solution (*c.f.* 6.65τ in CS_2 (27)) in the nmr experiment.

This octacarbonyl is not completely stable. It turned from orange to brown in colour and gave off incondensable gases when left under vacuum for two days in subdued lighting. $[Fe(CO)_4(GeMeH)]_2$ is known to eliminate CO to form the heptacarbonyl, $Fe_2(CO)_7(GeMeH)_2$, and traces of higher molecular weight species on weak illumination (29).

5.3 Trimethylgermyl(methylgermyl)tetracarbonyliron(0), $Fe(CO)_4(GeMe_3)(GeMeH_2)$

5.3.1 Preparation of $Fe(CO)_4(GeMe_3)(GeMeH_2)$

$KMn(CO)_5$, (from *ca.* $Mn_2(CO)_{10}$, 560 mg, 1.4 mmol, $NaK_{2.78}$, 6 mmol), together with $Fe(CO)_4(GeMe_3)_2$ (1502 mg, 3.7 mmol of wine - slightly brown in colour) and Et_2O (25 ml) were allowed to react at room temperature for 15 minutes. The volatile components of the mixture were pumped out of the reaction vessel. $Mn(CO)_5(GeMe_3)$ (*ca.* 451 mg, 1.4 mmol) plus unreacted $Fe(CO)_4(GeMe_3)_2$ was recovered after pumping the reaction vessel for a further six hours. $GeClMeH_2$ (150 mg, 1.2 mmol) and hexane (20 ml) were added to the $[Fe(CO)_4(GeMe_3)]^-$. After five minutes the initial deep wine-coloured $[Fe(CO)_4(GeMe_3)]^-$ and colourless solution had formed an orange solution. After ten minutes reaction time the solution was green in colour. After fifteen minutes reaction time the volatiles were pumped out of the reaction vessel to leave a grey-white salt and greenish - brownish oil. $GeMe_3H$ was found in the most volatile

fraction of the material which condensed out of the reaction vessel. The product was condensed into three different nmr tubes. Solvent was added and the nmr of these solutions was recorded before other spectropic data was collected. $[Fe(CO)_4(GeMeH)]_2$ was found in the reaction vessel residues together with a small amount of unidentified material which exibits a 2045 cm^{-1} band in the infrared.

5.3.2 Characterisation of $Fe(CO)_4(GeMe_3)(GeMeH_2)$

No mass spectral evidence was obtained for this compound. A very weak spectrum of $[Fe(CO)_4(GeMeH)]_2$ was found when attempts were made to do so. The solution spectrum of a yellow solution of the product which turned green before the spectrum was recorded shows infrared bands at 2074 mw, 2060 m, 2044 mw, 2021 wsh, 2015 msh, 2008 s, 1988 s cm^{-1}. This species was unstable and an extra band appeared at 2067 w, while the 2015 sh increased in intensity to become a medium-strong band, within *ca.*15 minutes. The bands at 2060 m and 2008 s cm^{-1} in this spectrum are attributed to $[Fe(CO)_4(GeMeH)]_2$, the band at 2044 cm^{-1} may be νGeH of $GeMe_3H$? (*cf.* 2049 cm^{-1}, gas (169)).

The ^1H nmr spectrum of $Fe(CO)_4(GeMe_3)(GeMeH_2)$ in benzene was recorded on green solutions which initially gave broad signals. After ten minutes the spectrum showed a strong singlet at 9.44τ assigned to $GeMe_3$, coincident with the $GeMeH_2$ methyl triplet at *ca.*9.45τ $^3J_{HGeCH}$ = 3.4 Hz. The GeH quartet is centred at 6.12τ . A singlet 9.71τ (3%) and small peaks at *ca.* 9.62τ and 9.66τ were observed throughout the recording of the nmr spectrum but do not appear to increase significantly. $GeMe_3H$ (9.82τ doublet, *c.a.*5.90τ multiplet, $^3J_{HGeCH}$ = 3.2Hz) was initially present (*c.a.* 3%) together with a trace of $[Fe(CO)_4(GeMeH)]_2$ (8.90τ doublet, $^3J_{HGeCH}$ = 3.4 Hz) and a small singlet at 8.76τ. $GeMe_3H$

accounted for 60% of the total signal intensity from all the methyl groups after 80 minutes in the nmr probe. At this point, $[Fe(CO)_4(GeMeH)]_2$ accounts for *ca.* 15% of the methyl signal, 4% is accounted for by the singlet at 8.76τ and another small singlet was observed at 7.81τ. These findings can be summarised thus:

$$2Fe(CO)_4(GeMe_3)(GeMeH_2) \xrightarrow[80\ min]{60\%} 2GeMe_3H + [Fe(CO)_4(GeMeH)]_2 + (GeMeX_3)$$

5.4 Trimethylgermyl(dimethylgermyl)tetracarbonyliron(0), $Fe(CO)_4(GeMe_3)(GeMe_2H)$

5.4.1 Preparation of $Fe(CO)_4(GeMe_3)(GeMe_2H)$

$KMn(CO)_5$, (from $Mn_2(CO)_{10}$ 469 mg, 1.2 mmol), $Fe(CO)_4(GeMe_3)_2$ (*ca.* 1700 mg, 4 mmol) and Et_2O (50 ml) were stirred at room temperature for 30 minutes. Et_2O, $Fe(CO)_5$ and $Mn(CO)_5(GeMe_3)$ were removed in vacuo. Unreacted $Fe(CO)_4(GeMe_3)_2$ was extracted in hexane (20 ml) followed by two 5 ml rinses, leaving a pink-white anion. $GeXMe_2H$ (125 mg, *ca.* 0.7 mmol, X = Cℓ, Br) and pentane (2 ml) were allowed to react at room temperature for ten minutes during which time the solution turned a pale orange colour. The more volatile components of the reaction mixture were removed in vacuo.

When no more material condensed out of the reaction vessel, the diffusion pump was switched on, and a U-trap with an nmr tube attached was inserted between the reaction vessel and pump. After 2½ hours, no more material appeared to be condensing into the U-trap. Yellow, oily $Fe(CO)_4(GeMe_3)(GeMe_2H)$ filled the nmr tube to a height of 1.2 cm. Hexane extraction of the residues shows $[Fe(CO)_4(GeMe_2)]_2$ to be the only carbonyl-containing species. Unreacted $GeXMe_2H$ and pentane were added back into the white solid remaining in the reaction vessel. A negligible quantity of further product was observed. Final extraction of residues in hexane gave no evidence of any further $[Fe(CO)_4(GeMe_2)]_2$

5.4.2 Characterisation of $Fe(CO)_4(GeMe_3)(GeMe_2H)$

A paucity of spectra makes identification of this compound rather tenuous. Attempts to obtain solution infrared of this compound resulted only in clean $[Fe(CO)_4(GeMe_2)]_2$ spectra. Likewise, the mass spectra show $[Fe(CO)_4(GeMe_2)]_2$ as the dominant pattern. Weak envelopes at lower *m/e* values indicate that more than just the 'octacarbonyl' species was present. A neat sample of '$Fe(CO)_4(GeMe_3)(GeMe_2H)$' indicated very weak broad *maxima* at *ca.* 9.33τ ($GeMe_3$ singlet?) *ca.* 9.41τ ($GeMe_2H$?) and 5.79τ (GeH?). After *ca.*15 minutes in the nmr probe the sample was withdrawn as *ca.*60% of the signal was now attributed to $GeMe_3H$? *ca.*9.9τ and $[Fe(CO)_4(GeMe_2)]_2$? *ca.*8.8τ.

In summary,

$$Fe(CO)_4(GeMe_3)(GeMe_2H) \xrightarrow[15\ min]{60\%} GeMe_3H + [Fe(CO)_4(GeMe_2)]_2 + (other?)$$

5.5 Survey of the properties of $Fe(CO)_4(GeMe_{3-x}H_x)(GeMe_{3-y}H_y)$

5.5.1 Comparison of nmr parameters in $Fe(CO)_4(GeMe_{3-x}H_x)(GeMe_{3-y}H_y)$ species

Table 5.6, page 213, shows the range of nmr shifts and coupling constants found for the methylgermyl-tetracarbonyliron species. No trend is seen in the methyl chemical shift values, which all come in a narrow range of *ca.* $\pm$ 0.2 ppm. The GeH chemical shift reflects the inductive effect of the methyl substituents and falls into distinct regions:

GeH_3 protons 6.53-6.47τ

GeH_2 protons 6.13-6.07τ

GeH protons 5.84-5.79τ

The coupling constant $^3J_{HGeCH}$ tends to decrease from $GeMeH_2$ species to $GeMe_2H$ species (*c.f.*, 3.4 Hz with 3.2 Hz). The same phenomenon is also evident in the parent hydrides: (168)

$GeMeH_3$ ^3J = 4.2 Hz,

$GeMe_2H_2$ ^3J = 3.8 Hz,

$GeMe_3H$ ^3J = 3.4 Hz

This trend is also apparent in the manganese derivatives,

$Mn(CO)_5(GeMeH_2)$ ^3J = 3.8 Hz, C_6H_6

$Mn(CO)_5(GeMe_2H)$ ^3J = 3.6 Hz, C_6H_6

Taken together, the ^1H nmr parameters obtained for unsymmetrically substituted-methyl-germyl-iron carbonyls obtained in this work are fully self-consistant. Thus, this data strongly supports the attribution of the more highly substituted species where self-reaction to give involatile solids and methylgermane(s) precludes other means of identification.

TABLE 5.6

Proton nmr data for $Fe(CO)_4(GeMe_{3-x}H_x)(GeMe_{3-y}H_y)$ complexes

Compound, (C_6H_6 solution)	CH_3, τ	GeH_3 τ, GeH_2 τ, GeH τ	^3J, Hz
$Fe(CO)_4(GeH_3)_2$ [a]		6.50s	
$Fe(CO)_4(GeMeH_2)(GeH_3)$	9.49t	6.47s 6.11q	3.4
$Fe(CO)_4(GeMeH_2)_2$	9.51t	6.13q	3.4
$Fe(CO)_4(GeMe_2H)(GeH_3)$	9.49d	6.48s 5.84h	3.2
$Fe(CO)_4(GeMe_2H)(GeMeH_2)$	9.44d 9.38t	6.07q 5.80h	3.4 3.2
$Fe(CO)_4(GeMe_3)(GeH_3)$	9.49s	6.53s	
$Fe(CO)_4(GeMe_3)(GeMeH_2)$	9.45s 9.44t	6.12q	3.4
$Fe(CO)_4(GeMe_2H)_2$	9.41d	5.83h	3.2
$Fe(CO)_4(GeMe_3)(GeMe_2H)$ [b]	9.41s 9.33d	5.79h	?
$Fe(CO)_4(GeMe_3)_2$	9.43s		

a - C_6D_6 reference (26); s = singlet, d = doublet, t = triplet, q = quartet, h = heptet (usually only 5 peaks are seen).

b - Very broad signals, approximate chemical shift values only.

5.5.2 Comparison of the infrared stretching frequencies of $Fe(CO)_4(GeMe_{3-x}H_x)(GeMe_{3-y}H_y)$

Although there is no linear trend there is a tendency toward decrease in the average CO stretching frequency as the number of methyl groups increases (*ca.* 20-25 cm^{-1} for an increase from 0 to 6 Me groups). Typically, the average νCO value shifts to higher frequency as substituents at the metal become more electronegative. This reduces the electron density of the metal available for dπ-pπ back bonding with the antibonding orbitals of the CO ligand. A decrease in the electron density of the CO antibonding orbitals results in an increase in the bond order of the C-O bond - hence increasing the stretching force constant and increasing the energy at which the νCO mode occurs.

In these species, νCO_{ax} (a_{11}) is the most sensitive to the change in the number of methyl groups on the GeR_3 ligand (*ca.* 4 to 5 cm^{-1} decrease in frequency for each Me group which is added, see Table 5.7). This trend is also apparent in methylgermyl manganese and cobalt carbonyls (17,19,20,39).

The consistent decrease in the νCO_{ax} (a_{11}) mode in these compounds supports in particular, the following identifications made in this work:

(i) $Fe(CO)_4(GeMeH_2)_2$: Here values obtained in this work and Jager's (178) are more consistent with other molecules of this type than the values reported by Bonny (29).

(ii) $Fe(CO)_4(GeMe_2H)_2$: Despite the problems caused by its rapid self-reaction, the solution values obtained in this work are seen to be realistic and in line with these methylgermyltetracarbonyliron derivatives (*c.f.* solid film spectra (30)).

TABLE 5.7

$\nu CO_{ax}(a_{11})$ modes in $Fe(CO)_4(GeMe_{3-x}H_x)(GeMe_{3-y}H_y)$: cm^{-1}

Compound [a]	Frequency (cm^{-1})	Compound [a]	Frequency (cm^{-1})
$Fe(CO)_4(GeH_3)_2$	2092		
$Fe(CO)_4(GeMeH_2)(GeH_3)$	2088		
$Fe(CO)_4(GeMeH_2)_2$	2082	$Fe(CO)_4(GeMe_2H)(GeH_3)$ [b]	2084
$Fe(CO)_4(GeMe_3)(GeH_3)$ [b]	2078	$Fe(CO)_4(GeMe_2H)(GeMeH_2)$	2077
$Fe(CO)_4(GeMe_2H)_2$	2073	$Fe(CO)_4(GeMe_3)(GeMeH_2)$	2073
$Fe(CO)_4(GeMe_3)(GeMe_2H)$	?		
$Fe(CO)_4(GeMe_3)_2$	2065		

a Values obtained from solution spectra (C_6H_{12} or C_6H_{14}) unless otherwise stated.

b These values have been shifted -7 cm^{-1} in line with the shift from gas to solution spectra. (See Table 5.8).

(iii) $Fe(CO)_4(GeMe_3)(GeMeH_2)$: This contained several decomposition products, but possibly infrared evidence for this compound is manifest in the 2073 cm^{-1} mode.

Vibrational spectra, 900-50 cm^{-1} region

For compounds of the type $Fe(CO)_4(GeMe_{3-x}H_x)(GeMe_{3-y}H_y)$, the lower region, 900-650 cm^{-1}, is a more sensitive and diagnostic region than the carbonyl stretching region. Table 5.9, page 217, shows the key absorptions of the δGeH, ρCH_3 and νGeC modes in species of type $GeXH_3$, $GeXMeH_2$ and $GeXMe_2H$.

TABLE 5.8

The major features of the carbonyl stretching frequencies of $Fe(CO)_4(GeMe_{3-x}H_x)(GeMe_{3-y}H_y)$ complexes, cm^{-1}

$Fe(CO)_4(GeH_3)_2$			$Fe(CO)_4(GeMeH_2)(GeH_3)$		$Fe(CO)_4(GeMeH_2)_2$			$Fe(CO)_4(GeMe_2H)(GeH_3)$	
gas	C_6H_{12}	Raman	Gas	Raman	Gas	C_6H_{12}	Raman	Gas	Raman
2101 s	2092 s	2099 s	2094 s	2091 s,p	2089 m	2082 ms 2051 sh	2086 m,p	2091 m	2084 vs
2042 vvs		2042 vs	2034 vvs		2030 vs		2040 w,sh	2040 vs?	
2020 vs	2024 vs	2023 vs	2017 sh 2012 vs	2023 vvs		2015 s	2014 s	2021 s?	2018 vvs
	2009 vvs				2007 s	1996 vs	2009 vs		

$Fe(CO)_4(GeMe_2H)_2$ C_6H_{14}	$Fe(CO)_4(GeMe_3)(GeH_3)$ gas	$Fe(CO)_4(GeMe_2H)(GeMeH_2)$ C_6H_{12}	$Fe(CO)_4(GeMe_3)(GeMeH_2)$ C_6H_{14}	$Fe(CO)_4(GeMe_3)_2$ C_6H_{12}
2073 m	2085 m	2077 m	2073 ?	2065s
2007 s	2036 s			
2001 vvs	2023 s	2010 s	2013 ?	2003 s 2000 s
1988 ms	2004 vs	1991 vs	1987 ?	1980 vs

See Tables: 3.5, 4.2, 3.6, 4.9, 3.11, 5.3, 3.14.

TABLE 5.9

Key absorptions in the 900-500 cm^{-1} region of some $GeMe_xH_y$ species

$GeXH_3$	δGeH_3			ρGeH_3
$GeBr_3$ [a]	872	832		579
$Mn(CO)_5(GeH_3)$ [b]	880	818		508
$Re(CO)_5(GeH_3)$ [c]	886	817		539
$Co(CO)_4(GeH_3)$ [d]	877	810		529
$Fe(CO)_4(H)(GeH_3)$ [e]	900	821		570
$Fe(CO)_4(GeH_3)_2$	890	835	809	529
$Fe(CO)_4(GeMeH_2)(GeH_3)$	883	811		534
$Fe(CO)_4(GeMe_2H)(GeH_3)$	882	808		537
$Fe(CO)_4(GeMe_3)(GeH_3)$	878	817		534

see references a (171), b (17), c (50), d (38), e (26), and tables 3.5, 4.2, 4.9, 5.3.

$GeXMeH_2$	GeH_2 band + ρCH_3	GeH_2 wag	νGeC
$GeC\ell MeH_2$ [f]	883 868 (3), 846	717	616
$GeBrMeH_2$ [f]	883 868 864	705	620, 610
$GeIMeH_2$ [f]	882 864, 853 840	694	614, 607
$Mn(CO)_5(GeMeH_2)$ [g]	881 877 838	695	609
$Co(CO)_4(GeMeH_2)$ [h]	887 873 838	702	615
$Fe(CO)_4(GeMeH_2)_2$	876 837	693	615
$Fe(CO)_4(GeMeH_2)(GeH_3)$	883 836	691	619

see references f (174b), g (39), h (19) and Tables 3.6, 4.2.

TABLE 5.9 (continued)

$GeXMe_2H$	δGeH	ρCH_2	νGeC
$GeC\ell Me_2H$ [i]	688 668	862, 841, 770	628, 618, 600
$GeBrMe_2H$ [i]	669	861, 842, 768	625, 617, 598
$GeIMe_2H$ [i]	654	867, 839, 763	615, 591
$Co(CO)_4(GeMe_2H)$ [j]	672, 662	848, 758	600, 592
$Mn(CO)_5(GeMe_2H)$ [j]	672, 655	837, 730	612, 580
$Fe(CO)_4(GeMe_2H)_2$	695-,675	875, 842, 725,	609,
$Fe(CO)_4(GeMe_2H)(GeH_3)$	662	865, 836, 728	573

see references i (174a), j (20) and Tables 3.11, 4.9.

$GeXMe_3$	ρCH_3	νGeC
$GeC\ell Me_3$ [k]	839	621
$[GeMe_3]_2$ [l]	827, 803	594, 555
$Mn(CO)_5(GeMe_3)$ [m]	825,	588, 559
$Fe(CO)_4(GeMe_3)_2$	829, 819, 809	586, 554
$Fe(CO)_4(GeMe_3)(GeH_3)$	829	557

See references k (197a), l (197b), m (191a) and Tables 3.14, 5.3.

One or more relatively strong methyl-rocking modes are consistently found in the 840-830 cm^{-1} region and these overlap with GeH_3 or GeH_2 bending modes in the unsymmetrically substituted compounds. The symmetric GeH_3 deformation is found consistently in the 820-810 cm^{-1} region and often shows a type A contour. The GeH_2 group is characterised by the wag around 700 cm^{-1}. When a GeH group is present, a weak GeH deformation about 660 cm^{-1} can be picked out. Only for $Fe(CO)_4(GeH_3)_2$ can in- and out-of-phase combinations of GeH deformation modes be traced. νGeC modes are attributed to bands in the region 620-550 cm^{-1} but are relatively weak and not always easy to distinguish from the δFeCO modes which also occur here. νGeC modes can be identified from the Raman as only these modes are likely to be polarised in this region.

TABLE 5.10

Key absorptions in the 650-50 cm^{-1} region of some $Fe(CO)_4L_2$ species

Compound	δFeCO	νFeC	νFeGe	δCGeFe δCFeGe δGeFeGe
$Fe(CO)_4(H)_2$	642 vs,	428 m		
$Fe(CO)_4(H)(GeH_3)$	623 vs,	432 vs,	226 vs,	102 vvs,
$Fe(CO)_4(GeH_3)_2$	628 vs,	434 vs,	229 vs, 216 m,	105 vvs
$Fe(CO)_4(GeMeH_2)(GeH_3)$	627 s,	440 s,	225 s,p	
$Fe(CO)_4(GeMeH_2)_2$	643 w,	448 m,p	210 s,	113 vs, 103 vvs, 58 vw,
$Fe(CO)_4(GeMe_2H)(GeH_3)$	628 s	440 s	229 s	
$Fe(CO)_4(GeMe_2H)_2$	643 w, 623 s	444 vw		
$Fe(CO)_4(GeMe_3)(GeH_3)$	624 s			
$Fe(CO)_4(GeMe_3)_2$	623 s	445 ms,p	200 vs,	105 vvs

See Tables: 3.5; 4.2; 3.6; 4.9; 3.11; 5.3; 3.14., and reference (26).

Strong δFeCO mode(s) are found in the region 650-600 cm^{-1} in these iron complexes, see Table 5.10, page 218.

νFeC occurs typically around 450-430 cm^{-1} in Raman spectra, although little attention has been paid to this region in infrared spectra (12,14). One or two strong νFeGe modes in the region 230-220 cm^{-1} of the Raman spectrum have been recorded. Slight polarisation of the 227 s mode in $Fe(CO)_4(GeMeH_2)(GeH_3)$ is consistent with the overlap of a polarised and a depolarised component ($a_1 + b_1$). Raman *maxima* less than 115 cm^{-1} have been ascribed to δCGeFe, δCFeGe and δGeFeGe modes

5.6 Comparison of carbonyl infrared spectra of $[Fe(CO)_4]_2(GeMe_{2-x}H_x)(GeMe_{2-y}H_y)$ species;

Although the octacarbonyl species reported in this work are often recorded as being orange or green, sublimation of these materials gives white solid, octacarbonyl. The 'coloured' impurities are thought to be present in only very minor quantities.

The carbonyl-stretching regions of the octacarbonyls are very interesting. Taking first the simple species, $[Fe(CO)_4(GeR_2)]_2$, spectra match the literature examples (*c.f.* Figure 1.11, page 27). The four B_{nu} modes of the idealised D_{2h} symmetry are assigned as follows: (59);

B_{3u} is the most intense band while the weak b_{1u} (*eq.*) mode may occur on either side of it, or may be unresolved. The axial B_{1u} mode is the highest frequency and the B_{2u} mode is intermediate in energy and varies in intensity. These vibrations all decrease in frequency from $GeR_2 = GeH_2 > GeMeH > GeMe_2$, paralleling the changes for the $Fe(CO)_4(GeMe_{3-x}H_x)(GeMe_{3-y}H_y)$ species. Additional weak features in the $GeR_2 = GeMeH$ and $GeMe_2$ spectra may indicate that the true symmetry is less than D_{2h}

Two species are thought to have a one μ-GeMeH group combined with, respectively, a μ-GeH_2 or a μ-$GeMe_2$. From the nature of their preparations, a mixture of the corresponding pairs of $[Fe(CO)_4GeR_2]_2$ species cannot be excluded. However, it is possible to assign the four main modes, as shown in Table 5.11, page 221, in a manner that is consistent in frequency and intensity with the three basic species discussed above. These two each show three 'extra' *maxima* which may arise from impurities or may, again, reflect the true, relatively low, symmetry.

TABLE 5.11

The carbonyl infrared spectrum of $[Fe(CO)_4]_2$ $(GeMe_{2-x}H_x)$ $(GeMe_{2-y}H_y)$; cm^{-1}

$[Fe(CO)_4(GeH_2)]_2$ a	$b[Fe(CO)_4]_2(GeMeH)(GeH_2)$	$[Fe(CO)_4(GeMeH)]_2$ c	$[Fe(CO)_4]_2(GeMe_2)(GeMeH)$ d	$[Fe(CO)_4(GeMe_2)]_2$ e	Tentative Assignment
2067 s	2063 s	2060 s	2056 s	2052 vs	νCO_{ax}, b_{1u}
2026 s	2026 ms	2022 mw	2021 w	2025 w	νCO_{eq} b_{2u}
2017 vvs	2017 s	2008 vs	2000 vs	2001 ws	νCO_{ax} b_{3u}
Overlapped	2011 s	2012 sh	2005 s	1988 m	νCO_{eq} b_{1u}
	2067 m	2067 w	2060 sh	2060 sh	extra bands
	2059 mw		2053 ms	2040 w	
	2009 sh		2016 mw		

See Figures: a,5.3, b,4.4, c,3.3, d,4.12, e,3.4.

5.7 Self-reaction of $Fe(CO)_4(GeMe_{3-x}H_x)(GeMe_{3-y}H_y)$ species

The self-reactions of $Fe(CO)_4(GeMe_{3-x}H_x)(GeMe_{3-y}H_y)$ are briefly summarised in Table 5.12, page 223. While certain aspects of these reactions remain unresolved, firm points about the self-reaction which have been established are:

(a) There is no ready germane elimination between GeH_3 groups (see also (27));

(b) Self-reaction occurs only where there is a possibility of eliminating a methylgermane;

(c) Where there is a choice between the elimination of two germanes, that germane with the most methyl groups is eliminated in preference. In cases where a second hydride was found, it appears slowly in small quantities, and may be the result of further condensation of the initial product;

(d) The rate at which self-reaction occurs appears to be largely dependent on the number of methyl groups in the compound. Where there is the same number of methyl groups per molecule, *e.g.*, $Fe(CO)_4(GeMeH_2)_2$ and $Fe(CO)_4(GeMe_2H)(GeH_3)$ the molecule which can eliminate the more methyl-substituted germane is the molecule which undergoes self-reaction the most rapidly;

Points which are not so firm are:

(e) There appears to be no indication of major differences between reactions occurring in solution (followed by ^1H nmr) and in the studies on neat liquids (followed by separation, identification and weighing of products)

TABLE 5.12

Summary of the self-reaction of $Fe(CO)_4(GeMe_{3-x}H_x)(GeMe_{3-y}H_y)$ complexes (dark, RT)

$Fe(CO)_4(GeH_3)_2 \longrightarrow$ no reaction	(27)
$Fe(CO)_4(GeMeH_2)(GeH_3) \xrightarrow{54d}$ 11% $GeMeH_3$, $[Fe(CO)_4(GeH_3)]_2(GeMeH)$	
$Fe(CO)_4(GeMeH_2)_2 \xrightarrow{25d}$ 22%$GeMeH_3$, $[Fe(CO)_4(GeMeH_3)]_2$	(29)
$Fe(CO)_4(GeMe_2H)(GeH_3) \xrightarrow{6\ d}$ 32%$GeMe_2H_2$, $[Fe(CO)_4(GeH_2)]_2$, $[Fe(CO)_4(GeH_3)]_2(GeMe_2)$	
$Fe(CO)_4(GeMe_2H)(GeMeH_2)^b \xrightarrow{3\ hr}$ 10%$GeMe_2H_2$, $[Fe(CO)_4]_2(GeMe_{2-x}H_x)(GeMe_{2-y}H_y)$	
$Fe(CO)_4(GeMe_3)(GeH_3) \xrightarrow{2\ d}$ 45%$GeMe_3H$, $[Fe(CO)_4(GeH_2)]_2$	
$Fe(CO)_4(GeMe_3)(GeMeH_2)^b \xrightarrow{80\ min}$ 60%$GeMe_3H$, $[Fe(CO)_4(GeMeH)]_2$, (GeMe)?	
$Fe(CO)_4(GeMe_2H)_2 \xrightarrow{3\ d}$ 26%$GeMe_2H_2$, $[Fe(CO)_4(GeMe_2)]_2$	(30)
$Fe(CO)_4(GeMe_3)(GeMe_2H)^b \xrightarrow{15\ min}$ 60%$GeMe_3H$, $[Fe(CO)_4(GeMe_2)]_2$, other?	
$Fe(CO)_4(GeMe_3)_2^c \longrightarrow$ no reaction .	

a - After *ca.*, 15 days at 55°C CO, H_2, GeH_4, GeO_2H_x, $Fe_2Ge_2(CO)_8H_x$, and Fe_3Ge_3 species were recovered together with 80% unreacted $Fe(CO)_4(GeH_3)_2$ (27).

b - While some samples were more stable, others were even more reactive under ostensibly the same conditions.

c - Bonny (181) reports that after several weeks in an nmr tube (CS_2solvent, RT) $(Me_3Ge)_2O$ was formed.

e.g., Compare reactions of $Fe(CO)_4(GeMeH_2)(GeH_3)$;

neat; 30% reaction in 84 days (0.35% per day)

C_6H_6; 43% reaction in 122 days (0.36% per day).

(f) Removing one of the products of the self-reaction (*e.g.*, dissolved germane or by precipitating octacarbonyl) may facilitate the reaction. For example, evolution of methylgermane was commonly observed when a $Fe(CO)_4(GeMe_{3-x}H_x)$-$(GeMe_{3-y}H_y)$ species was transferred in vacuo.

No separate experiments were done to obtain data for the self-reaction of $Fe(CO)_4(GeMe_2H)(GeMeH_2)$, $(Fe(CO)_4(GeMe_3)(GeMe_2H)$ or $Fe(CO)_4(GeMe_3)(GeMe_2H)$. The values given in Table 5.12, for these species indicate the typical rates with which some samples self-reacted. These values give a realistic indication of the experimental difficulties which were encountered in the isolation and identification of these species.

(g) Samples are very sensitive to adventitous traces of impurity Compare for example, different samples of $Fe(CO)_4(GeMe_2H)(GeMeH_2)$: One sample in benzene was observed by nmr spectroscopy to undergo 48% self-reaction in approximately two hours while another solution sample showed 10% self-reaction in three hours and yet a third, a neat sample, showed no sign of dimethylgermane (nor monomethylgermane elimination) in three hours.

Samples used for spectroscopic studies were typically screened by the nmr experiment before and/or after) other spectroscopic data was collected. Only samples which showed little or no decomposition in the nmr experiment were used to collect other data in the more highly substituted species.

5.7.1 Speculative self-reaction mechanisms

Three mechanisms for the self-reaction of $Fe(CO)_4(GeR_3)_2$ R = Me, H species can be envisaged; the first steps of each are shown:

(i) Intramolecular reaction with the formation of a germylene intermediate.

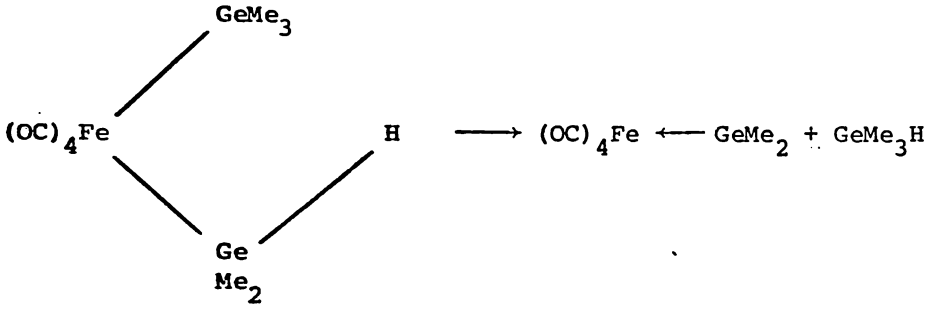

(ii) Intermolecular four-centre exchange reaction.

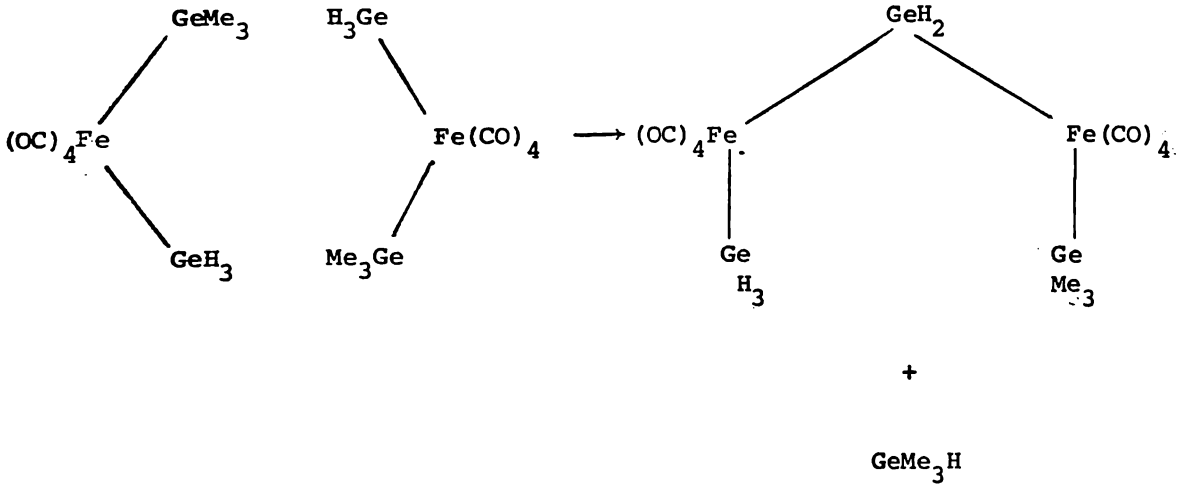

(iii) Free radical mechanism

$$(OC)_4Fe(GeMe_3)(GeH_3) \longrightarrow (OC)_4Fe(GeH_3)^{\bullet} + GeMe_3^{\bullet}$$

$$(OC)_4Fe(GeMe_3)(GeH_3) + GeMe_3^{\bullet} \rightarrow (OC)_4Fe(GeMe_3)(GeH_2)^{\bullet} + GeMe_3H$$

While the first step in the reaction sequence could be explained by any one or all of these mechanisms, it is not necessary that the second stage of the reaction should also involve the same mechanism.

(i) The intramolecular formation and attack of a germylene intermediate at another $Fe(CO)_4(GeR_3)_2$ molecule has been proposed (27,30). It was suggested that either;

(ia) the stability of the germylene intermediate was the critical factor in this process, and this increased with the number of methyl groups or,

(ib) the $GeMe_2$ moiety was more effective at bridging two iron atoms than either GeMeH or GeH_2.

However, results from this work are not compatible with these proposals about the effect of the methyl substitutuent.

Here, where a choice was available in the unsymmetrically substituted $Fe(CO)_4(GeR_3)(GeR'_3)$ species, the most methyl substituted germane was eliminated to leave the least methyl substituted bridging germanium moiety. If, alternatively, it is assumed that the critical step in the formation of $[Fe(CO)_4(GeR_2)]_2$ in these systems is driven by the leaving of the most methyl substituted germane with the concomittant formation of the least stable germylene intermediate, then the germylene intermediate scheme is compatible with the experimental observations. The traditional view of combination of two germylene intermediates *e.g.*,

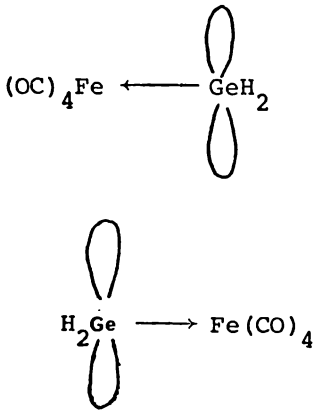

is compatible with all the experimental evidence except the formation of an Fe_2Ge_3 intermediate species. But this intermediate species could be formed *via* a four-centre reaction of an $[Fe(CO)_4(GeR_3)]$ species with $Fe(CO)_4(GeR_3)_2$ (27,30).

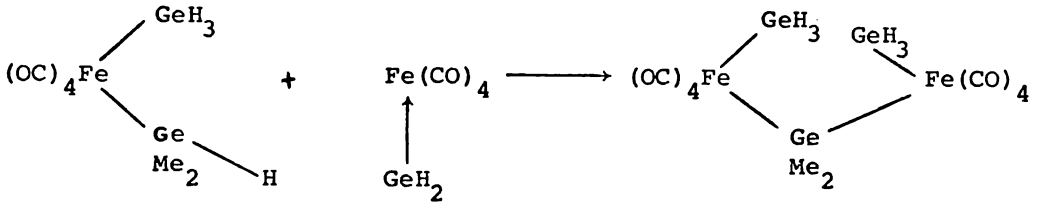

Another five-coordinate iron-germylene intermediate, $[Fe(CO)_4(GeR_2)]$, however, could not be proposed as the second intramolecular step to form $[Fe(CO)_4(GeR_2)]_2$.

(ii) A four-centre exchange mechanism as outlined in scheme (A) is compatible with all the experimental observations obtained in this work.

SCHEME A

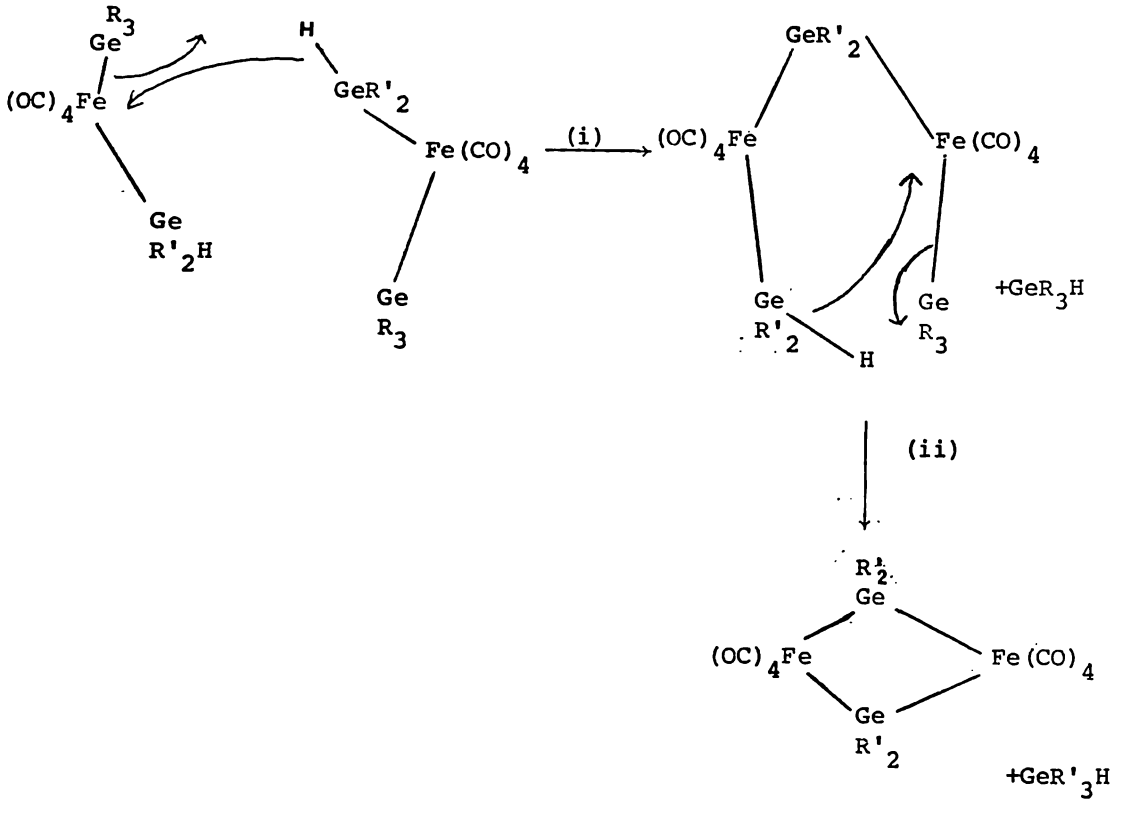

(iia) If incipient Ge→H bond formation is a critical step in the formation of a $Fe_2(\mu\text{-}GeR_2)$ species then this is compatible with the 'activation' of this process on methyl group substitution (*c.f.* $Fe(CO)_4(GeH_3)_2$ where no reaction occurs).

(iib) As Ge-H bonds are somewhat weaker than Ge-C bonds germanium hydride elimination in scheme (A) at room temperature is possible while at the same time, this mechanism precludes the possibility of methyl transfer, or of the self-reaction of $Fe(CO)_4(GeMe_3)_2$ *via* an exchange mechanism at room temperature.

(iic) Elimination of the most highly substituted germane may also be the result of a relief in steric crowding.

(iid) The formation of $[Fe(CO)_4(GeH_3)]_2GeR_2$ species is fully consistant with this mechanism. It is suggested that the elimination of GeH_4 between two GeH_3 groups does not readily occur (compare the stability of $Fe(CO)_4(GeH_3)_2$ to self-reaction). Thus the reaction of $Fe-(GeH_3)$ species stops at this stage.

In contrast, where methylgermyl groups are present, as in an intermediate such as $(Me_{3-x}GeH_x)Fe(CO)_4\mu-(GeR_2)Fe(CO)_4(Ge,Me_{3-y}H_y)$ $(y+x\neq6)$, then the second condensation would be very much favoured since it is intramolecular. Thus the Fe_2Ge_3 intermediate was identified only where GeH_3 groups were present.

Small amounts of GeH_4 formed in the latter stages of the self-reaction of $Fe(CO)_4(GeMeH_2)(GeH_3)$ and $Fe(CO)_4(GeMe_2H)(GeH_3)$ is compatible with a small amount of reaction in $[Fe(CO)_4(GeH_3)]_2(GeR_2)$ *i.e.*,

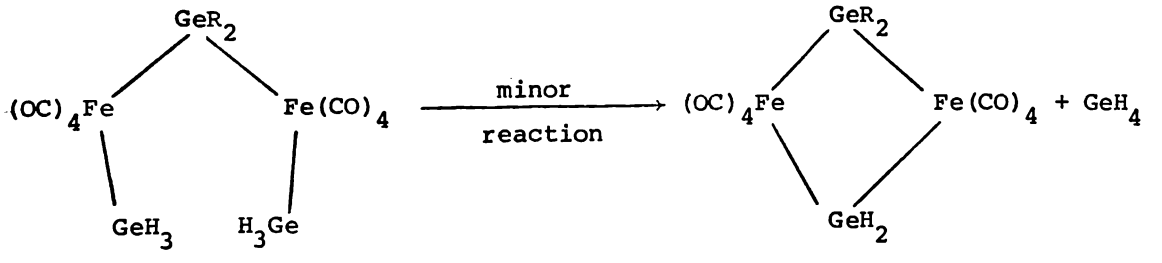

This is also consistant with the formation of unsymmetrically substituted $[Fe(CO)_4]_2(GeR_2)(GeR_2')$ species.

(iii) The sensitivity of the self-reaction of $Fe(CO)_4(GeMe_{3-x}H_x)(GeMe_{3-y}H_y)$ species toward impurities, heat and light, the elimination of the most highly substituted germane, the freedom of these reactions from side-products, and then vastly varying rates of self-reaction in some cases are all factors which are characteristic of reactions involving free radicals (198).

SCHEME B

$$Fe(CO)_4(GeMe_3)(GeH_3) \xrightarrow{\text{initiator}} Fe(CO)_4(GeH_3)^{\cdot} + GeMe_3^{\cdot}$$

$$Fe(CO)_4(GeMe_3)(GeH_3) + GeMe_3^{\cdot} \longrightarrow Fe(CO)_4(GeMe_3)(GeH_2)^{\cdot} + GeMe_3H$$

$$Fe(CO)_4(GeH_3)^{\cdot} + Fe(CO)_4(GeMe_3)(GeH_2)^{\cdot} \longrightarrow (OC)_4Fe(H_3Ge)\text{-}GeH_2\text{-}Fe(GeH_3)(CO)_4$$

Scheme (B) outlines a speculative free radical mechanism. As the self-reaction rate is typically slow, the concentration of free radicals at any time is expected to be very small. Thus, lack of observation of Ge_2Me_6 is not inconsistent with this mechanism.

The only factors which raise doubts about this radical mechanism are A, the necessity to postulate the combination of two radicals in the third step, and B, the observation of sharp ^{1}H nmr signals during the reaction.

The base-catalysed facile reversible homolysis of complexes of the type $[Fe(CO)_4(M'R_2)]_2$ has been proposed by Marks and Newman (43). It would not be impossible for traces of impurities in $Fe(CO)_4(GeR_3)_2$ samples to provide a similar catalytic mechanism for self-reaction where an alternative process would proceed slowly in the absence of this homolytic reaction scheme.

This discussion is necessarily speculative, but shows that the observed reaction products can be rationalised in acceptable ways, and suggests ways in which further work could clarify the nature of these reactions.

CHAPTER SIX

REACTIONS BETWEEN $Mn(CO)_5(GeMe_{3-x}H_x)$ AND $Co_2(CO)_8$

6.1 Introduction

GeH_4 reacts with $Co_2(CO)_8$ in hexane (15 weeks) to form essentially $[Co_2(CO)_7]_2Ge$ (109) and a "small amount" of $[Co_3(CO)_9][Co(CO)_4]Ge$. This compound has also been prepared by the reaction between GeI_4 and $Na(CO)_4$ (109).

As well as reacting GeH_4 with $Co_2(CO)_8$, Gerlach (20) also studied the reaction between $Mn(CO)_5(GeMe_2H)$ and $Co_2(CO)_8$ by nmr. He reported that, after 50 minutes reaction time, while the temperature was slowly raised from -30^o to 0^o, the $Mn(CO)_5(GeMe_2H)$ signals diminished to nothing and were replaced by new signals at 8.75τ and 8.88τ, the latter of which also disappeared within this time, ($SiCl_4$, TMS).

These signals were ascribed to $[Mn(CO)_5][Co(CO)_4]GeMe_2$ and $[Co(CO)_3(GeMe_2)]_2$ respectively. No hydride species were observed during this reaction. The reaction was worked up two days later, no further nmr data was obtained because of the poor resolution. Incondensable gases. $SiCl_4$, TMS and a carbonyl species exhibiting bands at 2115 wm, 2075 m sh, 2065 ms, 2050 s sh, 2045 vs, 1825 m, cm^{-1} in C_6H_{12}, together with other very weak bands, made up the volatile components of this reaction, which were obtained after sublimation. Three bridging CO modes were observed in nujol on standing. The major component of the mass spectrum was $Co_4(CO)_{12}$. (Note, the sample was exposed to air during sampling). Evidently, the lower region of the mass spectrum was "rather mixed". On assuming that $[Mn(CO)_5][Co(CO)_4]GeMe_2$ was formed (after comparison with the phenyl analogue (21)) the mass spectrum was found to fit very well with the observed envelopes of peaks "with clear germanium isotope patterns showing in some cases". The spectrum was not assigned in detail due to the "many obvious anomalies, both within and outside the assigned envelopes". No

mass spectral data was reported. The most plausible explanation for $Co_4(CO)_{12}$ (20) was thought to be the large excess of $Co_2(CO)_8$ (0.45 mmol) used *cf.* $Mn(CO)_5GeMe_2H$ (0.25 mmol).

$[Co_3(CO)_9][Mn(CO)_5]Ge$ has recently been isolated from the reaction between $[Co_2(CO)_7]_2Ge$ and $[Mn(CO)_5]^-$ (115a). This compound was characterised by its mass spectrum and infrared spectrum. It was thought to arise *via* the reactions

$$[Co_2(CO)_7]_2Ge \rightarrow [Co_3(CO)_9][Co(CO)_4]Ge + Mn(CO)_5^-$$

$$\downarrow$$

$$[Co_3(CO)_9][Mn(CO)_5]Ge + Co(CO)_4^- \quad ...6.1$$

In this chapter, reactions between $Co_2(CO)_8$ and $Mn(CO)_5(GeH_3)$, $Mn(CO)_5(GeMeH_2)$ and $Mn(CO)_5(GeMe_2H)$ are described.

6.2 Reactions between $Mn(CO)_5(GeH_3)$ and $Co_2(CO)_8$

6.2.1 Experimental details

6.2.1.1 Mn:Co ratio *ca* 1:1

As $Mn(CO)_5(GeH_3)$ (1.07 mmol), $Co_2(CO)_8$ (1598 mg, 0.47 mmol), and hexane (3 ml) in a sealed tube warmed up to room temperature, the solution started bubbling and turned red-orange-black in colour. The reaction mixture was left at room temperature for five hours. On opening the Carius tube, incondensable gas (*ca.*0.5 mmol), hexane and a trace of $Mn(CO)_5H$, and $Mn(CO)_5(GeH_3)$ (157 mg, 0.58 mmol) were recovered. The involatile residues were extracted with hexane (*ca.* 20 ml) then with CH_2Cl_2 (*ca.* 20 ml). No insoluble material remained. The infrared spectrum of the hexane-extracted material shows absorption *maxima* in the carbonyl region at 2083 w, 2078 w, 2062 w, 2053 w, 2041 w, 2033 vw, 2023 m, 2018 m, 2008 s, 1869 vw, 1842 vw, cm^{-1}. The carbonyl stretching region of the material extracted by CH_2Cl_2 was similar, although weaker, and the 2018 cm^{-1} band is diminished relative to the rest.

6.2.1.2 Mn:Co ratio *ca.* 1:2

$Mn(CO)_5(GeH_3)$ (0.98 mmol), hexane (3 ml) and $Co_2(CO)_8$ (321 mg, 0.94 mmol), were left at room temperature for five hours. Bubbling and a deep orange-black solution occurred as the reaction mixture was warmed up. Incondensable gases (1.1 mmol) were pumped out of the Carius tube. The involatile material was extracted under nitrogen by hexane (*ca.* 20 ml). The infrared spectrum of this extract shows bands at 2115 w, 2083 w, 2078 m, 2062 w, 2053 br w, 2041 s, 2034 w, 2022 ms, 2018 ms, 2012 w, 2008 w, 1869 vw, 1842 vw, cm^{-1}. A hexane spectrum of the material extracted by CH_2Cl_2 shows *maxima* (cm^{-1}) at 2115 m, 2078 m, 2062 w, 2052 sh, 2041 s, 2021 m.

6.2.1.3 Mn:Co ratio *ca.* 1:3

Reaction between $Mn(CO)_5(GeH_3)$ (346 mg, 1.28 mmol) and $Co_2(CO)_8$ (691 mg, 2.02 mmol) in hexane, (3 ml, RT, 5 hr), proceeded in a similar fashion to that of the above $Mn(CO)_5(GeH_3)$: $Co_2(CO)_8$ reactions. Incondensable gases (*ca.* 2.4 mmol) were removed in vacuo, together with hexane. The Carius tube was then broken in half and some of the solid material was set aside for a mass spectrum. The remaining solid was extracted successively with hexane (*ca.* 20 ml) and CH_2Cl_2 (*ca.* 25 ml). The hexane soluble fraction showed infrared bands (cm^{-1}) at 2083 m, 2079 s, 2062 s, 2053 s, 2040 s, 2034 s, 2023 s, 2018 s, 2011 ms, 2002 w, 1990 vw sh, 1867 m, 1842 w. The carbonyl infrared spectrum of the CH_2Cl_2 fraction is illustrated in Figure 6.1, page 235: band *maxima* (cm^{-1}) occur at 2078 m, 2053 w, 2042 mw sh, 2040 vs, 2022 m, 1867 w, 1842 w.

Figure 6.1

The carbonyl infrared spectrum of $[Co_3(CO)_9][Mn(CO)_5]Ge$: cm^{-1}

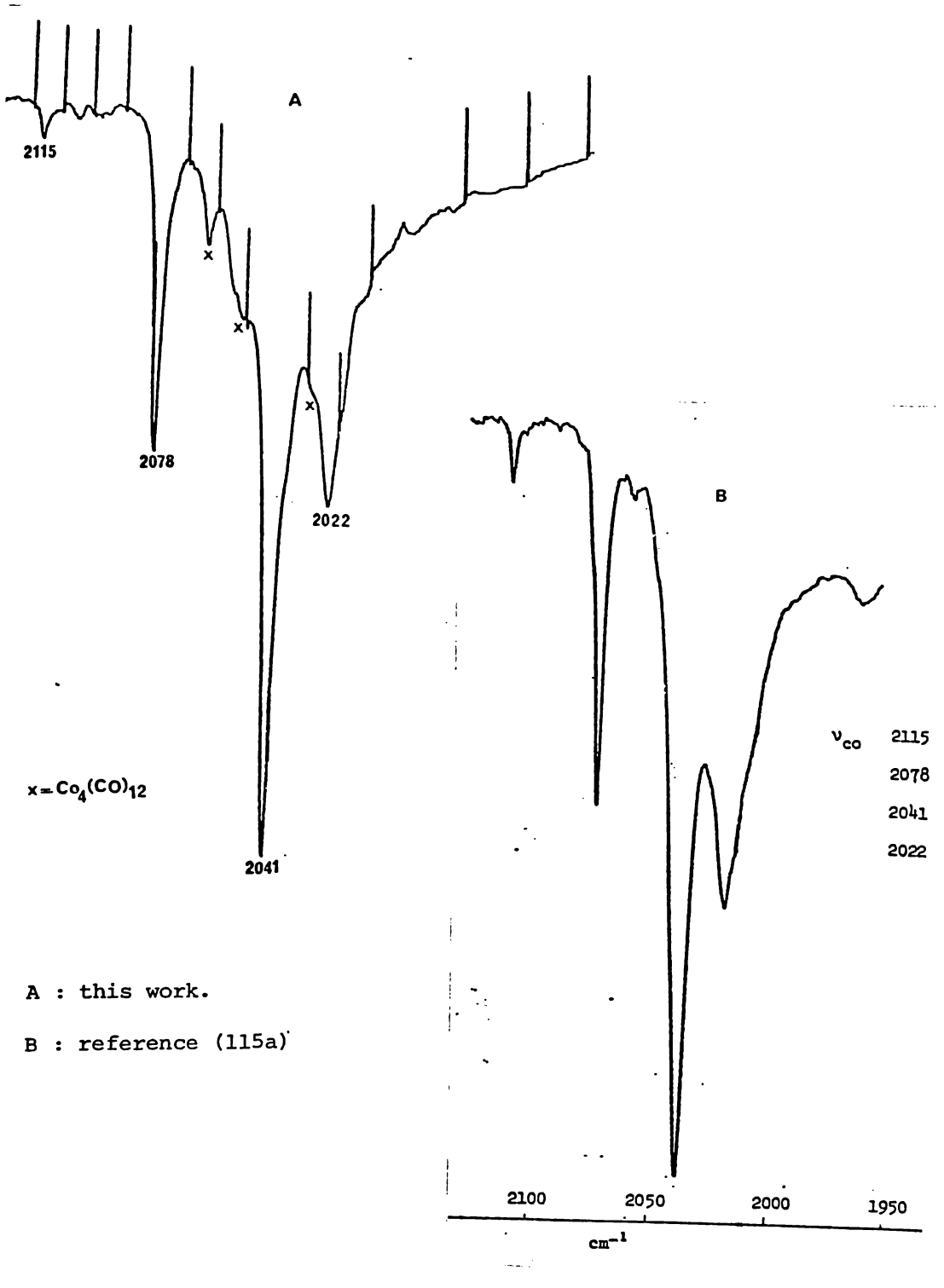

A : this work.

B : reference (115a)

Little evidence is seen for partially substituted species such as $[Co_2(CO)_7][Mn(CO)_5]GeH$ or $[Co(CO)_4][Mn(CO)_5]GeH_2$ which might have been expected to dominate the 1:2 Mn:Co and 1:1 Mn:Co reactions if these were the more favoured products. The unknown species with a bridging νCO mode at 1842 cm^{-1} in the 1:2 and 1:3 Mn:Co reactions suggests that a bridging $[Co_2(CO)_7]GeXY?$ species may be formed. The identity of the species in the 1:1 Mn:Co reaction which has a strong 2008 cm^{-1} νCO mode is not known.

6.2.2 Discussion of reactions involving $Mn(CO)_5(GeH_3):Co_2(CO)_8$

Table 6.1, page 238, shows products obtained from each of the above reactions.

The evidence of the non-volatile products suggests that the major reaction is complete substitution of all the GeH bonds.

$$Mn(CO)_5GeH_3 + 1.5Co_2(CO)_8 \longrightarrow [Co_3(CO)_9][Mn(CO)_5]Ge + 1.5H_2 + 3CO \quad (6.2)$$

The characterisation of the product is discussed in Section 6.2.3. The volume of incondensable gas observed is of the right order of magnitude. The ratio of incondensable to $Mn(CO)_5(GeH_3)$ consumed increases as the Mn:Co ratio increases. However, values are subject to enormous errors due chiefly to factors arising from the temperature gradient in the system (*e.g.*, a 4^oC increase in the temperature from -199^o to -195^o increases the vapour pressure of CO from *ca.* 28 cmHg to 50 cmHg (195))

Aside from the 1:1 Mn:Co reaction where $Co_4(CO)_{12}$ occurs in a similar amount, $[Co_3(CO)_9][Mn(CO)_5]Ge$ is the major component in the reaction residues. The mass spectrum given in Table 6.4, page 242, is that recorded on solid material from the 1:3 Mn:Co reaction before solvent extraction. This spectrum shows that $[Co_3(CO)_9][Mn(CO)_5]Ge$ is the most dominant component of the involatile residue

The infrared spectrum shown in Figure 6.1, page 235, compares the spectrum obtained after C_6H_{14} extraction of the 1:2 Mn:Co reaction with $[Co_3(CO)_9][Mn(CO)_5]Ge$ prepared by Duffy (115a). The spectrum is essentially the same as Duffy;s.

Thus, although yields were not determined, the qualitative examination of these reactions shows that equation (6.2) is the dominant process even when there is a deficit of cobalt,

TABLE 6.1

Qualitative comparison of products obtained from reactions between $Mn(CO)_5(GeH_3)$ and $Co_2(CO)_8$

1:1 Mn : Co reaction Reactants $Mn(CO)_5(GeH_3)$ (1.07 mmol) : $Co_2(CO)_8$ (0.47 mmol)

Products (i) Incondensible gases 0.5 mmol

(ii) Volatile species $Mn(CO)_5(GeH_3)$ (together with a trace only of $Mn(CO)_5H$), 0.58 mmol

(iii) Hexane extraction of residues Small amounts of $Co_4(CO)_{12}$ and $[Co_3(CO)_9][Mn(CO)_5]Ge$ and an unidentified species with a strong νCO at 2008 cm^{-1}).

(iv) CH_2Cl_2 extraction Following hexane extraction the remaining material was extracted in CH_2Cl_2 (20 ml.) The infrared spectrum of this sample shows $Co_4(CO)_{12}$, $[Co_3(CO)_9][Mn(CO)_5]Ge$ and a very much diminished band at 2008 cm^{-1}.

Summary: $Mn(CO)_5(GeH_3)$ + $Co_2(CO)_8$ ⟶ H_2/CO + $[Co_3(CO)_9][Mn(CO)_5]Ge$ + $Co_4(CO)_{12}$
(0.49 mmol) (0.47 mmol) (0.5 mmol) (similar quantities)
+ an unidentified species (characterised by a 2008 cm^{-1} band.)

1:2 Mn : Co reaction Reactants $Mn(CO)_5(GeH_3)$ (0.98 mmol) : $Co_2(CO)_8$ (0.94 mmol)

Products (i) Incondensible gases 1.1 mmol

(ii) Hexane extraction of residues $[Co_3(CO)_9][Mn(CO)_5]Ge$, $Co_4(CO)_{12}$ (approximately equal intensities of the strongest νCO modes), a little $Mn(CO)_5(GeH_3)$, a trace of the species with the 2008 cm^{-1} band, and a further species showing 2083 w, 2012 w, 1842 vw.

(iii) CH_3Cl_2 extraction of residues $[Co_3(CO)_9][Mn(CO)_5]Ge$

Summary: $Mn(CO)_5(GeH_3)$ + $Co_2(CO)_8$ ⟶ H_2/CO $[Co_3(CO)_9][Mn(CO)_5]Ge$
(<0.98 mmol) (0.94 mmol) (1.1 mmol) (major product)
+ $Co_4(CO)_{12}$ + trace of $[Co_2(CO)_7]X$?

1:3 Mn : Co reaction Reactants $Mn(CO)_5(GeH_3)$ (1.28 mmol) : $Co_2(CO)_8$ (2.02 mmol)

Products: (i) Incondensible gases 2.4 mmol

(ii) Hexane extraction νCO modes of $[Co_3(CO)_9][Mn(CO)_5]Ge$ and $Co_4(CO)_{12}$ are of similar intensity. Weaker bands at 2083, 2011, 2002 and 1842 cm^{-1} are also evident and $Mn(CO)_5GeH_3$ is present as shown by its 2018 cm^{-1} absorption.

(iii) CH_2Cl_2 extraction The bulk of the reaction residue $[Co_3(CO)_9][Mn(CO)_5]Ge$ remains after C_6H_{14} extraction and is extracted by CH_2Cl_2

Summary: $Mn(CO)_5(GeH_3)$ + $Co_2(CO)_8$ ⟶ H_2/CO + $[CO_2(CO)_9][Mn(CO)_5]Ge$
(<1.28 mmol) (2.02 mmol) (2.4 mmol) (major product)
+ $Co_4(CO)_{12}$ + trace of $[Co_2(CO)_7]X$?

6.2.3 Characterisation of $[Co_3(CO)_9][Mn(CO)_5]Ge$

As the symmetry of this molecule is C_s, all fourteen carbonyl stretching modes are infrared allowed. Though, assignment of carbonyl bands in the infrared spectrum in terms of the superposition of bands (based on local symmetry) arising from the $Mn(CO)_5$ unit ($\nu CO = 2a_1+e$, *ir*) and the $Co_3(CO)_9$ unit ($\nu CO = 2a_1+3e$, *ir*) is an attractive simplification, such arguments must be treated with caution. There is no reason to exclude mixing between the terminal $Mn(CO)_5$ carbonyl modes and the CO modes of the $Co_3(CO)_9$ unit. A similar problem arises in the cobalt analogue, $[Co_3(CO)_9][Co(CO)_4]Ge$. If we examine first, the cobalt species, it can be seen from Table 6.2, page 240 , that the carbonyl modes of $Co(CO)_4GeR_3$ species fall in the same regions as bands arising from $[Co_3(CO)_9]GeR$ compounds. Thus $[Co_3(CO)_9][Co(CO)_4]Ge$ shows only four bands arising from ^{12}CO stretches, which can be assigned as superposition of $Co(CO)_4$ and $Co_3(CO)_9$ spectra.

Since the carbonyl stretches of the $Mn(CO)_5Ge$ unit likewise fall in similar regions to those of the $Co_3(CO)_9Ge$ one, (Table 6.3, page 241), again an unexpectedly simple spectrum is observed for $[Co_3(CO)_9][Co(CO)_4]Ge$ where the four clear bands may be understood as a superposition of spectra of the contributing groups. It is clear from Figure 6.1, page 235, however, that neither 2040 cm^{-1} nor the 2022 cm^{-1} contour is "clean" and each probably includes two or three components.

Thus, the carbonyl region of the vibrational spectrum is characteristic of the compound but, like that of $[Co_3(CO)_9][Co(CO)_4]Ge$, it is unexpectedly simple in appearance. No conclusion can be drawn about interactions between $Mn(CO)_5$ and '$Co(CO)_3$' modes.

TABLE 6.2

Comparison of carbonyl infrared spectra of $[Co_3(CO)_9]Ge$ species, $[Co(CO)_4]GeH_3$ and $[Co_3(CO)_9][Co(CO)_4]Ge$; cm^{-1}

$[Co_3(CO)_9]GeMe$ (194) a	$[Co_3(CO)_9]GePh$ (194) b	Assignment	$[Co_3(CO)_9][Co(CO)_4]Ge$ (20) a	Assignment	$[Co(CO)_4]GeH_3$ (38) c	Assignment
2105 m	2104 vw	A	2111 vw	A+P	2017 s	P
2082 s	2082 s	B	2082 s	B		
2056 s	2056 s)	C				
2046 sh	2044 vw)		2044 vs	C+D+Q	2046 vs	Q
2030 s	2036 s	D				
2025? m	2025 m	E	2027 mw	E+R	2025 vvs	R

weak ^{13}CO modes have been omitted from this table, a hexane, b cyclohexane, c gas phase

TABLE 6.3

Comparison of the carbonyl infrared spectra of $[Co_3(CO)_9][M(CO)_x]Ge$ and $[Mn(CO)_5]GeH_3$; cm^{-1}

$[Co_3(CO)_9][Co(CO)_4]Ge$ (20,112) a	$[Co_3(CO)_9][Mn(CO)_5]Ge$ (115a) a	Assignment	$[Mn(CO)_5]GeH_3$ (17) b	Assignment
2111 vw	2115 w	A+X	2112 m	X
2082 s	2078 m	B		
2044 vs	2041 vs	C+D+Y	2034 s	Y
2027 mw	2022 ms	E+Z	2020 vvs	Z

weak ^{13}CO modes have been omitted, a hexane, b gas phase.

The mass spectrum (See Table 6.4, page 242) of the solid material before extraction by hexane and $CH_2C\ell_2$ shows envelopes identical to those obtained by Duffy (115a), together with a trace of $Co_4(CO)_{12}$ and one weak-medium peak at 296-288 ($Co_2(CO)_6Ge^+$?).

The major fragmentation pathway in $[Mn(CO)_5][Co_3(CO)_9]Ge$ is clearly CO loss. Manganese is the only metal atom with any propensity to fragment from the metal skeleton. This matches the stability of the Co_3Ge^+ unit, seen in the mass spectra of other $[Co_3(CO)_9]GeR$ species.

TABLE 6.4

The mass spectrum of $[Co_3(CO)_9][Mn(CO)_5]Ge$

Assignment	Apparent mass *m/e*	relative intensity a	(115a)
$Co_3Mn(CO)_{14}Ge^+$	700-694	m	17
$Co_3Mn(CO)_{13}Ge^+$	672-666	s	47
$Co_3Mn(CO)_{12}Ge^+$	644-638	m	23
$Co_3Mn(CO)_{11}Ge^+$	616-610	w	6
$Co_3Mn(CO)_{10}Ge^+$	588-582	vvw	3
$Co_3Mn(CO)_9Ge^+$	560-554	m	25
$Co_3Mn(CO)_8Ge^+$	532-526	s	88
$Co_3Mn(CO)_7Ge^+$	504-498	vs	100
$Co_3Mn(CO)_6Ge^+$	476-470	s	63
$Co_3Mn(CO)_5Ge^+$	448-442	s	74
$Co_3Mn(CO)_4Ge^+$	420-414	s	63
$Co_3Mn(CO)_3Ge^+$	392-386	s	90
$Co_3Mn(CO)_2Ge^+$	364-358	s	54
$Co_3Mn(CO)Ge^+$	336-330	s	56
Co_3MnGe^+	308-302	w	94
Co_3Ge^+	253-247	s	73

a This work, impurity peaks were also observed at 516 vvw $Co_4(CO)_{10}^+$, 488 vvw $Co_4(CO)_9^+$, 460 w $Co_4(CO)_8^+$, 432 m $Co_4(CO)_7^+$, 404 w $Co_4(CO)_6^+$, 376 w $Co_4(CO)_5^+$, 320 wm $Co_4(CO)_3^+$, 292 w $Co_4(CO)_2^+$, and 296-288 wm $Co_2(CO)_6Ge^+$?

6.3 Reaction between $Mn(CO)_5(GeMeH_2)$ and $Co_2(CO)_8$

6.3.1 Experimental details

$Mn(CO)_5GeMeH_2$ (264 mg, 0.93 mmol) and $Co_2(CO)_8$ (342 mg, 1.0 mmol) were reacted in hexane (3 ml) for ten minutes. Bubbling occurred and an orange-brown-yellow colour formed within about five minutes of reaction. Incondensable gases (*ca.* 0.6 mmol), traces of $HMn(CO)_5$ and $Mn(CO)_5(GeMeH_2)$ (71 mg, 0.25 mmol), were condensed out of the reaction vessel. The residues were extracted in hexane (25 ml). This extract showed carbonyl infrared bands at *ca.* 2109 w, 2082 w, 2076 m, 2063 w, 2052 sh w, 2047 m, 2030 m, 2020 w, 2014 ms, 2006 m, 1996 w, 1864 vw, 1834 w, cm^{-1}.

The remaining orange material dissolved in $CH_2C\ell_2$ (8 ml). Figure 6.2, page 244, illustrates the carbonyl infrared spectrum of this material. Absorption *maxima* (cm^{-1}) occur at 2109 w, 2076 s, 2049 s, 2030 ms, 2020 vs, 2014 s, 2002 w, 1836 mw. The ^1H nmr spectrum in benzene of this sample shows a very weak singlet at 8.51τ. After solid material had been removed for analysis by infrared, mass and nmr spectroscopy 112 mg, of product remained.

Figure 6.2

The carbonyl infrared spectrum of $[Co_2(CO)_7][Mn(CO)_5]GeMe$: cm^{-1}

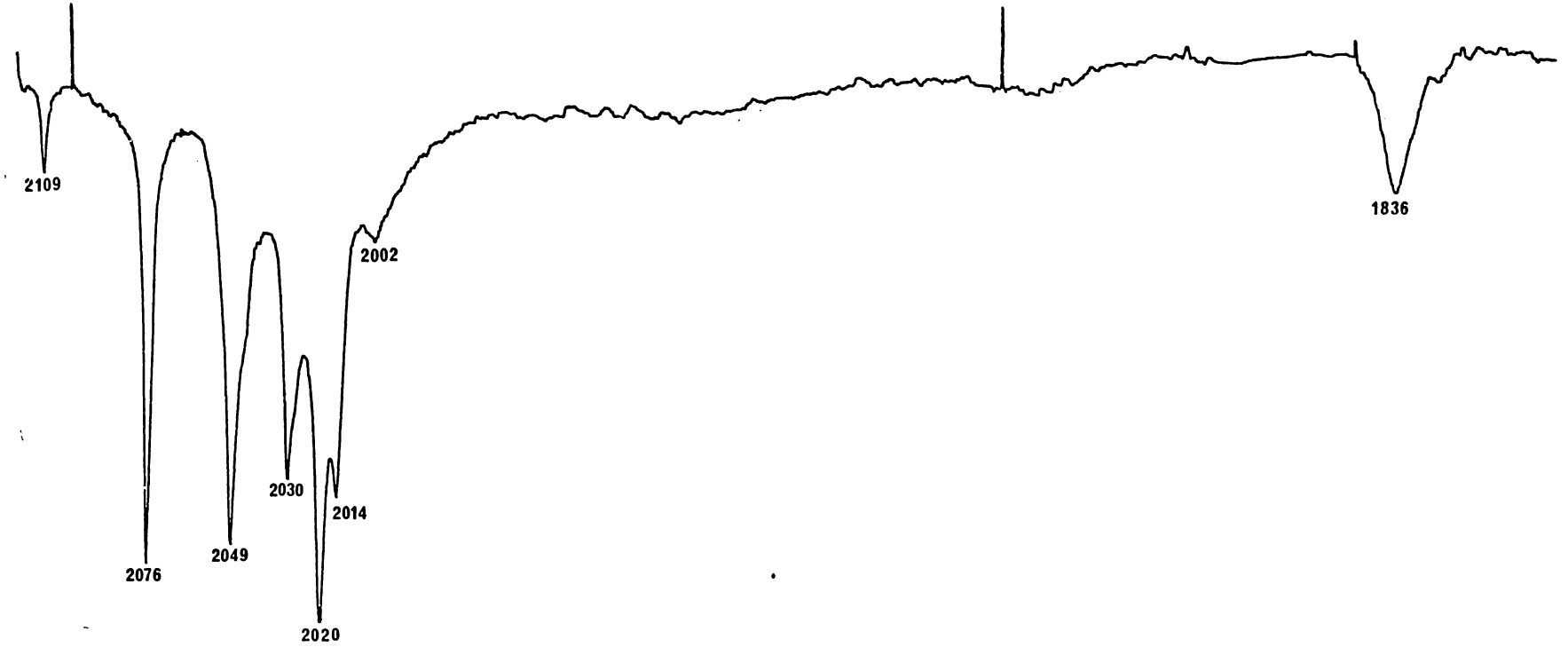

6.3.2 Discussion of reaction between $Mn(CO)_5(GeMeH_2)$ and $Co_2(CO)_8$

This reaction can be summarised as follows:

(i) Incondensable gases, 0.6 mmol

(ii) Volatile species, $Mn(CO)_5(GeMeH_2)$ (*ca.* 0.25 mmol), $Mn(CO)_5H$ trace

(iii) Hexane extract, $[Co_2(CO)_7][Mn(CO)_5]GeMe$, $Co_4(CO)_{12}$ and a small amount of an unidentified material with νCO bands at 2082 and 2006 cm^{-1}.

(iv) CH_2Cl_2 extract, $[Co_2(CO)_7][Mn(CO)_5]GeMe$ in excess of 0.18 mmol (material had been removed for infrared, mass and nmr spectroscopic studies).

These observations give the equation:

$$Mn(CO)_5(GeMeH_2) + Co_2(CO)_8 \rightarrow H_2/CO + [Co_2(CO)_7][Mn(CO)_5]GeMe + Co_4(CO)_{12} + Mn(CO)_5H + \text{unknown}$$

(0.68 mmol) (1.0 mmol) (0.6 mmol) (>0.18 mmol) (weak component) (trace) (trace)

The characterisation of $[Co_2(CO)_7][Mn(CO)_5]GeMe$ is discussed in the following section. As with $Mn(CO)_5GeH_3$, the recovered products suggest that the dominating reaction is:

$$Mn(CO)_5GeMeH_2 + Co_2(CO)_8 \rightarrow [Co_2(CO)_7][Mn(CO)_5]GeMe + H_2 + CO \quad (6.3)$$

No significant amount of partially substituted species, such as $[Co(CO)_4][Mn(CO)_5]GeMeH$ was indicated. However, although the Mn:Co ratio used was close to the 1:2 required by equation (6.3), about a quarter of the manganese did not react. There was no insoluble residue so that less soluble high molecular weight products can be excluded.

The $Co_2(CO)_8$ used (brown-orange colour) was not sublimed before use. The brown colour suggests $Co_4(CO)_{12}$ formation before reaction. Unreacted $Mn(CO)_5GeMeH_2$ could arise from a 1:1 Mn:Co reaction if $Co_4(CO)_{12}$ contaminated the $Co_2(CO)_8$ initially, thus, also accounting for the recovery of $Co_4(CO)_{12}$.

6.3.3 Characterisation of $[Co_2(CO)_7][Mn(CO)_5]GeMe$

The mass spectrum of the orange solid extracted by $CH_2C\ell_2$ is the best evidence for the formulation of this compound as a compound of the type $Co_2Mn(CO)_{12}GeMe$, see Table 6.5, page 249. The mass spectrum is similar to other germanium-containing carbonyl compounds as it shows, a weak parent ion, loss of CO as the dominant fragmentation process; and the bulk of the ion current is carried by ions retaining Co_2MnGe. All the remaining fragment ions are relatively weak and include $Mn(CO)_xGeMe^+$ species arising from scission of the metal-metal bonds. An unusual ion is the medium intensity ion at *m/e* = 274-265 which is tentatively attributed to $Mn(CO)_5Ge^+$ and involves metal loss which is otherwise observed only for the stripped skeleton.

The total fragmentation pattern suggests independent $Mn(CO)_x$ and $Co_2(CO)_y$ units. Hence the formulation of this species as $[Co_2(CO)_7][Mn(CO)_5]GeMe$ rather than $[CoMn(CO)_8][Co(CO)_4]GeMe$, which would be equally acceptable in terms of electron counting (18 electron rule).

This formulation is also intuitively more convincing as $Co_2(\mu\text{-}CO)$ species are common, whereas there are very few compounds where manganese atoms are bridged by CO. This may be because Mn is forced to be seven coordinate in a bridging situation, whereas the corresponding cobalt moiety is six coordinate.

cf.

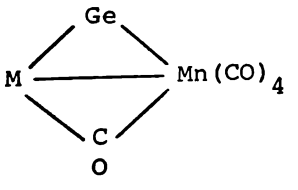

and

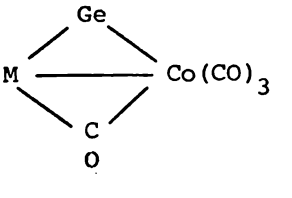

TABLE 6.5

The mass spectrum of $[Co_2(CO)_7][Mn(CO)_5]GeMe$

Tentative assignment	apparent mass	relative intensity
$MnCo_2(CO)_{12}GeMe^+$	600-594	w
$MnCo_2(CO)_{11}GeMe^+$	572-566	m
$MnCo_2(CO)_{10}GeMe^+$	544-538	m
$MnCo_2(CO)_9GeMe^+$	516-510	vvw
$MnCo_2(CO)_8GeMe^+$	488-482	vw
$MnCo_2(CO)_7GeMe^+$	460-454	w
$MnCo_2(CO)_6GeMe^+$	432-426	ms
$MnCo_2(CO)_5GeMe^+$	404-398	s
$MnCo_2(CO)_4GeMe^+$	376-370	ms
$MnCo_2(CO)_3GeMe^+$	348-342	m
$MnCo_2(CO)_2GeMe^+$	320-314	vs
$MnCo_2(CO)GeMe^+$	292-286	ms
$MnCo_2GeMe^+$	264-258	s
$MnCo_2Ge^+$	249-243	s
Co_2Ge^+	193-187	w
other fragments include:		
$Mn(CO)_5Ge^+$?	274-265	m
$Mn(CO)_3GeMe^+$	230-224	w
?	215-211	w
$Mn(CO)_2GeMe^+$	202-196	w

Also, Mn-Mn bonds are longer than Co-Co bonds, so this may add to the strain when Mn adopts a bridging CO.

As the proposed species $[Co_2(CO)_7][Mn(CO)_5]GeMe$ is of C_1 symmetry, twelve carbonyl-stretching modes are expected in the infrared. Table 6.6, page 250, compares the values obtained for this compound with those obtained for related species. The position and intensity of the carbonyl bands in the infrared spectra are consistent with its formulation as $[Co_2(CO)_7][Mn(CO)_5]GeMe$. Note, as in Section 6.2.3, that the modes of the $Mn(CO)_5$ unit are expected in similar positions to those of $Co(CO)_4$. It is interesting that whereas $[Co_2(CO)_7][Co(CO)_4]GeR$ show two bridging CO frequencies for both R=Me and Ph, the manganese species shows only one. As there is only one bridging νCO, two isomers of the tricobalt compounds must exist in similar proportions. For the manganese-dicobalt species, it is likely that steric factors lead to the predominance of the isomer with the $Mn(CO)_5$ group remote from the bridging region.

The very weak signal peak at *ca.* 8.51τ could arise from the product, compare,

$[Co_2(CO)_7]GeMe_2$	9.37τ	(C_6D_6)	(58)
$[Co_2(CO)_7][Co(CO)_4]GeMe$	8.07τ	($SiCl_4$)	(154)
$[Co_2(CO)_6](GeMe_2)_2$	9.0-8.7τ	(varies with T., $CF_2Cl_2CH_2Cl_2$)	(86)

However, the solubility is low, the peak is weak and an impurity (such as apiezon grease) cannot be excluded.

It is interesting to compare the stability of species containing the $[Co_2(CO)_7]Ge$ unit. $[Co_2(CO)_7]GeMe_2$ is both air sensitive and thermally unstable, rapidly decomposing below 25^0C to deposit $Co_4(CO)_{12}$ (58). $[Co_2(CO)_7][Co(CO)_4]GeMe$, $[Co_2(CO)_7][Co(CO)_4]GePh$ and $[Co_2(CO)_7][Co(CO)_4]GeBr$ are stable at room temperature but lose CO on

TABLE 6.6

The carbonyl infrared spectrum of $[Co_2(CO)_7][Mn(CO)_5]GeMe$ and some related species, cm^{-1}

$[Co_2(CO)_7][Mn(CO)_5]GeMe$ hexane[a]	$[Co_2(CO)_7][Co(CO)_4]GePh$ cyclohexane[b]	$[Co_2(CO)_7][Co(CO)_4]GeMe$ hexane[c]	$[Co_2(CO)_7]GeMe_2$ hexane[d]	$[Co_2(CO)_7]GePh_2$ hexane[e]	$[Mn_2(CO)_9]GeMe_2$ cyclohexane[f]
2109 w	2104 w	2105 m		2100 s	2100 (1)
2076 s	2082 s	2082 s	2087 s		
2049 s	2056 s	2056 s	2048 vs	2060 vs	2060 (4)
	2044 w	2046 sh			
2030 s	2036 vs	2030 s		2036 vs	
2020 vs	2025 m	2020/5 m	2025 vs	2019 s	
2014 s	2014 m	2007 w	2008 vs	2006 w,sh	2010 vs
2002 w	1998 w	1998 w	1998 sh		
			1965 w		1970 (4.5)
	1850 w	1850 m			
1836 mw	1835 sh	1838 w	1840 m	1840 s	1835 (0.5)

a - This work,
b - See reference (107)
c - See reference (154) and also reference (194)
d - See references (20, 58, 77)
e - See reference (157)
f - See reference (58)

warming, to give clusters; $[Co_3(CO)_9]GeR$. In contrast, $[Mn_2(CO)_9]GeMe_2$ is very stable, decomposing at its melting point, 144-143°C.

For $[Co_2(CO)_7][Mn(CO)_5]GeMe$ therefore, instability at ambient temperatures to form a Mn(μ-CO)Co species is not expected. Formation of a Co_2MnGe cluster could not be completely ruled out and would be interesting to investigate.

6.4 Reaction between $Mn(CO)_5(GeMe_2H)$ and $Co_2(CO)_8$

6.4.1 Experimental details

6.4.1.1 Preparation of $Mn(CO)_5(GeMe_2H)$

$NaMn(CO)_5$ (from $Mn_2(CO)_{10}$, 753 mg, 1.93 mmol), $GeXMe_2H$ (241 mg ; a mixture of $GeCl Me_2H$ and $GeBrMe_2H$ and possibly GeX_2MeH?) and Et_2O (5 ml) were shaken together for ten minutes at room temperature. The volatiles were removed leaving a white-orange coloured involatile material. Following fractionation, $Mn(CO)_5GeMe_2H$ (415 mg, 1.82 mmol) together with traces of mercury was recovered.

6.4.1.2 Reaction between $Mn(CO)_5GeMe_2H$ and $Co_2(CO)_8$

A solution of $Mn(CO)_5(GeMe_2H)$ (415 mg, 1.82 mmol) in hexane was poured onto $Co_2(CO)_8$ (297 mg, 0.87 mmol) under a nitrogen atmosphere. The solution turned brown, bubbling occurred and pressure was built up. After ten minutes at room temperature, the volatile material was pumped out of the tap-adapted Carius tube. $Mn(CO)_5(H)$ was very evident in the lowest volatile material (*ir*). The nmr spectrum of this volatile material gave a spectrum of $Mn(CO)_5(GeMe_2H)$, 9.39τ doublet, 5.83τ pentet, ^3J= 3.4Hz, and $Mn(CO)_5H$, 18.2τ singlet, in a mole ratio of 1.44:1, an unidentified singlet at 7.79τ (Intensity = 1/6 the intensity of $Mn(CO)_5(GeMe_2H)$, hexane ? 8.7τ., H_2 ? 5.7τ (*cf.* gaseous 5.66τ (196)). The nmr of orange-yellow sublimable material gives only infinitesimally small singlets at 9.63τ, 9.45τ, 9.25τ, 8.87τ, 8.78τ. Nmr spectra of unsublimable material gives peaks due to traces of solvent and apiezon grease only. The infrared spectrum of the sublimed material, yellow oil-white solid, shows absorption *maxima* in the carbonyl region at 2103 w, 2088 w, 2078 ms, 2056 mw, 2051 m, 2025 ms, 2015 vs,

2011 s, 2004 s, 1992 mw, 1982 w, 1841 w, cm^{-1}. Material which did not sublime (although it may have-given more time), shows carbonyl infrared stretching modes at 2103 mw, 2088 vw, 2078 s, 2061 w, 2053 w, 2034 w, 2028 m, 2023 m, 2015 vs, 2010 vs, 2003 vs, 1990 s, 1981 w, 1866 w, 1841 w, cm^{-1} in hexane.

The very weak mass spectrum of the sublimed material shows major monogermanium envelopes at,

Apparent mass	Relative intensity	Tentative assignment
302-295	vs	$Mn(CO)_5GeMe_2H^+$
274-267	s	$Mn(CO)_4GeMe_2H^+$
246-239	s	$Mn(CO)_3GeMe_2H^+$
218-211	s	$Mn(CO)_2GeMe_2H^+$
203-196	mw	$Mn(CO)_2GeMeH^+$
190-183	ms	$Mn(CO)GeMe_2H^+$
175-168	s	$Mn(CO)GeMeH^+$
147-140	mw	$MnGeMe^+$

6.4.2 Identification of products and discussion

The ^{1}H nmr spectrum of the volatile components from the reaction mixture show unreacted $Mn(CO)_5(GeMe_2H)$, $Mn(CO)_5H$, H_2 and a small unidentified singlet at 7.79τ. Nmr spectra of less volatile components do not reveal any useful information - the infinitesimally small peaks may account for material with low solubility or soluble impurities. Tentative suggestions for some of these peaks include starting material (9.45τ), germanium oxide species (9.63τ), while the peaks at 9.25τ, 8.87τ and 8.78τ could be products or traces of elements.

The infrared spectrum of the volatile components is dominated by $Mn(CO)_5H$. The infrared spectrum of the sublimed yellow oil-white solid contains absorptions at 2088w, 2056 mw, 2051 m, 2025 ms, and 1841 w cm^{-1}, which are largely absent from the infrared spectrum of the hexane fraction. Both spectra share bands at 2078 s, 2015 vs, 2010 vs, 2003 vs, 1990 s, 1981 w. Table 6.7, page 255, compares these values with infrared carbonyl modes in related complexes. Figure 6.3, page 256, shows spectra of $[Co(CO)_4]_2GeXY$ complexes together with the hexane fraction of the volatile material obtained in this section. Looking at the pattern of intensities and the regions in which these occur, it seems that there is no infrared evidence against the formulation of the hexane extract in this work and the tentative formulation of $[Co(CO)_4][Mn(CO)_5]GeMe_2$ species made in a similar reaction (20).

TABLE 6.7

The carbonyl infrared spectra of some dimethygermyl, manganese and cobalt carbonyls : cm^{-1}

Sublimed material[a] e	hexane extraction[a]	(20) d,f sublimed	(20) volatile product[b]	$[Co(CO)_4]_2GeMe_2$ (58)[f]	$[Mn(CO)_5]_2GeMe_2$ (58)[f]	$[Co_2(CO)_7]GeMe_2$ (20)[e]	$[Mn_2(CO)_9]GeMe_2$ (58)[f]
			2135, 2130				
			~2120 vw,sh				
			2115 wm				
2103 w	2103 mw	2105 m		2105 (2)	2105 (2.5)		2100 (1)
2088 w		2090 w,sh		2090 (6)		2087	
2078 ms	2078 s	2080 s			2080 (8)		
			2075 m,sh				
		2060 ms	2065 ms				2060 (4)
2056 mw							
2051 m					2045 (2)	2048	
		2040 s,sh		2035 sh			
2025 ms		2025 s,sh		2025 (6.5)		2025	
2015 vs	2015 vs	2015 vs					
2011 s	2010 vs	2010 vs,sh	2010 vw	2010 (7)	2010 (9.5)	2008	2010 vs
2004 s	2003 vs	2005 vs	2005 vs				
					2000 (9.5)		
				1995 (4.5)		1998 sh	
1992 mw	1990 s	1990 s					
					1985 (8.5)		
1982 mw	1981 w	1980 m,sh	1980 vw				
			1975 vw	1960	1955 (2)	1965	1970 (4.5)
1841 w			1825 m			1840 (8)	1835 (0.5)

a - This work, see Section 6.4.

b - See reference (20) and Section 6.4.

c - Compare with 2099, 2081, 2032, 2025, 2019, 2007, 1997 (20).

d - Bands at 665 s, 655 s, 545 ms were also recorded.

e - Hexane.

f - Cyclohexane.

g - Gas.

$Co_2(CO)_6(GeMe_2)_2$ (58), 2075 (1.5), 2035 (4), 2010 (4), 1985 (4.5) $Mn_2(CO)_8(GeMe_2)_2$ (58), 2035 (4), 2005 (8.5), 1995 sh, 1990 (8), 1962 (8), 1844 (0.2), 1823 (0.2).

Figure 6.3

The carbonyl infrared spectrum of $[Co(CO)_4][Mn(CO)_5]GeMe_2$ and some $[Co(CO)_4]_2GeXY$ species; cm^{-1}

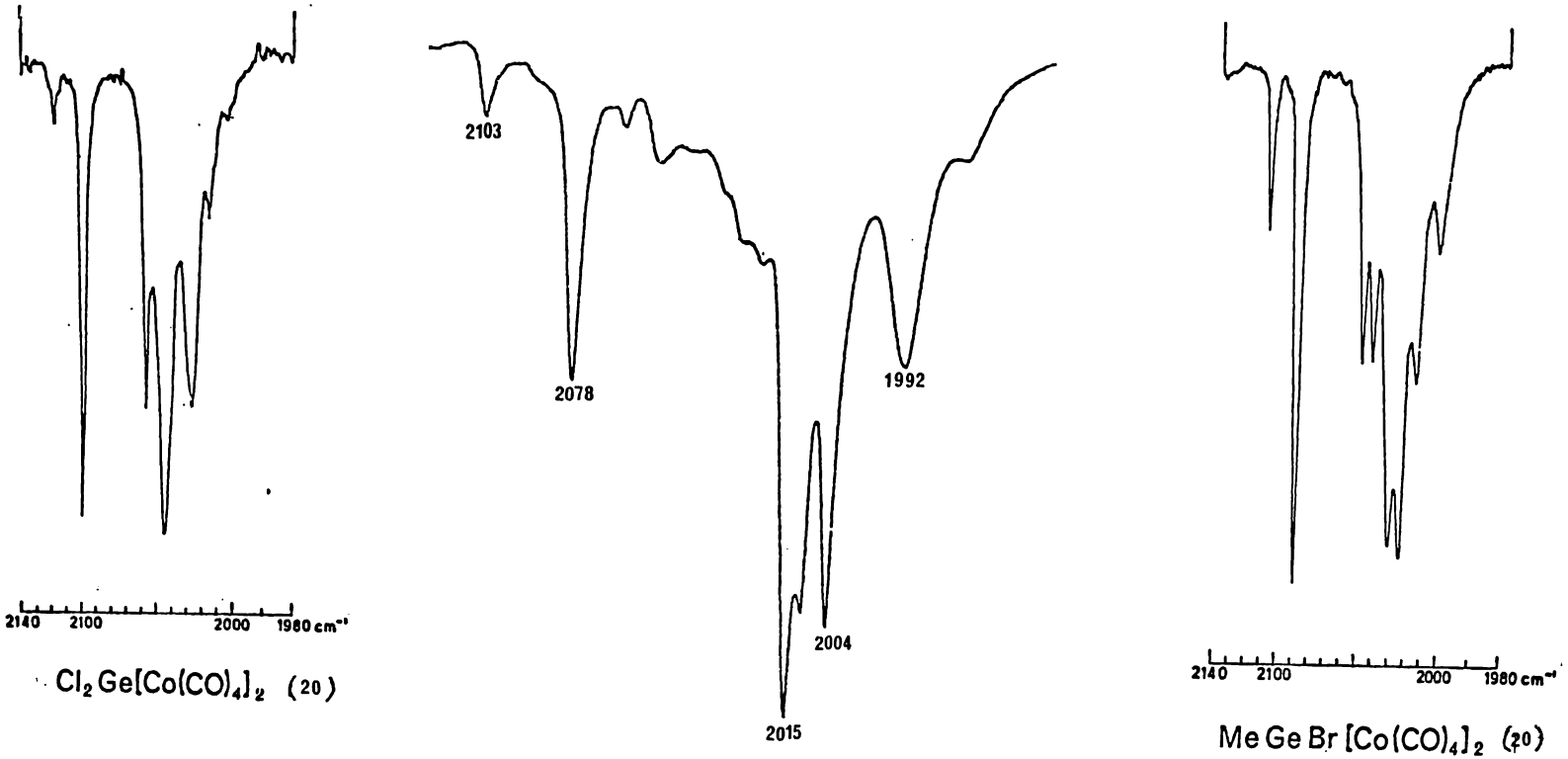

$Cl_2Ge[Co(CO)_4]_2$ (20)

$[Co(CO)_4][Mn(CO)_5]GeMe_2$

$MeGeBr[Co(CO)_4]_2$ (20)

Certainly, all the CO stretches are predicted to be infrared active as the symmetry of this compound is very low. C_s (predict 7a' + 2a''). As seen with other polymetallic carbonyls, there is a fair degree of mixing between the infrared allowed modes so fewer bands than are expected are usually observed.

The second component in the sublimed material which contains a bridging CO group remains unidentified.

The mass spectrum of the sublimed material is very weak. This is because it was taken after C_6H_6 had been added for the nmr study. Though the nmr spectrum shows very little material, the weak mass spectrum shows clearly, envelopes arising in predicted positions for unreacted $Mn(CO)_5(GeMe_2H)$ see page 253.

The mass spectrum of some material which did not sublime shows a clean weak spectrum ascribed to $[Mn(CO)_5][Co_2(CO)_7]GeMe$, where the P^+, $P-3CO^+$, $P-4CO^+$ and $P-5CO^+$ ions are too weak to be observed (*cf.*. Table 6.5, page 248). Extraction of the crude product before sublimation has envelopes attributable to $Mn(CO)_5(GeMe_2H)$, $[Mn(CO)_5][Co_2(CO)_7]GeMe$ a new series of envelopes separated by *m/e*= 28 which is thought to arise from $[Mn(CO)_5][Co(CO)_4]GeMe_2$. An unassigned peak occurs at *m/e*=16 units above the new series of ions.

The mass spectrum of the solid which did not sublime shows no envelopes attributable to $Mn(CO)_5(GeMe_2H)^+$ but shows envelopes at *m/e*=572-566 w, 544-538 w, 432-426 m, 404-398 s, 376-370 m, 348-342 m, 320-314 s, 292-286 s, 264-258 vs, 249-243 m, 206-200 w, 193-187 w, attributable to $[Co_2(CO)_7][Mn(CO)_5]GeMe$. The mass spectrum of a crude sample before sublimation shows a strong series of envelopes attributable to $Mn(CO)_5GeMe_2H$, and weak series of envelopes ascribed to $[Co_2(CO)_7][Mn(CO)_5]GeMe$ (as above) and new envelopes at :

Apparent mass	Relative intensity	Tentative assignment
495-483	w	?
473-467	w	$MnCo(CO)_9GeMe_2^+$
445-438	mw	$MnCo(CO)_8GeMe_2^+$
418-409	w	$MnCo(CO)_7GeMe_2^+$
390-380	mw	$MnCo(CO)_6GeMe_2^+$
361-353	m	$MnCo(CO)_5GeMe_2^+$
331-325	s	$MnCo(CO)_4GeMe_2^+$
230-225	w	$Mn(CO)_3GeMe^+$

Related compounds such as $[Mn(CO)_5]_2SiR_2$ R=H,Cℓ (16), $[Mn(CO)_5]_2GeMe_2$, $[Co(CO)_4]_2GeMe_2$ (58), $[Mn(CO)_5][Co(CO)_4]GePh_2$ (21), $[Mn(CO)_5][Co(CO)_4]SiClH$, $[Co(CO)_4]_2SiH_2$ (16), $[Mn(CO)_5]_2SnH_2$, $[Re(CO)_5]_2SnH_2$ (21) are all reasonably stable. $[Mn(CO)_5]GeMe_2$ and $[Co(CO)_4]_2GeMe_2$ melt at 79.5-78°C and 44.5-43°C respectively with no signs of decomposition (58). $[Mn(CO)_5][Co(CO)_4]GeMe_2$ by extention would be expected therefore to be stable also.

The major products recovered from this reaction were identified as $Mn(CO)_5(GeMe_2H)$, $[Mn(CO)_5][Co(CO)_4]GeMe_2$ and a little $[Co_2(CO)_7][Mn(CO)_5]GeMe$. Collman *et al.*, have prepared $[Mn(CO)_5][Co(CO)_4]GePh_2$ from an analogous reaction in high yields (no details were given).

6.4.3 Discussion of the reaction products obtained from reaction between $Mn(CO)_5(GeMe_2H)$ and $Co_2(CO)_8$

The appearance of copious amounts of hydride, $Mn(CO)_5H$ was not seen in reactions between $Co_2(CO)_8$ and $Mn(CO)_5(GeH_3)$ or $Mn(CO)_5(GeMeH_2)$. The appearance of $Co(CO)_4H$ has previously been postulated for reactions of the type:

$$M'R_3H + Co_2(CO)_8 \longrightarrow Co(CO)_4M'R_3 + Co(CO)_4H$$

$Co(CO)_4H$ is thought to undergo further reaction,

e.g $2Co(CO)_4H \longrightarrow Co_2(CO)_8 + H_2$

or $Co(CO)_4H + M'R_3H \longrightarrow Co(CO)_4M'R_3 + H_2$

No $Co(CO)_4H$ has been detected in any reactions between $Mn(CO)_5GeMe_{3-x}H_x$ and $Co_2(CO)_8$ in this work.

The formation of nmr detectable (*ca.* .5-20 mg) quantities of $Mn(CO)_5H$ may indicate that a different reaction is taking place in reactions where only one H is available per molecule to react.

Alternative suggestions for the presence of the $Mn(CO)_5H$ include different and/or catalysed reaction pathways resulting from

(i) Mercury contamination. In this reaction, traces of mercury in the $Mn(CO)_5(GeMe_2H)$ would have been transferred into the reaction system. Pouring a hexane solution of the less volatile $Mn(CO)_5(GeMe_2H)$ into the reaction vessel in this case contrasts with condensing the more volatile $Mn(CO)_5GeMeH_2$ and $Mn(CO)_5GeH_3$ into the Carius reaction tube in previous cases.

(ii) Oxygen contamination. As the reactants were allowed to react under a nitrogen atmosphere which was known to contain traces of oxygen, this species too, may be responsible for an alternative reaction pathway.

$[Co_2(CO)_7][Mn(CO)_5]GeMe$ is unexpected. One plausible explanation for the product $[Co_2(CO)_7][Mn(CO)_5]GeMe$ is from reaction of $Mn(CO)_5GeMeH_2$ impurity. The $Mn(CO)_5(GeMe_2H)$ used in this reaction was identified by its gas phase infrared spectrum. A small portion of $Mn(CO)_5(GeMeH_2)$ can not be ruled out as the bulk sample was not checked by nmr analysis before further reaction.

Further studies are required to definitively establish the formation and spectral properties of $[Mn(CO)_5][Co(CO)_4]GeMe_2$; whether in fact, this is the sole, or dominant product from this reaction; what the minor products are *e.g.*, GeMe species or $M(CO)_xH$ species.

Nmr reaction studies may also reveal the nature of the reaction intermediates.

6.5 Overview

Routes to mixed manganese and cobalt clusters have included reactions involving anion exahange, and reactions between neutral hydrides and carbonyls.

As $Mn(CO)_5^-$ only appears to displace terminally bonded $Co(CO)_4$ units, which are rare in cobalt carbonyl chemistry - cobalt compounds tend to be more thermodynamically stable in cluster situations. Lack of suitable precursors may retard the formation of the mixed metal clusters *via* this route.

In reactions with manganese hydrides and $Co_2(CO)_8$, it appears that $Co(CO)_4$ displaces hydrogen to give the mixed manganese cobalt derivative in often clean, fast reactions with good yields. (*cf.*, reactions with germanium, silicon and tin hydrides, Section 2.4.1)

It may be that reaction of $Co_2(CO)_8$ with GeH_2 moiety to produce H_2 and CO is faster and cleaner than reactions where only one Ge-H is available to react. In this latter case, there is evidence from this work for the formation of hydride species *e.g.*, $Mn(CO)_5H$ (*cf.*, Section 2.4.1) The hydrides are unstable and are thought to further react. This may account for secondary products obtained in reaction with $Mn(CO)_5(GeMe_2H)$.

But certainly, once one or two hydrogen atoms have been replaced, the remaining hydrogen(s) appear to be more reactive. The 1:1 $Mn(CO)_5(GeH_3)$: $Co_2(CO)_8$ reactions indicate that competition for the $Co_2(CO)_8$ does not occur; rather, the main product is the fully substituted product. No evidence is seen for partially substituted species.

Mixed metal complexes could be built up taking advantage of the reactivity of the functional M'-H unit. As can be seen in the tetracarbonyliron system, subtle changes in substituents can produce marked changes in the reactivity of the functional Ge-H groups towards condensation and the formation of higher molecular species. Reactions between iron carbonyl compounds, *e.g.*, $[Fe(CO)_4(GeH_2)]_2$ and $Co_2(CO)_8$ would be interesting to pursue.

It would also be interesting to see whether CO could cause condensation to some extent to reverse (See Section 2.)

e.g., $[Co_3(CO)_9][Mn(CO)_5]Ge + \quad CO \longrightarrow [Co(CO)_4]_3[Mn(CO)_5]Ge$

and to see whether mixed metal clusters will close up with loss of CO.

REFERENCES

(1) HEIN, F., POBLOTH, H., Z.Anorg. Allg. Chem., 1949, *248*, 84, Chem. Abstr. 1941, 37, 2676.

(2) VYAZANKIN, N.S., RAZUVAEV, G.A., KRUGLAYA, O.A., Organomet. Chem. rev. 1968, *3*, 323.

(3) BROOKS, E.H., CROSS, R.J., Organomet. Chem. rev.(A), 1970, *6*, 227.

(4) AYLETT, B.J., Adv. Inorg. Chem. Radiochem. 1968, *11*, 294.

(5) YOUNG, J.F., Adv. Inorg. Chem. Radiochem, 1968,*11*, 91.

(6) GLOCKLING, F., STOBART, S.P., M.T.P. International review of Science, Inorg. Chem. Seriesone, 1972, *6*, 63.

(7) HSIEH, A.T.T., M.T.P. International review of Science, Inorg. Chem., Series two, 1975, *6*, 109.

(8) ANG, H.G., LAU, P.T., Orgonomet. Chem. rev. (A), 1972, *8*, 235.

(9) CUNDY, C.S., KINGSTON, B.M., LAPPERT, M.F., Adv. Organomet Chem., 1973, *11*, 253.

(10) HOFLER, F., Topics in Current Chemistry, 1974, *50*, 129.

(11) AYLETT, B.J., Organomet. Chem. rev. 1980, (being J.Organomet. Chem., Library, 1980, *9*, 327.

(12) BONNY, A., Coordination Chem. rev. 1978, *25*, 229.

(13) NICHOLSON, B.K., MACKAY, K.M., GERLACH, R.F., Reviews on Silicon, Germanium, Tim and Lead compounds, 1981, in press.

(14) MACKAY, K.M., NICHOLSON, B.K., Comprehensive Organometallic Chemistry, Pergamon Press, Chapter 43, in press.

(15) AYLETT, B.J., CAMPBELL, J.M., J.Chem. Soc. (A), 1969, 1916.

(16) ABRAHAM, K.M., URRY, G., Inorg. Chem., 1973, *12*, 2850.

(17) GEORGE, R.D., MACKAY, K.M., STOBART, S.R., J. Chem. Soc.(D), 1972, 1505.

(18) MASSEY, A.G., PARK, A.J., STONE, F.G.A., J.Am.Chem.Soc.,1963, *85*, 2021.

(19) GRAHAM, B.W.L., MACKAY, K.M., STOBART, S.R., J.Chem. Soc (D), 1975, 475.

(20) GERLACH, R.F., MSc. Thesis, University of Waikato, 1976,

(20b) GERLACH, R.F., D.Phil.Thesis, University of Waikato, 1978.

(21) COLLMAN, J.P., HOYANO, J.K., MURPHY, D.W., J.Am. Chem. Soc., 1973, *95*, 3424.

(22) WONG, F.S., MACKAY, K.M., J. Chem. Res.(S), 1980, 109.

(23a) AYLETT, B.J., CAMPBELL, J.M., WALTON, A., J.Chem. Soc.(A), 1969, 2110.

(23b) AYLETT, B.J., CAMPBELL, J.M., WALTON, A., Inorg.Nucl.Chem. Lett., 1968, *4*, 79.

(24) AMBERGER, E., MULHOFER, E., STERN, H., J.Organomet. Chem, 1969, *17*, 5.

(25) KING, R.B., PANNELL, K.H., BENNETT, C.R., ISHAQ, M. Organomet. Chem., 1969, *19*, 327.

(26a) STOBART, S.R., J. Chem. Soc, (D), 1972, 2443.

(26b) STOBART, S.R., Inorg. Nucl. Chem. Lett., 1971, *7*, 219.

(27) BONNY, A., D.Phil, University of Waikato, 1976.

(28) BONNY, A., MACKAY, K.M., J. Chem. Soc. (D), 1978, *11*, 1569.

(29) BONNY, A., MACKAY, K.M., J. Chem. Soc. (D), 1978, 506.

(30) BONNY, A., MACKAY, K.M., J. Chem. Soc. (D), 1978, *7*, 722.

(31) BROOKS, E.H., GRAHAM, W.A.G., Abstr. of 4th Int.Conf.on Organomet. Chem, 1969, Bristol.

(32) FLITCROFT, N., HARBOURNE, D.A., PAUL, I., TUCKER, P.M., STONE, F.G.A., J. Chem. Soc. (A), 1966, 1130.

(33) WONG, F.S., MACKAY, K.M., Inorg. Chim. Acta., 1979, *39*, L21.

(34) AYLETT, B.J., CAMPBELL, J.M., J. Chem. Soc.(A), 1969, 1910.

(35) HAGEN, A.P., MACDIARMID, A.G., Inorg. Chem. 1967, *6*, 686.

(36) FIELDHOUSE, S.A., CLELAND, A.J., FREELAND, B.H., MANN, C.D.M., O'BRIEN, R.J., J. Chem. Soc.(A), 1971, 2537.

(37) CHALK, A.J., HARROD, J.F., J. Am. Chem. Soc. 1967, *89*, 1640.

(38) GEORGE, R.D., MACKAY, K.M., STOBART, S.R., J. Chem. Soc.(D) 1972, 974.

(39) GRAHAM, B.W.L., D.Phil. Thesis, University of Waikato, 1973.

(40) WONG, F.S., MACKAY, K.M., J. Chem. Soc.(D), 1978, *12*, 1752.

(41) HACKET, P., MANNING, A.R., J.Organomet. Chem, 1974, *66*, C17.

(42) STOBART, S.R., Inorg. Synth., XV, 174.

(43) MARKS, T.J., NEWMAN, A.R., J.Am. Chem. Soc., 1973, *95*, 769.

(44) KNOX, S.A.R., STONE, F.G.A., J.Chem. Soc., (A), 1971, 2874.

(45) KUMMER, R.K., GRAHAM, W.A.G., Inorg. Chem. 1968, *7*, 1208.

(46) CHALK, A.J., HARROD, J.F., J.Am. Chem. Soc., 1965,*87*, 1134.

(47) TRIPLETT, K., CURTIS, M.D., Inorg. Chem., 1976, *15*, 431.

(48) BROOKS, E.H., ELDER, M., GRAHAM, W.A.G., HALL, D., J.Am. Chem. Soc., 1968, *90*, 3587.

(49) JETZ, W., GRAHAM, W.A.G., J. Organomet. Chem. 1974, *69*, 383.

(50) MACKAY, K.M., STOBART, S.R., J.Chem. Soc.(D), 1973, 214.

(51) CLELAND, A.J., FIELDHOUSE, S.A., FREELAND, B.H., O'BRIEN, R.J., J. Organomet. Chem., 1971, *32*, C15.

(52) CLARK, H.C., HAUW, T.L., J.Organomet. Chem, 1972, *42*, 429.

(53) HOWARD, J., KNOX, S.A.R., STONE, F.G.A., WOODWARD, P., J. Chem. Soc. Chem. Commun.,1970, 1477.

(54) KERBER, R.C., PAKKANEN, T., Inorg. Chim.Acta, 1979,*37*, 61.

(55) ASH, M.J., BROOKES, A., KNOX, S.A.R., STONE, F.G.A., J.Chem. Soc.(A), 1971, 458.

(56) VANCEA, L., POMEROY, R.K., GRAHAM, W.A.G., J.Am. Chem. Soc. 1976, *98*,1408.

(57) BRATERMAN, P.S., Metal Carbonyl Spectra, Organometallic Chemistry, Series of Monographs, Academic Press Inc., 1975.

(58) JOB, R.C., CURTIS, M.D., Inorg. Chem., 1973, *12*, 2514.

(59) KAHN, O., BIGORGNE, M., J. Organomet. Chem, 1967, *10*, 137.

(60) JAGER, N.W., M.Sc. Thesis, University of Waikato, 1979.

(61) COTTON, F.A., KRAIHANZEL, C.S., J.Am. Chem.Soc (A), 1962, *84*, 4433.

(62) ORGEL, L.E., Inorg. Chem., 1962, *1*, 25.

(63) POILBLANC, R., BIGORGNE, M., J.Organomet. Chem. 1966, *5*, 93.

(64) POMEROY, R.K., GRAY, R.S., EVANS, G.O., GRAHAM, W.A.G., J.Am. Chem. Soc., 1972, *94*, 272.

(65) BIGORGNE, M., J. Organomet. Chem., 1975, *94*, 161.

(66) PANKOWSKI, M., BIGORGNE, M., J. Organomet. Chem., 1969, *19*,393.

(67) DAVIDSON, G., Introductory group theory for chemists, Applied Science Publishers, 1971.

(68) COLLMAN, J.P., MURPHY, D.W., FLEISCHER, E.B., SWIFT, D., Inorg. Chem., 1974, *13*, 1.

(69) BOR, G., J. Organomet. Chem., 1975, *94*, 181.

(70) DALTON, J., PAUL, I., STONE, F.G.A., J. Chem. Soc.,(A), 1968, 1215.

(71) DELBEKE, F.T., CLAEYS, E.G., VAN DER KELEN, G.P., EECKHAUT, Z., J.Organomet. Chem. 1970, *25*, 213.

(72) KAHN, O., BIGORGNE, M., C.R.Acad, Sc.Paris, 1968, *t261*, 2483.

(73) PATMORE, D.J., GRAHAM, W.A.G., Inorg. Chem., 1967, *6*, 981.

(74) JOHNSON, B.F.G., LEWIS, J., ROBINSON, P.W., MILLER, J.R., J.Chem. Soc.,(A), 1968, 1043.

(75) GRYNKEWISH, G.W., MARKS, T.J., Inorg.Chem, 1976,*15*, 1307.

(76) KNOX, S.A.R., PHILLIPS, R.P., STONE, F.G.A., J. Chem. Soc., (D), 1974, 658.

(77) KUMMER, D., FURRER, J., Z.Naturforsch, 1971, *B26*, 162.

(78) SCHMID, G., BALK, H.J., J. Organomet. Chem, 1974,*80*, 257.

(79) CLARK, H.C., RAKE, A.T., J. Organomet, Chem. 1974,*82*, 159.

(80) POMEROY, R.K., GRAHAM, W.A.G., J.Am.Chem. Soc., 1972, *94*, 276.

(81) ADAMS, R.A., BRICE, M.D., COTTON, F.A., Inorg. Chem., 1974, *13*, 1080.

(82) VANCEA, L., BENNETT, M.J., JONES, C.E., SMITH, R.A., GRAHAM, W.A.G., Inorg. Chem, 1977, *16*, 897.

(83) POMEROY, R.K., VANCEA. L., CALHOUN, H.P., GRAHAM, W.A.G., Inorg. Chem, 1977, *16*, 1508.

(84) BALL, R., BENNETT, M.J., Inorg. Chem, 1972, *11*, 1806.

(85) ADAMS, R.D., COTTON, F.A., CULLEN, W.R., HUNTER, D.L., MIHICHUK, L., Inorg. Chem, 1975, 14(b), 1395.

(86) ADAMS, R.D., COTTON, F.A., J.Am.Chem. Soc., 1970, *92*, 5003.

(87) FLOOD, T.C., DISANTI, F.J., CAMPBELL, K.D., Inorg. Chem, 1978, *17*, 1643.

(88) MARKS, T.J., GRYNKEWICH, G.W., J. Organomet. Chem.,1975, *91*, C9.

(89) EVANS, J., JOHNSON, B.F.G., LEWIS, J., MATHESON, T.W., NORTON, J.R., J. Chem. Soc.(D), 1978. 626.

(90) GLADFELTER, W.L., GEOFFROY, G.L., Inorg. Chem.,1980, *19*, 2579.

(91) COLTON, R., McCORMICK, M.J., Coord. Chem.,rev. 1980, *31*, 1.

(92) JETZ, W., GRAHAM, W.A.G., Inorg. Chem.,1971, *10* , 4.

(93) COTTON, F.A., WILKINSON, G., Advanced Inorganic Chemistry, Interscience Publishers, 1972, 3rd Edition.

(94) HOWARD, J.A.K., KELLETT, S.C., WOODWARD, P., J.Chem. Soc.(D), 1975, 2333.

(95) HOYANO, J.K., GRAHAM, W.A.G., Inorg.Chem., 1972, *11*, 1265.

(96) BEHRENS, V.H., GÖRTING, K., MERBACK, P., MOLL, M., Z.Anorg. Allg.Chem., 1979, *454*, 67.

(97) BIKOVETZ, A.L., KUZMIN, O.V., VDOVIN, V.M., KRAPIVIN, A.M., J. Organomet. Chem., 1980, *194*, C33,

(98) TRIPLETT, K., CURTIS, M.D., J.Am. Chem. Soc., 1975, *97*, 5747.

(99) ZIMMER, J.C., HUBER. M., C.R.Acad. Sc,Paris, 1968, *t267*, 1685.

(100) HARRISON, P.G., KING, T.J., RICHARDS, J.A., J.Chem. Soc.(D), 1975, 2097.

(101) GILMORE, C.J., WOODWARD, P., J.Chem. Soc.(D), 1972, 1387.

(102a) WATKINS, S.F., J. Chem. Soc. (A), 1969, 1552.

(102b) CROZAT, M.M., WATKINS, S.F., J.Chem, Soc.(D), 1972, 2513.

(103) ELDER, M., Inorg. Chem., 1969, *8*, 2703.

(104) ELDER, M., HALL, D., Inorg. Chem., 1969, *8*, 1425.

(105) DONG, D., FOUST, A.S., GRAHAM, W.A.G., Abs. 6th Int.Conf. on Organomet. Chem. University of Massachusetts, August, 1973.

(106) TRIPLETT, K., CURTIS, M.D., Inorg. Chem., 1975, *14*, 2284.

(107) BALL, R., BENNETT, M.J., BROOKS, E.H., GRAHAM, W.A.G., HOYAND, J., ILLINGWORTH, S.M., J.Chem.Soc.(CC), 1970, 592.

(108a) HOWARD, J., WOODWARD, P., J.Chem.Soc., (A), 1971, 3648.

(108b) BROOKES, A., KNOX, S.A.R., STONE, F.G.A., J.Chem.Soc.(A), 1971, 3469.

(109a) GERLACH, R.F., MACKAY, K. M., NICHOLSON, B.K., ROBINSON, W.T., J.Chem. Soc.(D), 1981, *1*, 80.

(109b) GERLACH, R.F., MACKAY, K.M., NICHOLSON, B.K., J.Organomet. Chem., 1979, *178*, C30.

(110) KODEL, V.W., HAUPT, H.J., HUBER, F., Z.Anorg. Allg. Chem., 1979, *448*, 126.

(111) SWEET, R.M., FRITCHIE, C.J., SCHUNN, R.A., Inorg. Chem., 1967, *6*, 749.

(112) SCHMID, G., ETZRODT, G., J.Organomet. Chem., 1977, *131*, 477.

(113) BOESE, R., SCHMID, G., J.Chem. Soc. Chem. Commun., 1979, 349.

(114) McNEESE, T.J., WREFORD, S.S., TIPTON, D.L., BAU, R., J.Chem. Soc. Chem. Commun., 1977, 391.

(115a) DUFFY, D.N., D.Phil.Thesis, University of Waikato, 1981.

(115b) THOMPSON, R., M.Sc. Thesis, University of Waikato, 1981.

(115c) FOSTER, S.P., University of Waikato, Personal Communication. 1981.

(116a) ELLIS, J.E., J. Organomet. Chem., 1975, *86*, 1.

(116b) KING, R.B., Adv. Organomet. Chem., 1964, *2*, 157.

(117) BEHRENS, V.H., WEBER, R., Z.Anorg. Chem., 1955, *281*, 190.

(118) KING, R.B., STONE, F.G.A., Inorg. Synth., 1963, *7*, 196.

(119a) LONGONI, G., CHINI, P., CAVALIERI, A., Inorg.Chem., 1976, *15*, 3025.

(119b) COLLMAN, J.P., Acc. Chem., Res., 1975, *8*, 342.

(120) GLADYS, J.A., TAM, W., J. Org. Chem., 1978, *43*, 2279.

(121) BLANCHARD, A.A., COLEMAN, G.W., Inorg. Synth., Vol.II, 243.

(122) FARMERY, K., KILNER, M., GREATREX, R., GREENWOOD, N.N., J. Chem. Soc., 1969, 2339.

(123) TELLER, R.G., FINKE, R.G., COLLMAN, J.P., CHIN, H.B., BAU, R., J. Am.Chem.Soc., 1977, *99*, 1104.

(124) PANNELL, K.H., JACKSON, D., J.Am.Chem. Soc., 1976, *98*, 4443.

(125) COTTON, J.D., BRUCE, M.I., STONE, F.G.A., J.Chem.Soc.,(A), 1968, 2162.

(126) GEORGE, R.D., KNOX, S.A.R., STONE, F.G.A., J.Chem.Soc.(D)., 1972, 973.

(127) NICHOLSON, B.K., SIMPSON, J., J.Organomet. Chem., 1978,*155*, 237.

(128) DUFFY, D.N., NICHOLSON, B.K., J.Organomet. Chem., 1979,*164*, 227.

(129a) INKROTT, K., GOETZE, R., SHORE, S.G., J.Organomet.Chem., 1978,*154*, 337.

(129b) BRUNET, J., SIDOT, C., CAUBERE, P., J.Organomet. Chem., 1980,*204*,229.

(129c) REGER, D.L., FAUTH, D.J., DUKES, M.D., Syn. React. Inorg. Metal-Org. Chem., 1977, *7*, 151.

(130) DUFFY, D.N., MACKAY, K.M., NICHOLSON, B.K., ROBINSON, W.T., J. Chem. Soc.(D). In press.

(131) ELLIS, J.E., FLOM, E.A., J.Organomet. Chem., 1975,*99*, 263.

(132a) CURTIS, M.D., Inorg. Nucl. Chem. Lett., 1970, *6*, 859.

(132b) CURTIS, M.D., Inorg. Chem., 1972, *11*, 802.

(133) NASTA, M.A., MACDIARMID, A.G., J.Am. Chem. Soc., 1971,*93*, 2812.

(134) NASTA, M.A., MACDIARMID, A.G., SAALFELD, F.E., J.Am. Chem. Soc., 1972, *94*, 2449.

(135) BENNETT, M.J., GRAHAM, W.A.G., SMITH, R.A., STEWART, R.P., Jr. J.Am. Chem. Soc., 1973, *95*, 1685.

(136a) BERRY, A.D., MACDIARMID, A.G., Inorg. Nucl. Chem. Lett., 1969, *5*, 601.

(136b) CUNDY, C.S., LAPPERT, M.F., YUEN, C.K., J.Chem. Soc.(D)., 1978, *5*, 427.

(137) MACDIARMID, A.G., BAAY, Y.L., BALD, J.F., BERRY, A.D., GONDAL, S.K., HAGEN, A.P., NASTA, M.A., SAALFELD, F.E., MCDOWELL, M.V., Pure and Applied Chem. 1969, *19*, 431.

(138) AYLETT, B.J., COLQUHOUN, H.M., J.Chem. Res.(S), 1977, 148.

(139) JETZ, W., GRAHAM, W.A.G., Inorg. Chem., 1971, *10*, 1647.

(140) CORNWELL, A.B., HARRISON, P.G., J.Chem. Soc.(D), 1975,*20*,2017.

(141) SHRIVER, D.F., Acc. Chem. Res., 1970, *3*, 231.

(142) BURNHAM, R.A., LYLE, M.A., STOBART, S.R., J.Organomet. Chem., 1977,*125*, 179.

(143) MARKS, T.J., SEYAM, A.M., Inorg. Chem., 1974, *13*, 1624.

(144a) SCHMID, G., WELZ, E., Angew. Chem. Int.Ed.Engl. 1977,*11*, 785.

(144b) SAKURAI, H., KAMIYAMA, Y., NAKADAIRA, Y., Agnew.Chem.Int.Ed. Engl., 1978,*17*, 674.

(145) COTTON, J.D., KNOX, S.A.R., STONE, F.G.A., J.Chem. Soc.(A)., 1968, 2758.

(146) COTTON, J.D., KNOX, S.A.R., PAUL, I., STONE, F.G.A., J.Chem. Soc.(A)., 1967, 264.

(147a) KNOX, S.A.R., STONE F.G.A., J.Chem. Soc.(A)., 1969, 2559.

(147b) KNOX, S.A.R., MITCHELL, C.M., J. Organomet. Chem., 1969, *16*, p.67.

(148) DENNIS, L.M., JUDY, P.R., J.Am.Chem.Soc., 1929, *51*, 2321.

(149) BICHLER, R.E., CLARK, H.C., HUNTER, B.K., RAKE, A.K., J.Organomet. Chem., 1974, *69*, 367.

(150) BAAY, Y.L., MACDIARMID, A.G., Inorg. Nucl. Chem. Lett., 1967, *3*, 159.

(151) JETZ, W., SIMONS, P.B., THOMPSON, J.A.J., GRAHAM, W.A.G., 1966, *5*, 2217.

(152) KNOX, S.A.R., STONE, F.G.A., J.Chem. Soc.(A)., 1970, 3147.

(153) GONDAL, S.K., MACDIARMID, A.G., SAALFELD, F.E., McDOWELL, M.V., Inorg. Nucl. Chem. Lett., 1969, *5*, 413.

(154) GERLACH, R.F., GRAHAM, B.W.L., MACKAY, K.M., J.Organomet. Chem., 1979, *182*, 285.

(155) SCHMID, G., Angew. Chem., Int.Ed.Engl., 1978, *17*, 392.

(156) BASATO, M., FAWCETT, J.P., POE, A., J.Chem.Soc.(D)., 1974, 1350.

(157) FIELDHOUSE, S.A., FREELAND, B.H., O'BRIEN, R.J., J.Chem.Soc. Chem. Commun., 1969, 1297.

(158) ETZRODT, G., SCHMID, G., J.Organomet. Chem., 1979, *169*, 259.

(159) MALISCH, W., RIES, W., Angew, Chemie., 1978, *17*, 120.

(160) POMEROY, R.K., J. Organomet. Chem., 1979, 177, C27.

(161) BOS, K.D., BULTEN, E.J., NOLTES, J.G., J.Organomet. Chem., 1975, 92, 33.

(162) BIGORGNE, M., POILBLANC, R., PANKOWSKI, M., Spectrochim.-Acta., 1970, *26A*, 1217.

(163) BULTEN, E.J., BUDDING, H.A., J. Organomet. Chem, 1974,*82*, 121.

(164) GREENE, J., CURTIS, M.D., Inorg. Chem., 1978, *17*, 2324.

(165) SMITH, D.W., J.Chem. Soc.(D)., 1976, 834.

(166) SANDERSON, R. T., WILEY, J., Vacuum Manipulations of Volatile Compounds, 1948.

(167) JOLLY, W.L., DRAKE, J.E., Inorg.Synth., 1963, *7*, 34.

(168) VAN DE VONDEL, D.F., J.Organomet. Chem., 1965, *3*, 400.

(169) VAN DE VONDEL, D.F., VAN DER KELEN, G.P., Bull.Soc.Chim.Belges, 1965, *74*, 467.

(170a) GEISLER, T.C., COOPER, C.G., NORMAN, A.D., Inorg. Chem., 1972, *11*, 1710.

(170b) FREEMAN, D.E., RHEE, K.E., WILSON, M.K., J.Chem. Phys., 1961, *39*, 2908.

(171a) RHEE, K.H., WILSON, M.K., J.Chem. Phys., 1965, *43*, 333.

(171b) GRIFFITHS, J.E., SRIVASTAVA, T.N., ONYSZCHUK, M., Can. J. Chem., 1962, *40*, 579.

(171c) DRAKE, J.E., RIDDLE, C., J.Chem. Soc.(A)., 1969, 2114.

(172) EBSWORTH, E.A.V., FRANKISS, S.G., ROBIETTE, A.G., J. Mol. Spectrosc., 1964, *12*, 299.

(173a) DRAKE, J.E., HEMMINGS, R.T., RIDDLE, C., J.Chem.Soc.(A)., 1971, 600.

(173b) DRAKE, J.E., HEMMINGS, R.T., RIDDLE, C., J.Chem.Soc.(A)., 1970, 3359.

(173c) BENTHAM, J.E., CRADOCK, S., EBSWORTH, E.A.V., Inorg.Nucl. Chem. Lett, 1971, *7*, 1077.

(174a) BARKER, G.K., DRAKE, J.E., HEMMINGS, R.T., Can.J.Chem., 1974, *52*, 2622.

(174b) BARKER, G.K., DRAKE, J.E., HEMMINGS, R.T., Spectrochim. Acta., 1972, *28A*, 1113.

(174c) BARKER, G.K., DRAKE, J.E., HEMMINGS, R.T., RAPP, B., J.Chem. Soc.(A)., 1971, 3291.

(175) WONG, F.S., D.Phil. Thesis, University of Waikato, 1978.

(176) HEIN, F., HEUSER, E., Z.Anorg.Chem., 1947, *255*, 125. CHEM. ABSTR., *43*, 45966.

(177a) BRAUER, G., Handbook of preparative inorganic chemistry, VOL.1, 716, Reed, Riley, New York.

(177b) FOSTER, L.S., DRENAN, J.W., WILLISTON, A.F., Inorg.Synth, *2*, 109.

(177c) EMELEUS, H.J., MACKAY, K.M., J.Chem.Soc., 1961, 2676.

(177d) Reprint from Instrument, Vol.25, No.3, March 1952, Bethlehem Apparatus Co.,

(177e) LIMMER, A., By gas chromatography, University of Waikato, personal communication.

(178) JAGER, N.W., M.Sc. Thesis, University of Waikato, 1979.

(179) MOSS, J.R., GRAHAM, W.A.G., J. Organomet. Chem., 1969, *18*, p.24.

(180) MOEDRITZER, K., J. Organomet. Chem., 1966, *5*, 254.

(181) BONNY, A., MACKAY, K.M., J. Organomet. Chem., 1978, *144*, 389.

(182) BRADLEY, G.F., STOBART, S.R., J. Chem. Soc.(D)., 1974, 264.

(183) PATMORE D.J., GRAHAM. W.A.G., J. Chem. Soc. Chem. Commun., 1967, 7.

(184) VAN DEN BERG, G.C., OSKAM, A., J. Organomet. Chem., 1975, *91*, 1.

(185a) NESMEYANOV, A.N., ANISIMOV, K.N. KOLOBOVA, N.E., ICHANDOZH, V.N., Izv.Nauk.SSSR, Ser.khim. 1971, *2* , 462.

(185b) NESMEYANOV, A.N., KOLOBOVA, N.E., KHANDOZHKO, V.N., ANIMOV, K.N., Zhur.Obshchei.khim., 1974, *44* , 313.

(185c) GERLACH, R.F., GRAHAM, B.W.L., MACKAY, K.M., J.Organomet.Chem., 1976, *118*, C23.

(186) FIELD, D.S., NEWLANDS, M.J., J.Organomet. Chem, 1971, *27* , 213.

(187) VAHRENKAMP, H., Angew. Chemie., Int.Ed., 1978, *17* , 379.

(188) POMEROY, R.K., WIJESEKERA, K.S., Inorg.Chem., 1980, *19*, 3729.

(189) BLACKENEY, A.J., GLADYSZ, J.A., Inorg. Chimica Acta, 1980, *53* , L25.

(190) WATTERS, K.L., BUTLER, W.M., RISEN, W.M., Inorg. Chem., 1971, *10*, 1970.

(191a) BURNHAM, R.A., STOBART, S.R., J.Chem.Soc(D), 1973, *12*, 1269.

(191b) SPALDING, T.R., J.Organomet. Chem., 1978, *149*, 371.

(192a) MACKAY, K.M., University of Waikato, personal communication.

(192b) NICHOLSON, B.K., University of Waikato, personal communication.

(193) JOHNSON, B.F.G., LEWIS, J., WILLIAMS, I.G., WILSON, J.M., J.Chem. Soc (A), 1967, *2* , 341.

(194) ETZRODT, G., SCHMID, G., J. Organomet. Chem., 1979, *169* 259

(195) DODD, R.E., ROBINSON, P.L., Experimental Inorganic Chemistry, Elsevier Publishing Co., 1954.

(196) POPLE, J.A., SCHNEIDER, W.G., BERNSTEIN, H.J., High Resolution Nuclear Magnetic Resonance Spectroscopy, McGraw-Hill, New York, 1959.

(197a) VAN DE VONDEL, D.F., VAN DER KELEN, G.P., Bull. Soc. Chim. Belges., 1975,*74*, 453.

(197b) GEORGE, R.D., MACKAY, K.M., J. Chem. Soc.(A), 1969, 2122.

(198a) LAPPERT, M.F. LEDNOR, P.W., Adv. Organomental. Chem., 1976, *14*, 345.

(198b) COTTON, J.D., MORRIS, G.A., J. Organometal. Chem., 1978, *145*, 245.

(199) $Fe(CO)_4(SiMe_3)_2$ has just recently been claimed to have been prepared from $K_2Fe(CO)_4$ and $SiBrMe_3$.(189)